

REINFORCED MULTIPLE BOLT TIMBER CONNECTIONS

by

Richard Mastschuch

Dipl.Ing., Technical University in Košice, Slovakia, 1993

A THESIS SUBMITTED IN PARTIAL FULFILMENT OF
THE REQUIREMENTS FOR THE DEGREE OF

MASTER OF APPLIED SCIENCE

in

THE FACULTY OF GRADUATE STUDIES

Civil Engineering Department

We accept this thesis as conforming
to the required standard

THE UNIVERSITY OF BRITISH COLUMBIA

November 2000

© Richard Mastschuch, 2000

ABSTRACT

Bolted connections have been used in heavy timber construction for centuries. Yet design rules are very inconsistent and failure modes are often of a brittle nature, contrary to design rules that are based on a yield model approach. To improve the ductility of bolted connections especially in seismic design applications, reinforcing measures can be applied in the connection region. The reinforcement restrains the expansion of timber in the perpendicular-to-grain direction and is meant to prevent a sudden release of energy and the associated brittle failure of the connection.

This thesis reports on an experimental investigation into the effect of various reinforcing techniques on multiple bolt connections in glue-laminated timber (Glulam) and parallel strand lumber (PSL). Several reinforcing techniques were investigated; (i) threaded rods and glued-in rods were applied internally; (ii) truss plates, nailed plates and glued-on plates were used as a surface reinforcement. Different configurations and materials within each reinforcement group were compared.

A total of 79 specimens were tested, 58 under monotonic tension and 21 under reverse cyclic loads. All connections consisted of 2 rows of 5 bolts each, attached to 19mm thick steel side plates. As a pilot study, three replicas of each ten-bolt connection were tested in monotonic tension. From these results, the joints considered to display good strength, ductility and energy dissipation characteristics were later tested in cyclic static loading. The parallel strand lumber specimens were 89x140mm and glue-laminated specimens 89x130mm in cross section with the bolts penetrating the short distance (89mm). The connection geometry was in all cases based on the bolt diameter and followed the Canadian code rules in CAN/CSA 086.1-94. The end distance, and the bolt and row spacing were respectively 10d, 4d and 4d in all the connections. The slenderness of the bolts (l/d ratio) was varied by using different bolt diameters in the tests - 9.5mm(3/8"), 12.7mm(1/2") and 15.9mm(5/8"). The bolts (Grade 5) were tested in bending to obtain their yield stress.

The larger diameter (1/2", 5/8") bolted connections with lag screw and truss plate reinforcement exhibited brittle fractures (splitting and shear plug). The reinforcement helped to maintain the integrity of the connection and considerable nonlinear deformations occurred with a relatively small reduction in load.

The most promising reinforcement method consisted of coarse threaded lag screws (4mm thread) inserted perpendicular to the grain halfway between each of the connection bolts. These specimens reached the highest displacement ductility ratio (15 on average) in the 3/8" bolt

connections. Further achievement was achieved when the reinforcing rod was offset from the bolt, and higher ductility was reached when compared to the reinforcing rod in the mid-position.

Fine threaded ready rod (1.8mm thread) did not have adequate bond to prevent perpendicular-to-grain tension splitting. In these cases the connections failed suddenly and in brittle failure modes with a ductility ratio of 4.7 in 5/8" PSL and 6.1 in 1/2" Glulam connections.

The tests with the truss plates showed that the teeth of the truss plates were not long enough. Especially in the cyclic tests, the huge cumulative displacement caused the truss plates to prematurely pull out from the timber. Thus a more sudden drop in the strength and stiffness followed after the peak load, compared to the lag screw reinforced cases.

The use of epoxy glue with different forms of reinforcement (glued-on plates, glued-in rods and rebars) mostly increased the strength (-1.7%, 32.1% and 14% on average) but did not prevent sudden failures. Ductility ratios of 2.9, 4.1 and 4.2 (on average) were reached for the three bolt sizes.

Little plate crushing in the bolt location and nail bending were observed when finishing nails and thin plates (0.6mm) were used as reinforcement. When 2" spiral nails with 1.2 mm thick plate were used, the stiff nails caused cracking of the specimen at peak load and no plate crushing was observed. Both configurations failed in a brittle manner.

One of the specimens was reinforced with a stiffened truss plate. Whereas the truss plates in general acted as passive reinforcement only, in this case most of the force was directly transferred through truss plate teeth to the wood. The plate prematurely pulled out off the wood, which caused a brittle failure (ductility of 3.3).

The Glulam connections were stronger than their PSL equivalents, but less ductile. The damage on the Glulam specimens was less predictable and cracks typically propagated along the entire specimen length. Cracks in PSL joints stopped at 10-15cm from the last bolt due to the denser and random wood strand orientation in the PSL cross section.

TABLE OF CONTENTS

	ABSTRACT	ii
	TABLE OF CONTENTS.....	iv
	LIST OF FIGURES.....	vi
	LIST OF TABLES.....	ix
	ACKNOWLEDGMENTS.....	x
1.	INTRODUCTION, OBJECTIVES.....	1
2.	LITERATURE REVIEW.....	4
2.1.	Main Issues Related to the Behaviour of Multiple Bolted Timber Connections.....	4
2.1.1.	Introduction, Objectives.....	4
2.1.2.	European Yield Model.....	4
2.1.3.	Compression Parallel to Grain.....	6
2.1.4.	Shear Stresses.....	8
2.1.5.	Bolt Clearance and Precision of Manufacturing.....	10
2.1.6.	Bolt Spacing, Number of Rows.....	11
2.1.7.	Bolt End Distance, Ratio of Main Member Length to Bolt Diameter.....	12
2.1.8.	Influence of Timber Properties.....	14
2.1.9.	Group Factor and Load Distribution within the Row.....	15
2.1.10.	Bolt versus Dowel.....	17
2.1.11.	Possible Failure Modes and Their Causes.....	18
2.2.	Seismic Aspects of Timber Structures and Bolted Connections.....	20
2.2.1.	Performance of Low-Rise Timber Buildings in Recent Earthquakes (Brown, D., 1991).....	20
2.2.2.	The Seismic Behaviour of Timber Structures (B.Deam, A.King, 1994).....	21
2.3.	Truss Plate Reinforcement in Parallam (Hockey, 1999)	23
3.	MATERIALS USED.....	25
3.1.	Parallel Strand Lumber.....	25
3.2.	Glue Laminated Lumber.....	27
3.3.	Connectors	29
3.3.1.	Bolts-Technical Data.....	29
3.3.2.	Flexural Yield Stress of Bolts - Tests in Bending.....	29
3.4.	Reinforcement - Secondary Connectors.....	31
3.4.1.	Truss Plates.....	31
3.4.2.	Coarse Threaded Rods - Lag Screws.....	32
3.4.3.	Fine Threaded Rods - Ready Rods.....	32
3.4.4.	Nailed Steel Plates.....	33
3.4.5.	Epoxy Glued Steel Plates.....	34
4.	SPECIMENS.....	35
4.1.	List of Specimens – Chronology.....	35
4.1.1.	List of Specimens.....	35
4.1.2.	Specimen Configuration layouts.....	36
4.1.3.	Chronology of Choosing the Specimen Types.....	41
4.2.	Unreinforced Specimen Manufacturing.....	42
4.3.	Reinforced Specimen Manufacturing.....	43
4.3.1.	Truss Plates	43
4.3.2.	Coarse Threaded Rods - Lag Screws.....	43
4.3.3.	Fine Threaded Rods - Ready Rods.....	44
4.3.4.	Nailed Steel Plates.....	44
4.3.5.	Epoxy Glued Steel Plates.....	44
4.3.6.	Stiff Steel Plate Welded on Truss Plates.....	45
4.3.7.	Glulam Specimens.....	45

5.	TEST METHODS.....	46
5.1.	Test Apparatus.....	46
5.1.1.	Setup for Static Tests.....	46
5.1.2.	Setup for Cyclic Tests.....	50
5.2.	Test Descriptions.....	52
5.2.1.	Static (Tension) Tests.....	52
5.2.2.	Cyclic (Tension-Compression) Tests	52
6.	DATA ANALYSIS METHODS.....	54
6.1.	Joint Ultimate Load, Joint Ultimate Displacement.....	54
6.2.	Elastic Stiffness Calculations.....	54
6.3.	Displacement Ductility of the Connections.....	54
6.4.	Energy Dissipation of the Connections.....	55
6.5.	Bending Deflection of the Bolts after Connection Failure.....	55
6.6.	Specimen Density and Moisture Content after the Test.....	57
7.	TEST RESULTS.....	58
7.1.	Static Tension Tests	58
7.1.1.	Unreinforced Specimens.....	58
7.1.2.	Threaded Rods	60
7.1.3.	Truss Plates.....	67
7.1.4.	Nailed Plates.....	70
7.1.5.	Glued-on-Plates.....	74
7.1.6.	Glued-in-Rods.....	75
7.1.7.	Load Distribution among Bolts in a Row.....	77
7.1.8.	086.1-94 CSA Code Strength Calculation vs. Experimental 5-th Percentile Value of Unreinforced Connections.....	79
7.2.	Reverse Cyclic Tests.....	82
7.2.1.	Unreinforced Specimens.....	85
7.2.2.	Truss Plates	87
7.2.3.	Threaded Rods.....	89
7.2.4.	Displacement-Stiffness Relation	93
8.	DISCUSSION.....	94
8.1.	Static Tension Tests.....	94
8.2.	Reverse Cyclic Tests.....	97
9.	CONCLUSIONS AND RECOMMENDATIONS.....	100
	REFERENCES.....	102
	APPENDICES.....	105
	APPENDIX I - Single Test Results, Specimen Layouts, Load-Displacement Curves, Photographs of Tested Specimens in Static Tension and Cyclic Loading.....	105
	APPENDIX II - Static Test Comparisons in Size and Material.....	192
	APPENDIX III - a - Static Tension Tests - Numerical Data Summary.....	202
	b - Reverse Cyclic Tests - Numerical Data Summary.....	205
	c - Statistical Data from Single-Connector Bending Tests....	206
	d - Bolts Bending Deflection Values Measured after the Failure of the Connections Tested in Static Tension.....	208
	e - Density and Moisture Content Summary.....	210

LIST OF FIGURES

Figure 1.	Failure modes according to CSA 086.1-94 (European yield model).....	5
Figure 2.	Response of spruce loaded in compression parallel to grain (Tan, Smith 1999).....	6
Figure 3.	Local behaviour after yield in loading parallel to grain (Rodd 1973).....	6
Figure 4.	Assumed embedding stress distribution around the fastener hole (Jorissen, 1998).....	7
Figure 5.	Stresses perpendicular to grain – spruce 24x72mm, row of 4bolts M12 (Jorissen, 1998).....	8
Figure 6.	Shear stresses in a multiple bolted connection (Jorissen, 1998).....	9
Figure 7.	Shear stress depending on the perpendicular-to-grain stress (van der Put).....	10
Figure 8.	Effect of bolt clearance on the radial stress along contact of hole A of a single fastener in spruce (Rowlands <i>et al.</i> , 1982).....	10
Figure 9.	Bolt spacing = 7d (Yasumura, 1988).....	11
Figure 10.	Bolt spacing = 4d (Yasumura, 1988).....	11
Figure 11.	Relation between ultimate load per bolt and the number of rows -with four bolts in the row (Yasumura, 1988).....	12
Figure 12.	Relation between maximum load and end distance (Yasumura, 1987).....	13
Figure 13.	Load-slip plots of joints with three 6mm dowels in line with $l/d=3$ and 6 (Mischler <i>et al.</i> , 2000).....	14
Figure 14.	Typical load-slip plot of identical joints in hardwood and softwood (Mischler, 1998).....	14
Figure 15.	Load distribution among the 5 bolts for 173mm wide Douglas Fir main member and 51mm side plates - test results (Wilkinson, 1986).....	16
Figure 16.	Typical load-slip curves of the tested dowel and bolted joints (Hirai, 1990).....	17
Figure 17.	Possible failure modes of a bolted connection loaded in tension.....	19
Figure 18.	Structure load-displacement responses (Park, 1989).....	22
Figure 19.	Typical hysteresis curve for wood connection (Popovski, Prion, 1998).....	23
Figure 20.	Fabrication Procedure of Parallam® (Introduction to Wood Design, 1996).....	26
Figure 21.	Parallam® cross section with the orientation of the veneer strips (Hockey, 1999).....	26
Figure 22.	Fabrication procedure of Glulam (Introduction to Wood Design, 1996).....	28
Figure 23.	Typical Glulam beam (Introduction to Wood Design, 1996).....	28
Figure 24.	Technical data of the bolts	29
Figure 25.	Test setup for bolts tested in bending.....	30
Figure 26.	Load-displacement curves of the tested bolts and lag screw.....	30
Figure 27.	Truss plate dimensions.....	31
Figure 28.	Technical data of lag screw.....	32
Figure 29.	Technical data of ready rod.....	33
Figure 30.	Technical data of spiral nail.....	33
Figure 31.	Unreinforced specimen layouts	36
Figure 32.	Truss plate reinforced specimen layouts.....	37
Figure 33.	Rod reinforced specimen layouts (two end rods).....	38
Figure 34.	Lag screw reinforced specimen layouts (rods at the bolt positions).....	39
Figure 35.	Lag screw reinforced specimen layouts (single end rod).....	39
Figure 36.	Glued-on plate reinforced specimen layouts (1.2mm plate, epoxy).....	40
Figure 37.	Nailed-on plate reinforced specimen layouts (1.2mm plate, spiral nails).....	40
Figure 38.	Nailed-on plate reinforced specimen layouts (1.2, 0.6mm plate, finishing nails).....	41
Figure 39.	Mechanical setup for monotonic static tests.....	47
Figure 40.	Specimen mounted in the setup – close up view.....	48
Figure 41.	Schematic view on the testing equipment.....	49
Figure 42.	Close view on LVDT s.....	50
Figure 43.	Lateral support-system for cyclic loading.....	51
Figure 44.	Cyclic loading protocol (ISO, 1999).....	52
Figure 45.	Explanation of the ductility considerations.....	54
Figure 46.	Test setup for measuring the bending deflection of bolts.....	56
Figure 47.	Typical load-displacement (P- Δ) curves of the unreinforced 3/8”(TU-2), 1/2”(HU-1) and 5/8”(FU-8) PSL specimens tested in static tension.....	58
Figure 48.	Typical failure of unreinforced 1/2” PSL specimen.....	59
Figure 49.	Unreinforced (FU) vs. lag screw (FRR) and ready rod (FRRF) reinforced connections; typical P- Δ curves of 5/8” PSL specimens tested in static tension.....	60
Figure 50.	Bi-axial tear-out failure of lag screw reinforced 1/2” PSL specimen.....	61

Figure 51.	Configurations of the threaded rods in the specimen.....	61
Figure 52.	Unreinforced (HU) vs. two end rods (HRR); all P-Δ curves of ½” PSL specimens tested in static tension	62
Figure 53.	Single end rod (HRRS) vs. two end rods (HRR); all P-Δ curves of ½” PSL specimens tested in static tension.....	63
Figure 54.	Centered rods (HRR) vs. rods at the bolt locations (HRRSH); all P-Δ curves of ½” lag screw reinforced PSL specimens tested in static tension.....	63
Figure 55.	Influence of l/d ratio; typical P-Δ curves of the lag screw reinforced 3/8” (TRR), ½” (HRR) and 5/8” (FRR) PSL specimens tested in static tension.....	64
Figure 56.	Unreinforced (TU) vs. lag screw reinforced (TRR) connections; typical P-Δ curves of 3/8” PSL specimens tested in static tension.....	65
Figure 57.	Unreinforced (GHU) vs. lag screw (GHRR) and ready rod (GHRRF) reinforced connections; typical P-Δ curves of ½” Glulam specimens tested in static tension.....	65
Figure 58.	Unreinforced (GTU) vs. lag screw (GTRR) reinforced connections; typical P-Δ curves of 3/8” Glulam specimens tested in static tension.....	66
Figure 59.	Unreinforced (HU) vs. truss plate (HRT) and stiff truss plate (HRTW) reinforced connections; typical P-Δ curves of 1/2” PSL specimens tested in static tension.....	67
Figure 60.	Unreinforced (FU) vs. truss plate (FRT) and rotated truss plate (FRTT) reinforced connections; average P-Δ curves of 5/8” PSL specimens tested in static tension	67
Figure 61.	Typical row tear-out failure of ½” truss plate reinforced PSL specimen.....	68
Figure 62.	The configurations of regular truss plate (FRT) and transversely rotated truss plate specimen (FRTT).....	69
Figure 63.	Unreinforced (FU) vs. nailed plate type I (FRN-I) and II (FRN-II) reinforced connections; all P-Δ curves of 5/8” PSL specimens tested in static tension (spiral nails).....	71
Figure 64.	Unreinforced (HU) vs. nailed plate gauge 18 (HRN18) and 26 (HRN26); all P-Δ curves of 1/2” PSL specimens tested in static tension (finishing nails).....	71
Figure 65.	Unreinforced (FU-avg) vs. nailed plate gauge 18 (FRN18) and 26 (FRN26); typical P-Δ curves of 5/8” PSL specimens tested in static tension (finishing nails).....	72
Figure 66.	Shear plug failure of 5/8” 18 gauge nailed plate (finishing nails) reinforced PSL specimen.....	73
Figure 67.	Unreinforced (FU-avg) vs. epoxy glued-on plate reinforced (FRE)connections; all P-Δ curves of 5/8” PSL specimens tested in static tension	74
Figure 68.	Shear plug and row shear-out failure of 5/8” epoxy glued-on plate reinforced PSL specimens.....	75
Figure 69.	Unreinforced (HU) vs epoxy glued-in lag screw (HRER) and rebar (HRERe) reinforced connections; all P-Δ curves of 1/2” PSL specimens tested in static tension	76
Figure 70.	Failure along the reinf. screws of 1/2” epoxy glued-in lag screw reinforced PSL specimens.....	76
Figure 71.	The three bolt diameter deflection shapes after failure.....	77
Figure 72.	Average bolt bending-displacement distribution in a row of 5/8”, ½” and 3/8” 10-bolt	78
Figure 73.	Density-moisture content relation – PSL.....	80
Figure 74.	Single hysteresis loops at three stages – connection HRRC-3.....	84
Figure 75.	Static tension compared to the reverse cyclic behaviour – ½” 10bolt unreinforced connection in PSL.....	84
Figure 76.	Cyclic load-slip curves of unreinforced PSL connections	86
Figure 77.	Row shear-out failure of 1/2” unreinforced PSL specimen tested in reverse cyclic loading.....	87
Figure 78.	Row shear-out failure of 1/2” truss plate reinforced PSL specimen tested in reverse cyclic loading	87
Figure 79.	Cyclic behaviour of 5/8” and ½” 10 bolt truss plate PSL reinforced connections	88
Figure 80.	Cyclic behaviour of 3/8” 10 bolt lag screw PSL reinforced connections	89
Figure 81.	Cyclic behaviour of ½” 10 bolt lag screw PSL reinforced connections.....	90
Figure 82.	Cyclic behaviour of 5/8” 10 bolt lag screw PSL reinforced connections.....	91
Figure 83.	Row shear-out failure of 3/8” lag screw reinforced PSL specimen tested in reverse cyclic loading.....	91
Figure 84.	Failure of 3/8” lag screw reinforced Glulam specimens tested in reverse cyclic loading.....	91
Figure 85.	Lag screw reinforced; P-Δ curves of 3/8” Glulam specimens tested in reverse cyclic loading.....	92

Figure 86.	Fatigue failure of 3/8"(9.5mm) diameter bolts.....	92
Figure 87.	Relation between elastic stiffness and displacement at ultimate load.....	93
Figure 88.	Elastic stiffness and the ultimate force average values – static tension.....	95
Figure 89.	Ductility ratios of the connections tested in static tension.....	96
Figure 90.	Energy dissipation of the connections tested in static tension.....	96
Figure 91.	Ductility and energy dissipation improvement due to the reinforcement of the connections tested in static tension.....	97
Figure 92.	Elastic stiffness and the ultimate force average values – cyclic tests.....	98
Figure 93.	Summation of absolute values of ductility and energy dissipation – reverse cyclic tests.....	99

LIST OF TABLES

Table 1.	Yield stresses of the bolts from bending tests.....	30
Table 2.	The list of tested specimen configurations.....	35
Table 3.	Static tension test results – unreinforced joints in PSL	59
Table 4.	Static tension test results – 5/8 inch 10 bolt threaded rod reinforced joints in PSL (FRR-lag screw, FRRS-single end rod, FRRF-ready rod).....	61
Table 5.	Static tension test results – 1/2 inch 10 bolt threaded rod reinforced joints in PSL.....	64
Table 6.	Static tension test results – 3/8 inch 10 bolt threaded rod reinforced joints in PSL	65
Table 7.	Static tension test results – 1/2 inch 10 bolt threaded rod reinforced joints in Glulam.....	65
Table 8.	Static tension test results – 3/8 inch 10 bolt threaded rod reinforced joints in Glulam.....	66
Table 9.	Static tension test results – 1/2 inch 10 bolt truss plate reinforced joints in PSL.....	69
Table 10.	Static tension test results – 5/8 inch 10 bolt truss plate reinforced joints in PSL.....	70
Table 11.	Static tension test results – 5/8 inch 10 bolt nailed plate (spiral nails) reinforced joints in PSL...	72
Table 12.	Static tension test results – 1/2 and 5/8 inch 10 bolt nailed plate (finishing nails) reinforced joints in PSL.....	72
Table 13.	Static tension test results – 5/8 inch 10 bolt epoxy glued-on plate reinforced.....	75
Table 14.	Static tension test results – 1/2 inch 10 bolt epoxy glued-in rod reinforced joints in PSL.....	76
Table 15.	Code prediction vs. test fifth percentile connection strength (Glulam, PSL).....	82
Table 16.	Total results of the joints tested in static tension.....	94
Table 17.	Total results of the joints tested in reverse cyclic loading.....	97

ACKNOWLEDGEMENTS

I am very grateful to my supervisors Dr. Helmut Prion¹ and Dr. Frank Lam² for their guidance, valuable suggestions, and encouragement throughout this research. I am personally indebted to Dr. Prion for financing my graduate studies at UBC and both, Dr. Prion and Dr. Carlos Ventura³, for giving me the opportunity to work with them on the number of interesting research projects.

I would like to express my gratitude to Professor Ricardo Foschi⁴ for reviewing the manuscript from the technical point of view. I greatly appreciate Ms. Lani Levine's and Ms. Fiona Robertson's intensive effort, patience and the time spent on editing the manuscript grammatically.

Several UBC graduate students contributed to the successful completion of this project. I am very grateful to Blake Hockey's⁵ initial guidance with the experiments. Precious advice and friendly attitude of Jachym Rudolf⁵, David Moses⁵ and Marjan Popovski⁵ is very appreciated.

Appreciation is extended to the technicians of the Structures Laboratory, Mr. Harald Schrempp, Mr. John Wong, Mr. Doug Smith and Mr. Doug Hudniuk for the helpful participation in preparing the apparatus and instrumentation used in the experiments.

Extensive testing described in this report was possible by providing wood products from the companies Truss Joist Mac Millan and Lamwood.

Finally loving gratitude is given to my wife Tatiana, cousin Dr. Joseph Ragaz⁶, my mom Darina and sister Karin whose limitless love, patience, tolerance and financial and mental support was the difference that made this academic goal possible for me.

¹ Associate Professor, Departments of Civil Engineering and Wood Science, Faculty of Applied Science and Faculty of Forestry, University of British Columbia

² Associate Professor, Department of Wood Science, Faculty of Forestry, University of British Columbia

³ Associate Professor, Department of Civil Engineering, Faculty of Applied Science, University of British Columbia

⁴ Professor, Department of Civil Engineering, Faculty of Applied Science, University of British Columbia

⁵ Graduate Student, Department of Civil Engineering, Faculty of Applied Science, University of British Columbia

⁶ Clinical Associate Professor, Division of Medical Oncology, Department of Medicine, Faculty of Medicine, University of British Columbia

1. INTRODUCTION, OBJECTIVES

Whereas light woodframe construction is the most popular and efficient method for residential buildings, large open enclosed spaces are often required for commercial and industrial buildings. This precludes the use of such panelized systems and heavy timber framing presents a more practical solution.

Therefore, braced post and beam timber frames are often a suitable substitution for the light framing to gain efficiency of the building plan area. The high clearances of commercial buildings also increase the strength demand of the structural members in both vertical and horizontal directions. Several types of heavy timber bracing placed in certain locations of the structure are typically provided to resist lateral forces from wind and earthquake loads. Internal forces are more concentrated in the link elements of heavy timber braced systems compared to the shear walls of the light frames. This makes heavy timber frames very efficient, but also introduce challenges regarding the connections.

Aside from the element properties of the braced frames, their global behaviour is largely dependent on the end joints. Ideally, the connections should be designed for strength capacity approaching the capacity of the member. Proper detailing and suitable load-deformation characteristics of the connections are thus crucial to assure satisfactory performance. In earthquake risk zones the connections are required to fulfill a high ductility demand. In other words, they need to be designed to avoid failure in a brittle manner after reaching the peak load, while maintaining relatively high loads at higher displacements.

The choice of the connector is largely dependent on the size of the member. While nails are optimal for light timber frames, bolts and other connectors such as lag screws, shear plates and split rings would be more suitable for heavy timber frames, due to their higher strength and ease of connection assembly. Larger members often need to be equipped with more than one bolt (multiple bolted connections) in order to transfer higher member forces. Slender and mild (low carbon) steel bolts should be used to achieve the required ductility. Stocky and high carbon steel bolts were found to cause uneven distribution of forces among the bolts. Such load concentration initiates premature cracks in the wood and can cause brittle failure.

The properties of wood also influence ductility and strength of bolted connections. In recent years, new technology brought better use of commercial timber. New manufacturing processes were developed which minimize the occurrence of imperfections in the wood (e.g.

knots, voids etc) thus improving its strength and efficiency when compared to sawn timber. These composite timber products are manufactured by cutting logs into smaller strands or chips and integrating them under certain conditions back together. This idea of reconstituting small wood sections was initially applied in Glue laminated lumber (Glulam). Later the technology of gluing veneer was improved leading to products such as Laminated Veneer Lumber (LVL), Laminated Strand Lumber (LSL), and Parallel Strand Lumber (PSL). Glulam and PSL were used in this research with the intent to compare their different mechanical properties, especially shear and tension strength in the multiple bolt connections.

Design codes vary widely in their approach to the dimensioning of bolted connections. For example the Canadian capacity rules in CAN/CSA 086.1-94 are based on a plastic deformation model assuming ductile behaviour of both connection materials, namely bolts yielding and wood crushing. These equations are relatively accurate in predicting the joint strength capacity provided that sufficient spacing, end and edge distance is provided. Eventual failure modes are often different, however, especially in the case of multiple bolted connections, when the failures are often brittle. Also, there are no rules in any design code that would specifically apply to seismic design of bolted connections. Therefore further research should target all the important issues in this area.

Several previous research projects at UBC investigated bolted connections. Most of them were focused on single bolted joints. Schubert, (1998) tested plywood, fiberglass and a truss plate as surface reinforcement applied on PSL. Single bolted reinforced 2x4 inch specimens were tested in static tension and reverse cyclic loading. The tests showed that the reinforcement could significantly increase ductility and strength of the connection. Truss plates (Hockey, 1999) as reinforcement in various PSL specimen sizes were tested in monotonic tension, where the ductility gains due to the truss plate reinforcement were observed in connections with one or four bolts. Most of the ten-bolt connections still failed in a brittle manner, signaling that still more research has to be done with multiple bolted connections. While Hockey's thesis focused only on truss plate reinforcement, there are several other types of methods for reinforcement, which need specific attention.

In this thesis several techniques were investigated; (i) threaded rods and glued-in rods applied internally; (ii) truss plates, nailed plates and glued-on plates used as a surface reinforcement. Different configurations and materials within each reinforcement group were compared. Small groups (of 3) of different reinforcements were first tested in monotonic tension. The test results are described in detail in Sec.6.1. After the monotonic tests, the most ductile

connections were chosen to be further tested in reverse cycles (tension – compression). The obtained load-displacement graphs from the cyclic tests (Sec.7.2) (hysteresis diagrams) will be eventually used to simulate the connection behaviour in dynamic modeling of braced heavy timber frames.

The objective of this study was to investigate different types of reinforcement techniques to improve the behaviour of multiple bolted timber connections. Within each type of reinforcement, different hardware geometry was applied on the PSL and Glulam specimens to cover a wide range of configurations. Increased ductility and strength of the connections were priority. The following connection aspects were also investigated in this thesis: stiffness, ease of manufacturing, appearance, and efficiency of the connection.

2. LITERATURE REVIEW

2.1. Main Issues Related to the Behaviour of Multiple Bolted Timber Connections

2.1.1. Introduction, objectives

There has been relatively little literature written on the topic of multiple bolted connections (MBC) so far. More was done on single bolted joints because of their simplicity in terms of modeling and predicting the load-deformation behaviour and failure. Despite the development of high capacity computers, a full analysis of MBC still takes a considerable amount of time, especially when using finite element stress models in three dimensions. Furthermore, failure criteria of wood failure mode under complicated stress state are not available. Therefore, experimental research (testing) in most cases ends up to be more time efficient than computer analysis.

Several test results from previous research describing MBC are presented in this chapter. The most important information on the subject of reinforced connections is presented together with a description of the relevant issues. Finally to better understand the planned MBC testing, which is a core focus of this thesis, the different failure modes are explained at the end of the chapter.

2.1.2. European Yield Model

In the latest issue of the Canadian code CSA 086.1-94 the European Yield Model (EYM - proposed by Johanson, 1949) was adopted as the basic for design to predict the capacity of dowel type (nail, bolt and screw) connections. This model is based on equilibrium equations resulting from the free body diagram of a bolt in a wood member. All assumptions are based on the ductile behaviour of wood and/or the fasteners in the connection. The wood fibers are assumed to fail by full bearing and crushing in compression when resisting the load applied by the bolt. The bolts are assumed to bend and possibly yield, while creating a number of plastic hinges, dependent on the number of shear planes or the number of connection members (either two or three). The plastic hinge configuration is mainly related to the bolt slenderness (L/d ratio), the relative stiffness of the connecting materials and the level of fixity at the side plates. For example, there can be either two or four hinges in a three-member connection.

According to the EYM, four ductile yield failure modes are possible. Figure 1 shows the modes and design formulae used for each failure mode, which represents the unit lateral strength resistance. The smallest value would represent the critical mode and should be chosen as the factored resistance parallel (P_r) and perpendicular (Q_r) to the grain, respectively:

$$P_r = \phi P_U n_S n_F J_F \quad \text{and} \quad Q_r = \phi Q_U n_S n_F J_R$$

where $P_U = p_U (K_D K_{SD} K_T)$ $Q_U = q_U (K_D K_{SD} K_T)$

For explanation of symbols see Sec. 7.1.8., in which the code strength prediction is calculated.

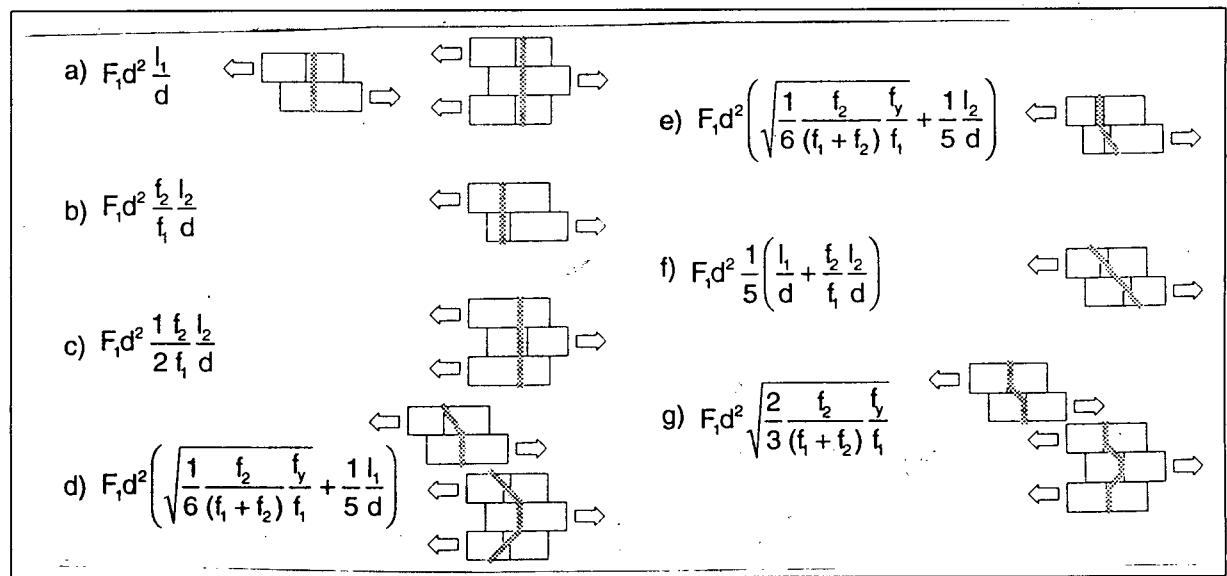


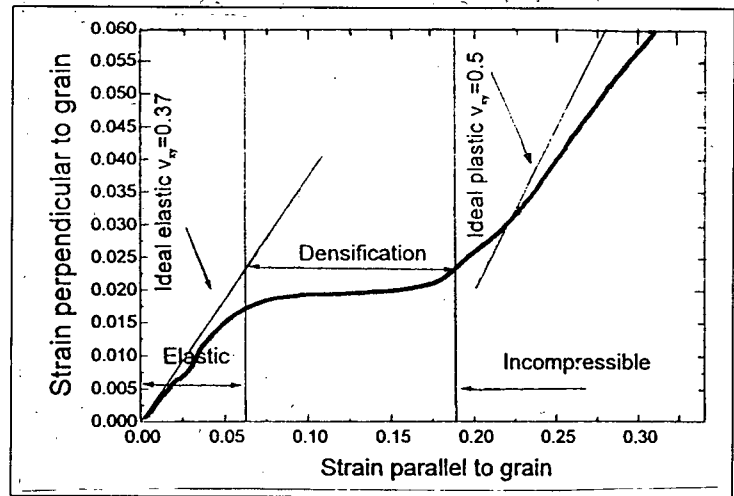
Figure 1. Failure modes according to CSA 086.1-94 (European yield model)

Later on Soltis *et al.* (1986) and McLain and Thangjitham (1983) experimentally confirmed that the EYM adequately estimates the strength capacity of bolted timber connections. Wilkinson (1992) found that the load at the 5%-of-bolt-diameter displacement accurately compared to the EYM capacity values. All the above-mentioned research was focused on connections with a single bolt. Other studies showed that factors such as specific wood gravity, bolt diameter, direction of loading (parallel or perpendicular to grain), wood species and bolt yield strength highly influence the dowel bearing strength (Wilkinson 1991). These effects will be explained further in the following sections.

2.1.3. Compression Parallel to Grain

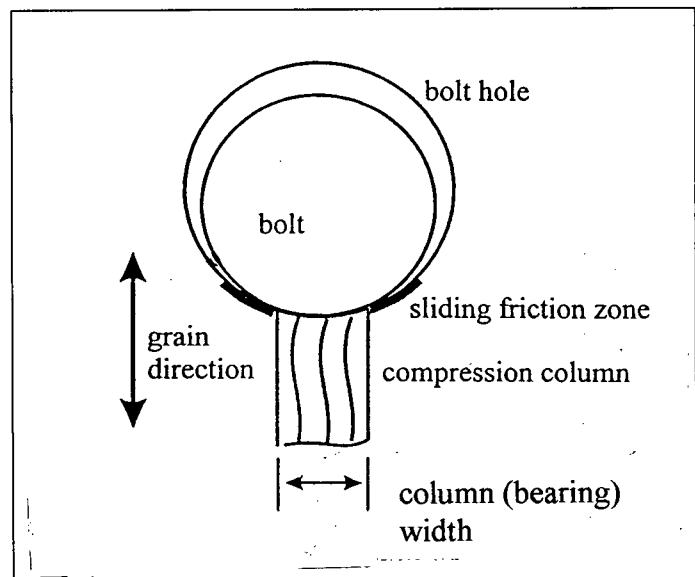
The compressibility of wood plays a significant role in the development of a failure mode in a connection. The timber fiber has an unusual stress-strain relationship when compressed. An unconstrained compression test (Fig.2) shows that the curve of longitudinal versus transverse strain exhibits three phases (Tan and Smith, 1999).

Figure 2. Response of spruce loaded in compression parallel to grain
(Tan and Smith, 1999)



In the initial elastic part the compressed fibers expand in the transverse direction as a result of the Poisson effect. During the densification part the fibres are crushed, and the voids are filled, creating a plateau on the curve. Once the compressibility limit is reached, lateral

Figure 3. Local behaviour after yield in loading parallel to grain
(Rodd, 1973)



expansion resumes, similar to plastic flow in ductile materials. The extensive strains in the transverse direction can cause cracks and expansion of the timber block. This phenomenon is causing the undesired brittle failure of wood. In the bolted connection case, the splitting is intensified by the “wedging force” and the “sliding friction zone” of the bolt depending on the stress concentration occurred due to clearance in the bolt hole (see Sec. 2.1.5). Friction between the bolt and the timber surface creates a compression column, the width of which is dependent on the bolt diameter and the hole tolerance. The column with the two shear planes causes the row shear failure (Fig.3).

The load in the perpendicular-to-grain direction can be calculated according to an analytical approach suggested by Kuipers (Jorissen,1998) (Fig.4):

The transverse load is:

$$V = y d \sigma_{h0} \frac{\frac{1 - \sin^2(\varphi)}{2} \cos(\varphi) - \left(\frac{\pi}{4} - \frac{\varphi}{2} - \frac{\sin(2\varphi)}{4} \right) \sin(\varphi)}{2 \cos(\varphi)} \quad (1.00)$$

If the angle of friction $\varphi = 30^\circ$, the transverse load $V = 0.1 y d f_h$. More realistic is the angle $\varphi = 18^\circ$ chosen by Werner, suggested by Rodd (Jorissen, 1998) ($f_h = \sigma_{h0}$ – embedding strength, ρ - density, $y = 2d$, d - bolt diameter).

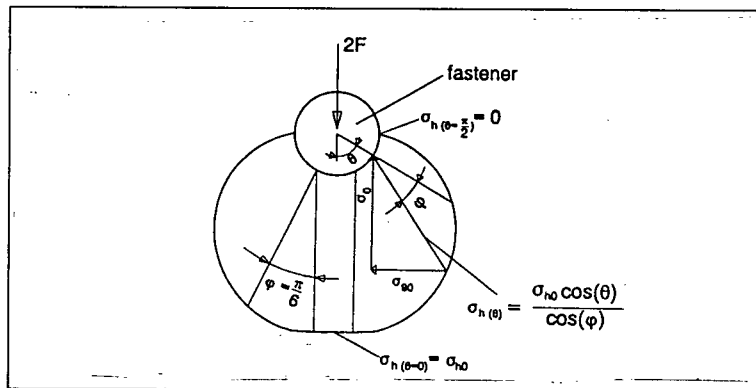


Figure 4. Assumed embedding stress distribution around the fastener hole (Jorissen, 1998)

In the multiple connector case, the transverse stresses are a maximum in the individual bolt positions and are overlapping each other. The overlapping stress accumulation is dependent on the bolt distance in the row. The bigger the distance is, the more independent the stresses are. Therefore as the code requires, designers should use the minimum spacing equal four times the bolt diameter to decrease the chance of wood failing due to local concentration of the perpendicular to grain stress.

According Equation (1.00), Jorissen (1998) calculated the transverse stress field for the connection with four bolts in a single row based on the model of a beam on an elastic foundation. The cumulative stresses are plotted in Fig. 5.

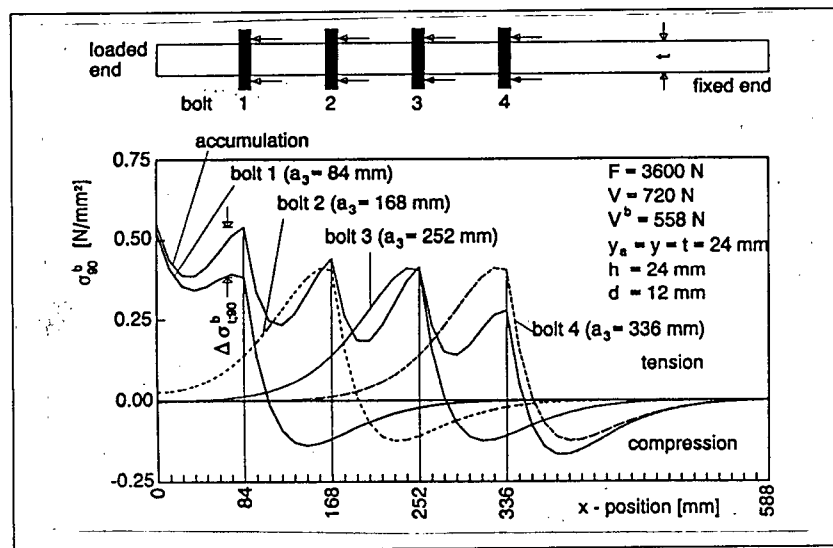


Figure 5. Stresses perpendicular to grain – spruce 24x72mm, row of 4 bolts M12 (Jorissen, 1998)

2.1.4. Shear Stresses

The shear stresses are also a limiting strength factor in MBCs. If the connection reaches its shear strength before the bolts yield and thus create plastic hinges, it can also end up cracking and failing in a brittle manner. The shear stresses are also accumulating in the bolt areas. The shear stresses at the loaded end were analyzed by Volkersen (Jorissen, 1998) and the formula (1.01) was developed.

Jorissen used this model for his aforementioned connection to plot the shear stresses along the row of bolts. The spruce specimen was loaded in the parallel to grain direction. Figure

cumulative part of the shear stress is present almost along the entire bolt spacing distance, but it is critical at the bolt positions, where the peak stresses are located.

$$\sigma_v = \frac{F (h_1 + h_2) f_v^2}{2 \omega E_0 G_c y_b h_1 h_2} \left[\frac{\cosh(\omega L_1)}{\sinh(\omega L_1)} \cosh(\omega x) - \sinh(\omega x) \right]$$

$$\omega = \sqrt{\frac{(h_1 + h_2)}{2 h_1 h_2} \frac{f_v^2}{E_0 G_c}}$$

$$h_2 = \frac{d}{2} \sin(\varphi)$$

$$h_1 = \frac{h - 2h_2}{2}$$

(1.01)

where: f_v - Shear strength [N/mm²]
 E_0 - Young's Modulus // Grain [N/mm²]
 $t = y$ - Member Thickness [mm]
 G_c - Critical Energy Release Rate [Nmm/mm²]
 φ - Embedding Stress Angle [deg]

Van der Put (Jorissen, 1998) proposed a relationship between shear strength and perpendicular to grain tension strength as shown in Fig. 7. According to this stress interaction envelope, a MBC connection could fail in a brittle manner by either reaching the wood critical shear stress or the wood critical perpendicular-to-grain stress at a certain bolt position.

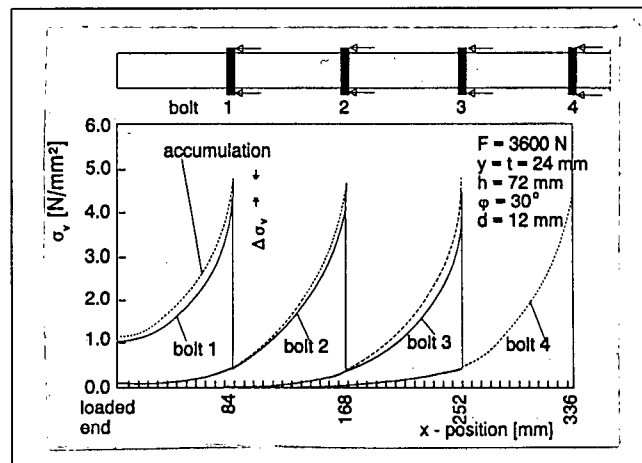


Figure 6. Shear stresses in a multiple bolted connection (Jorissen, 1998)

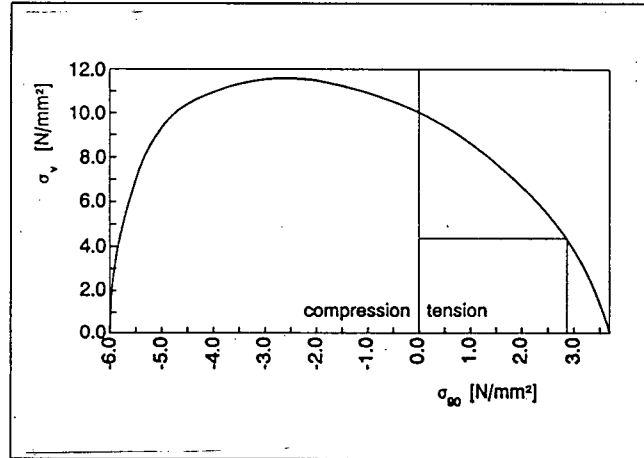


Figure 7. Shear stress depending on the perpendicular-to-grain stress (Van der Put) (Jorissen, 1998)

2.1.5. Bolt Clearance and Precision of Manufacturing

The clearance between a dowel-type connector and the hole in a timber member can significantly influence the connection behaviour to the extent of changing the failure mode. Lowlands *et al.* (1982) obtained experimental data from different clearance sizes or ratios between the diameter of bolt hole and the bolt diameter (r/R).

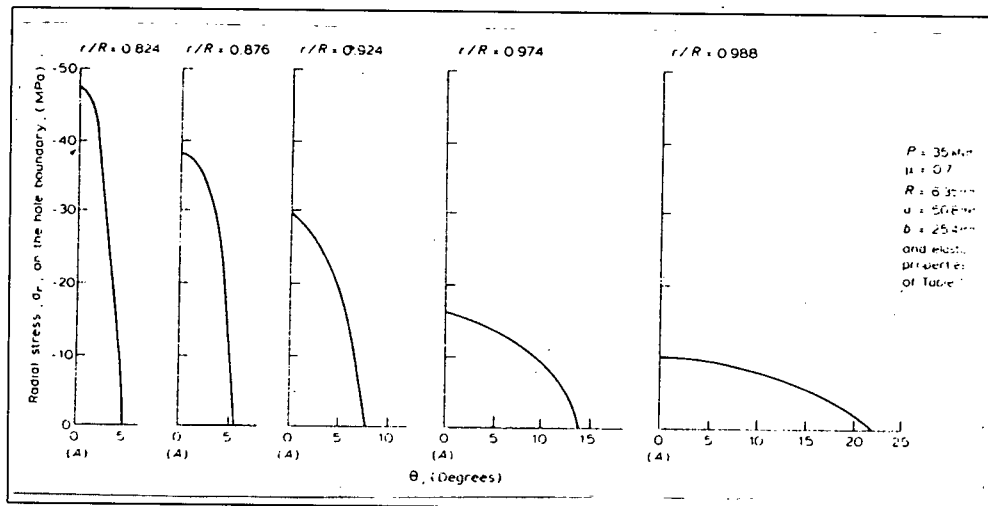


Figure 8. Effect on bolt clearance on the radial stress along contact of hole A of single fastener in spruce (Rowlands *et al.*, 1982)

The five plots (Fig.8) clearly show how the clearance significantly increases maximum contact radial stresses.

High concentrated stresses are not desirable and can cause uneven load distribution among the bolts, possibly initiating brittle failure. These results indicate the importance of manufacturing precision and the benefit of using tight fitting pin connections.

2.1.6. Bolt Spacing, Number of Rows

As explained in the “stresses” part above, the *bolt spacing* greatly influences the load per bolt by accumulation of the stresses in the bolt positions. Yasumura (1988) showed this phenomenon after testing spruce glue-laminated specimens in tension. One, two and three rows of 16mm diameter bolts with rows spaced at 40mm were used in the tests. The trend curves in Fig.9 with the bolt spacing of 7d are sloping much less than the specimens in Fig.10 with spacing of 4d, where the higher number of bolts is decreasing the load per bolt much more significantly. Fig.11 also indicates that as l/d increases the “number of bolts - load per bolt” relation slopes more significantly.

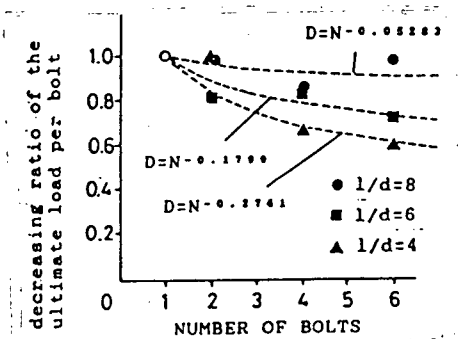


Figure 9. Bolt spacing = 7d
(Yasumura, 1988)

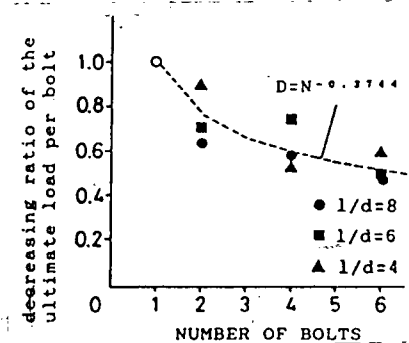


Figure 10. Bolt spacing = 4d
(Yasumura, 1988)

Fig.11 shows that for a small l/d ratio (4) the *number of rows* is not influencing the load per bolt very much, as opposed to bolts with a higher ratio ($l/d=8$). In the case of softer bolts as the number of row increases, the load per bolt decreases in almost linear relation.

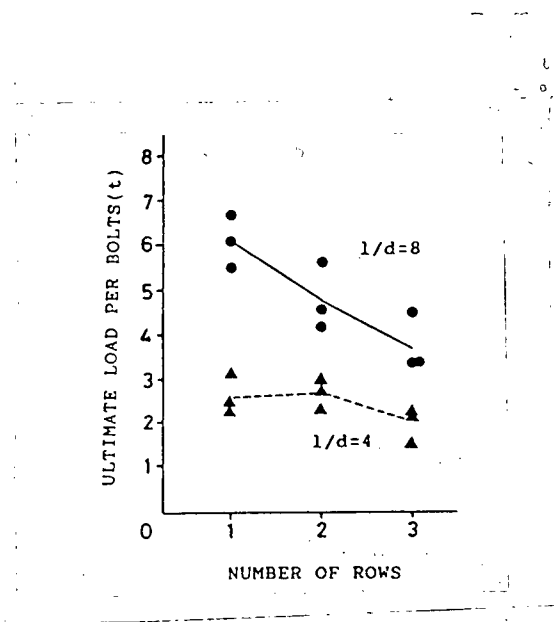


Figure 11. Relation between the ultimate load per bolt and the number of rows, specimens with four bolts in the row (Yasumura, 1988)

2.1.7. Bolt End Distance, Ratio of Main Member Length to Bolt Diameter

The bolt end distance has a significant influence on the maximum load of the joint. Beyond a certain end distance the maximum load remains constant, controlled by the embedding strength of the wood. For example, in Fig.12 (Yasumura, 1987) for $l/d = 2$ the limiting end distance is $5d$. Up to this limit the connection can fail due to shear or transverse tension in a brittle manner, because it does not reach the embedding strength limit. For different l/d ratios this limit is different. For seismic purposes, the point of transition from brittle to ductile failure modes is of interest, to assure joint ductile behaviour. Because of the even load distribution in the row of bolts, slender bolt connections tend to fail under higher loads. The higher embedding strength of slender bolts, as explained in the following relations, increases the strength of MBCs.

Equation (1.02), proposed by Fahlbusch (Jorissen, 1998), shows the non-linear relation between the embedding strength and the fastener diameter.

$$f_h = f_{h,10} (0.9 + 1/d) \quad [\text{N/mm}^2] \quad (1.02)$$

With: $f_{h,10}$ = embedding strength for a fastener diameter of 10 mm.
 d = fastener diameter [mm].

Equation (1.03) shows the linear relation suggested by Norén.

$$f_h = f_{h,10} (66-d)/56 \quad [\text{N/mm}^2] \quad (1.03)$$

As can be seen in Fig.12, an increase in bolt end distance increases the load capacity in brittle failure until a ductile failure mode starts to govern. For end distances beyond the critical value, wood crushing and bolt bending govern the connection behaviour. Spruce glulam and Douglas Fir specimens with wood side-plates were loaded in tension parallel to grain. The bolt diameters were 16 and 20mm. The connection holes were drilled with no clearance ($r/R=1$). The embedding strength of Spruce and Douglas Fir were respectively 36.9 MPa and 53.6 MPa, the bolt moment capacity was 490.5 MPa with first yielding at 245 MPa.

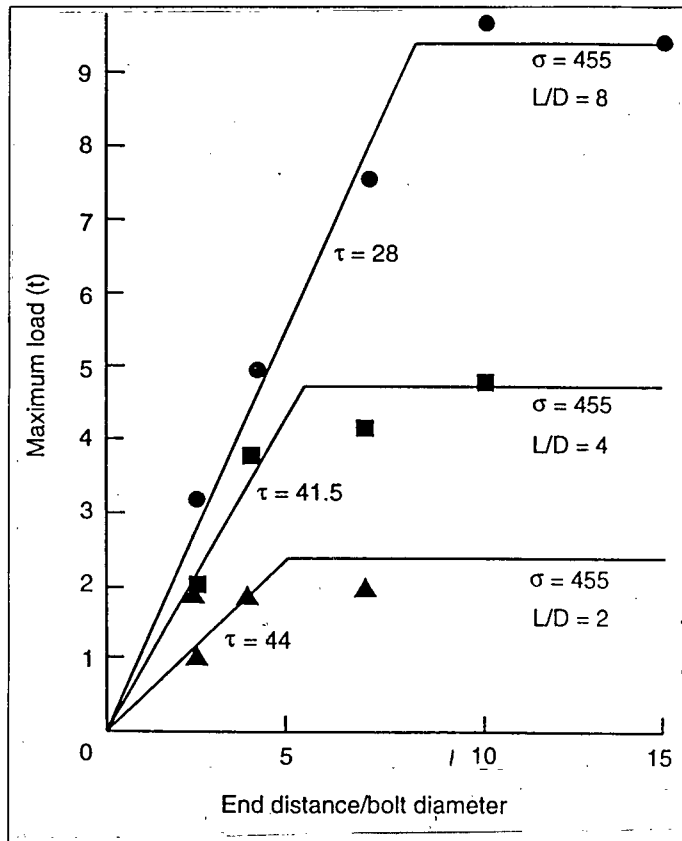


Figure 12. Relationship between maximum load and end distance (Yasumura, 1987)

The slenderness of a dowel-type connector has a significant influence on the failure mode of the connection as shown in Fig.13 (Mischler *et al.*, 2000). Dowels with slenderness ratio of 3 developed brittle failures with premature splitting and sudden loss of strength, whereas specimens with $l/d=6$ failed in a ductile way, and reached much higher loads and displacements.

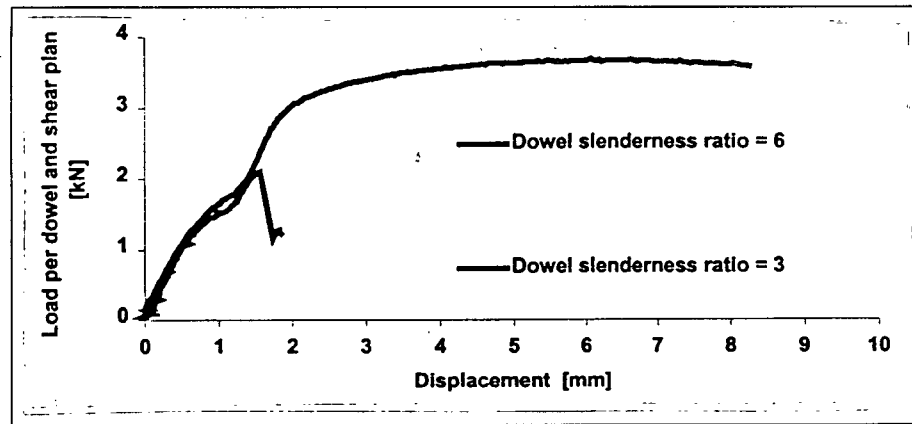


Figure 13. Load-slip plots of joints with three 6 mm dowels in line with $l/d=3$ and 6 (Mischler *et al.*, 2000)

2.1.8. Influence of Timber Properties

Different species have different embedding strengths as well as varying tension perpendicular to grain and shear strengths. This will influence the strength, stiffness and the type of failure of the connection. Different ultimate strength and displacement capacity of Spruce and

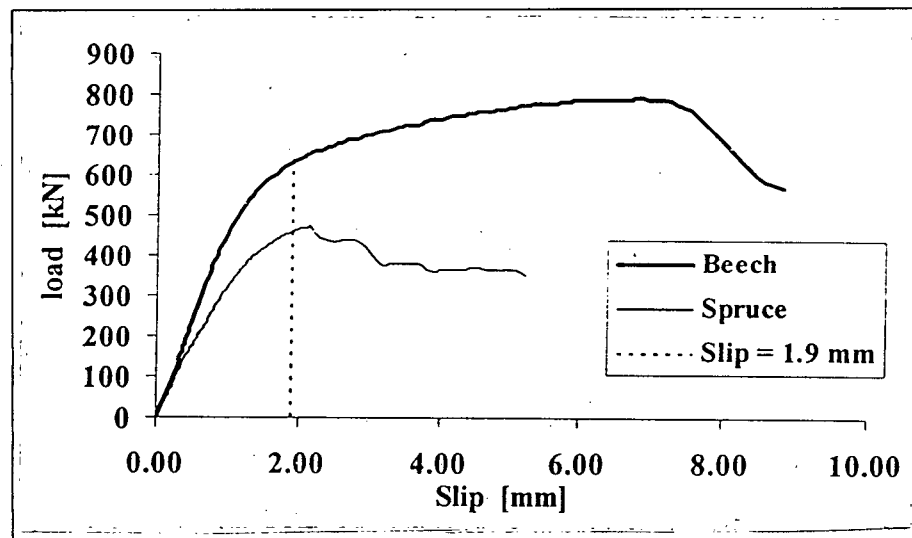


Figure 14. Typical load-slip plot of identical dowel joints in hardwood (Beech) and softwood (Spruce) (Mischler, 1998)

Beech multiple shear connections is shown in Fig.14 (Mischler, 1998). The higher load capacity of the beech specimens is mainly caused by the higher embedding strength of the wood. Also the tensile strength perpendicular to grain of hardwood such as beech is much higher than that of softwood (spruce).

2.1.9. Group Factor and Load Distribution within the Row

In design codes the configuration effects in bolted connections are often combined in so-called group factors. These have been derived from experimental studies on typical connections with fabrication tolerances as generally found in practice.

The Canadian code CSA 086.1-94 group factor J_G for bolts is largely based on Canadian (Massé *et al.*, 1988) and Japanese tests results (Yasumura, 1987). It reflects the influence of the L/d ratio, bolt-spacing ratio (s/d) and number of bolts in a row (N) on the total connection capacity. These three effects are combined in the following formula:

$$J_G = 0.33[L/d]^{0.5}[s/d]^{0.2} N^{-0.3} \leq 1.0$$

It can be concluded from this formula that the benefit from increasing the number of bolts in a row beyond 10 to 12 is so small, that it becomes inefficient. Therefore the formula is limited to 12 bolts in a row.

Later on Massé *et al.*(1988) introduced the end distance factor " J_L ", that accounts for a reduction of load as the end distance is reduced from prescribed $10d$ with a limit placed at $7d$.

Massé and Yasumura found out, that as the number of bolt rows is increased, the capacity of the bolts in the row decreased. The research also indicated that beyond three rows of bolts, the strength is not significantly increased. The factor " J_R " was added to the group factor formula so that:

$$\begin{aligned} J_R &= 1.0 \text{ for 1 row (or 1 bolt/row)} \\ &= 0.8 \text{ for 2 rows (2 or more bolts/row)} \\ &= 0.6 \text{ for 3 rows (2 or more bolts/row)} \end{aligned}$$

As recent research has shown (Tan and Smith, 1999), a small l/d ratio can cause an uneven load distribution in the row of bolts. Thus, due to the high concentration of the load in

one or two bolts, the connection can end up failing in a brittle manner. While one bolt is already undergoing plastic hinging, the other bolts may still be elastic. The hinging bolt is reaching the timber's "uncompressed zone" by crushing the wood fiber to its limit. Then the extensive tension in the transverse direction is initiated, causing a brittle crack in the member. The crack is quickly progressing along the row of bolts causing a global brittle failure. The EYM does not include this failure mode in its calculations, therefore it is not valid for multiple bolted connections with high strength short bolts (stocky bolts with small l/d ratios). Tan and Smith in their hybrid elasto-plastic model could predict the ultimate capacity of the connection and whether failure would be brittle or ductile, by using separate load-slip curves of the bolts in one row. But still, a multiple row model would have to be supplemented by separate calculation to predict the shear plug, usually occurring in the bolt group with several rows.

Another research project (Wilkinson 1986) investigated the influence of the bolt load-slip curves and fabrication imperfections on the distribution of the load in the row. The real bolt load-slip curves were obtained from tests and used for the analytical model to predict the overall connection load-displacement relation. The model accounting for the bolt curves and tolerances in drilling showed that these two factors are randomly distributed. Every distribution of the load in the row is unique and failure can be caused by any bolt, which is the main load carrier. These results indicate that the use of a single load-slip curve for designing a connection is not necessarily conservative. Therefore, the code should account for the mentioned random effects in

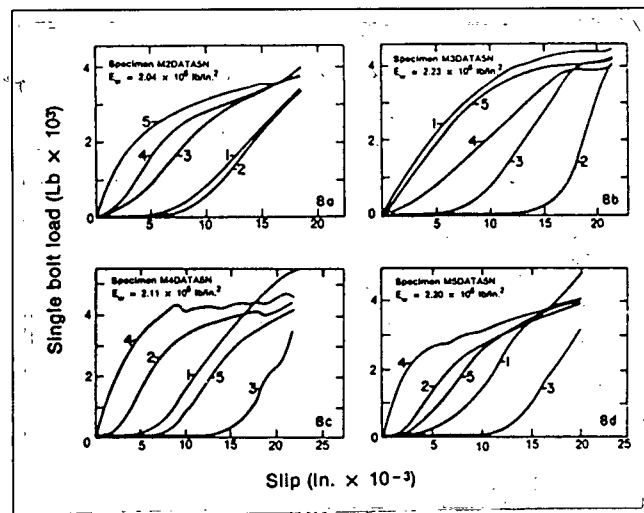


Figure 15. Load distribution among the 5 bolts for 173mm wide Douglas Fir main member and 51mm steel side plates – test results (Wilkinson, 1986)

the design calculations. This model could be used for predicting the distribution among the bolts, provided sufficient information about the bolts and imperfections in the connection is available. The particular bolt behaviour in the joint was closely related to the imperfections in the specimen manufacturing, and could thus be obtained only after the test, which was not a prediction any more. Wilkinson suggested gathering enough statistical data to be able to generate random load-slip curves that include the effect of fabrication defects. Fig.15 shows the variability and the lack of trend in the measured load-slip curves for five bolt connections with Douglas-Fir main members.

2.1.10. Bolt versus Dowel

The use of drift pins or dowels in North America is not very common, mainly due to the lack of precise manufacturing facilities. As mentioned before, dowels, when used for tight fit connections with proper l/d ratio are very ductile and can be useful in earthquake resistant design. Bolts are commonly used, which have certain disadvantages. Bolted connections typically become loose after time due to wood shrinkage in the perpendicular to grain direction. Therefore they have to be tightened after a certain exposure time. Another feature, which can be both an advantage and a drawback, is the bolt's ability to constrain the wood fibers. The bolt's head and nut, when the joint is loaded laterally (bolts in shear) causes a clamping force, that

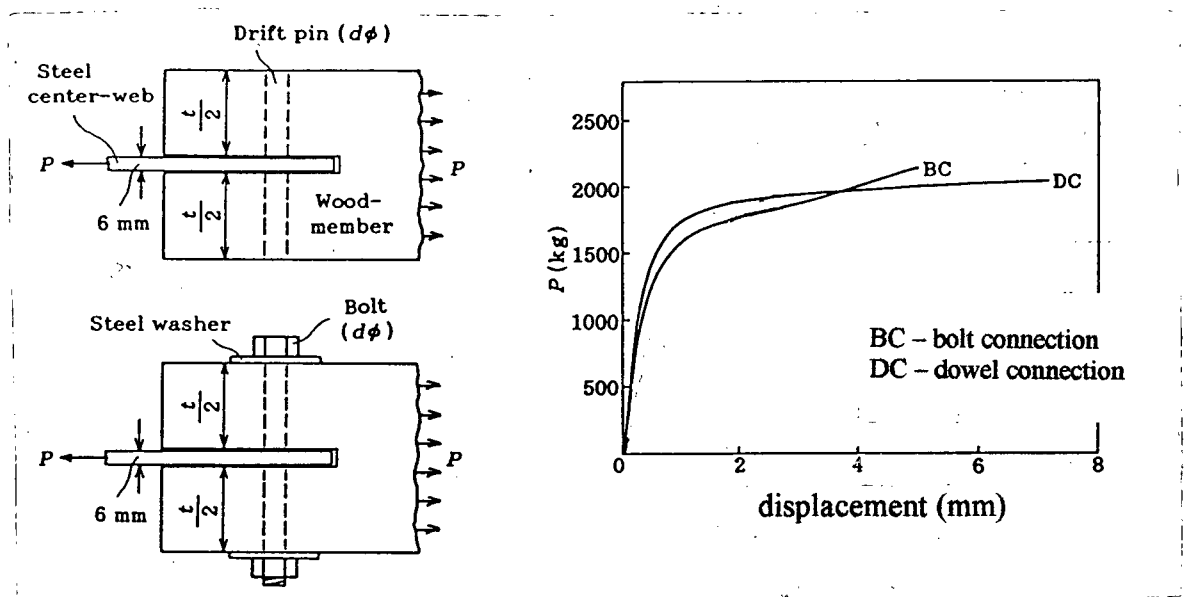


Figure 16. Typical load-slip curves of the tested dowel and bolted joints (Hirai, 1990)

reduces further expansion in the transverse direction and further bending deflection of the bolt.

This behaviour can also cause premature splitting and is a limiting factor for the ultimate displacement of the connection. On the other hand the advantage of a bolted joint compared to dowels is the higher ultimate strength. The bolts act similar to pre-stressed reinforcement in concrete and resist the transverse forces in the wood. Therefore, the ultimate strength of a bolted connection due to the end fixity of the wood tends to be higher than that of a dowel type connection. Both connection types are compared in Fig.16 (Hirai, 1990).

2.1.11. Possible Failure Modes and Their Causes

According to the aforementioned research, several factors have an influence on the behaviour of multiple bolted connections loaded in tension parallel to grain. The failure modes are dependent on one or more of the following:

- wood properties:
 - density
 - mechanical properties
 - moisture content
 - dimensions
- side plate properties
- bolt load-deformation relationship
- l/d ratio
- edge distance
- bolt spacing in the row
- number of rows
- row spacing
- precision of manufacturing

The reasons for brittle failure (*wood splitting, row shear, shear plug- uneven load distribution among the bolts, stress concentration*) can be cited as:

- end distance is too small
- low l/d ratio

- bolt spacing is too small
- precision of drilling is poor
- distance between rows is too small
- bolt yield stress is too high
- wet conditions

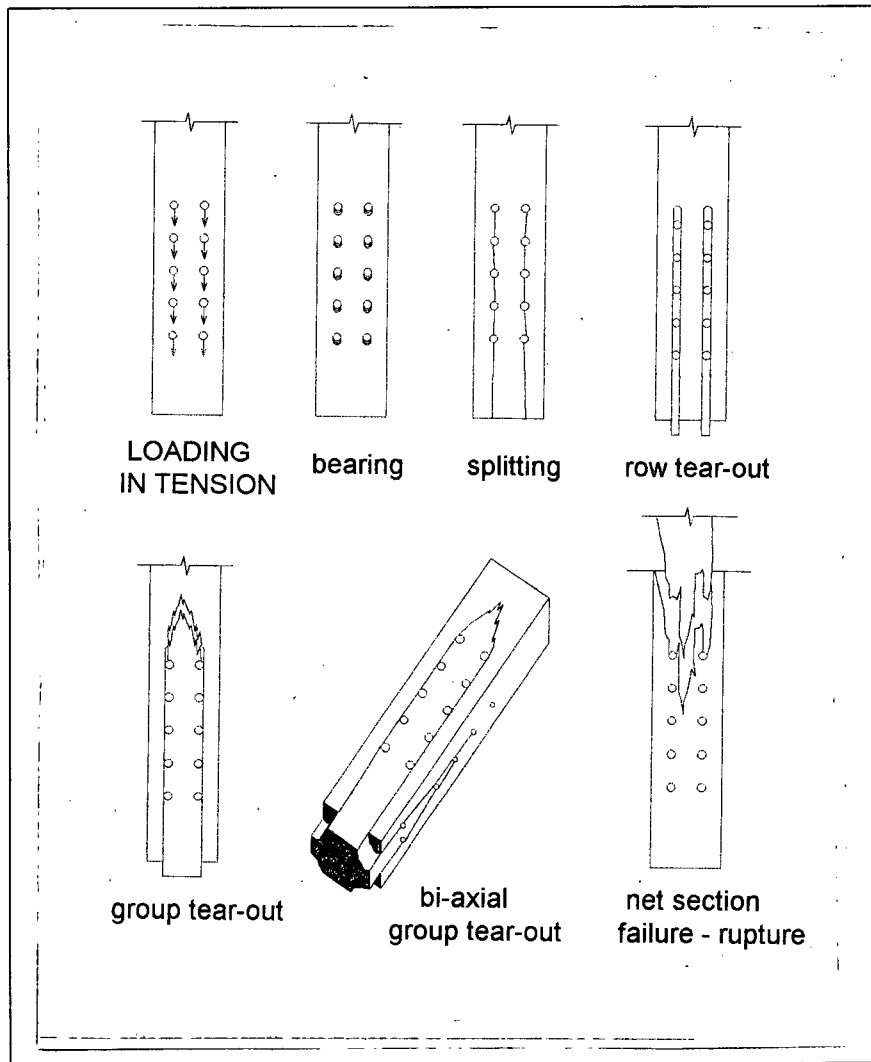


Figure 17. Possible failure modes of a bolted connection loaded in tension

Note: Also a combination of the four failure modes can occur.

Ductile Failure (*wood crushing*- bolts are yielding in bending, load is evenly distributed among the bolts)

- all rules, distances, properties, conditions are optimal

2.2. Seismic Aspects of Timber Structures and Bolted Connections

2.2.1. Performance of Low-Rise Timber Buildings in Recent Earthquakes

(Brown, D., 1991)

Engineers can learn the most from experience, and especially precious is the lesson learned from observing the failure of a structure. To illustrate the performance of buildings in earthquake the major failures that occurred in the San Fernando (1971) and the Loma Prieta (1989) Earthquakes are analyzed in the following section.

San Fernando Earthquake:

Widespread damage was observed during the earthquake. For example, a concrete hospital with moment resisting columns in the first storey and shear walls above was a total loss. Yet, wood frame structures in the near vicinity had little or no damage. The lesson there is that different building types respond differently to ground shaking and appropriate structural systems have to be designed accordingly.

In woodframe buildings there were several cases where let-in braces failed – either breaking in two, or the nails pulled out of framing or through the end of the board. Let-in bracing generally consists of 19x89mm or 19x140mm boards placed at 45-degree angle after studs and plates have been notched so that siding would fit flush against the framing. Sheathing is generally not provided. From experience, the let-in bracing should be limited in multistorey buildings to the lowest seismicity zones.

Another problem occurred in the low wood-frame walls (cripple walls), which are usually of much less height than a regular storey. They are used to elevate the ground floor above the foundation wall. The walls failed when not properly braced. It is recommended that the same bracing as used in the normal height wall should be used in the cripple walls.

Especially susceptible to earthquake forces were discontinuities in framing, e.g. split-level houses, which failed by splitting apart due to the ground shaking.

The major issue were large garage door openings, which were not sufficiently laterally supported. This is especially critical in cases where the garage projects out of the main building

with another living space above. The small columns could not take the big shear forces, causing the rotation of the side and back walls of the garage.

Loma Prieta Earthquake:

Houses built on sloped sites seemed to be particularly prone to damage, because of the slender columns of varying height supporting the houses. Plywood or other materials were used for sheathing those studs. Sometimes the sheathing or nailing was not adequate: spacing of the nails was bigger than the usual 150mm o.c. This caused a weak storey under the stiff superstructure, large deformations and sometimes collapse. Failures occurred in the longest poles or in the connection between the poles and the floor. A remedial solution could be to brace those columns with members resisting both tension and compression.

Structures in the San Francisco Marina district suffered major damage. They were built on filled ground that greatly amplified the ground accelerations. They also had almost no shear resistance in the lowest storey, which was often perforated with garage openings.

The author concluded that the Uniform Building Code provisions are adequate, provided they are understood by the consultant and the builder. Also, one has to follow the load path all the way down to the ground, provide sufficient load transfer through the diaphragms to shear walls and braces. Plan checking and inspection are key elements in achieving earthquake resistant structures.

2.2.2. The Seismic Behaviour of Timber Structures (B.Deam, A.King, 1994)

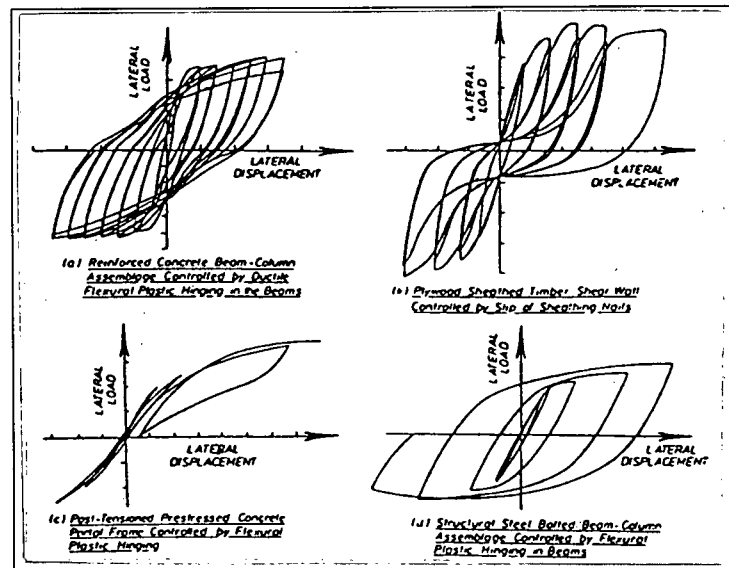
The design of timber structures is well covered in the codes to resist high wind loads, providing sufficient lateral stiffness and strength. From experience it is also known that well designed timber-framed structures typically survive earthquakes well. This is mainly because of their small mass, high damping and good distribution of the seismically induced forces. The forces are shared among a large number of elements with connections that can deform during an earthquake.

It is not economically feasible to design structures to withstand very large earthquakes without any damage. Most designers prefer a system to deform plastically in a controlled manner, while avoiding collapse (Dowrick, 1997).

direction of loading. From such test the load-deformation relationship “hysteresis loops” are obtained. The area bounded by the hysteresis loop is used as a measure of the energy absorbed by the tested structural element (Dowrick, 1977). Hysteresis loops produced by four different materials are reproduced in Fig.18 (Park, 1989). A fat loop represents significant energy dissipation, which is typical for reinforced concrete or steel elements. Prestressed concrete and timber, on the other hand, develop much narrower loops, which are pinched in the central region.

Figure 18. Structure load-displacement responses (Park, 1989)

- (a) Reinforced Concrete Beam-Column Assemblage
- (b) Plywood Sheathed Timber Wall
- (c) Post-Tensioned Prestressed Concrete Portal Frame
- (d) Structural Steel Bolted Beam-Column Assemblage



Historically it was thought that the pinched tiny loop of timber is undesirable, because of the small energy absorption (Park, 1989). This is clearly inconsistent with the low damage ratio experienced by timber buildings. The typical loop pinching of a wood connection is shown in Fig. 19 (Popovski, Prion 1998). The pinching is caused by the reduced stiffness and strength deterioration in dowel-type connections due to crushing of wood by the connector, creating a gap in the member. Then, in between the reverse cycles of the motion mostly the steel connectors carry the load in the joint.

The material and slenderness of the connectors used in timber joints greatly influences the ductility. Slender mild steel connectors, when evenly distributed in the wood member, appear to be ideal for the earthquake design. Nails for example, were found to be very favourable; they can resist many load reversals without significant strength reduction. Connections with dowels, when designed to be ductile, can also absorb a large amount of energy. Ductile behaviour can typically be obtained when slender and well distributed dowels or bolts are used in the joint

when designed to be ductile can also absorb a large amount of energy. Ductile behaviour can typically be obtained when slender and well distributed dowels or bolts are used in the joint design. Although the bolt material often has relatively high yield characteristics, choosing a smaller diameter and bigger end distance and bolt spacing can prevent brittle failures.

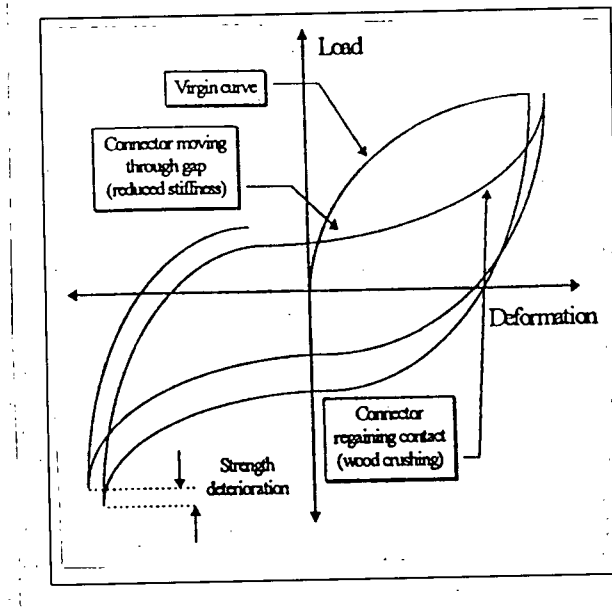


Figure 19. Typical hysteresis curve for wood connection (Popovski, Prion, 1998)

2.3. Truss Plate Reinforcement in Parallam (Hockey, 1999)

Hockey's thesis investigated the behaviour of truss plate reinforced bolted connections in parallel strand lumber (PSL). Because the truss plate reinforcement was one of several methods used for this project, the following quote might be appropriate:

"Static tension tests were performed on single bolt, group of four bolts and a ten bolt connection in 38x140 mm, 89x140 mm, and 133x191 specimens. Each test group had a set of 10 unreinforced connection specimens and 10 reinforced connection specimens."

"Connections in the 38x140 test specimens consisted of one 12.7mm (1/2") bolt and ten 12.7 mm bolts (two rows of 5 bolts). With the single bolt connections, average ultimate strength improvements of 36% and ductility improvements in excess of 278% were realized by reinforcing the connections. Reinforcement of the ten bolt connections did not effect the average ultimate strength, while ductility improved by 250%."

"Connections in the 89x140 test specimens consisted of one 15.9 mm (5/8") bolt and ten 15.9 mm bolts (two rows of 5 bolts). With the single bolt connections, average ultimate strength improvements of 12% and ductility improvements in excess of 104% were realized by

reinforcing the connections. For the ten bolt connections, reinforcement did not significantly change the average ultimate strength, while ductility improved by 5%.”

“Connections in the 133x191 test specimens consisted of one 22.2 mm bolt and four 22.2 mm bolts (two rows of 2 bolts). With the single bolt connections, average ultimate strength improvements of 3% and ductility improvements in excess of 143% were realized by reinforcing the connections. For the four bolt connections, the average ultimate strength was increased by 6%, while ductility improved by about 35%.”

The results for the truss plates show that there is no significant improvement both in strength and ductility when using the larger diameter bolts and bigger sizes of specimens. Therefore, for this study, wood specimens of 89x140mm cross section were combined with one size smaller bolts (12.7mm dia.), which is still practical and easy to install. Also, a comparison between the behaviour of truss plate reinforced and the threaded rod reinforced connections would be interesting to perform.

3. MATERIALS USED

3.1. Parallel Strand Lumber

Parallel strand lumber (PSL) is a high strength structural composite lumber product manufactured by gluing strands of wood together under heat and pressure. It is a proprietary product marketed under the trade name Parallam[®].

PSL can be made in long lengths but it is usually limited to 20m (66 ft.) by transportation constraints.

Manufactured at a moisture content of 11 percent, which is approximately the equilibrium moisture content of wood in most service conditions, PSL is less prone to shrinking, warping, cupping, bowing or splitting.

It is manufactured in Canada from Douglas fir and in the United States from Southern Pine from veneer strands from which most growth imperfections have been removed. This results in a product with consistent properties and high load carrying capacity. As smaller plantation and second growth timber finds its way into the market place, PSL provides a means of ensuring the availability of large dimension and high quality wood products.

MANUFACTURE OF PSL

The process of PSL manufacture as shown in Fig.20 is similar to the manufacture of plywood. Logs are peeled on a lathe to create veneer sheets, which are then oven dried. The veneer sheets are clipped into long narrow strands of up to 2.4m (8') in length and about 13mm (1/2") in width. Small pieces are screened out before the strands are coated with an exterior-type adhesive (phenol-formaldehyde). The strands are then laid-up in a random distribution oriented to the length of the member, and formed into a continuous billet, which is fed into a belt press. Under pressure and microwave generated heat, the glue is cured to produce a finished continuous billet 280 x 406mm (11" x 16") in cross-section. The billet is cross cut to desired lengths, rip sawn to produce rough dimensions or custom sizes and sanded down to finished dimensions. Larger dimensions are produced by edge gluing billets together, where techniques common to those used for the manufacture of glulam are performed. Fig. 21 shows a Parallam[®] cross-section with the orientation of the veneer strips.

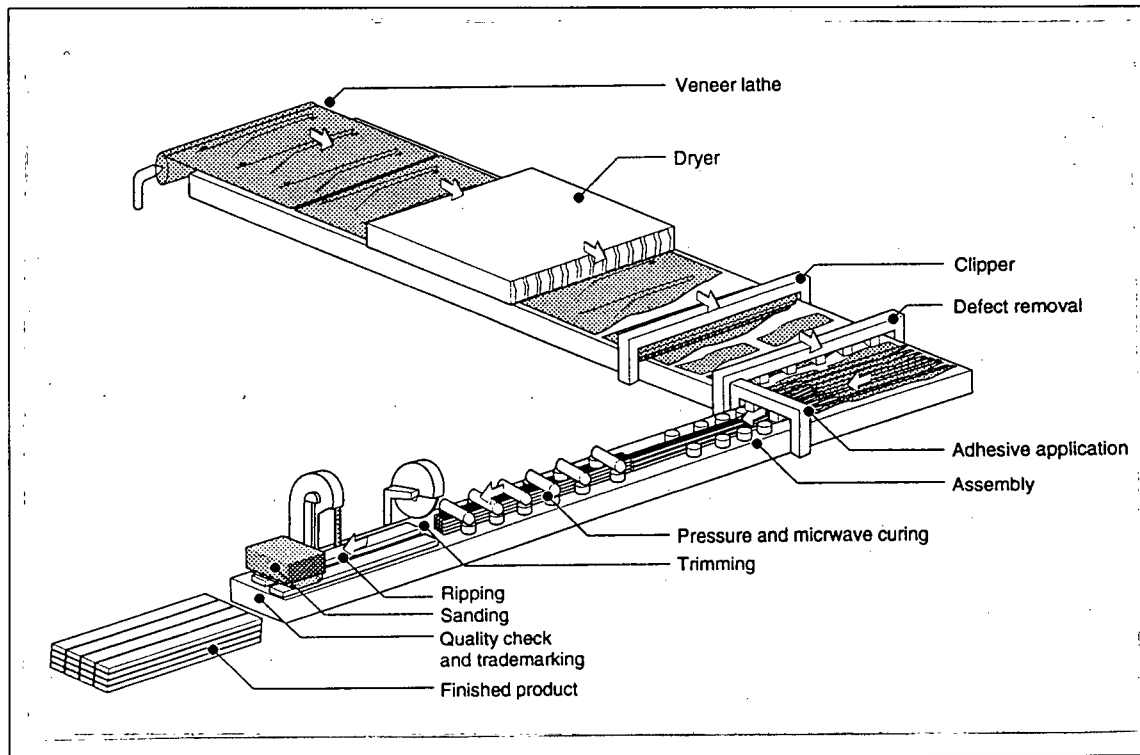


Figure 20. Fabrication Procedure of Parallam® (Introduction to Wood Design, 1996)

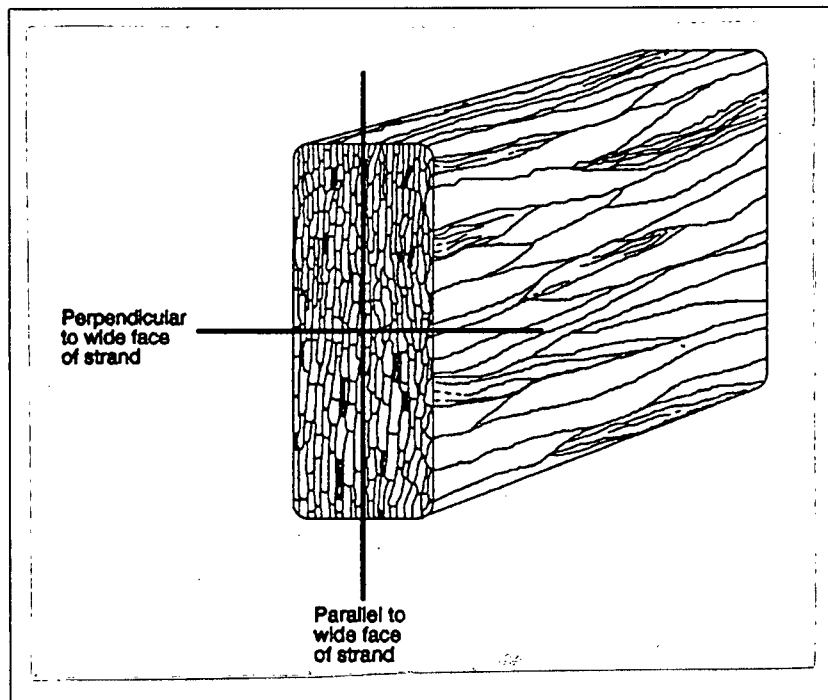


Figure 21. Parallam® cross section with the orientation of the veneer strips

(Hockey, 1999)

3.2. Glue Laminated Lumber

Glulam (glued-laminated timber) is a structural timber product manufactured by gluing together individual pieces of dimension lumber under controlled conditions. In the manufacture of glulam, the wood pieces are jointed and arranged in horizontal layers or laminations.

Laminating is an effective way of using high strength lumber of limited dimension to manufacture large structural members in many shapes and sizes. Glulam is used for columns and beams and frequently for curved members, which are to be loaded in combined bending and compression. The lumber used for manufacture is a special grade (lamstock) which is purchased directly from lumber mills. It is dried to maximum moisture content of 15 % and is planed to a closer tolerance than that required for dimension lumber.

Canadian glulam is manufactured in three species combinations: Douglas Fir-Larch, Hem-Fir and Spruce-Pine.

MANUFACTURE OF GLULAM

The special grade of lumber used for glulam, lamstock, is received and stored at the laminating plant under controlled conditions. Prior to glulam fabrication, all lumber is visually graded for strength properties and mechanically evaluated to determine the modulus of elasticity (E). These two assessments of strength and stiffness are used to determine where a given piece will be situated in a beam or a column. Once graded, the individual pieces of lamstock are finger jointed into full-length laminations of constant grade and each endjoint is proof tested.

The laminated lengths are then arranged according to the required grade combination for the product being manufactured. Each lamination moves through a glue applicator and gets laid up into the desired configuration. After positioning into a curved or straight shape the laminations are clamped and stored at a controlled temperature until the glue is fully cured.

After curing the member is moved to a finishing area, where it is patched, surface planed, and end trimmed. Additional drilling and notching for connections, sanding, staining or varnishing can be done at this time. As a final step, glulam members are wrapped in readiness for shipping (Fig.22).

Fig. 23 shows a typical glulam timber beam with finger-jointed lamination. In Canada, glulam members are manufactured to the standard CSA 0122 Structural Glued-Laminated

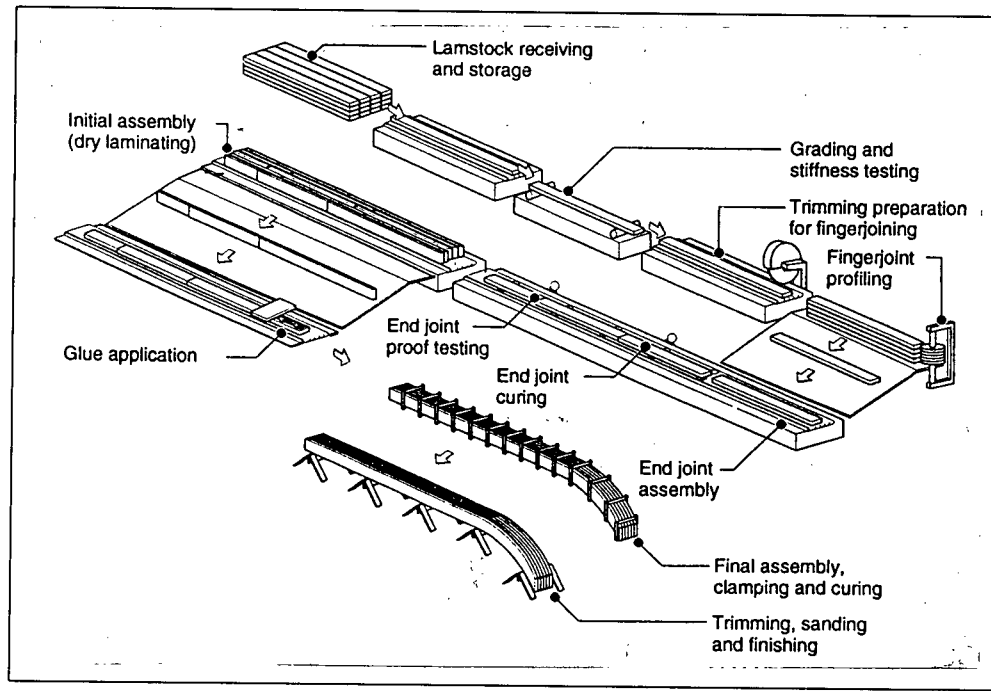


Figure 22. Fabrication Procedure of Glulam (Introduction to Wood Design, 1996)

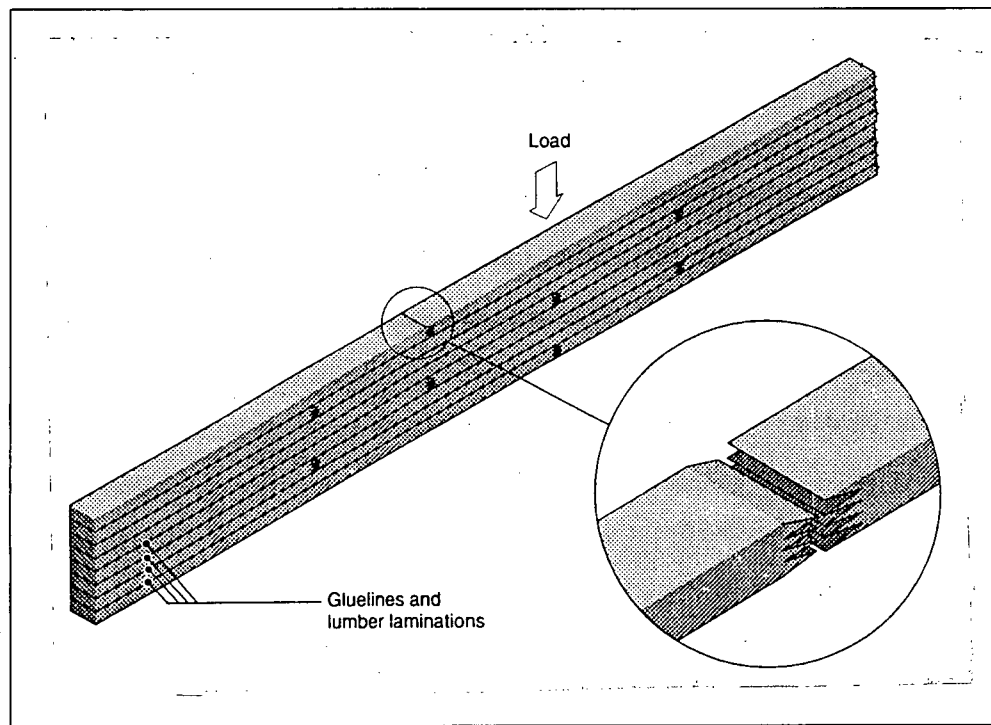


Figure 23. Typical Glulam Beam (Introduction to Wood Design, 1996)

Timber, and the manufacturers of glulam must be certified in accordance with CSA 0177 Qualification Code for Manufacturers of Structural Glued-Laminated Timber.

3.3. Connectors

3.3.1. Bolts

Bolts were chosen as the primary connectors according to CAN/CSA 086.1-94. Bolts with three diameters (3/8"-9.5mm, 1/2"-12.7mm and 5/8"-15.9mm) were used, all with hexagonal head.

Bolts of less than 9.5 mm diameter were not used in the current study since reinforcement techniques were believed to be the most effective with larger diameter bolts.

To achieve acceptable ductility levels in the connection it was decided to use medium carbon grade 5 bolts. To observe the effect of bolt diameter on the connection performance, three bolt sizes were chosen, namely, 3/8", 1/2" and 5/8". Technical data for these bolts are shown in Figure 24.

STEEL

FOR EXTRA STRENGTH

SAE GRADE 5

Material Spec. ASTM A 449

Length shown is under head to end in inches

C1035-1041

MEDIUM CARBON STEEL

Made to the dimensional requirements of I.F.I. Standard Hex. Cap Screws (B18.2.1, 1965)


For critical applications requiring greater fastener strength.

MINIMUM TENSILE STRENGTH (PSI)

Up to 1" dia. inclusive 120,000 PSI

Over 1" to 1-1/2" inclusive 105,000 PSI

FINISHED HEXAGON BOLTS



1970 Draft Revision of ANSI B18.2.1, 1965

BRIGHT ZINC CHROMATE PLATED

QUENCHED AND TEMPERED

MINIMUM THREAD LENGTH (Standard)

Up to 6" long: (2D + 1/4) Twice diameter plus 1/4 inch.

Over 6" long: (2D + 1/2) Twice diameter plus 1/2 inch.

NOTE: See listing on page B145 for Grade 5 Cap Screws with full thread length.

COARSE THREAD (U.N.C.) (U.S.S.)

UNIFIED STANDARD CLASS 2A FIT

DIA.	1/4"	5/16"	3/8"	7/16"	1/2"	9/16"	5/8"	3/4"
THD.	20	18	16	14	13	12	11	10
LENGTH▼	ORDER BY SPAE-NAUR NUMBERS LISTED BELOW							
4-1/2	326-312	326-318	HC-54	HC-68	HC-84	HC-98	HC-110	HC-245
5	326-329	HC-38	HC-55	HC-69	HC-85	HC-99	HC-110A	HC-118
6	326-326	HC-241	HC-242	HC-70	• HC-86	HC-100	• HC-111	HC-119

Figure 24. Technical data of the bolts

3.3.2. Flexural Yield Stress of the Bolts – Tests in Bending

Three groups of 5 bolts (15.9, 12.7, 9.5 mm) and one group of five 12.7mm diameter lag-screws were tested as simply supported beams in static bending. The tests were conducted on a SATEC universal testing machine in the Materials Laboratory of UBC. The bolts and screws were loaded by a concentrated ramp force in the mid-span. The average rate of loading (non-

hydraulic machine) was 2.0mm/min. The test was displacement-controlled. Every connector had the same 90 mm span. Supports were created by two 25.4 mm diameter steel cylinders welded onto a steel plate (Fig.25)

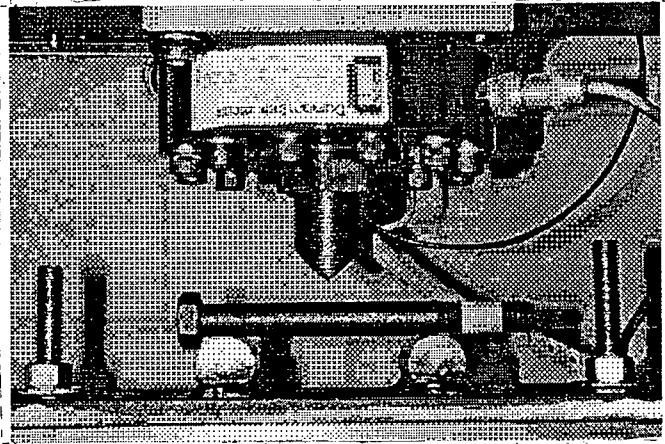


Figure 25. Test setup for bolts tested in bending

Connector	Diameter d_{avg} (d_{nom}) [mm]	Plastic Mod Z [mm ³]	Load 1st y. F _y [N]	Load (5%) F ₅ [N]	1st Yield M. M _{y1} [Nmm]	Pl.Moment M _{pl} [Nmm]	1st Yield S $f_{y1}=M_{y1}/z$ MPa	Pl.Stress $f_{pl}=M_{pl}/z$ MPa
Lag Screw	9.50 (12.7)	142.9	3000	4100	67500	92250	472	646
Bolt	15.71 (15.9)	646.2	22000	29400	495000	661500	766	1024
Bolt	12.53 (12.7)	327.9	11000	14200	247500	319500	755	974
Bolt	9.40 (9.5)	138.4	4500	5900	101250	132750	731	959

Table 1. Yield stresses of the bolts tested in bending

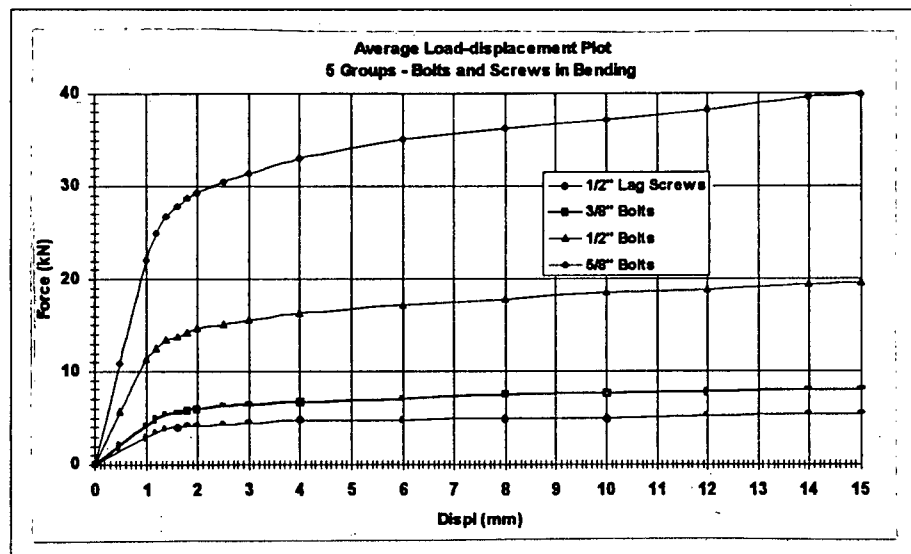


Figure 26. Load –Displacement curves of the tested bolts and the lag screw

The load-displacement curves of all the connectors were very consistent with a mean coefficient of variation of 0.02 (Tab.1). All the curves had a linear elastic portion followed by gradual softening and a constant strain-hardening modulus. The average load-displacement curves for each group of connectors are displayed in Fig.26.

3.4. REINFORCEMENT - SECONDARY CONNECTORS

3.4.1. Truss plates

The truss plates used in this study were 0.8 mm thick with dimensions 92x148mm. They were made of galvanized steel plates punched so the teeth were shaped like prongs with the tip of the teeth flush with the underside of the plate.

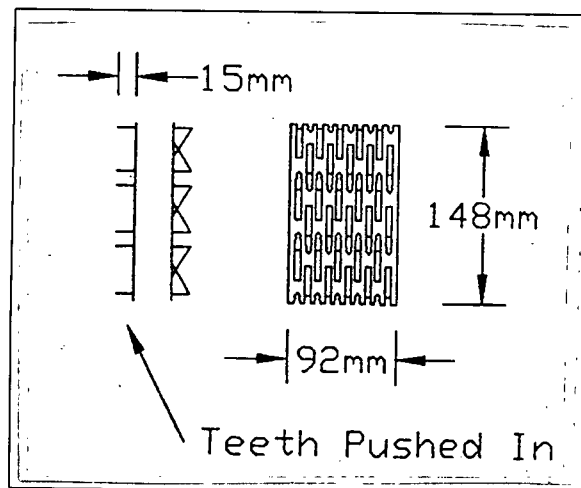



Figure 27. Truss Plate
Dimensions

These truss plates are specially designed for do-it-yourself craftsmen who do not have access to a press and need to hammer in the teeth one by one (Fig.27). They were manufactured by LumberLock, a division of Mitek Canada, and are not an engineered type. They are no longer manufactured but are still obtainable in most lumber yards. These truss plates were chosen for consistency, and be able to make direct comparison with the results obtained by Hockey (1999).

Nowadays, Mitek makes truss plates that are more suitable for assembly of trusses with the teeth longer and not bent. The straight teeth are much stiffer than the prong type, therefore there is less chance that the teeth will bend before they penetrate the wood fiber.

3.4.2. Coarse Threaded Rods - Lag Screws

The threaded part of regular 10" long galvanized lag screws with 1/2" (12.5 mm) shank diameter were used as transverse reinforcement of the connections. The threaded part of the screw was 5 1/2" long and the smooth part (no thread) was 4" (100mm) long. The thread was of a coarse type with 4mm-thread pitch. The thread depth was 1.5 mm. The shank diameter in the threaded part was 3/8" (9.5 mm). Figure 28 shows the technical data of the lag screws used in the tests.

Identification Grade Mark	Specification	Fastener Description	Material	Nominal Size Range (in.)	Mechanical Properties		
					Proof Load (psi)	Yield Strength Min (psi)	Tensile Strength Min (psi)
 No Grade Mark	SAE J429 Grade 1	Bolts, Screws, Studs	Low or Medium Carbon Steel	1/4 thru 1-1/2	33,000	36,000	60,000
	ASTM A307 Grades A&B		Low Carbon Steel	1/4 thru 4			
	SAE J429 Grade 2		Low or Medium Carbon Steel	1/4 thru 3/4, Over 3/4 to 1-1/2	55,000 33,000	57,000 36,000	74,000 60,000

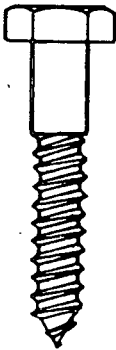
STEEL LAG SCREWS HEXAGON HEAD  HOT GALVANIZED Finish For maximum protection	1"
	1-1/4"
	1-1/2"
	1-3/4"
	2"
	2-1/2"
	3"
	3-1/2"
	4"
	4-1/2"
	5"
	5-1/2"
	6"
	7"
	8"
	9"
	10"
	12"

Figure 28. Technical data of lag screw

3.4.3. Fine Threaded Rods - Ready Rods


Another type of threaded rod used for the transverse reinforcement was a fine-thread steel rod, so called "ready rod". Ready rod is commonly available and comes in 24" (254mm) to 144" (3658mm) lengths. This means it has to be cut to the desired length. The one used for the experiment was of 3/8" (9.5mm) shank and was initially cut to approximately 7" (178mm) length to allow space for a power wrench. After installation into the specimen it was cut to the width of the specimen - 5 1/2" (140mm).

The thread of the ready rod with thread pitch of approximately 1.8mm and depth 1mm (1/2"-13) was finer than that of the lag screw. The rod was not galvanized. Figure 29 shows a catalogue entry for this type of threaded rod.

STEEL

THREADED RODS

Right-hand Threads
THREADED FULL LENGTH



"INCH" SIZES

Grade: C1010 (or better)
ASTM spec A-307
Minimum tensile strength
50,000 to 60,000 psi

The versatile do-it-yourself rod for making U-bolts, eye-bolts, hangers, ladder rungs, and many types of special items. Cold-drawn steel bends easily without heating. Just cut to desired length and use.


Finishes: Plain and ZINC PLATED

THREAD SIZE	ORDER BY SPAE-NAUR NUMBERS LISTED BELOW									
	Plain 24" Lgth.	Zinc Pltd. 24" Lgth.	Plain 36" Lgth.	Zinc Pltd. 36" Lgth.	Plain 72" Lgth.	Zinc Pltd. 72" Lgth.	Plain 120" Lgth.	Zinc Pltd. 120" Lgth.	Plain 144" Lgth.	Zinc Pltd. 144" Lgth.
•1/2"-13			TR-8	TR-8ZP	866-017	866-017ZP	866-065	866-065ZP	866-081	866-081ZP

Figure 29. Technical data of ready rod

3.4.4. Nailed Steel Plates

Figure 30. Technical data of spiral nails



NAILS - SPIRAL STD. BRIGHT

SPIRAL STANDARD NAIL

Tree Island Industries

For general construction use where ease of driving and greater holding power are required. Effective against shock loads and vibrations, holding power increases from 50% to 200%.

Finish - Bright.

50 lb Carton.

Length	Gauge	
1-1/2"	13-1/2	D361-0029..... 41
2"	12-1/2	B361-0052..... 42

Galvanized steel plates were used to reinforce the specimen on its surface. The 18 gauge plates were nailed with a pneumatic nailer using the spiral nails 2" (51mm) long and of 12-1/2 gauge. A sample of spiral nail is displayed in Figure 30.

Another kind of nail used was the finishing nail that hammered in was the 26 gauge galvanized plate manually. The nails were 1/16" (1.6mm) thick and 1 1/2" (38.1mm) long with an

oval-shape. Because the nails were significantly smaller, the code allowed tighter (20mm) spacing between them and thus many nails could be used (134 pieces per 5/8" bolt connection).

3.4.5. Epoxy Glued Steel Plates

G2 epoxy glue made by Formulators of Canada Ltd. was used as the glue for connecting the galvanized steel plates to the PSL specimens. Its manufacturers represent this glue as being formulated for good bonding to oily and acidic woods. They also specify that it is a permanent waterproof bond for most woods and metals, all rocks and gems and concrete and non-waxy plastics. It has two components – resin and hardener.

In the experiment the epoxy had less brittle behaviour when mixed in a ratio of 1:1. The curing time is usually 24h at 20°C and 48h at 10°C(50°F). The specimen was left to cure for a period of 27 hours because of the laboratory temperature that was 18°C at that time.

4. SPECIMENS

4.2. List of Specimens - Chronology

4.1.1. List of Specimens

Type			Symbol	Repl.	Bolt diam.	Bolts	Reinf	Configuration Specification	I/d
[Nr.]	[mater.]	[test]	[short]	[Nr.]	[in] ([mm])	[Nr.]	[Y/N]	[reinforcement description]	[]
1	PSL	Static monot.	TU	3	3/8" (9.5)	10	No	unreinforced	9.3
2	PSL	Static monot.	HU	2	1/2" (12.7)	10	No	unreinforced	7
3	PSL	Static monot.	FU	10	5/8" (15.9)	10	No	unreinforced	5.6
4	PSL	Static monot.	HRT	2	1/2" (12.7)	10	Yes	truss plates	7
5	PSL	Static monot.	FRT	9	5/8" (15.9)	10	Yes	truss plates	5.6
6	PSL	Static monot.	HRTW	1	1/2" (12.7)	10	Yes	stiff plate welded on a truss plate	7
7	PSL	Static monot.	FRTT	2	5/8" (15.9)	10	Yes	every 2nd truss plate 90deg rot.	5.6
8	PSL	Static monot.	FRR	2	5/8" (15.9)	10	Yes	lag screws - two end screws	5.6
9	PSL	Static monot.	HRR	2	1/2" (12.7)	10	Yes	lag screws - two end screws	7
10	PSL	Static monot.	TRR	3	3/8" (9.5)	10	Yes	lag screws - two end screws	9.3
11	PSL	Static monot.	HRRSH	2	1/2" (12.7)	10	Yes	lag screws at the bolt location	7
12	PSL	Static monot.	HRRS	2	1/2" (12.7)	10	Yes	lag screws - single end screw	7
13	PSL	Static monot.	FRRS	2	5/8" (15.9)	10	Yes	lag screws - single end screw	5.6
14	PSL	Static monot.	FRRF	2	5/8" (15.9)	10	Yes	ready rods - two end rods	5.6
15	PSL	Static monot.	FRE	2	5/8" (15.9)	6	Yes	epoxy glued 1.2 mm galv. plates	5.6
16	PSL	Static monot.	FRN -1	1	5/8" (15.9)	10	Yes	(spiral) nailed 1.2mm galv plates	5.6
17	PSL	Static monot.	FRN -2	1	5/8" (15.9)	10	Yes	(spiral) nailed 1.2mm galv plates	5.6
18	PSL	Static monot.	HRN18	1	1/2" (12.7)	10	Yes	(finish.) nailed 1.2mm galv. plate	7
19	PSL	Static monot.	FRN18	1	5/8" (15.9)	10	Yes	(finish.) nailed 1.2mm galv. plate	5.6
20	PSL	Static monot.	HRN26	1	1/2" (12.7)	10	Yes	(finish.) nailed 0.6mm galv. plate	7
21	PSL	Static monot.	FRN26	1	5/8" (15.9)	10	Yes	(finish.) nailed 0.6mm galv. plate	5.6
22	PSL	Static monot.	HRER	2	1/2" (12.7)	10	Yes	epoxy glued-in lag screw	7
23	PSL	Static monot.	HRERe	2	1/2" (12.7)	10	Yes	epoxy glued-in rebar M10	7
24	Glulam	Static monot.	GTU	3	3/8" (9.5)	10	No	unreinforced	9.3
25	Glulam	Static monot.	GHU	3	1/2" (12.7)	10	No	unreinforced	7
26	Glulam	Static monot.	GTRR	3	3/8" (9.5)	10	Yes	lag screws - two end screws	9.3
27	Glulam	Static monot.	GHRR	3	1/2" (12.7)	10	Yes	lag screws - two end screws	7
28	Glulam	Static monot.	GHRRF	3	1/2" (12.7)	10	Yes	ready rods - two end rods	7
29	PSL	Reverse cyclic	TU-C	1	3/8" (9.5)	10	No	unreinforced	9.3
30	PSL	Reverse cyclic	HU-C	3	1/2" (12.7)	10	No	unreinforced	7
31	PSL	Reverse cyclic	FU-C	3	5/8" (15.9)	10	No	unreinforced	5.6
32	PSL	Reverse cyclic	TRR-C	1	3/8" (9.5)	10	Yes	lag screws - two end screws	9.3
33	Glulam	Reverse cyclic	GTRR-C	1	3/8" (9.5)	10	Yes	lag screws - two end screws	9.3
34	PSL	Reverse cyclic	HRR-C	3	1/2" (12.7)	10	Yes	lag screws - two end screws	7
35	PSL	Reverse cyclic	FRR-C	3	5/8" (15.9)	10	Yes	lag screws - two end screws	5.6
36	PSL	Reverse cyclic	HRT-C	3	1/2" (12.7)	10	Yes	truss plates	7
37	PSL	Reverse cyclic	FRT-C	3	5/8" (15.9)	10	Yes	truss plates	5.6

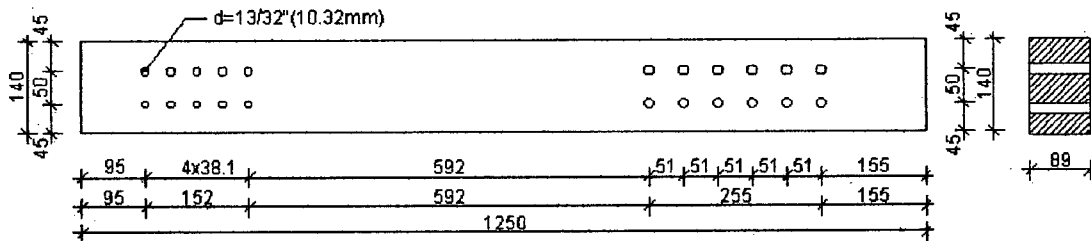
Explanation of Specimen Symbols:

T	3/8" Bolt	E	Epoxy Glued	SH	Offset (Shifted) Rod (away from the Bolt)
H	1/2" Bolt	F	Fine Threaded (Ready) Rod	TT	Truss Plate Transversely Rotated
F	5/8" Bolt	N	Nailed Plate	W	On-Truss Plate Welded Steel Plate
U	Unreinforced	T	Truss Plate	Re	Reinforcing Bar No.10 (11.3mm)
R	Reinforced	R(F)	Lag Screw (Ready Rod)	18	18 gauge (1.2 mm) galvanized steel plate
G	Glulam	S	Single Rod at the End	26	26 gauge (0.6mm) galvanized steel plate

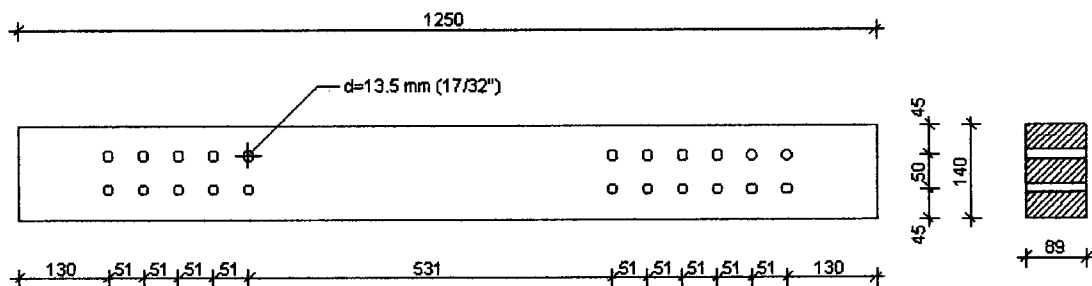
Table 2. The list of tested specimen configurations

4.1.2. Specimen configuration layouts

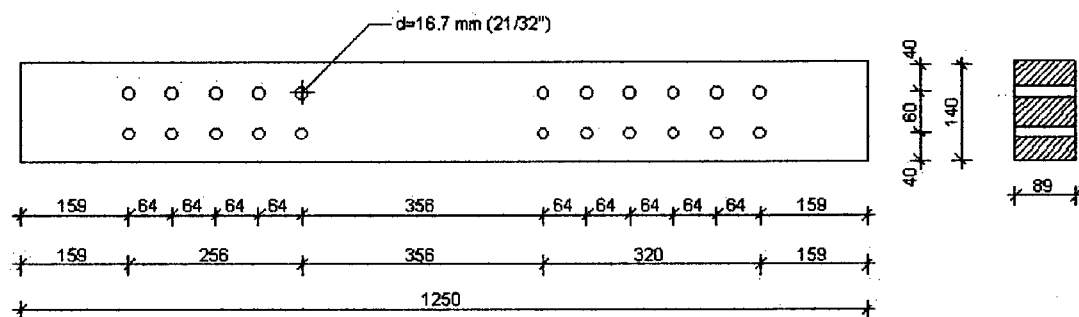
TU, GTU, TU-C



HU, GHU, HU-C



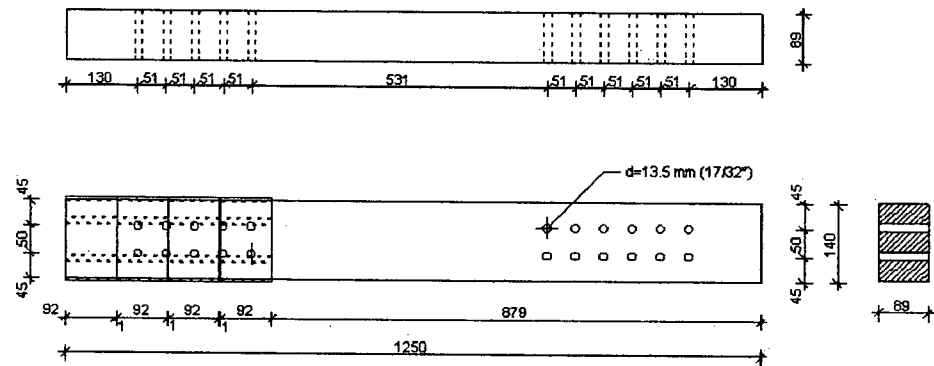
FU, FU-C



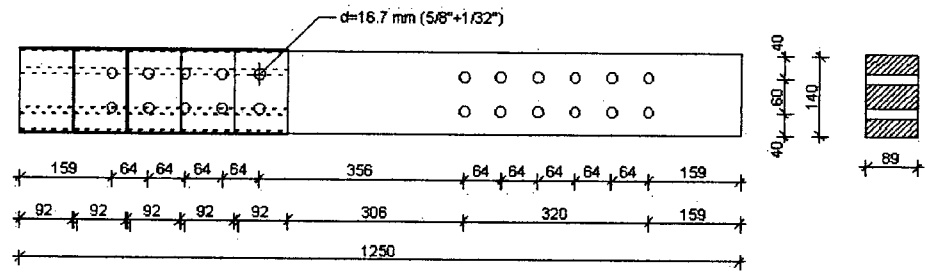
(All measurements in mm)

Figure 31. Unreinforced specimen layouts

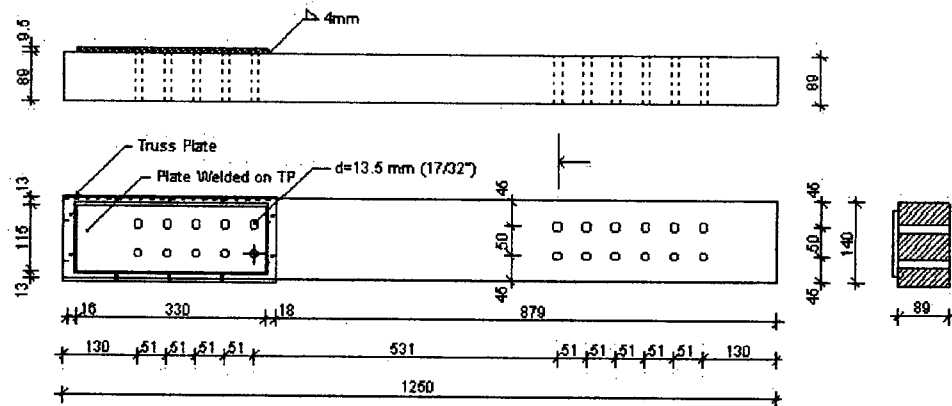
HRT, HRT-C



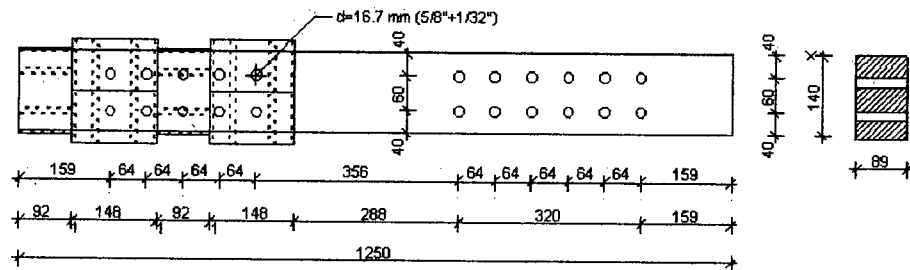
FRT, FRT-C



HRTW



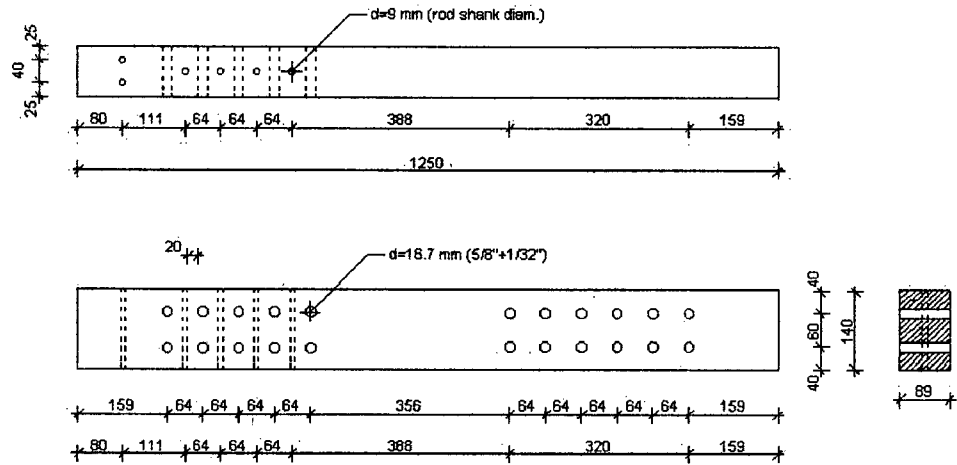
FRTT



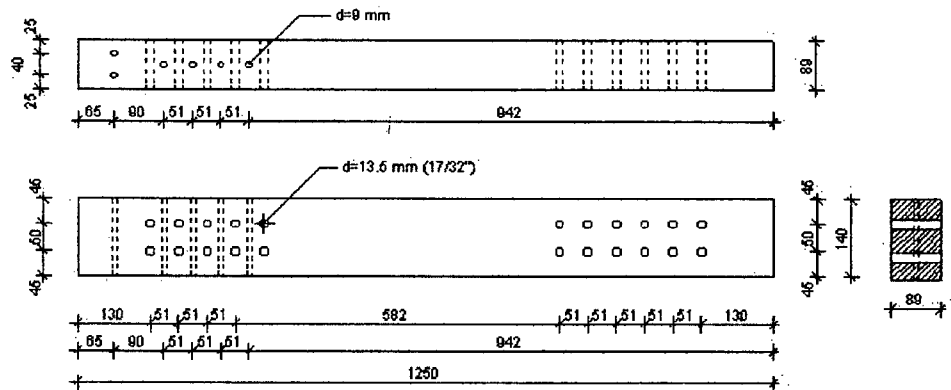
(All measurements in mm)

Figure 32. Truss plate reinforced specimen layouts

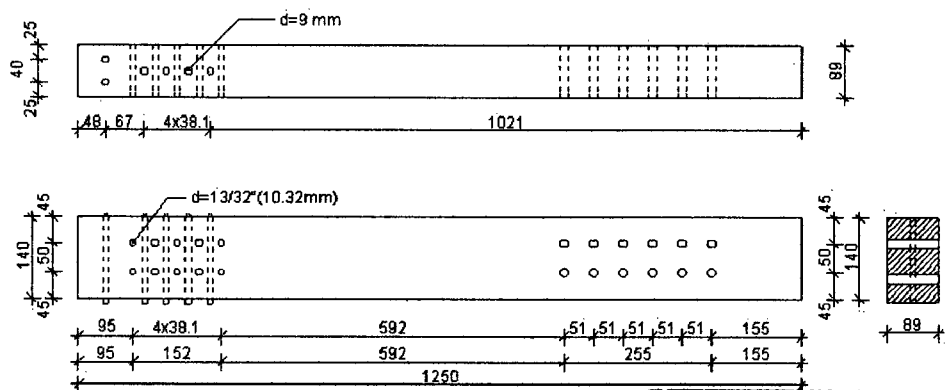
FRR, FRRF, FRR-C



HRR, GHRR, GHRRF, HRER, HRERe, HRR-C



TRR, GTRR, TRR-C, GTRR-C



(All measurements in mm)

Figure 33. Rod reinforced specimen layouts (two end rods)

HRRSH

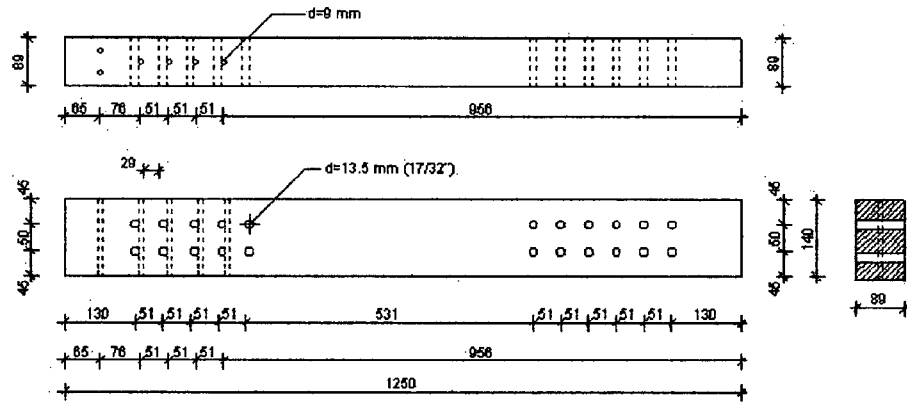
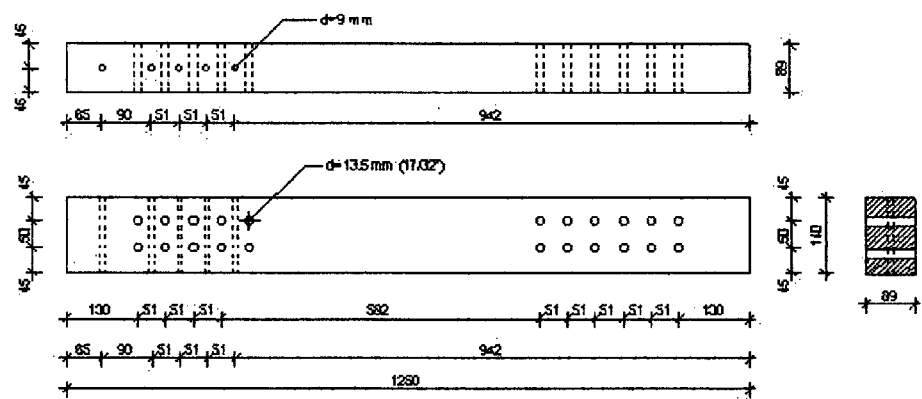
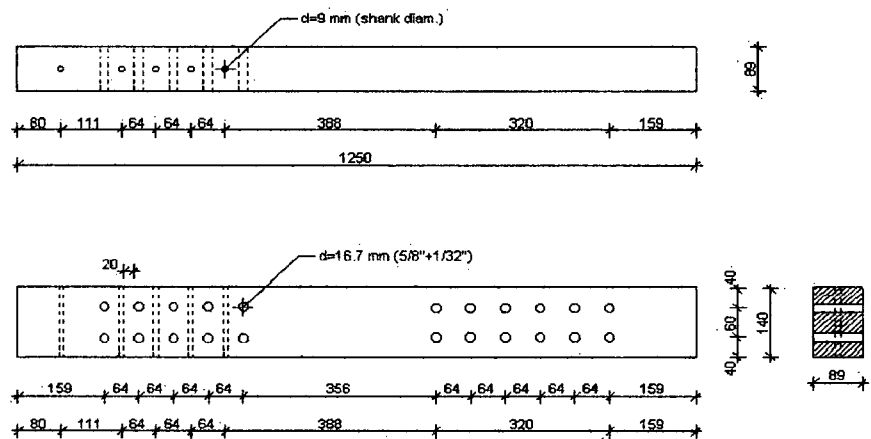


Figure 34. Lag screw reinforced specimen layouts (rods at the bolt positions)

HRRS



FRRS



(All measurements in mm)

Figure 35. Lag screw reinforced specimen layouts (single end rods)

FRE

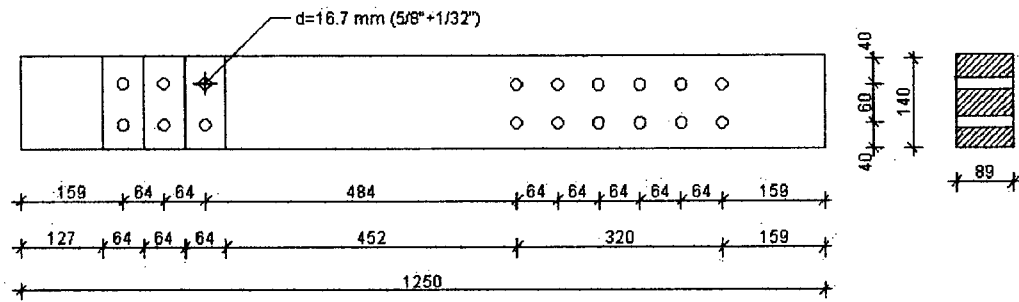
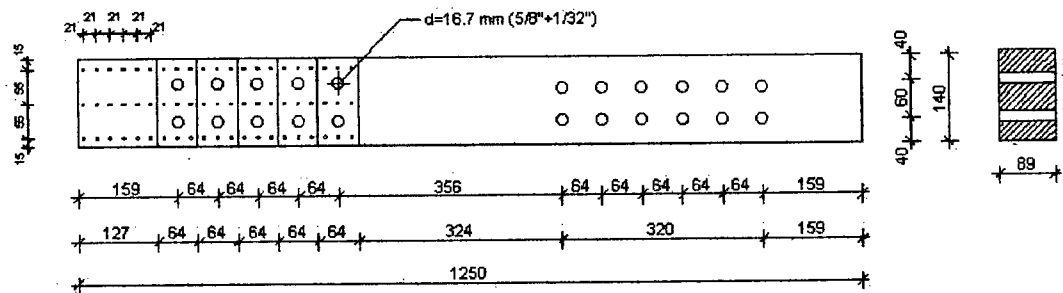
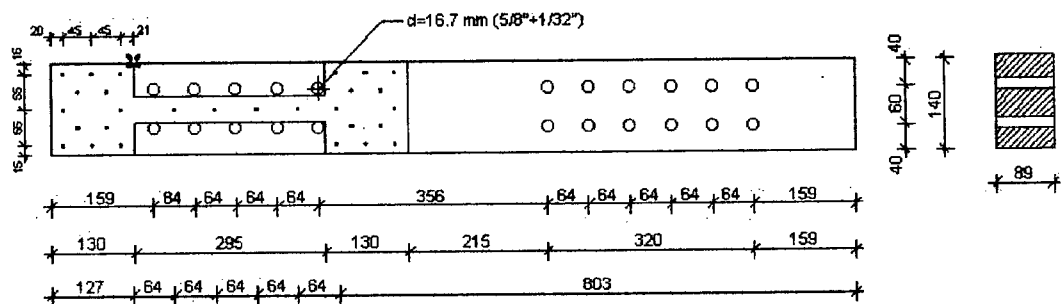


Figure 36. Glued-on plate reinforced specimen layouts (1.2mm plate, epoxy)

FRN-type I



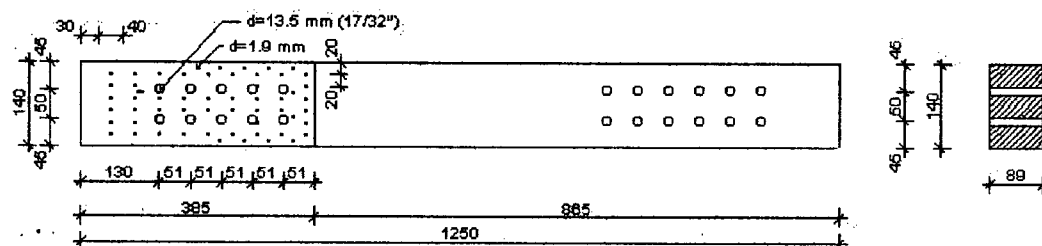
FRN-type II



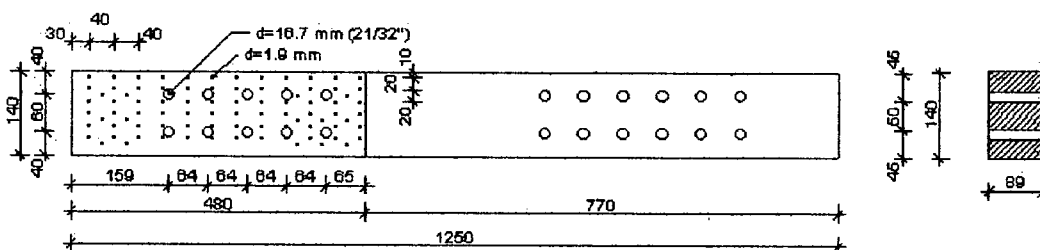
(All measurements in mm)

Figure 37. Nailed-on plate reinforced specimen layouts (1.2mm plate, spiral nails)

HRN 18, HRN 26



FRN 18, FRN 26



(All measurements in mm)

Figure 38. Nailed-on plate reinforced specimen layouts (1.2, 0.6mm plate, finishing nails)

4.1.3. Chronology of Choosing the Specimen Types

The list of symbols shown in Table 2 was evolving through time and the types of specimens and the number of replicas were changing based on the obtained test results. The initial idea was to study only reinforcement techniques for 1/2" and 5/8" bolted connections, which represents commonly used joints for 140x89mm PSL cross sections. These initial tests were performed in the period from February to July 1999.

It was suspected that the stiff truss plate (steel plate welded on truss plates), epoxy glued-in rods and epoxy glued-on plates would be less ductile. Therefore, only one replica of this type was tested.

The 5/8" unreinforced and truss plate reinforced specimens (10 of each) were tested by Hockey (1999) and the intent was to compare them to the rest of present test results. Therefore they were included in the list of specimens.

For multiple (10) bolt specimens, the effect of truss plate reinforcement largely diminished (Hockey, 1999). That is why the idea of rotated truss plates was developed and two replicas of FRTT were made.

In the case of threaded rods, different configurations (location and number of rods) were tested. Two replicas were made for HRRS, HRRSH and FRRS. Their configurations are briefly described in the list of specimens (Tab 2).

It was a very time-consuming process to manufacture the nailed (spiral nails) plate specimens, thus only one replica was made. Also, it was not certain whether the results would be satisfactory or not. When all the nailed specimens failed in a brittle manner, this method was abandoned. In December 1999 these results initiated the manufacture of another set of nailed plate specimens. Due to previous lack of ductility, thinner plates (gauge 26) and smaller (finishing) nails were used with $\frac{1}{2}$ " and $\frac{5}{8}$ " diameter bolts.

In January 2000, to investigate connection behaviour in other large size composite materials, specimens made of Glulam (Douglas Fir) were tested. These results showed minor differences but were not convincing.

Therefore, new $\frac{3}{8}$ " bolt equivalents of each specimen materials with traditional reinforcement (unreinforced, truss plate and lag screw reinforced) were tested (3 of each).

When all the aforementioned configurations were tested, only the ones with the most ductile results were chosen for reverse cyclic testing. For the sake of comparison, cyclic tests were also performed on the unreinforced specimens. One replica of each $\frac{3}{8}$ " diameter bolt specimens and three of each $\frac{1}{2}$ " and $\frac{5}{8}$ " bolt specimens were tested in February 2000.

4.2. Unreinforced Specimen Manufacturing

The PSL 1250-mm long specimens were cut out of a 4m long 89x140 ($3\frac{1}{2}$ " x $5\frac{1}{2}$ ") mm section PSL piece. For each of the three bolt diameters, two side plates were drilled with the appropriately sized holes. The holes were overdrilled by 0.8 mm ($\frac{1}{32}$ ") in diameter to facilitate insertion of the bolts during the assembly of the connection. Drilling bits of two diameters were used:

$\frac{1}{2}$ " (12.7 mm) bolt - $\frac{17}{32}$ " (13.5 mm) hole

$\frac{5}{8}$ " (15.9 mm) bolt - $\frac{21}{32}$ " (16.7 mm) hole

The side plates were used as templates for drilling the transverse holes in the specimen. The same bit size was used for drilling the specimen and the side plates. The same procedure was kept for the glulam specimens. The only difference was in the size of the specimen – 89x130 (3 ½"x 5 1/8"). The layouts of unreinforced specimens are shown in Fig 31.

4.3. Reinforced Specimen Manufacturing

4.3.1. Truss Plates

After the specimens were manufactured (procedure in Sec.4.2), the truss plates were applied on one side with the exact location assured. They were pressed evenly on the specimen surface by a hydraulic press. The same procedure was followed for the opposite side of the specimen. The truss plates were installed in accordance with CSA 086.1-94 section 10.8.

Once again, the testing steel side plates were used as templates for drilling through the truss plates. The purpose was to ensure that the holes were in the same place as those drilled in the specimen previously, and to lead the drilling bit through an uneven surface of the truss plate. The specimen drawings are displayed in Fig.32.

4.3.2. Coarse Threaded Rods (Lag Screws)

After the specimen was manufactured (procedure in Sec.4.2), the holes for the threaded rods- lag screws were predrilled perpendicular to the direction of the bolts. In order to obtain friction where the threads penetrate the wood, the leading holes were drilled to be the same size as the diameter of the shank in the threaded part of the screw. The lag screws had a hexagonal head so the electric power tool easily turned the screw to cut the thread in the specimen. Soap or any non-petroleum lubricant could have been used to make turning easier and prevent burning the wood fibre, but this was not necessary in this case because of the coarse thread size. After the screw was inserted only its cone tip was protruding out of one side of the specimen. The protruding unthreaded part of the screw on the other side was cut off using the cutting blade of an electric grinder. The entire threaded part of the screw was used and its length was equal to the depth of the hole. The specimen drawings are displayed in Figs. 33, 34 and 35.

4.3.3. Fine Threaded Rods - Ready Rods

The specimen fabrication to this point was the same as that described in section 4.3.2. The holes for the fine threaded rods (ready rods) were predrilled perpendicular to the direction of the bolts. To obtain friction where the threads penetrate the wood, the leading holes were drilled to the same size as the diameter of the shank in the threaded part of the rod. It was necessary to attach two hexagonal nuts to the rod to be able to turn the rod in the specimen by using the electric power wrench. This time a non-petroleum lubricant had to be used to make turning easier, and to prevent burning of the wood fiber. The protruding threaded part of the rod on one side of the specimen was cut off using the cutting blade of an electric grinder. The specimen drawings are displayed in the same figure as for the lag screw (same dimensions) (Fig.33).

4.3.4. Nailed Steel Plates Type

After the specimen was manufactured (procedure in Sec.4.2), the galvanized side plates (described in section 3.3.4) were cut to the right size from a 4'x8' (1.2x2.4m) sheet. They were overdrilled by 1/16" to fit the bolt holes in the specimen. The plates were then either manually nailed (finishing nails)(see nails in Sec. 3.3.4) or nailed with a pneumatic nailer (spiral nails) onto the specimens. The same procedure was followed for both sides of the specimen. The specimen drawings are displayed in Fig.37 (spiral nails) and Fig.38 (finishing nails).

4.3.5. Epoxy Glued Steel Plates

After the specimen was manufactured (procedure in Sec.4.2) the galvanized side plates (described in section 2.3.4) were cut to the right size from 4'x8' (1.2x2.4m) sheet and overdrilled by 1/16" in diameter to fit the holes for the bolts in the specimen. On the side where the plates were to be glued they were roughened with an electric grinder to create an adhesive surface. The plates were then epoxy glued (see epoxy in sec. 3.4.5) and weighed down during the drying and hardening period (48 hours). The same procedure was followed symmetrically for both sides of the specimen. Excessive glue hardened on the specimen sides was cut off with a construction knife. The specimen drawings are displayed in Fig.36.

4.3.6. Stiff Steel Plate Welded on Truss Plates

The HRTW specimen was prepared by using a truss plate specimen with a thick steel plate welded to the truss plates on both sides as shown in Fig.32.

4.3.7. Glulam Specimens

The glulam specimens were made in the same way as their PSL equivalents. That is why they are not displayed on the drawings. The only difference was in the size of their cross section which was $3 \frac{1}{2}$ " by $5 \frac{1}{8}$ ". The three lamellas were laid perpendicularly to the bolts in the following thicknesses; first $1 \frac{3}{8}$ ", then $\frac{5}{8}$ ", then $1 \frac{3}{8}$ ", together making a piece equal $5 \frac{1}{8}$ " in width. This symmetrical section was chosen for the purpose to obtain good tension properties (18t-E). The glulam specimens were prefabricated, made of Douglas Fir and their length was 1250mm.

5. TEST METHODS

5.1. Test Apparatus (Fig.39)

5.1.1. Setup for Static Tests (mechanical part)

A 100 kip (445 kN) actuator and a 300 kip load cell were suspended from a modular steel moment frame. The frame consisted of two I-section columns 4773 mm high and a channel beam 2745 mm long. The actuator, the load cell and the specimen were suspended from the beam using six 1" diameter bolts (Fig.39). The specimen was attached at each end to the side plates (19 mm thick -ASTM A36) which were then attached to pins securing it to the load cell and the floor (Fig.40). Because the setup was a pin-pin connection it behaved as a truss member. Precautions were taken to keep the secondary moments caused by unintentional eccentricities to a minimum. Every part of this steel system was designed so it would not possibly yield anywhere but in the connection zone under study, located at the top part of the specimen. The lower part of the specimen was designed to be stronger; 12 bolts, tightened by a power wrench, were used to move the failure to the top, which was only a 10-bolt finger tightened connection. The top plates were shimmed to avoid friction in the steel-wood-steel planes. Additionally, to also cause failure in the top, a gap of approximately 0.5mm was allowed in-between the two materials. Because of its relatively low mass (10.4kg), the (PSL or GLULAM) specimen was mounted without the use of a crane. The maximum stroke of the jack was ± 76 mm (152 mm total).

The two LVDT's (displacement measuring devices) were screwed to the surface of the middle of the specimen, and the moving parts of the LVDT's were touching the "L" brackets attached to the bottom parts of the top steel side plates (Fig.42). The actuator was displacement controlled by an MTS servo controller.

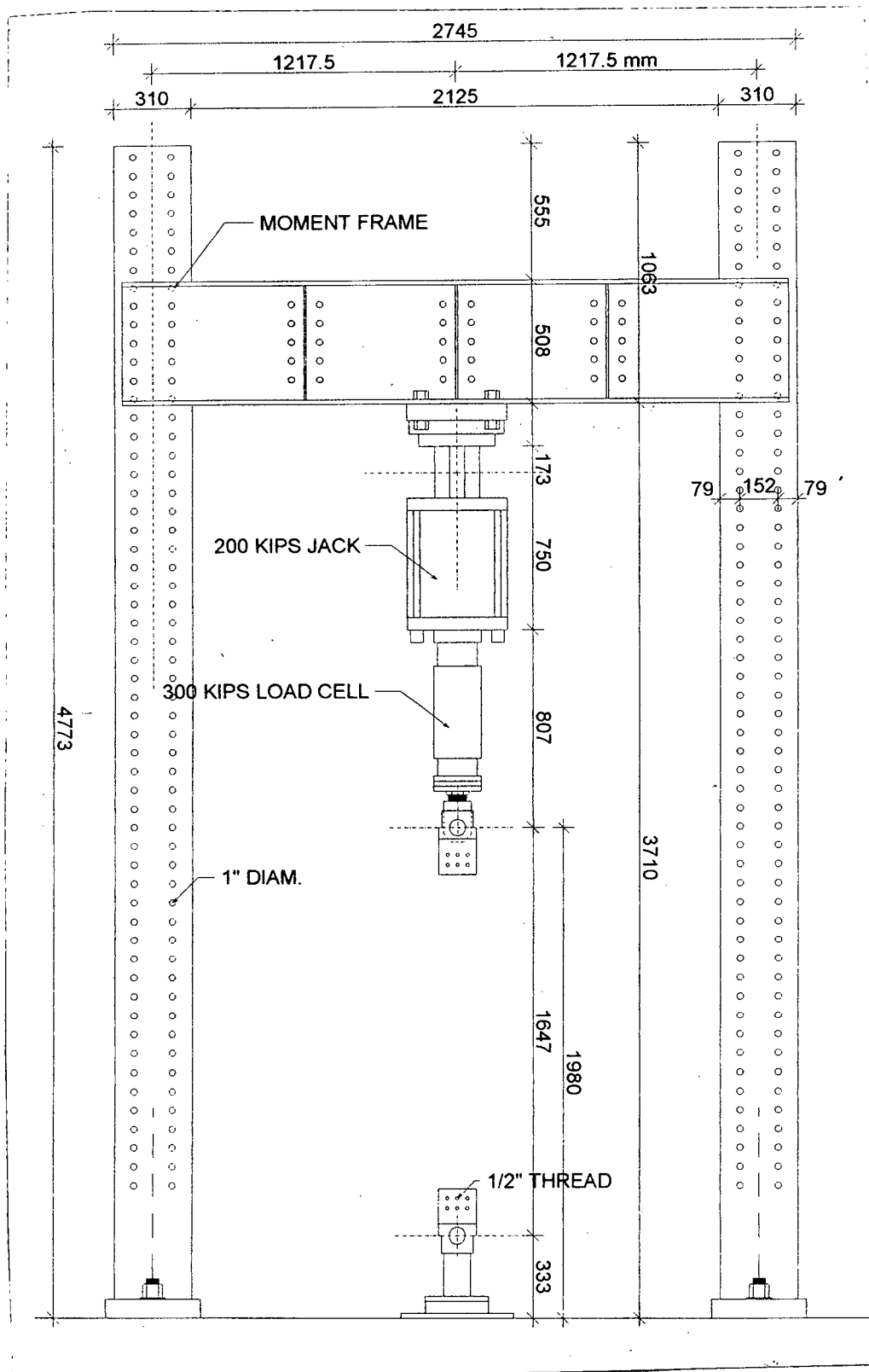


Figure 39. Mechanical setup for monotonic static tests

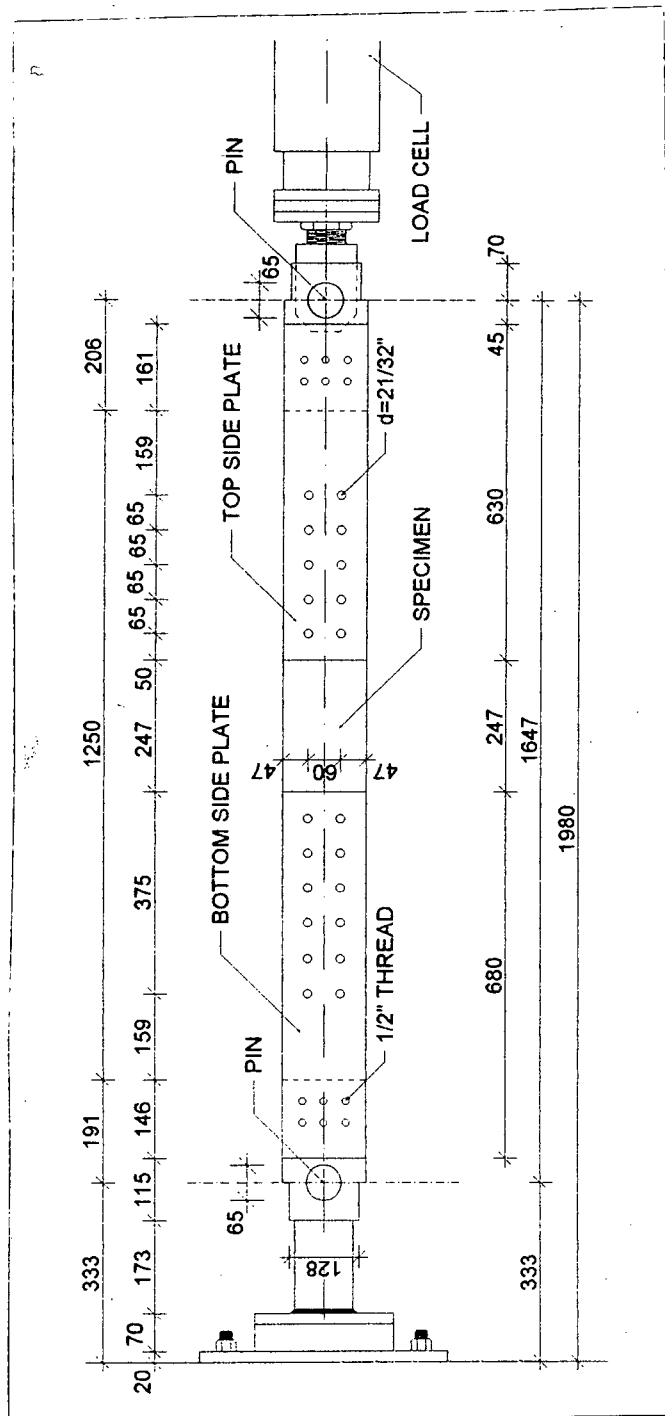


Figure 40. Specimen mounted in the setup – close up view

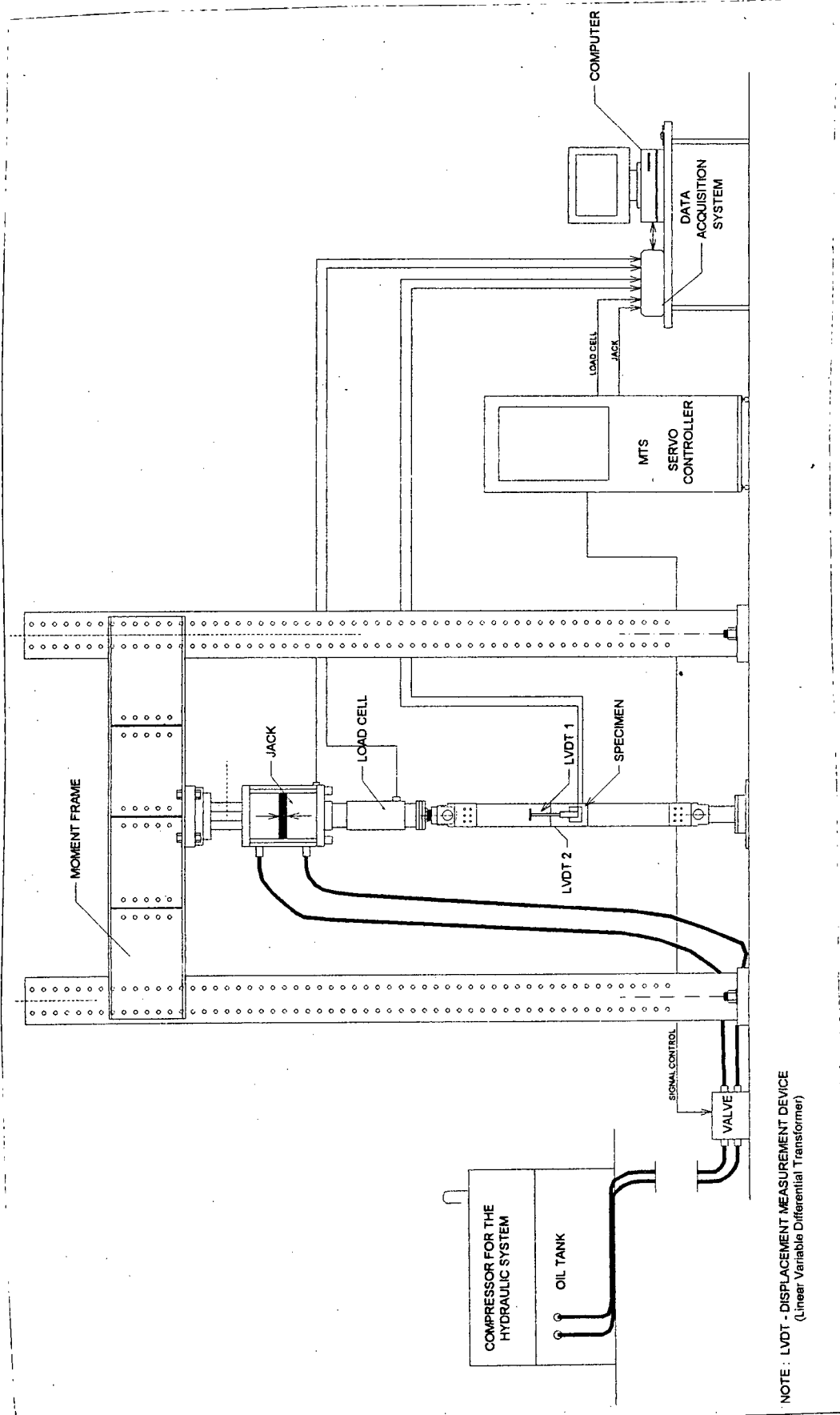


Figure 41. Schematic view of testing set-up

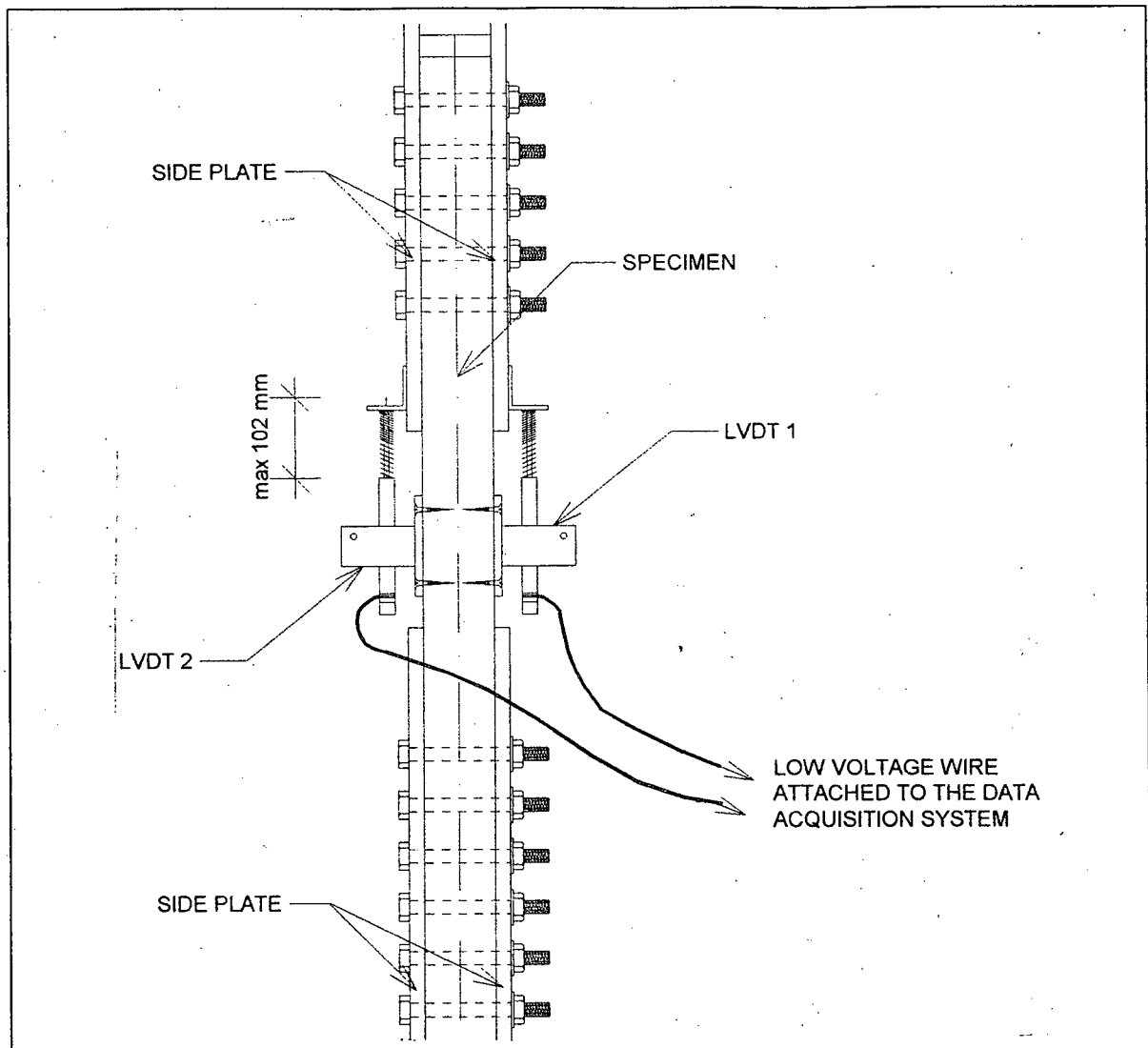


Figure 42. Close up view on LVDT's

5.1.2. Setup for Cyclic Tests

The same frame and equipment were used for the static cyclic loading as for the static tension loading, except lateral support was needed for testing in compression. The main members of the lateral support were two 8x8" (203x203 mm) I beams attached to the moment frame. Four rollers, two in each direction were attached in the lateral support beams (Fig.43).

The rollers were placed approximately in the centre of the specimen. A 1mm slack was left in each direction.

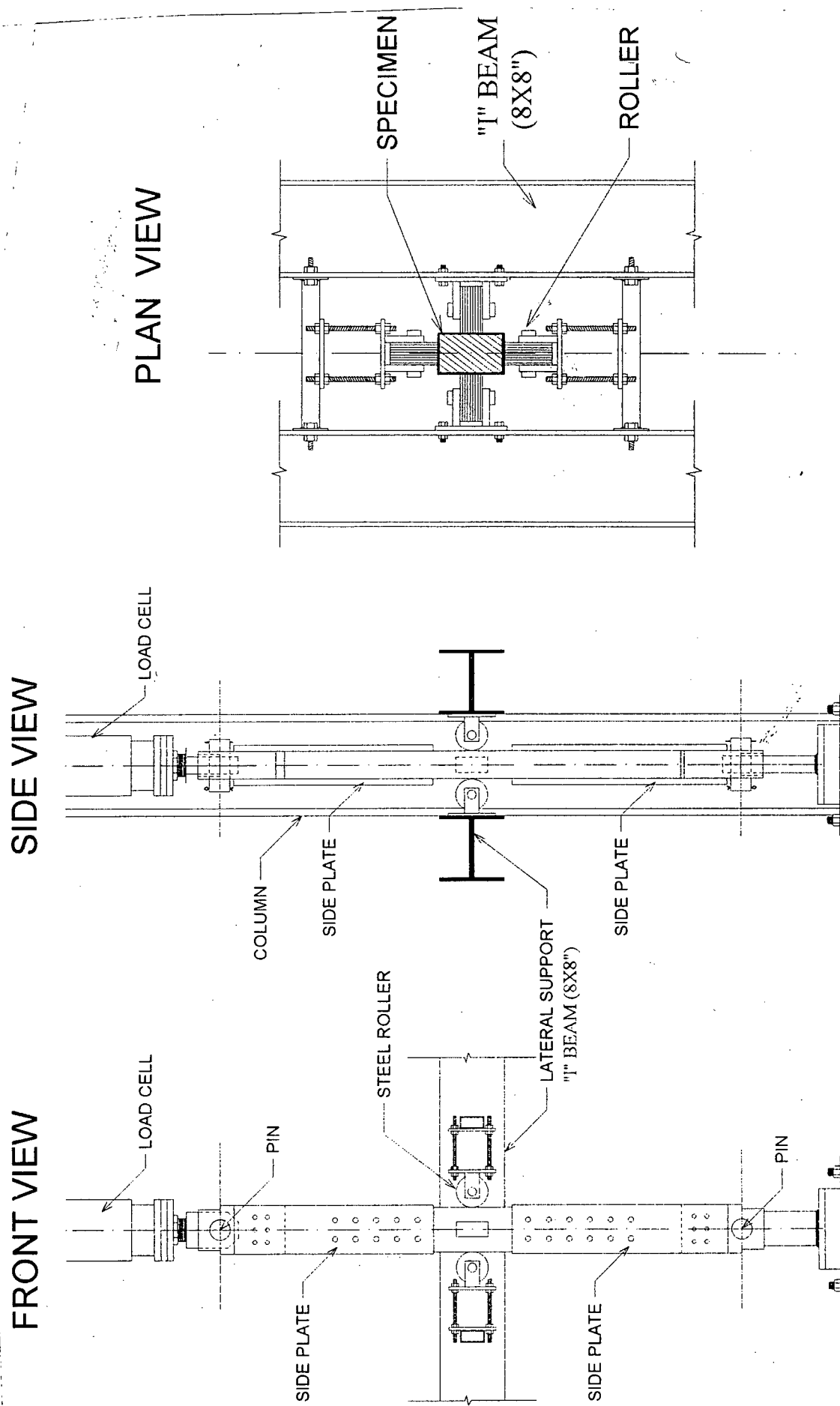


Figure 43. Lateral support system for reverse cyclic loading.

5.2. Test Descriptions

5.2.1. Static (Tension) Tests

The tension-loading rate was 0.7mm/min, causing first fracture to occur within about 6 min while the entire test lasted about 17 minutes. Every test was continued up to a displacement of 40mm to obtain consistent input for calculating energy dissipation. The data acquisition system collected the data with a frequency of one set per second, so at the end of the test, at 40mm displacement, the computer had collected approximately 1200 points on the load-deflection curve. The software "Labtech Notebook" was used for the data monitoring and recording. The collected data were then analyzed using Microsoft Excel.

5.2.2. Cyclic (Tension-Compression) Tests

The same MTS-controller and acquisition systems were used for the cyclic tests. In this case the displacement input was reverse cyclic (tension-compression). The following figure shows the cyclic test protocol (ISO, 1999). It is the draft protocol for quasi-static cyclic testing of timber connections. The displacement amplitude was expressed as a percentage of the displacement at ultimate load reached during static tension tests for the same type of specimen.

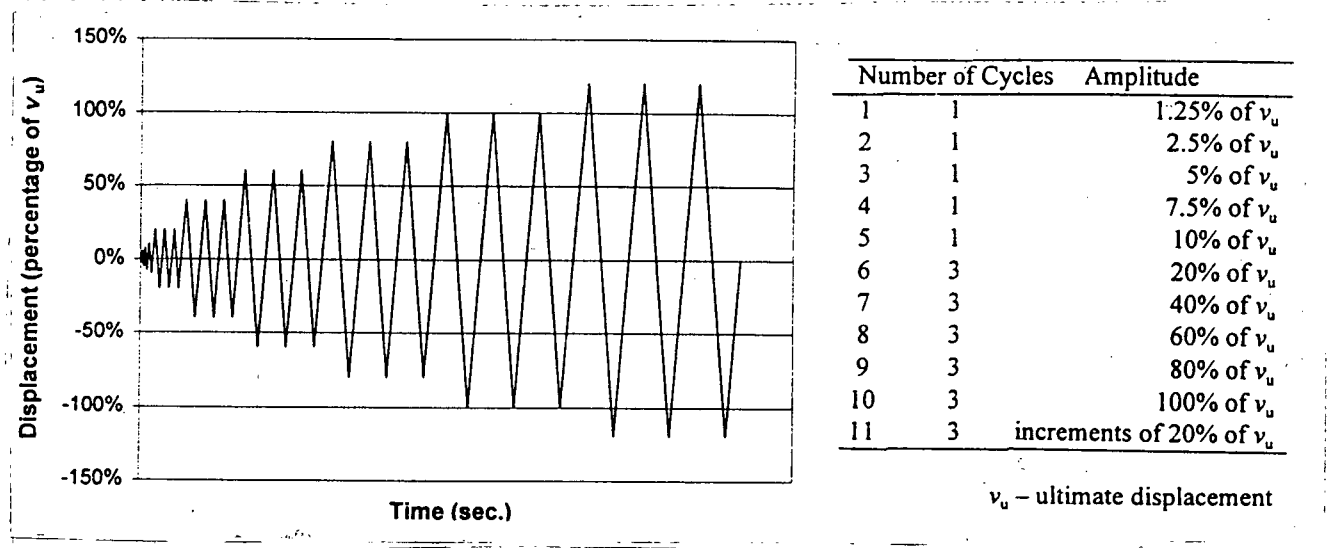


Figure 44. Cyclic loading protocol (ISO, 1999)

The protocol was followed up to and including application of the failure load (80% of ultimate displacement). After this only one cycle per step was used until 40mm displacement

was reached. The tests were displacement-controlled to prevent a sudden failure when the maximum load was reached. Due to the slow performance of the hydraulic system and poor tracking ability, the displacement control was done manually through adjustment of the stroke.

The cyclic loading rate was displacement controlled on average 16mm/min, causing first fracture to occur in approximately 9 min while the entire test lasted about 33 minutes. The data acquisition system collected the data with a frequency of one point per second, so at the end of the test at 1900mm (cumulative average) displacement, the computer collected approximately 2000 points on the load-deflection curve. The same data analysis software was used for these tests as for the static tension tests.

6. DATA ANALYSIS METHODS

6.1. Joint Ultimate Load, Joint Ultimate Displacement

The maximum load carried by the connections during the static and cyclic tests was obtained from the test data. The ultimate displacement was considered as the displacement value in mm at 80 % of maximum load after the peak load.

6.2. Elastic Stiffness Calculations

The elastic stiffness was calculated from the linear part of the load-displacement graph, where the slope of a line connecting the two points on the curve at 50% and 20% of max. load:

$$k_e = (F_{50} - F_{20}) / (D_{50} - D_{20}) \quad (1.04)$$

6.3. Displacement Ductility of the Connections

The following formula was used to calculate the displacement ductility of the connections:

$$\mu = D_{80} / D_{50} \quad (1.05)$$

The quantities in the formula are explained by the following figure:

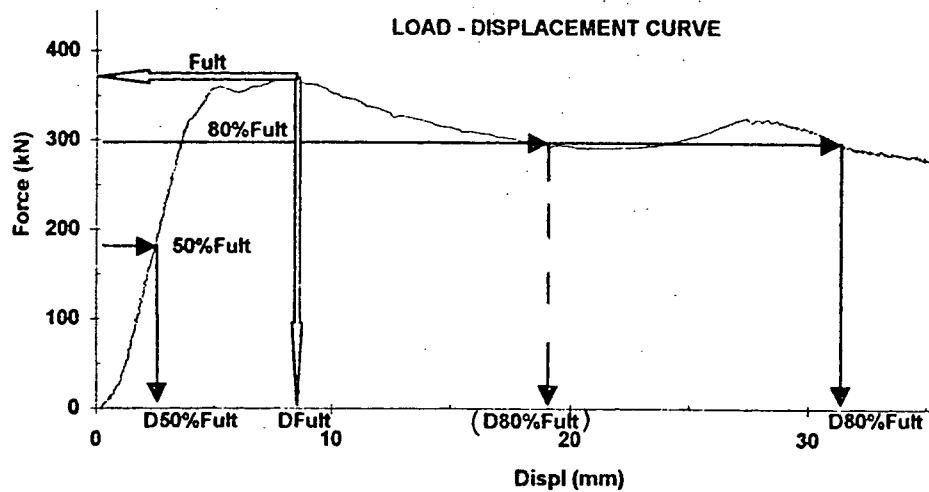


Figure 45. Explanation of ductility considerations

Fig. 45 shows that in some cases (lag screw reinforced joints) there were two peaks on the load-slip curve, thus two possible options for displacement at 80% of max load occurred. In this case, the higher displacement was considered to obtain a measure of ductility.

In the cyclic test case ductility was calculated according to the same formula, and the values of the envelope of the cyclic diagram in the tension part was considered.

6.4. Energy Dissipation of the Connections

Fig. 45 shows that when two peaks occur, the ductility formula is not a unique measure of the connection behaviour. It does not fully explain the behaviour of the connection by division of the two numbers. The dissipated energy is much better, because it is integrating entire area under the load-slip curve.

The dissipated energy of the connections was calculated using the full set of points from the load-deflection curves of the tested specimens. Energy is the area under the curve, which was approximated using numerical integration. The following formula was used to obtain dissipated energy of the part of the graph up to the point “n”:

$$\Sigma E_i = \Sigma [(D_i - D_{i-1}) * (F_i + F_{i-1}) / 2] \quad (1.06)$$

D_i – displacement [mm] of the point “i” on the load-displ. curve

F_i – load [N] of the point “i”

$i = 1, 2 \dots n$

where n is the point at 40 mm displacement

The energy dissipation was integrated up to 40 mm displacement for the static tension tests, which meant around 1200 points were considered. In the case of the reverse cyclic tests the energy dissipation data were calculated up to 100 mm of cumulative displacement reached by the particular connection.

6.5. Bending Deflection of the Bolts after Connection Failure

Almost all the bolts bent in the static tension tests were measured. Some of the data were lost or miss-numbered within a particular row of bolts. The bolt deflections from the cyclic tests were not measured, since their deflections were changing over the protocol history. Even if they had been recorded at the end of the test, it would not have reflected the true failure bending deflection.

Each inspected bolt was numbered according to its position in the joint. The mid-span deflections were measured by a dial gauge with 1/1000 inch (0.025mm) scale attached to a magnetic stand (Fig. 46). The bolts were put on the same simply supporting system as was used in the bolt bending deflection tests described in Sec. 3.3.1. All the deflection data are listed in the Appendix III-d and distribution among the bolts within the row is explained in Sec.7.1.7.

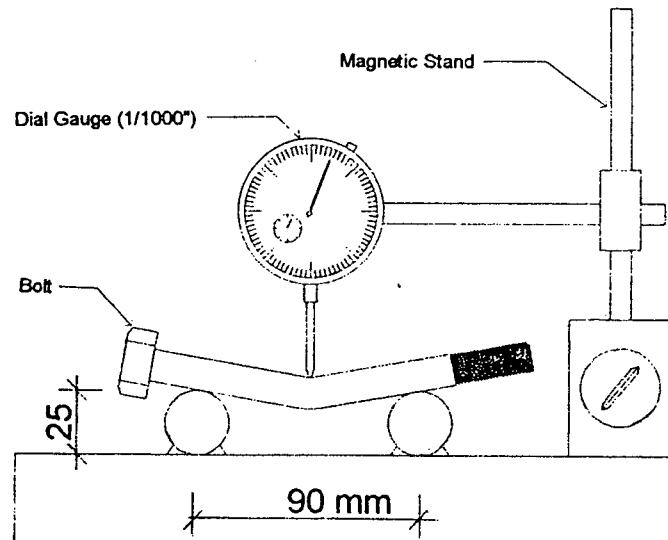


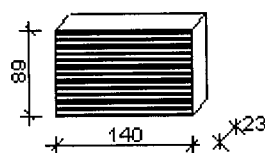
Figure 46. Test setup for measuring the bending deflection of bolts

6.6. Specimen Density and Moisture Content after the Test

Every specimen was tested after each test for its moisture content and density, using the oven-drying method according to the code ASTM D-4442-84. The following article explains the procedure in detail.

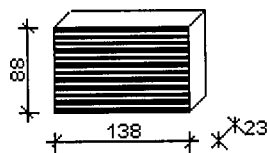
Sample Calculation of Density and Moisture Content – Specimen HRR1

Right after the load test, a block was cut out of the specimen 5" from the end and its properties were measured :



Dimensions: 140 × 88 × 23 mm
Volume: 287 e3 mm³ = 0.000287 m³
Mass: 186.88 g = 0.187 kg
Density: 652.104 kg/m³

Dimensions measured after approximately 3 days * of oven drying:



Dimensions: 138 × 88 × 23 mm
Volume: 291 e3 mm³ = 0.000291 m³
Mass: 172.71 g = 0.172 kg
Density: 592.577 kg/m³

$$\begin{aligned}\text{Mass of water: } & M_w - M_s \\ &= 186.88 \text{ g} - 172.71 \text{ g} \\ &= 14.17 \text{ g}\end{aligned}$$

$$\begin{aligned}\text{Moisture content: } & M_w / M_s \times 100\% \\ &= 14.17 / 172.71 \text{ g} \times 100\% \\ &= 8.2\%\end{aligned}$$

$$\begin{aligned}(\text{Wet Density} - \text{Dry Density}) / \text{Dry Density} \times 100\% \\ &= 652.104 - 592.577 / 592.177 \times 100\% \\ &= 10.05\%\end{aligned}$$

The endpoint of the drying time was reached when the mass loss in a 3-hour interval was equal to or less than twice the selected balance sensitivity. The balance sensitivity for 0.01% MC precision was 0.1 mg, the specimens were dried to 0.2 mg or less mass loss in a 3-hour period.

7. TEST RESULTS

7.1. STATIC TENSION TESTS

A summary of test results is presented in this chapter with comparisons and comments. Part of the test results are the load-displacement graphs where either all the curves or only typical curves were chosen because it was not possible to generate average curves in all the cases due to the test data inconsistency. The number of data points and their locations do not match since most of the tests were speeded up after the peak load to reach the desired consistent 40mm displacement value for calculating ductility. Nevertheless, it was still possible to average the numerical quantities that are shown in the following tables. The system by which the test data were analyzed was explained in Chapter 6.

The detailed individual numerical data and load-deflection curves of the connections are summarized in Appendix I with the comparisons in Appendix II.

7.1.1. Unreinforced Specimens (HU, FU and TU)

Ten 5/8"(15.9mm) 10-bolt, two 1/2"(12.7mm) 10-bolt and three 3/8" 10-bolt unreinforced specimens were tested in static tension. Fig.47 shows typical load-displacement curves.

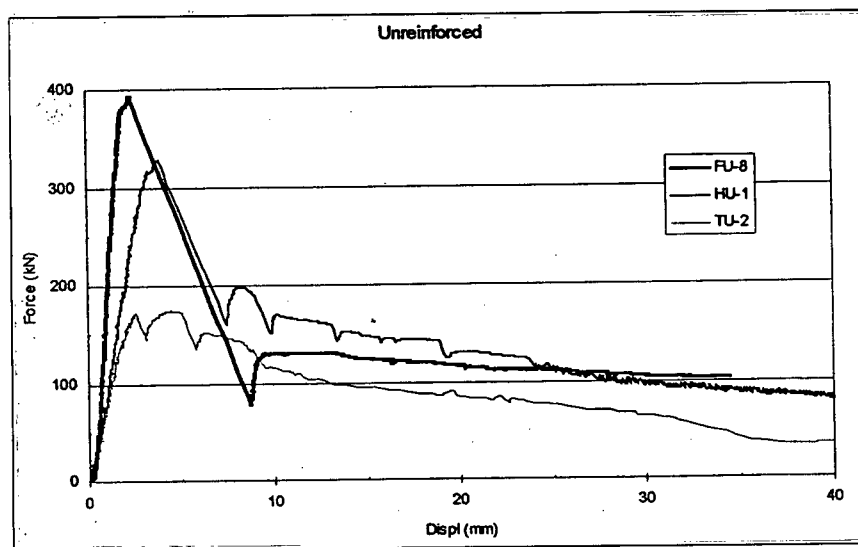


Figure 47. Typical load-displacement (P-Δ) curves of the unreinforced 3/8"(TU-2), 1/2"(HU-1) and 5/8" (FU-8) PSL specimens tested in static tension

The 1/2" and 5/8" unreinforced specimens were similar in their very brittle behaviour, characterized by a sudden drop after the peak load was reached. The 3/8" specimen failed in a

more ductile manner. The ultimate strength capacities of the 1/2" and 5/8" specimens were very similar, while half as much (175 kN) was carried by the 3/8" bolt connection. The 3/8"-bolt connection behaved in a much more ductile manner, although the fracture pattern was still of a brittle nature. In general it can be said that the initial-elastic stiffness decreased and ductility increased with increased L/d ratio, indicating that slender bolts have a softening influence on the global connection behaviour.

The failure mode for the 5/8"-bolt specimens was mainly row tear out and group tear-out. The 1/2" and 3/8"-bolt specimens failed in a combination of row splitting and row tear-out (Fig.48). These failure modes are common for brittle connections.

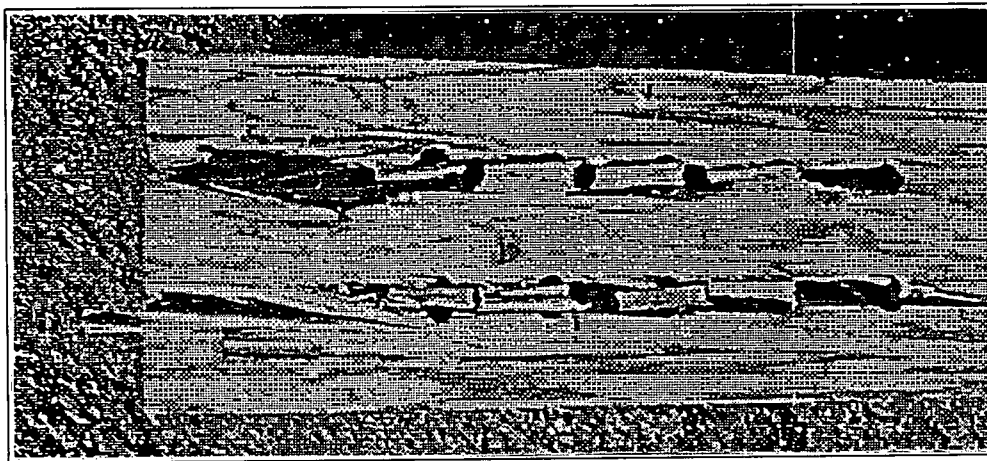


Figure 48. Typical failure of unreinforced 1/2" PSL specimen

Specimen Symbol	Bolt d. [in]	Force Ult. [kN]	Diff [%]	Stiffness [kN/m]	Diff [%]	Energy Dis [Nm]	Diff [%]	Ductility []	Diff [%]	Failure Mode
FU-Avg	5/8"	372.5		275.3		4173.2		3.8		group shear, row shear
HU-Avg	1/2"	288.3	-22.6	119.4	-56.6	5246.0	25.7	2.6	-31.1	row split, row shear
TU-Avg	3/8"	175.34	-52.9	79.77	-71.0	3113.22	-25.4	4.85	27.6	row split, row shear

Table 3. Static tension test results – unreinforced joints in PSL

The results from Table 3 indicate that the smaller diameter bolts improved the connection behaviour with increased ductility and energy dissipation. The 3/8"-bolt connections showed a dramatic change in the behaviour by shifting towards a more ductile failure mode. This indicates that little improvement could be expected by reinforcing these connections.

The individual test data are shown in Appendix I and the comparisons of the three different bolt diameter joints are listed in Appendix II.

7.1.2. Threaded Rods

Two types of threaded rods were used as reinforcement in the tests, namely lag screws with a coarse thread and ready rods with a fine thread. The rods were placed transversely to the direction of the loading, the bolts and the grain direction. The use of the coarse thread was meant to increase the bond between the reinforcement and the wood.

The four 5/8" 10-bolt reinforced specimens (two of each size of thread) had the same initial stiffness and about the same ultimate strength, but soon after the maximum load at 4mm displacement, the curve of the fine thread specimen abruptly dropped to 100 kN (Table 4). The coarse thread specimens experienced a gradual decline in load and had a sudden drop in capacity at a displacement of about 20mm (Fig. 49).

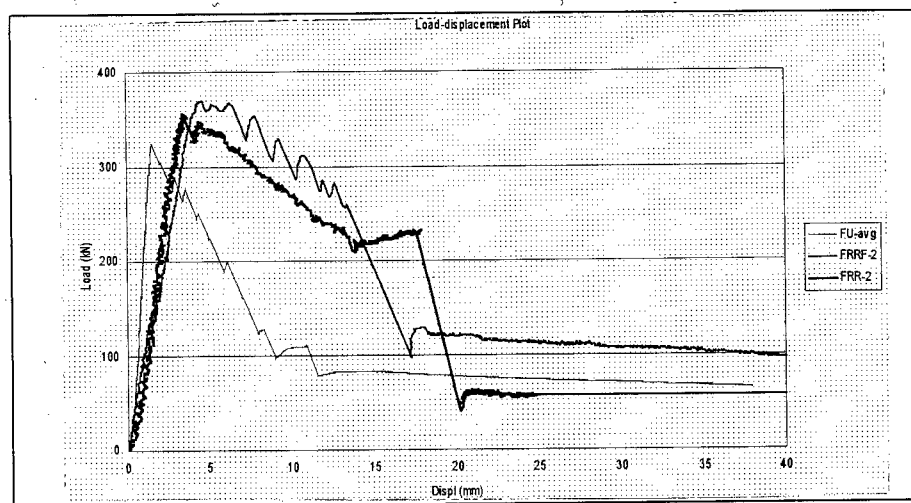


Figure 49. Unreinforced (FU) vs. lag screw (FRR) and ready rod (FRRF) reinforced connections; typical P-Δ curves of 5/8" PSL specimens tested in static tension

Compared to the unreinforced specimens, the difference in ductility improvement between the ready rod and the lag screw was not significant: 25% for FRRF and 33% for FRR (average from two tests each). The lag screw specimens were carrying 200 kN at 20 mm, whereas the ready rod joints dropped down to 100 kN at the same displacement. The lag screw reinforcement significantly improved the energy dissipation compared to the ready rod. The load-slip curve was also smoother.

Both ready rod reinforced specimens (FRRF) failed when the ready rod stripped through the wood fibers. The failure mode was group bi-axial tear out (Fig. 50), which means that row shear-out occurred with the two rows of bolts as well as the reinforcing rods.

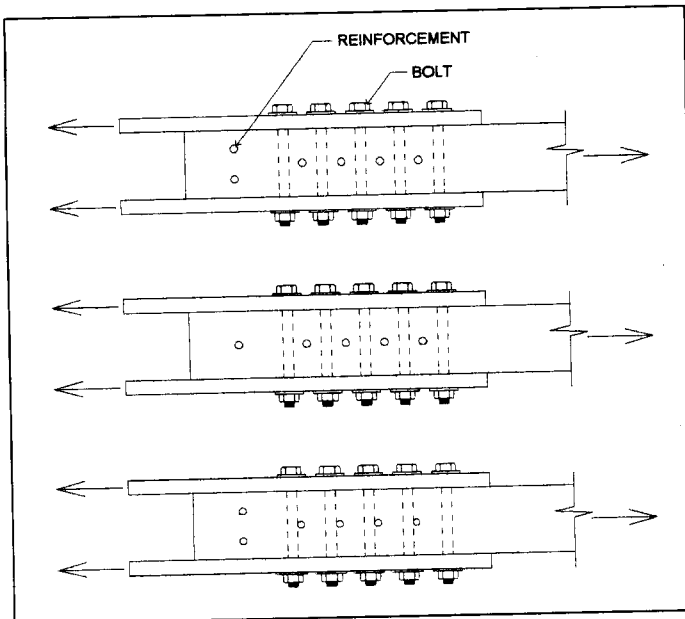
Specimen Symbol	Bolt d. [in]	Force Ult. [kN]	Diff [%]	Stiffness [kN/m]	Diff [%]	Energy Dis [Nm]	Diff [%]	Ductility []	Diff [%]	Failure Mode
FU-Avg	5/8"	372.5		275.3		4173.2		3.8		group shear, row shear
FRR-Avg	5/8"	346.32	-7.0	156	-43.3	6594.24	58.0	5.055	33.0	group shear
FRRS-Avg	5/8"	389.2	4.5	119.9	-56.4	6781.0	62.5	4.3	11.8	group shear, net section
FRRF-Avg	5/8"	373.2	0.2	92.6	-66.4	6241.9	49.6	4.7	24.9	group shear

Table 4. Static tension test results – 5/8 inch 10 bolt threaded rod reinforced joints in PSL (FRR-lag screw, FRRS-single end rod, FRRF-ready rod)



Figure 50. Bi-axial tear-out failure of lag screw reinforced 1/2" PSL specimen

Although it is often thought that a minimal amount of transverse reinforcement is sufficient, these tests have shown that the reinforcing elements carry a significant load, particularly in the post-ultimate region. Fine thread proved to lack sufficient bond with the wood, and the coarse threaded lag screws performed much better.



- (a) Two end rods (HRR)
- (b) Single end rod (HRRS)
- (c) Rods moved away from the potential contact with bolts (HRRSH)

Figure 51. Configurations of the threaded rods in the specimen

The placement of the rods in the connection was also considered, this time with a ½" bolt connection. Three reinforcement configurations were tested in static tension. For all the connections lag screws were used as reinforcing elements in the transverse direction. The HRR type had single reinforcing rods placed halfway between the bolts, with two rods at the end of the connection. The HRRS had a single rod at the end. The HRRSH had the rods moved away from the bolts (touching the neighboring bolts) so that a larger travelling distance of the bolts was allowed (Fig. 51).

Due to the use of the same size of bolts, all the lag screw load-displacement curves had the same elastic stiffness. When compared to the unreinforced specimens, the three reinforced specimens had the following increase in ductility – HRR:137%; HRRS:378%; HRRSH:236% (Fig. 52, 53 and 54 Table 5). Even though the curves were not consistent enough to make firm conclusions, the increased tendency of reinforced specimens was unmistakable. One of the offset rod connections (HRRSH-1) was much smoother and showed promising second peak on the load-displacement curve. The increased distance between the bolt and the reinforcing rod improved the behaviour significantly by increasing the amount of wood that would be able to absorb energy without adding stress concentrations that could lead to brittle failures. The latter was the case with HRR specimens, which failed soon after the bolts came in contact with the reinforcing rods. In the HRRSH specimens a secondary peak was observed in the load-displacement curve, when the reinforcing rods started to participate in carrying load. It was a

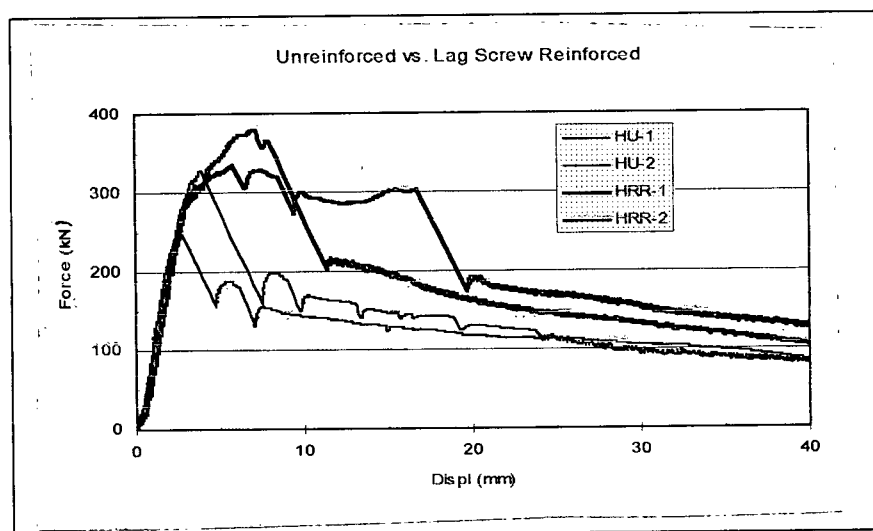


Figure 52. Unreinforced (HU) vs. two end rods (HRR); all P-Δ curves of ½" PSL specimens tested in static tension

much smoother load transfer mechanism, compared to the HRR specimens, with a large amount of wood acting as a compressible cushion between bolt and reinforcing rod. This increased the ductility, with the drop of the load delayed up to 25 mm displacement. The average ductility was significantly higher in the specimens with the offset rods (HRRSH) and single reinforcing rods (HRRS) in the end zone.

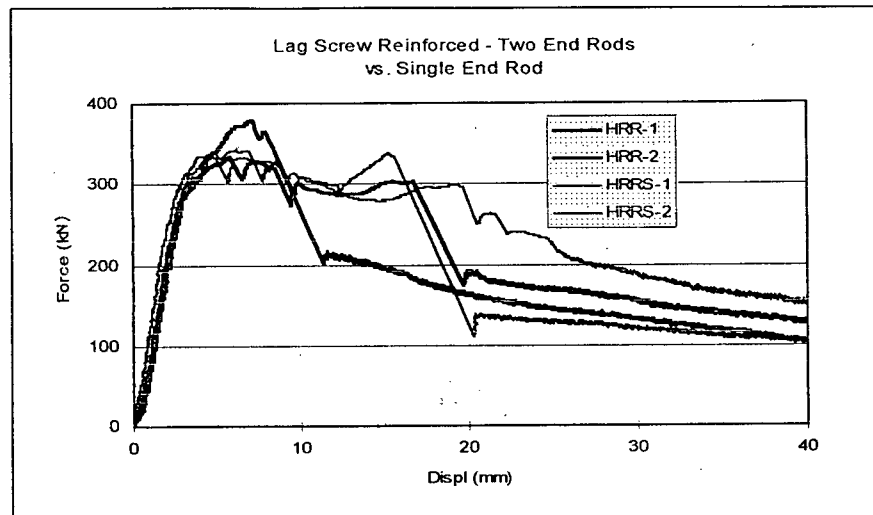


Figure 53. Single end rod (HRRS) vs. two end rods (HRR); all P-Δ curves of ½" PSL specimens tested in static tension

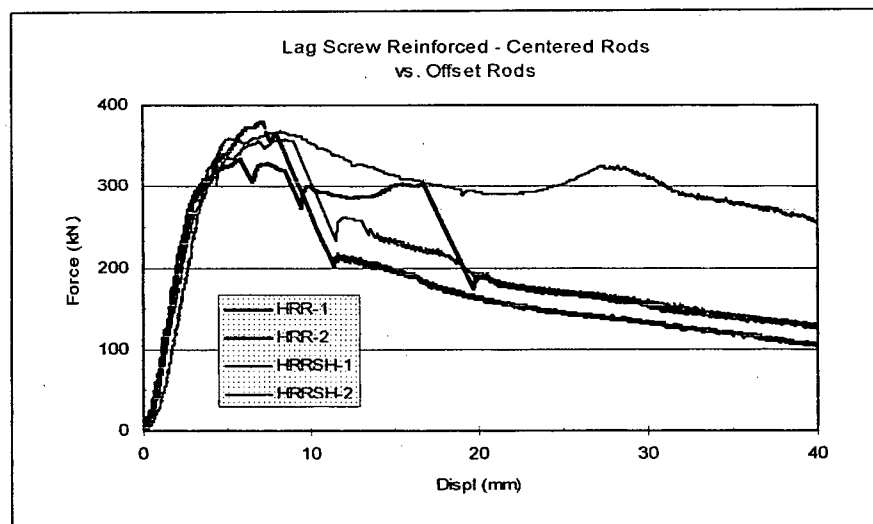


Figure 54. Centered rods (HRR) vs. rods at the bolt locations (HRRSH); all P-Δ curves of ½" lag screw reinforced PSL specimens tested in static tension

All three types of reinforced specimens failed in bi-axial group tear-out, except one (HRRSH 1), which failed in row tear-out.

Specimen Symbol	Bolt d. [in]	Force Ult. [kN]	Diff [%]	Stiffness [kN/m]	Diff [%]	Energy Dis [Nm]	Diff [%]	Ductility []	Diff [%]	Failure Mode
HU-Avg	1/2"	288.3		119.4		5246.0		2.6		row split, row shear
HRR-Avg	1/2"	357.0	23.8	124.9	4.7	7900.2	50.6	6.2	137.2	group shear, row shear
HRRS-Avg	1/2"	340.8	18.2	128.2	7.5	8747.5	66.7	12.5	378.1	group shear, row shear
HRRSH-Avg	1/2"	363.1	25.9	110.2	-7.7	9990.4	90.4	8.8	236.5	group shear, row shear

Table 5. Static tension test results – 1/2 inch 10 bolt threaded rod reinforced joints in PSL

The influence of bolt slenderness (l/d ratio) of 3/8", 1/2" and 5/8" lag screw reinforced specimens is shown in Fig. 55. When considering the bolt size, the best results were obtained using the 3/8"10-bolt connection (TRR). The ductility ratio ranged from 8 to 24, and the ultimate strength averaged at the 300 kN level which was very close to the higher diameter bolt connection values.

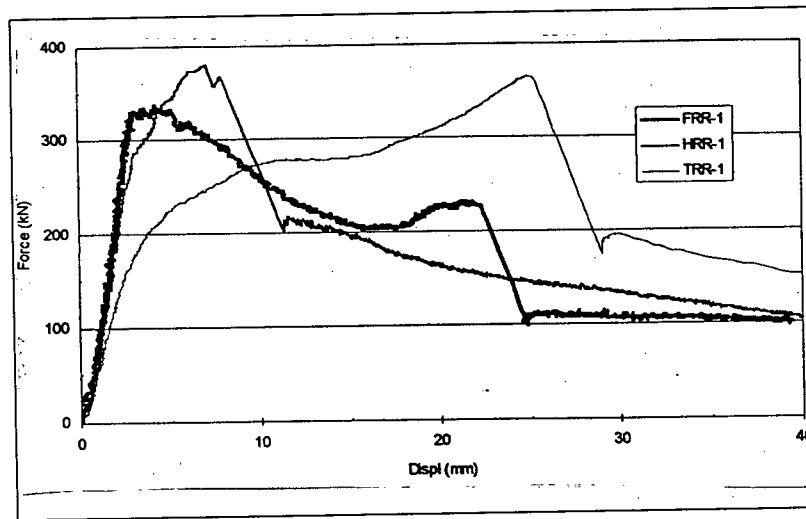


Figure 55. Influence of l/d ratio; typical $P-\Delta$ curves of the lag screw reinforced 3/8" (TRR-1), 1/2" (HRR-1) and 5/8" (FRR-1) PSL specimens tested in static tension

Also the force drop-off happened far beyond the usual 4mm displacement observed so far (22 mm). This improvement with the more slender bolts ($l/d = 9.3$), also almost changed the failure mode to a ductile one and the load-slip curve to a smooth one. The specimen started failing in wood crushing, no cracks were initially observed and the load at failure was almost evenly distributed among the bolts (see Sec.7.1.7).

At the end the specimen failed in a brittle failure mode. Fig. 56 and Table 6 show the improvements due to the lag screw reinforcement in the PSL 3/8" 10 bolt connections.

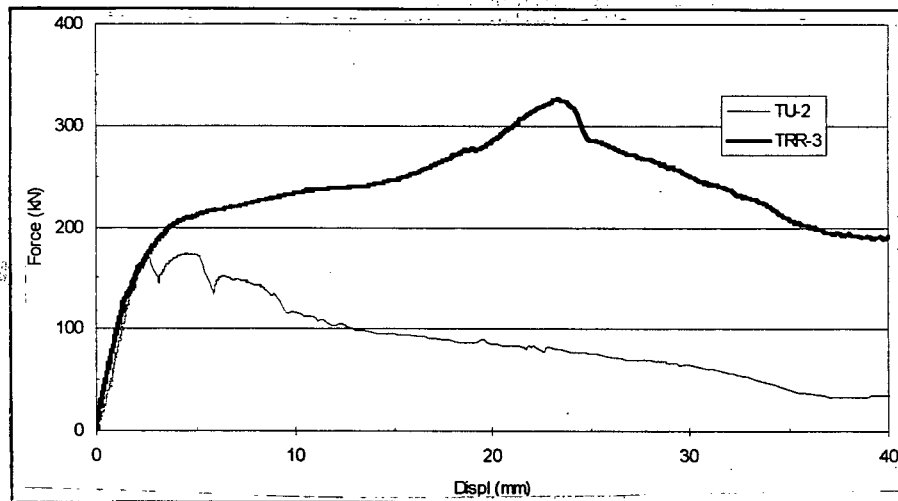


Figure 56. Unreinforced (TU) vs. lag screw reinforced (TRR) connections; typical P-Δ curves of 3/8"PSL specimens tested in static tension

Specimen Symbol	Bolt d. [in]	Force Ult. [kN]	Diff [%]	Stiffness [kN/m]	Diff [%]	Energy Dis [Nm]	Diff [%]	Ductility []	Diff [%]	Failure Mode
TU-Avg	3/8"	175.34		79.77		3113.22		4.85		group shear, row split
TRR-Avg	3/8"	325.26	85.5	87.3467	9.5	9186.3367	195.1	15.18	213.0	group shear, row shear

Table 6. Static tension test results – 3/8 inch 10 bolt threaded rod reinforced joints in PSL

Glulam 3/8"-bolt connections (GTU,GTRR) (Fig. 58) had a similar increase in

Specimen Symbol	Bolt d. [in]	Force Ult. [kN]	Diff [%]	Stiffness [kN/m]	Diff [%]	Energy Dis [Nm]	Diff [%]	Ductility []	Diff [%]	Failure Mode
GHU-Avg	1/2"	306.57		115.03		2841.32		2.34		group shear, row shear
GHRR-Avg	1/2"	346.34	13.0	100.59	-12.6	6659.66	134.4	4.69	100.4	group shear, row split
GHRRF-Avg	1/2"	337.61	10.1	89.6267	-22.1	6446.7333	126.9	6.1233	161.7	group & row shear, split

Table 7. Static tension test results – 1/2"-10 bolt threaded rod reinforced joints in Glulam

ductility and energy absorbed (Table 8) compared to their 1/2" (GHU,GHRR) equivalents (Fig.57) (Table 7).

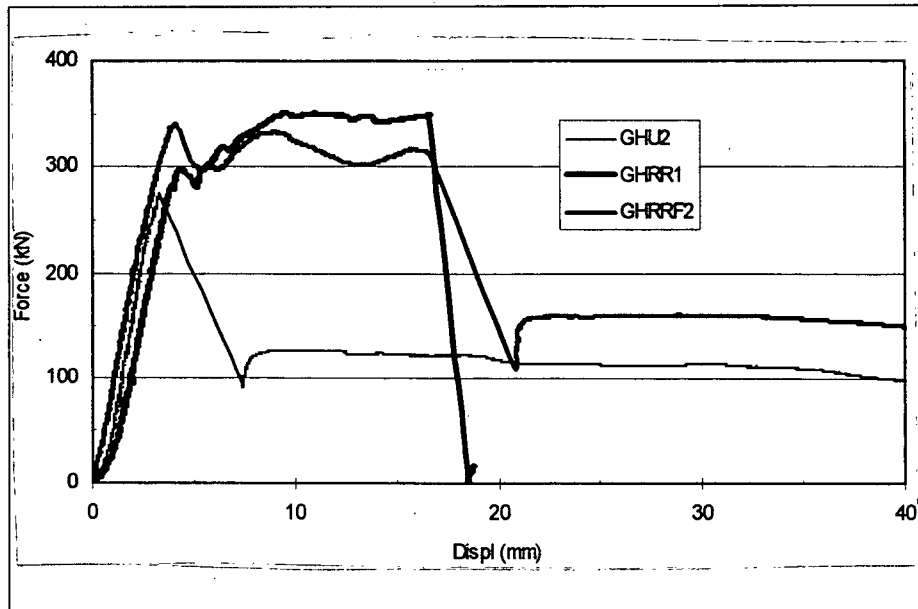


Figure 57. Unreinforced (GHU) vs. lag screw (GHRR) and ready rod (GHRRF) reinforced connections; typical P-Δ curves of 1/2" Glulam specimens tested in static tension

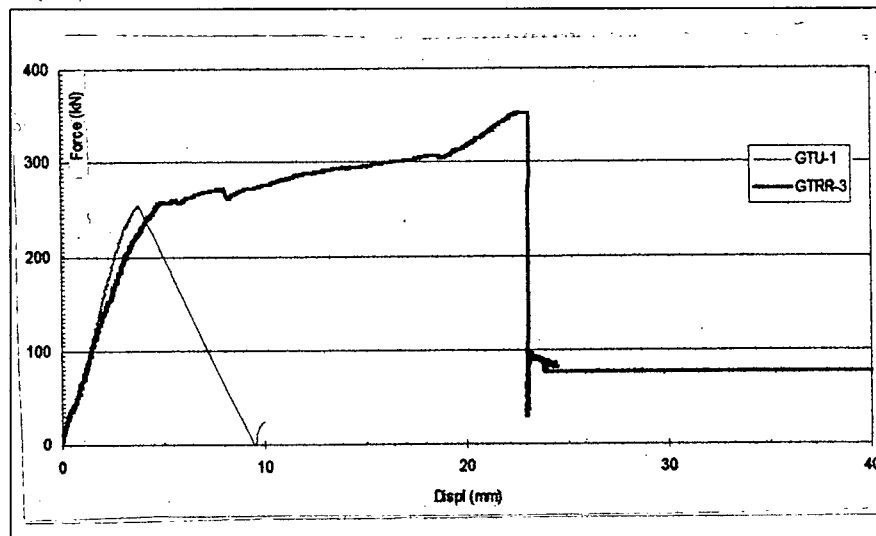


Figure 58. Unreinforced (GTU) vs. lag screw (GTRR) reinforced connections; typical P-Δ curves of 3/8" Glulam specimens tested in static tension

Specimen Symbol	Bolt d. [in]	Force Ult. [kN]	Diff [%]	Stiffness [kN/m]	Diff [%]	Energy Dis [Nm]	Diff [%]	Ductility []	Diff [%]	Failure Mode
GTU-Avg	3/8"	260.8		78.53		3458.54		4.13		row shear, row split
GTRR-Avg	3/8"	354.26	35.8	74.6	-5.0	7531.71	117.8	8.75	111.9	row shear, row split

Table 8. Static tension test results – 3/8 inch 10 bolt threaded rod reinforced joints in Glulam

7.1.3. Truss Plates

The truss plate reinforced specimens (HRT, FRT) experienced varying levels of increase in ductility compared to the unreinforced specimens (HU, FU): 5.3% for the 5/8" (Table 10) and 172.9% for the 1/2" bolted connections (Table 9). The 1/2" bolt reinforced specimens had 29% more improvement in ductility than their 5/8" bolt equivalents (Tab 9,10).

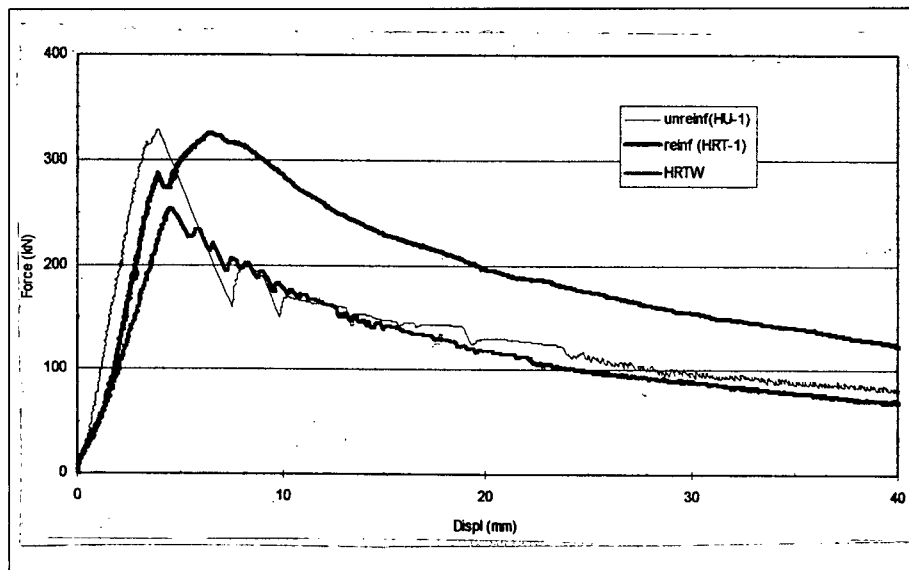


Figure 59. Unreinforced (HU) vs. truss plate (HRT) and stiff truss plate (HRTW) reinforced connections; typical P-Δ curves of 1/2" PSL specimens tested in static tension

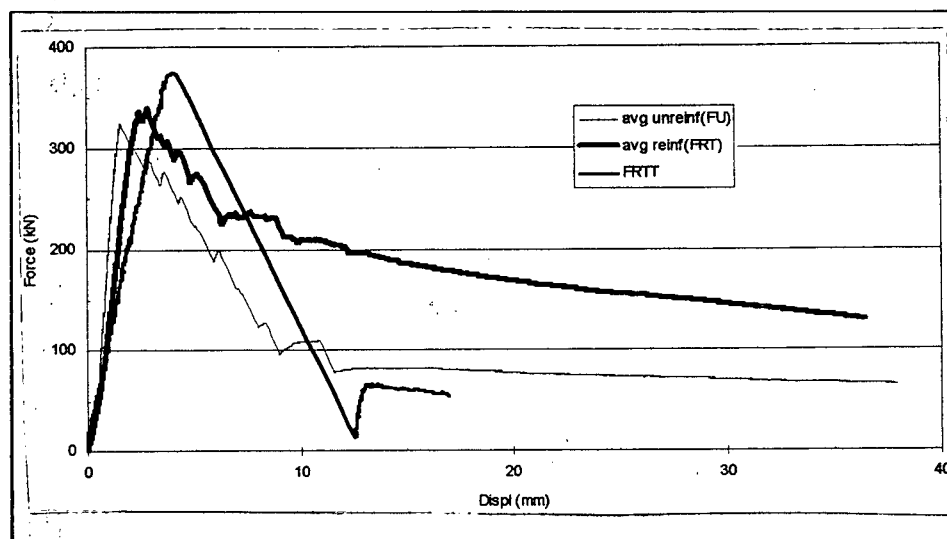


Figure 60. Unreinforced (FU) vs. truss plate (FRT) and rotated truss plate (FRTT) reinforced connections; average P-Δ curves of 5/8" PSL specimens tested in static tension

The curve in Fig. 59 is much smoother for the $\frac{1}{2}$ " reinforced connections than for the $\frac{5}{8}$ " ones (Fig. 60). Again, the initial-elastic stiffness of the $\frac{1}{2}$ " bolt joint was much lower than that of the $\frac{5}{8}$ " one. Even though, the post-ultimate strength capacity of the $\frac{1}{2}$ " bolt connection was not significantly higher compared to the $\frac{5}{8}$ " connection.

The typical failure modes for reinforced $\frac{5}{8}$ " bolt specimens were row splitting, row tear-out and group tear-out.

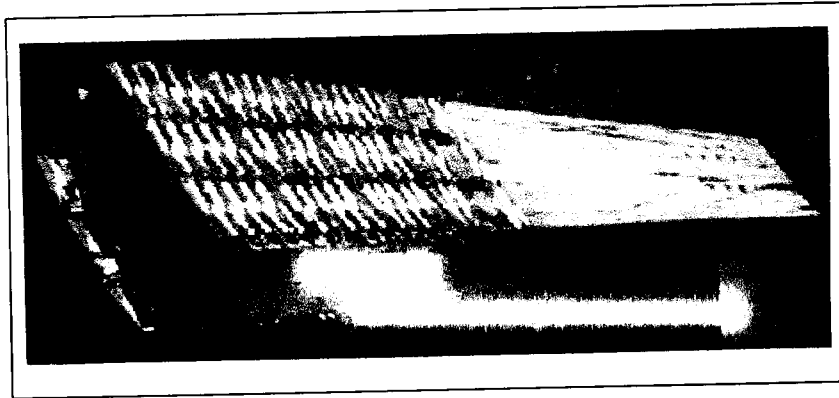


Figure 61. Typical row tear-out failure of $\frac{1}{2}$ " truss plate reinforced PSL specimen

The reinforced $\frac{1}{2}$ " bolt specimens failed in a combination of row splitting and row tear-out (Fig. 61). Although the holes in the reinforcement truss plates were $\frac{1}{32}$ " over-drilled, the truss plates were crushed by the bolts in the direction of the tension loading. This meant, that the truss plates were also load carrying elements in the longitudinal as well as transverse direction. The truss plate geometry was such that the outer teeth were not active as they were located on the edge, therefore not contributing to the joint reinforcing action. Similarly, the inner teeth happened to fall on the line of the two bolt rows, which might have accelerated the shear action along the two rows of bolts. These are some of the factors that contributed to the relatively early failures.

The idea of transferring a significant part of the load fully through the truss plate was tried in specimen (HRTW), which had a stiff, load carrying steel plate welded to the regular truss plate specimen. Most of the load was transferred from the bolts into the thick plate and then into the truss plate. The teeth were not long enough to withstand the pullout forces and little benefit was gained. The results showed that the transfer of the load directly to the truss plate significantly decreased the total joint energy absorption by avoiding crushing of the wood by the bolts.

The initial stiffness was lower than that of the unreinforced specimen (HU) indicating a different load path, namely through the truss plate instead of directly from bolt to wood. The curves almost matched in their post-ultimate region. The energy dissipation was 13% lower than the reinforced specimens.

Another drawback was that the fabrication of the welded-on steel plate was difficult and very tedious, and the fumes from welding galvanized truss plates were very toxic. Also the two plates were very thick, and the specimen connection became very heavy.

Specimen Symbol	Bolt d. [in]	Force Ult. [kN]	Diff [%]	Stiffness [kN/m]	Diff [%]	Energy Dis [Nm]	Diff [%]	Ductility []	Diff [%]	Failure Mode
HU-Avg	1/2"	288.3		119.4		5246.0		2.6		row split, row tear-out
HRT-Avg	1/2"	316.7	9.8	97.1	-18.7	7900.1	50.6	7.2	172.9	row shear
HRTW	1/2"	254.2	-11.8	62.0	-48.0	4930.5	-6.0	3.3	26.0	row shear

Table 9. Static tension test results – 1/2 inch 10 bolt truss plate reinforced joints in PSL

The result from this test have illustrated the importance of clearly identifying the major load path and assuring adequate capacity for a controlled failure mode. The role of the truss plate has to be defined (reinforcing element or load carrying element) and the connectors have to be designed accordingly.

The 5/8"10-bolt specimens with truss plates transversely rotated (90 degree angle) after every second row (FRTT in Fig. 62) were tested with the idea to prevent longitudinal movement initiated by the shear stresses at the peak load. In other words, the objective was to prevent a shear plug failure.

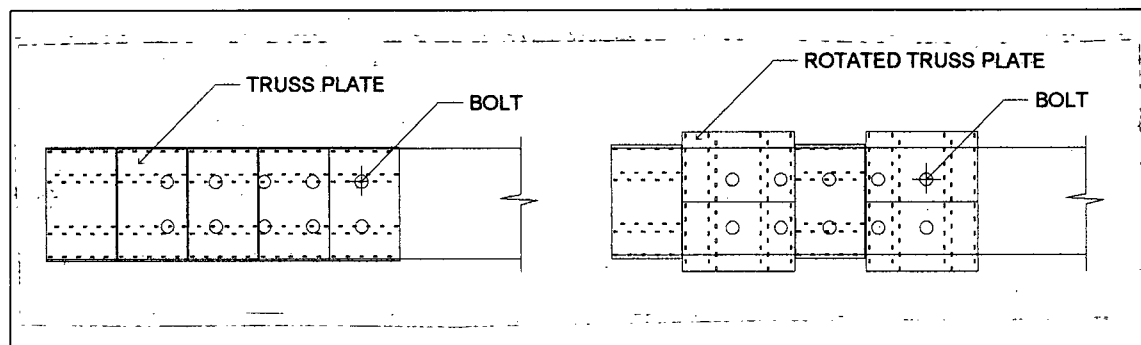


Figure 62. The configurations of regular truss plate (FRT) and transversely rotated truss plate specimen (FRTT)

The opposite result was obtained, however as the failure was brittle (Fig. 60). The ultimate force was by 0.5% lower compared to the unreinforced joints (FU), the ductility was lower by 3.1% and, most significantly, the energy dissipation dropped by 40% (Table 10). There were not enough lateral teeth to hold the specimen together, because half of the teeth were placed in the perpendicular direction. The rotation actually caused the teeth to cut the wood fibers and decrease the net section area of the specimen. The shear plug was not prevented.

Specimen Symbol	Bolt d. [in]	Force Ult. [kN]	Diff [%]	Stiffness [kN/m]	Diff [%]	Energy Dis [Nm]	Diff [%]	Ductility []	Diff [%]	Failure Mode
FU-Avg	5/8"	372.5		275.3		4173.2		3.8		group shear, row shear
FRT-Avg	5/8"	364.93	-2.0	179.15	-34.9	7129.89	70.9	4	5.3	group & row shear, split
FRTT-Avg	5/8"	370.5	-0.6	93.2	-66.2	2491.3	-40.3	3.7	-3.3	group shear

Table 10. Static tension test results – 5/8 inch 10 bolt truss plate reinforced joints in PSL

Globally, the experience from the truss plate connection tests showed that smaller diameter bolts and truss plate reinforcement improved the connection behaviour and increased ductility and energy dissipation of the connection. Also, some energy was absorbed by crushing the truss plate surface (not only by the withdrawal action of the teeth) in order to obtain even distribution of the load among the materials. All the truss plate teeth need to be placed in the direction parallel to the grain in order to obtain maximum withdrawal resistance and to prevent cutting the wood fibers. The truss plate should act primarily in the perpendicular to grain and perpendicular to load direction, functioning as a reinforcing element only.

7.1.4. Nailed Plates

Spiral Nails:

Two types - one of each - nailed plate reinforced specimens were tested in static tension. They were all 5/8" 10-bolt connections. Type I represented 6 separate nailed plates positioned at every pair of bolts leaving one mm gap between the plates. Type II was of the same thickness (18 gauge) plate cut to obtain an "I" shape.

The purpose was to transfer the load to the rear end (less perpendicular to grain stress sensitive) of the specimen, and to prevent cracking along the nail line (nails located only at the two ends), which was a detriment as observed in Specimen type I.

Both curves are compared with the unreinforced specimen (Fig.63). And again, there is almost no improvement in the behaviour of the two: the same initial slope, slight increase in the ultimate strength, and almost no increase in ductility (FRN I +16.6%, FRN II -13%)(Table 11).

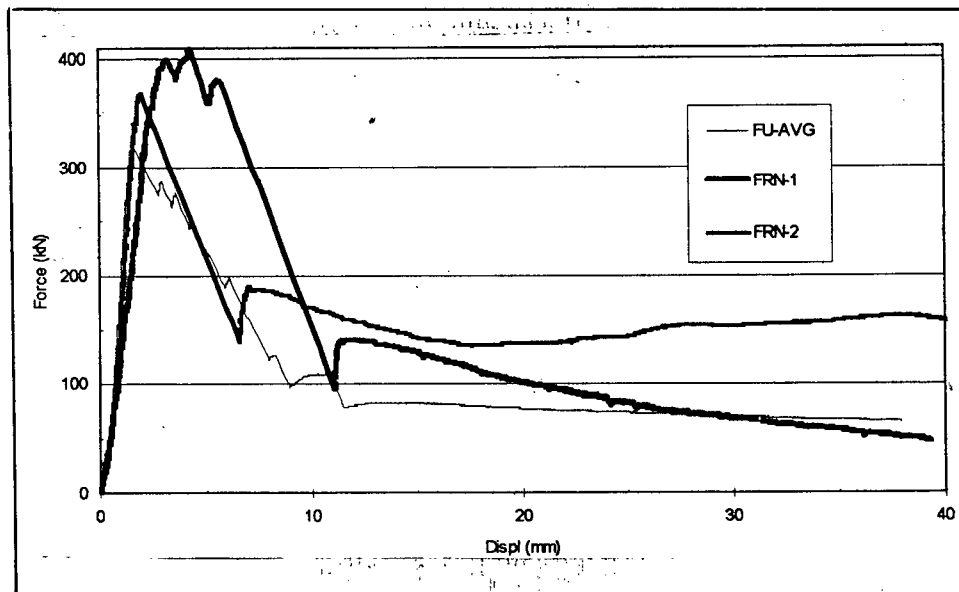


Figure 63. Unreinforced (FU) vs. nailed plate type I (FRN-I) and II (FRN-II) reinforced connections; all P-Δ curves of 5/8" PSL specimens tested in static tension (spiral nails)

Finishing Nails:

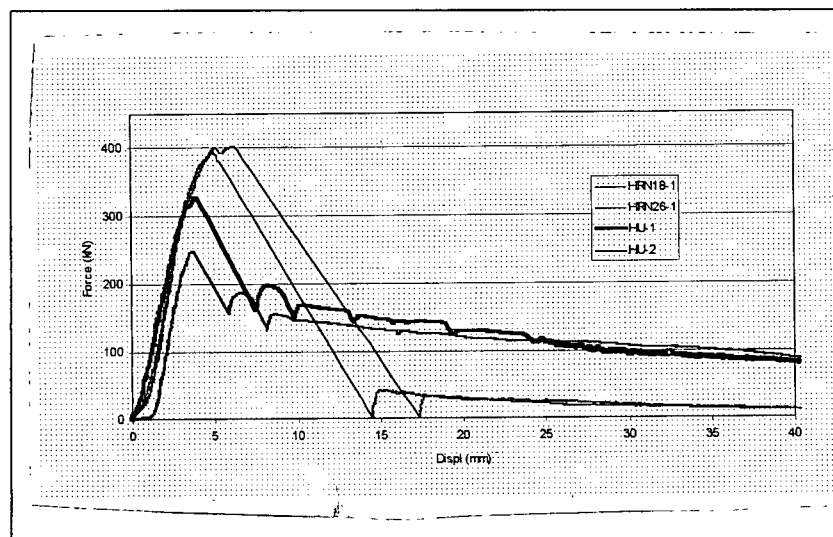


Figure 64. Unreinforced (HU) vs. nailed plate gauge 18 (HRN18) and 26 (HRN26); all P-Δ curves of 1/2" PSL specimens tested in static tension (finishing nails)

The nails were probably too large as they were very stiff, they cut the fibers and were not contributing to ductility and were badly positioned. Cracks occurred exactly on the nail lines.

Specimen Symbol	Bolt d. [in]	Force Ult. [kN]	Diff [%]	Stiffness [kN/m]	Diff [%]	Energy Dis [Nm]	Diff [%]	Ductility []	Diff [%]	Failure Mode
FU-Avg	5/8"	372.5		275.3		4173.2		3.8		group shear, row shear
FRN-I	5/8"	409.27	9.9	154.65	-43.8	5454.49	30.7	4.43	16.6	group shear
FRN-II	5/8"	368.23	-1.1	270.33	-1.8	6645	59.2	3.31	-12.9	row shear

Table 11. Static tension test results – 5/8 inch 10 bolt nailed plate (spiral nails) reinforced joints in PSL

The experience from the use of thick sturdy nails, which were cutting the specimen along the fibers, led to another set of experiments. This time much smaller finishing nails were meant to create a yielding field of thin pins with the load evenly distributed in all the materials. Also, two different gauges of galvanized plates were tried and the objective was to achieve crushing

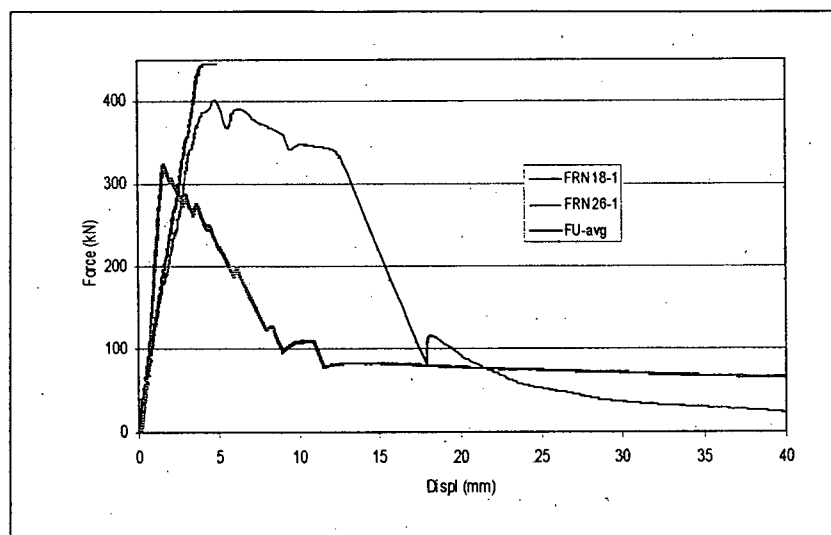


Figure 65. Unreinforced (FU-avg) vs. nailed plate gauge 18 (FRN18) and 26 (FRN26); typical P-Δ curves of 5/8" PSL specimens tested in static tension (finishing nails)

Specimen Symbol	Bolt d. [in]	Force Ult. [kN]	Diff [%]	Stiffness [kN/m]	Diff [%]	Energy Dis [Nm]	Diff [%]	Ductility []	Diff [%]	Failure Mode
HU-Avg	1/2"	288.3		119.4		5246.0		2.6		row split, row shear
HRN18	1/2"	392.8	36.2	134.92	13.0	3529.22	-32.7	3.02	15.3	group shear
HRN26	1/2"	398.92	38.4	131.28	10.0	4195.35	-20.0	3.74	42.7	group shear
FU-Avg	5/8"	372.5		275.3		4173.2		3.8		group shear, row shear
FRN18	5/8"	>445	N/A	112.75	N/A	N/A	N/A	N/A	N/A	not reached
FRN26	5/8"	400.22	7.4	95.07	-65.5	6176.65	48.0	6.77	78.2	group shear

Table 12. Static tension test results – 1/2 and 5/8 inch 10 bolt nailed plate (finishing nails) reinforced joints in PSL

to create a yielding field of thin pins with the load evenly distributed in all the materials. Also, two different gauges of galvanized plates were tried and the objective was to achieve crushing and local yielding of the plate at the bolt position.

Similar crushing as for the truss plates was observed. A soft nailed plate was designed to simulate this behaviour of a truss plate with longer and slender teeth. Both plate gauges were tested on the ½" and 5/8" 10-bolt connection (Fig. 64, 65).

Even though different nail sizes and plate thicknesses were used, the results obtained were not desirable in most of the configurations (Table 12).

Although some increase in ductility and energy dissipation was observed, the failure was sudden and brittle in all cases. The FRN18 connection reached the capacity of the actuator (445kN), because of its high stiffness and strength, therefore it could not fail. Promising results were obtained with the thin plate specimen (FRN26), where both energy dissipation and ductility improvements were positive and of high value.

The expected crushing damage at the bolt was observed in the 0.6mm plate, but the finishing nails were not suitable for such high loads. The nails were pulled through the galvanized plate. The 1.2mm plates were too stiff and they attracted high loads into the joint, causing high shear stresses along the bolts and splitting the connection. A typical brittle failure mode is shown in Fig. 66.

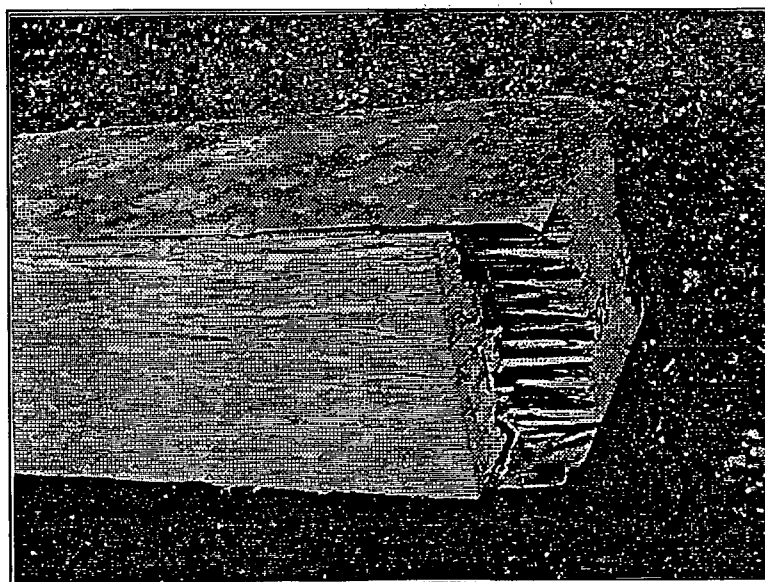


Figure 66. Shear plug failure of 5/8"18 gauge nailed plate (finishing nails) reinforced PSL specimen.

7.1.5. Glued-on Plates

In the case of epoxy glued-on steel plates, a 10-bolt connection, because of its high strength, was reduced to six 5/8" bolt connection. When the 10-bolt case was initially tested, the actuator reached its capacity (450kN) and failure could not be achieved.

The epoxy glued plates were separately placed on both specimen surfaces, one plate per two parallel bolts. Also, there was one plate glued on the end area of the joint with no holes punched in it.

The results were very consistent, but very brittle; similar to the unreinforced equivalents with the same strength and little lower initial stiffness (Fig. 67). The ductility was even decreased by 22.3% (Table 13).

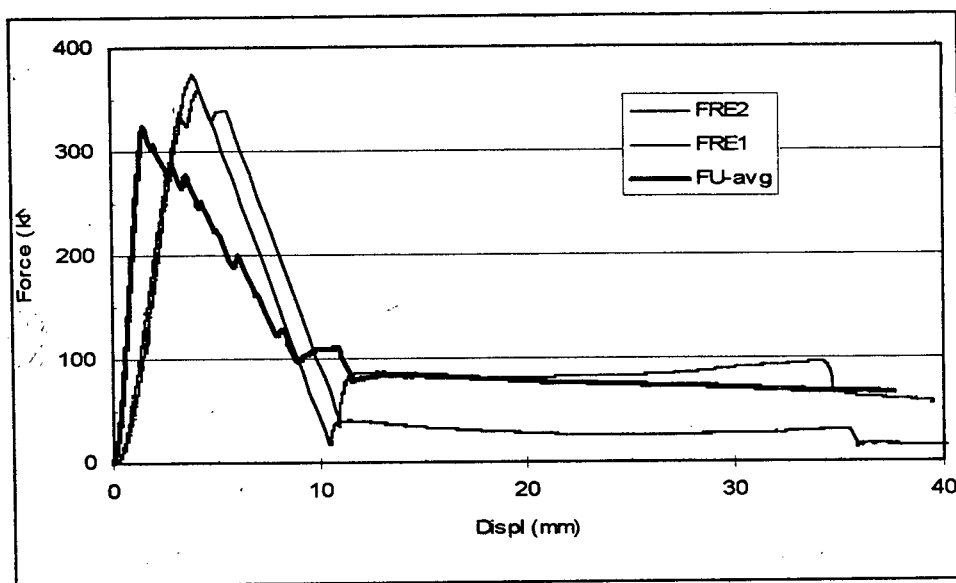


Figure 67. Unreinforced (FU-avg) vs. epoxy glued-on plate reinforced (FRE) connections; all P-Δ curves of 5/8" PSL specimens tested in static tension

Specimen FRE-1 failed by row shear, and FRE-2 by group shear. In both cases all the glued plates peeled off the surface, which can be attributed to the different Young's moduli of the epoxy, wood and steel resulting in significant shear stresses along the glued planes. The failure surface consisted of approximately 50% glue-steel interface and 50% wood failure.

the epoxy, wood and steel resulting in significant shear stresses along the glued planes. The failure surface consisted of approximately 50% glue-steel interface and 50% wood failure.

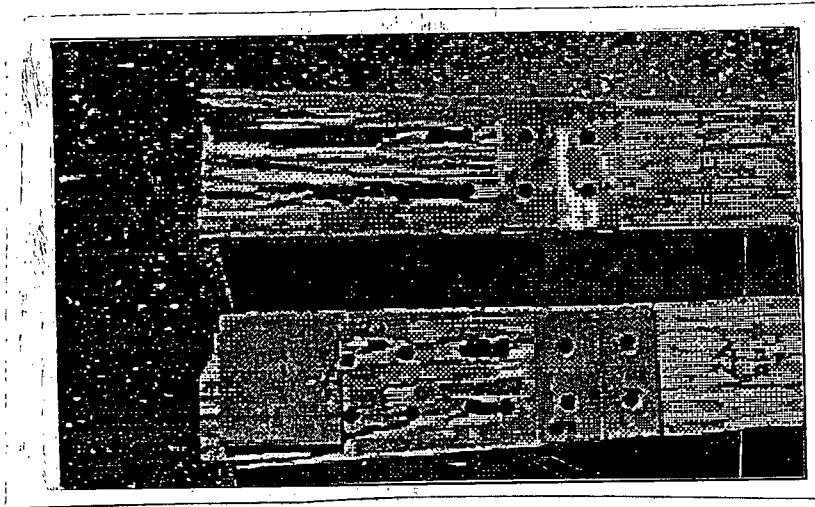


Figure 68. Shear plug and row shear-out failure of 5/8" epoxy glued-on plate reinforced PSL specimens

Specimen Symbol	Bolt d. [in]	Force Ult. [kN]	Diff [%]	Stiffness [kN/m]	Diff [%]	Energy Dis [Nm]	Diff [%]	Ductility []	Diff [%]	Failure Mode
FU-Avg	5/8"	372.5		275.3		4173.2		3.8		group shear, row shear
FRE-Avg	5/8"	366.075	-1.7	129.695	-52.9	1712.915	-59.0	2.95	-22.4	group shear, row shear

Table 13. Static tension test results – 5/8 inch 10 bolt epoxy glued-on plate reinforced joints in PSL

7.1.6. Glued-in-Rods

The behaviour of glued-in rebars (HRERe) and glued-in lag screws (HRER) was compared in the 1/2" 10-bolt connection tension tests. The glue (epoxy) was meant to fill the gap between the reinforcing element and the wood. In the case of the lag screw the gap was minimal because the hole was the same as the shank of the screw in its threaded part. The glue was expected to increase the stiffness of the connection, which was not confirmed in the results in Table 14 and the graph in Fig. 69. The initial stiffness of the joint was in both cases the same as that of the unreinforced specimen. The ductility increased by 55-60 % and the energy absorption was on the same level. The glued in rebar connections reached on average 328 kN and the glued-in lag screw joints 380 kN. Both joint configurations failed in a brittle failure mode. All four joints developed a group bi-axial shear plug (Fig 70).

As expected, the lag screw specimens failed at much higher displacements than the rebar connections (6 mm). This was probably due to the higher withdrawal resistance of the screw in

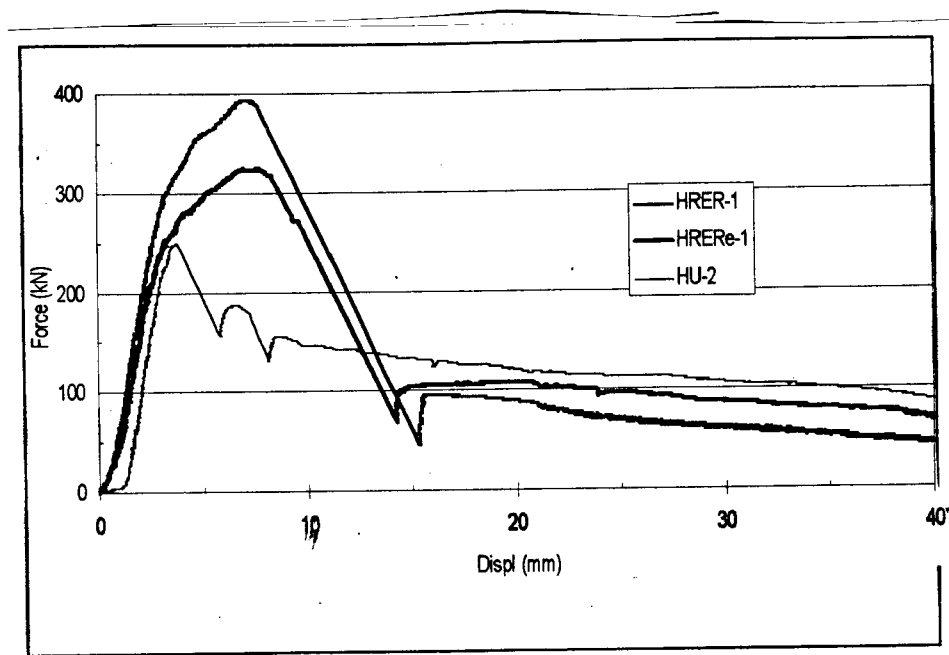


Figure 69. Unreinforced (HU) vs epoxy glued-in lag screw (HRER) and rebar (HRERe) reinforced connections; all P-Δ curves of 1/2" PSL specimens tested in static tension

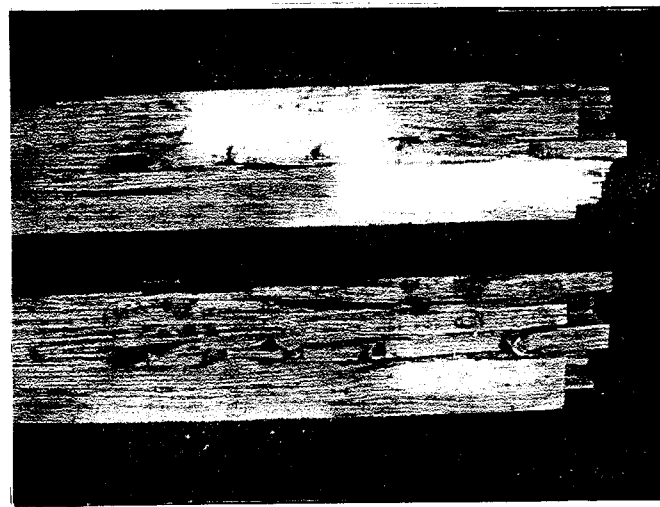


Figure 70. Failure along the reinforcing screws of 1/2" epoxy glued-in lag screw reinforced PSL specimens

Specimen Symbol	Bolt d. [in]	Force Ult. [kN]	Diff [%]	Stiffness [kN/m]	Diff [%]	Energy Dis [Nm]	Diff [%]	Ductility []	Diff [%]	Failure Mode
HU-Avg	1/2"	288.3		119.4		5246.0		2.6		row split, row shear
HRER-Avg	1/2"	380.88	32.1	96.92	-18.8	6372.48	21.5	4.07	55.3	group shear
HRERE-Avg	1/2"	328.74	14.0	105.45	-11.6	4756.98	-9.3	4.23	61.5	group shear

Table 14. Static tension test results – ½ inch 10 bolt epoxy glued-in rod reinforced joints in PSL

7.1.7. Load Distribution among Bolts in a Row

The distribution of the applied connection load among the bolts was of interest after testing the specimens in tension. It was technically complicated to measure the midspan deflection of the bolts during the test, therefore the results were obtained after the failure at 40mm total displacement, after the specimen had been dismantled from the test setup. The measured deflections therefore did not include the elastic deformations. Although the residual plastic deformations are not strictly a measure of load, it does indicate the progression of deformation, which is assumed to resemble the deformation distribution pattern in the elastic range. It was found that lower diameter bolts ($3/8"$, $1/2"$) bolts had reached the yield plateau at the end of the test, which was always at a displacement of 40mm. In some cases, $5/8"$ bolts did not have any plastic deformations.

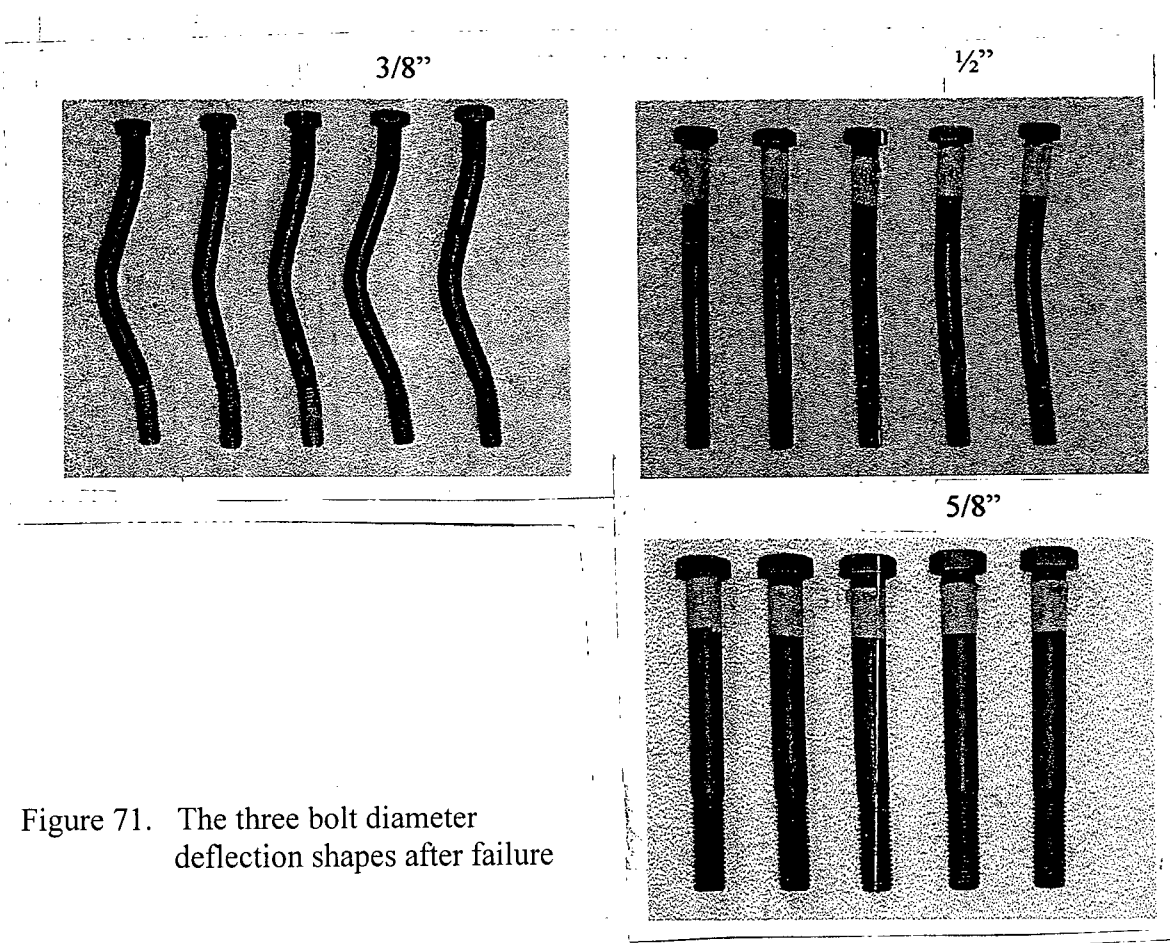


Figure 71. The three bolt diameter deflection shapes after failure

As the previous single connector bending tests showed (Sec 3.2.2.), the bolts approximately followed a bilinear elasto-plastic load-slip curve.

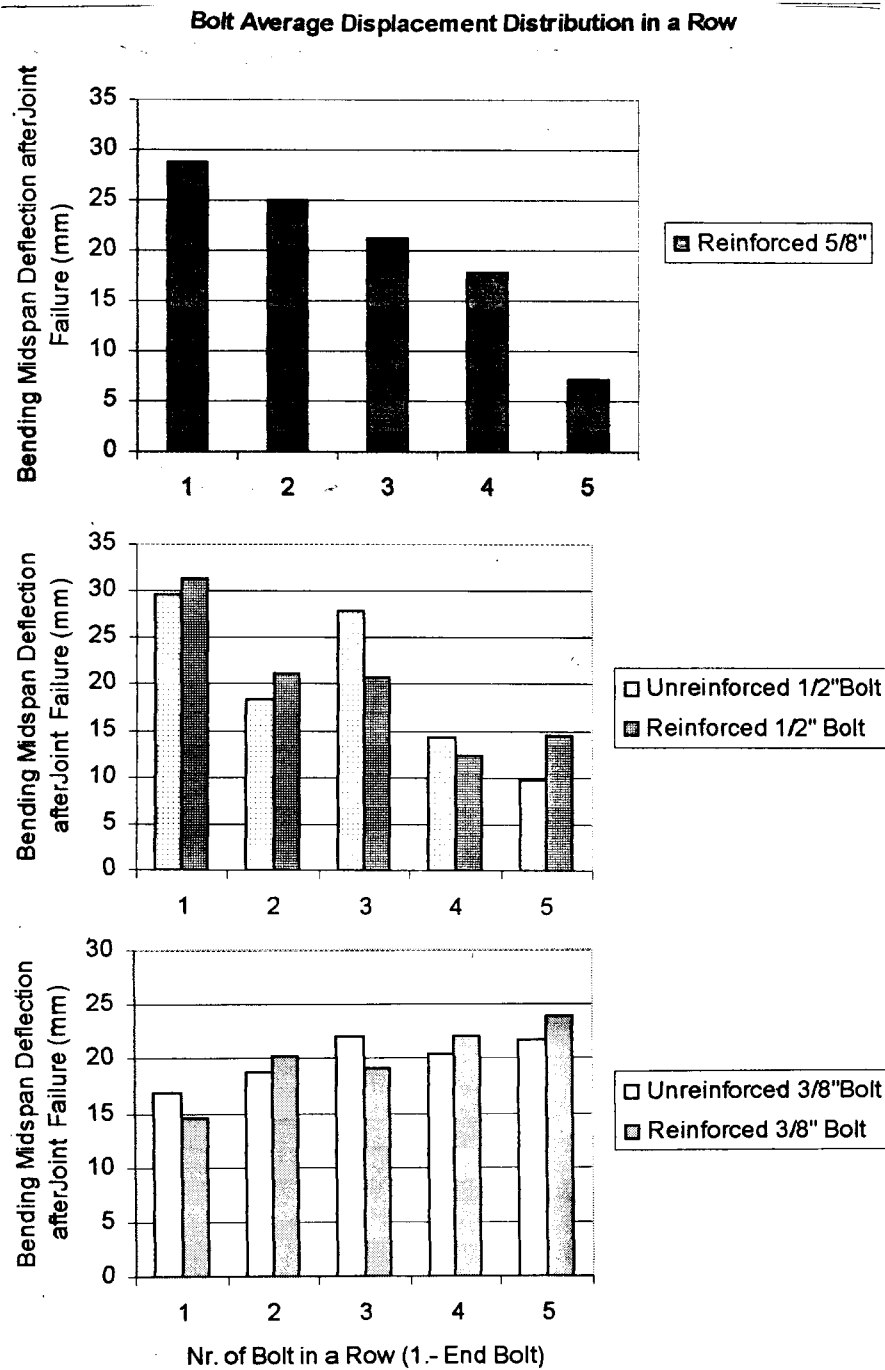


Figure 72. Average bolt bending-displacement distribution in a row of 5/8", 1/2" and 3/8" 10-bolt reinforced and unreinforced connections

The deflection of the bolts used in the connections was measured according to the procedure that is shown in Sec. 6.5. The data were averaged and divided into the three groups according to the bolt diameters (3/8", 1/2" and 5/8"). The other aspect considered was if the connection was reinforced or not.

As can be seen on the charts (Fig. 71, 72), in the 5/8" bolt reinforced case the majority of the load was carried by the end bolt and decreased towards the last bolt in the row. As the bolt diameter was reduced the deflection was gradually redistributed almost in the opposite order. Both the unreinforced and reinforced equivalents on average followed similar distribution patterns in each diameter case. In the 9.5mm case the distribution was more equalized, indicating a better load distribution.

7.1.8. 086.1-94 CSA Code Strength Calculation vs. Experimental 5-th Percentile Value of Unreinforced Connections

The code value of ultimate load was compared to the tested fifth percentile of the load obtained from the tension tests. All adjustment factors were set to be equal to 1.0, except the group factor J_F , and the load duration factor K_D , that were calculated according to the code. The mean tested value for density used in the embedding strength formula was used in the code calculations. A separate value was used for the two materials PSL and Glulam. To satisfy consistent moisture content conditions as used for the code formula for embedding strength (Hilson, Larsen, Smith, Whale), the density at 12% of moisture content was used for both materials. By coincidence the Glulam timber had the mean moisture content of 12%, therefore its measured mean density was used in the calculations. In the case of PSL, the moisture content was in the range of 7.4-10.6%. Therefore, the density was interpolated from the tested values to obtain the density at 12% using the linear relation in the graph (Fig. 73). All PSL and Glulam data from monotonic tests were used for this purpose. The moisture content was always measured after the test.

Also, the true measured value of the bolt yield stress was used in the code calculations. The five bolts of each 15.9, 12.7, 9.5 mm in diameter were tested in bending using the same stock of bolts as were used for the static tension and reverse cyclic tests (see Sec. 7.1.7.).

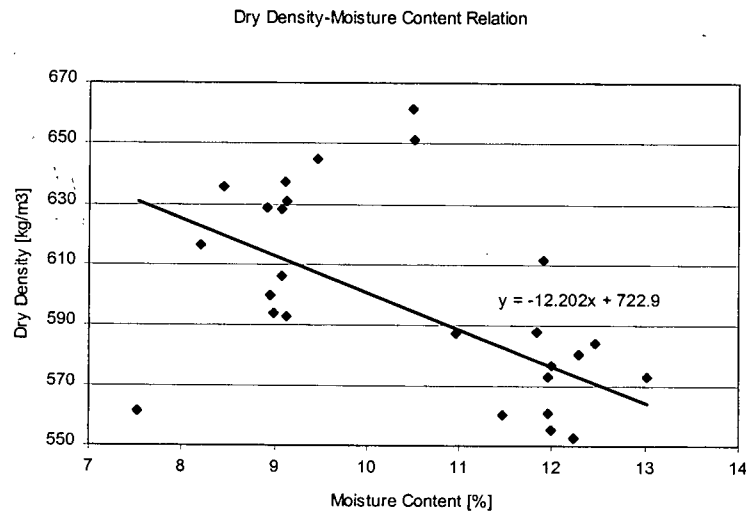


Figure 73. Density-moisture content relation – PSL reinforced and unreinforced connections

Factored lateral resistance of a 10 bolt 89x140 steel-wood-steel connection in PSL loaded parallel to grain for 3/8"(9.5 mm) diameter bolt
(CSA O86.1-94 sec.10.4.4.1):

$$P_r = \phi \cdot P_u \cdot n_s \cdot n_f \cdot J_F$$

$$\phi = 1.0$$

$$P_u = p_u (K_D K_{SF} K_T)$$

$$K_D = 1.25 \text{ (standard duration of loading)}$$

$$K_{SF} = 1.0 \text{ (service conditions-dry)}$$

$$K_T = 1.0 \text{ (fire retardant treatment- not treated)}$$

$$n_s = 2 \text{ (nr. of shear planes per bolt)}$$

$$n_f = 10 \text{ (nr. of bolts)}$$

$$J_F = J_G \cdot J_L \cdot J_R = 0.82(1.0)(0.8) = 0.666$$

$$J_G = 0.33(l/d)^{0.5}(s/d)^{0.2}N^{-0.3} \text{ (for 2-12 bolts in a row)}$$

$$J_G = 0.33(89/9.5)^{0.5}(51/9.5)^{0.2}5^{-0.3} = 0.82$$

$$J_L = 1.0 \text{ (for loaded end distance)}$$

$$J_R = 0.8 \text{ (nr. of rows- 2)}$$

$$l = 89 \text{ mm (main member thickness)}$$

$$d = 9.5 \text{ mm (bolt diameter)}$$

$$s = 4d = 38 \text{ mm (bolt distance in the row)}$$

$$N = 5 \text{ (nr. of bolts in a row)}$$

$p_u = 7.84 \text{ kN}$ – the unit lateral resistance, which was the smallest from:

(10.4.4.-page121)

- a) $F_1 \cdot d^2 \cdot l_1 / d = 82.89 \text{ kN/shear plane}$
- c) $F_1 \cdot d^2 / 2 \cdot f_2 / f_1 \cdot l_2 / d = 12.73 \text{ kN}$
- d) $F_1 \cdot d^2 \{ [1/6 \cdot f_2 / (f_1 + f_2) \cdot f_y / f_1] + l_1 / 5d \}^{0.5} = 7.84 \text{ kN}$
- g) $F_1 \cdot d^2 \{ [2/3 \cdot f_2 / (f_1 + f_2) \cdot f_y / f_1] \}^{0.5} = 10.68 \text{ kN}$

$$F_1 = 0.8f_1 = 0.8(574) = 459.2 \text{ MPa}$$

$$f_2 = 63G(1 - 0.01d) = 63(0.49)[1 - 0.01(9.5)] = 37.63 \text{ (embedd. strength-main member)}$$

$$G = 0.66 \text{ (tested interpolated density of PSL at 12\% moisture)}$$

$$f_y = 929 \text{ MPa (bolt bending yield stress – from the real bending tests)}$$

$$\text{(ASTM A449 CSA G40.21- grade 5 is 350 MPa)}$$

$$f_1 = 574 \text{ Mpa (side member yield stress was not tested– ASTM A36 CSA G40.21)}$$

$$l_2 = 89 \text{ mm (main member thickness)}$$

$$l_1 = 19 \text{ mm (side member thickness)}$$

$$\underline{P_r = \phi \cdot P_u \cdot n_s \cdot n_f \cdot J_F = 1.0(9.8)(2)(10)(0.66) = 128.89 \text{ kN}}$$

The code values calculated according to the aforementioned spreadsheet were compared to the fifth percentile of the strength from the test results.

The fifth percentile was determined from the formula valid for normal distribution :

$$x_p = m_x \pm k\sigma$$

where m_x is the mean value of the strength obtained from the tension tests, k is coefficient which varies for different percentile values (in the lower 5 % case $k = -1.645$), σ is the standard deviation equal to :

$$\sigma = \text{cov}^* m_x$$

where $\text{COV} = 0.1$ is coefficient of variation obtained from the statistical data of the previous research project (Hockey, 1999)

The following unreinforced connections were compared :

10-15.9 mm (5/8") bolt in PSL,
10-12.7 mm (1/2") bolt in PSL,
10- 9.5 mm (3/8") bolt in PSL,

10-12.7 mm (1/2") bolt in Glulam,
10- 9.5 mm (3/8") bolt in Glulam

The tested fifth percentile and calculated code strength values of unreinforced specimens are summarized in the Table 15.

Glulam Symbol	P _{ult} (avg) [kN]	P(5%) [kN]	Code Value [kN]	Difference [%]
GHU-Avg	306.57	256.14	154.73	65.54
GTU-Avg	260.80	217.90	100.90	115.96

PSL Symbol	P _{ult} (avg) [kN]	P(5%) [kN]	Code Value [kN]	Difference [%]
FU-Avg	372.50	311.22	201.32	54.59
HU-Avg	288.30	240.89	158.10	52.37
TU-Avg	175.34	146.50	103.11	42.08

Table 15. Code prediction vs. test fifth percentile connection strength (Glulam, PSL)

These results indicate that the code predictions are on the conservative side, probably because they had been based on the European yield model assumptions. The tests showed that the failure modes of multiple bolted connections were almost always brittle. Only the 3/8" diameter bolt connection (GTU, TU) was partially approaching the ductile-plastic modes by its wood crushing mode, which was more significant than in the 5/8" and 1/2" bolt case. The yield load would be expected to be higher in more ductile cases (3/8"). This is apparent in the 3/8"-bolt PSL connection case. The difference in strength between the code prediction and the test result of the glulam 3/8" unreinforced joints is lower than in the 1/2" unreinforced connections. The difference in strength of Glulam in the code and according to the test results could have been caused by variability in the wood product and approximate assumptions of the material properties in the code.

7.2. REVERSE CYCLIC TESTS

The ISO-standard protocol (Sec. 5.2.2) was followed, where the displacement amplitudes were gradually increased in steps, with equal steps expressed as 20% of the displacement at maximum load from the monotonic tension tests (e.g. 4mm x 20% = 0.4mm step). This way 100% displacement was reached after 15 cycles (5x3cycles). Due to different displacements of different connection configurations in monotonic tests, the displacement steps of cyclic protocols varied (Appendix III):

- 5/8" unreinforced connections in PSL (FU-C)

0.4mm

- 5/8" lag screw reinforced connections in PSL (FRR-C)	0.8mm
- 5/8" truss plate reinforced connections in PSL (FRT-C)	0.8mm
- 1/2" unreinforced connections in PSL (HU-C)	0.8mm
- 1/2" lag screw reinforced connections in PSL (HRR-C)	0.8mm
- 1/2" truss plate reinforced connections in PSL (HRT-C)	0.8mm
- 3/8" unreinforced connections in PSL (TU-C)	0.8mm
- 3/8" lag screw reinforced connections in PSL (TRR-C)	4.0mm
- 3/8" lag screw reinforced connections in Glulam (GTRR-C)	2.5mm

For each amplitude the cycle was repeated three times. The first single cycles were skipped, because sensitivity of the electronic controller was lower than the protocol displacements. After the maximum load of the particular connection had been reached, the number of cycles per step was reduced from three to one.

The hysteresis loops of dowel-like connections are usually pinched, which was confirmed with all the tested bolted specimens. The loops were relatively more slender in the cases where the ultimate displacements of the static tension tests were smaller (mostly unreinforced joints). Therefore the displacement protocol steps were chosen to be relatively small. The load-slip diagrams were diagonally symmetrical about both horizontal and vertical axes. All the tested connections in most cases failed in tension, also the ultimate strength was lower in the tension part. Although the data in both parts of the graph were collected, due to the symmetry only the quantities in the tension part were considered for numerical comparison.

After each cycle with the same amplitude (the same displacement step) the strength degradation was observed. This drop in load was caused by damage in the wood fibers, which was the most severe at the second cycle of each displacement step. This degradation decreased the energy dissipation of subsequent cycles but it did not seem to have a significant influence on the connection ductility. In the zero-displacement zone most of the load was carried by the bolts, and the energy was dissipated by the bolts yielding in bending.

The hysteresis loops were changing throughout the protocol. Single loops of the 12.7mm 10-bolt lag screw reinforced joint at three stages are shown in Fig 74. The loop in the near-elastic part was slender with a steep slope of stiffness. In the stage that included the peak load (second loop), significant energy was dissipated as represented by a much larger area of the loop and also the middle "slack" zone was significantly wider. That meant the bolts were greatly contributing to the joint energy dissipation by yielding in bending. The third loop reflected behaviour at the

second peak, when the reinforcing rods approached the bolt position. That increased the strength of the joint, but the slack zone was also reduced. This indicates excessive wood crushing around the bolts, which reduces the bending contribution of the resistance.

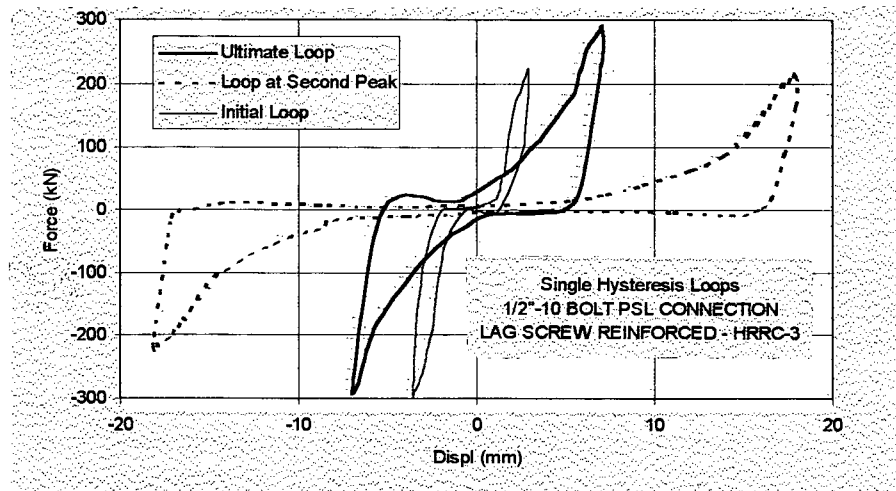


Figure 74. Single hysteresis loops at three stages –connection HRRC-3

When the same type of connections tested in monotonic tension were compared to the reverse cyclic tests, the monotonic tension curve in terms of behaviour followed the envelope of the cyclic diagram in all cases, but was higher in strength capacity by approximately 18 % as can be seen in Fig. 75.

All the individual data sets are documented in Appendix I.

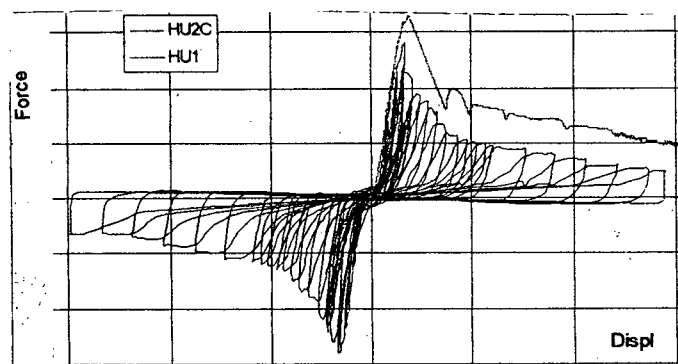


Figure 75. Static tension compared to the reverse cyclic behaviour – $\frac{1}{2}$ " 10 bolt unreinforced connection in PSL

7.2.1. Unreinforced Specimens

The most significant pinching was observed in the unreinforced connections. Each of the three diameters of the bolts (15.9, 12.7, 9.5 mm) had a different influence on the connection behaviour. 15.9 mm bolt connections (FU 1-3) were the most brittle and the least energy absorbing with the stiffest elastic part and the most sudden post-ultimate drop. The average displacement value at ultimate load reflected this behaviour. As the L/d ratio of the bolts increased (5.6, 7.0, 9.3) the average displacement at ultimate load gradually increased respectively as follows: 2.93, 3.75 and 5.12 mm.

This softening of the connection as the bolt L/d ratio was increased, is recognized to a certain degree in all the connections. This trend is shown separately for each type of connection tested in reverse cyclic loading in Fig. 87 in the following section 7.2.4., where the elastic stiffness against the ultimate displacement was plotted.

The 9.5mm (3/8") bolt connection had the highest ductility ratio (5.4), a distinctly more ductile failure mode with significant wood crushing, although splitting still occurred at large displacements. Ductility of the 1/2" and 5/8" unreinforced connections was much lower; 1.7 and 1.6 respectively.

The load capacity (5 to 10kN) in the "slack" zone of the load-slip graph was more significant with the 3/8" bolt connections, compared to the 1/2" and 5/8" connections (5kN and almost 0kN).

This is due to the fact that the more slender bolts dissipated significant amount of energy through cyclic bending, whereas mostly irrecoverable crushing dominated the behaviour of more stocky bolts. In the latter case a gap would open up around the bolt along the entire length, leading to the slackness around the neutral displacement position.

Average energy dissipation after 100mm of cumulative cyclic displacement for 5/8", 1/2" and 3/8" unreinforced connections was 483, 2191 and 1580Nm respectively. The three unreinforced connections with three bolt sizes are plotted in Fig. 76.

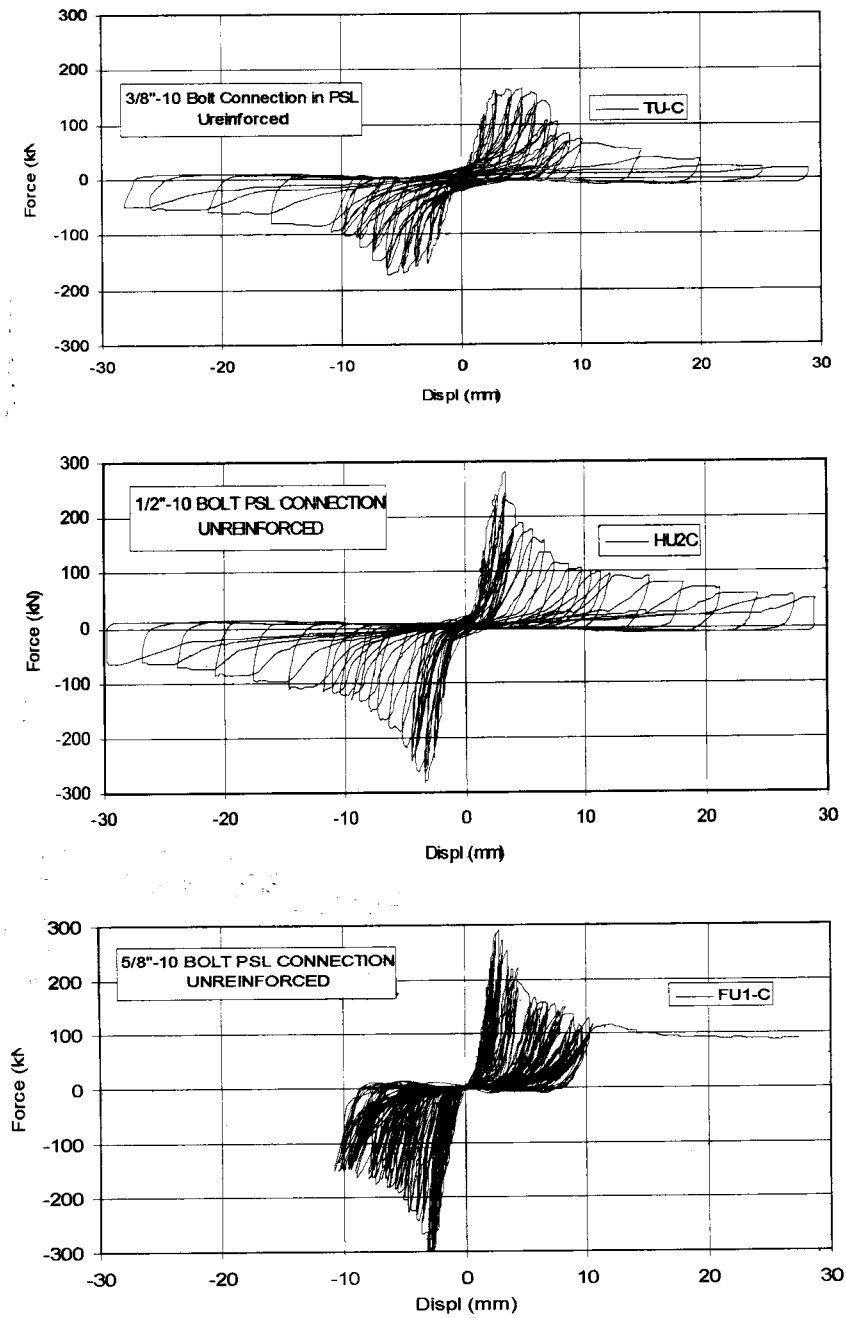


Figure 76. Cyclic load-slip curves of unreinforced PSL connections

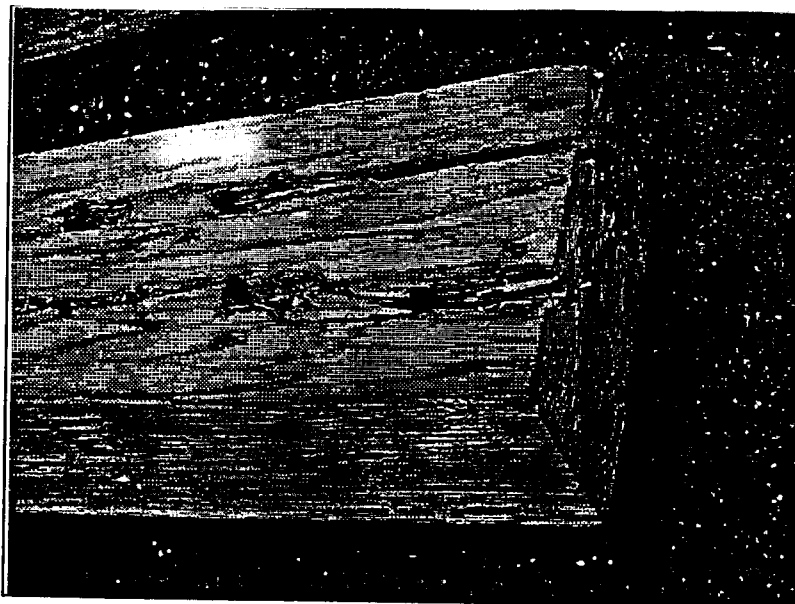


Figure 77. Row shear-out failure of 1/2" unreinforced PSL specimen tested in reverse cyclic loading

7.2.2. Truss Plates (Gang Nail Plates)

Due to the variability in the PSL specimens, truss plates showed a decrease in the joint elastic stiffness (-15.5% and -22.4% in 5/8" and 1/2" bolt case respectively).

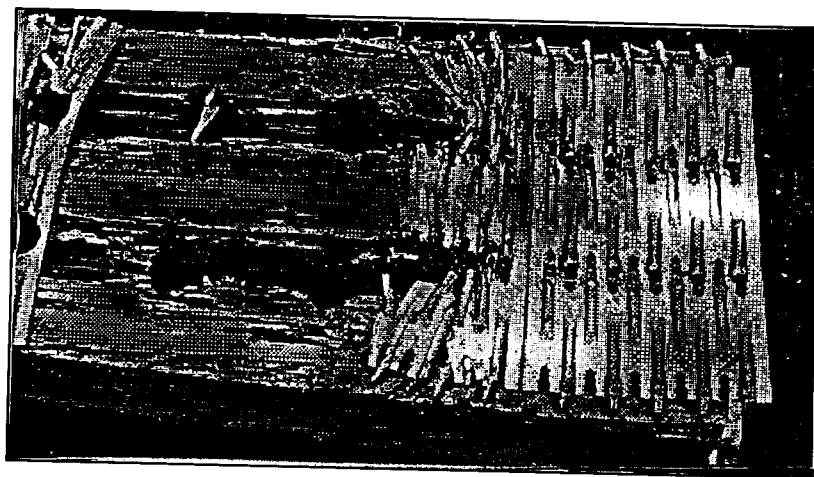


Figure 78. Row shear-out failure of 1/2" truss plate reinforced PSL specimen tested in reverse cyclic loading

Reinforcement increased the ductility by 12.7% and 18.7%, compared to the unreinforced connections. The strength capacity change for the 5/8" and 1/2" bolt connections was +18% and -5% respectively. Average energy dissipation after 100mm of cumulative cyclic displacement for 5/8" and 1/2" truss plate reinforced connections was 2454 and 2025Nm respectively. These

values were not compared to the energy dissipation of unreinforced connections, because it was not conclusive due to different displacement step in the loading protocol of each connection type (see Sec.7.2).

All the truss plate reinforced specimens failed in either one of the brittle failure modes: row shear and row splitting (Fig. 78).

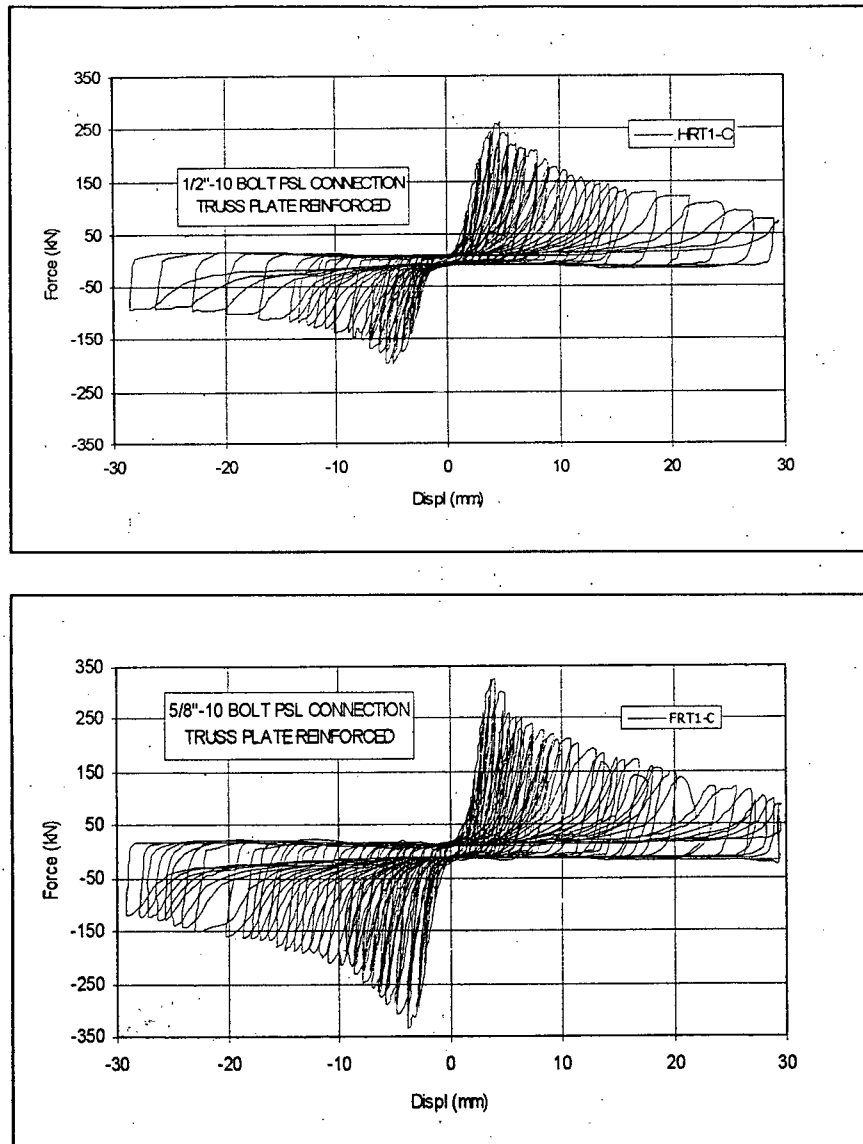


Figure 79. Cyclic behaviour of 5/8" and 1/2" 10-bolt truss plate reinforced connections

After the failure, all the truss plates were crushed on their surface and the teeth were bent. As mentioned in the static tests section, the truss plate teeth were not long enough to remain lodged in the wood for such large displacements and eventually the whole truss plate was

withdrawn from the wood fibers causing a radical drop in strength and stiffness. The cyclic motion proved to be more detrimental to the truss plate connection behaviour, compared to the static tension loading.

The 5.9mm (3/8") truss plate connections were not tested in cyclic loading, because the lag screw connections showed better results in the static tension tests.

Fig. 79 shows the hysteresis curves for the two truss plate connections tested under cyclic loading.

7.2.3. Threaded Rods – Lag Screws

In the case of the lag screw reinforced joints, the higher L/d ratio of the bolts also had a positive influence on the connections. A 60% increase in strength was observed for the 9.5mm case, and 13.6% for the 15.9mm case. The 12.7mm bolted connection had no increase in strength compared to the unreinforced connection (-3.5%). Compared to the unreinforced joints, the 1/2" bolt connections experienced the largest increase in ductility (191%). Even if the 3/8" bolt connection reached on average the highest ductility ratio (8.67), its relative increase in ductility was small (60%), because the unreinforced specimens behaved quite well (ductility of 5.43). As observed before, the 5/8" bolt joints had on average the lowest ductility (4.85, 81 % improvement over the unreinforced connections). The load-slip curves of the 3/8" (TRR-C), 1/2" (HRR-C) and 5/8" (FRR-C) 10-bolt lag screw reinforced connections are shown respectively in Fig.80, 81 and 82.

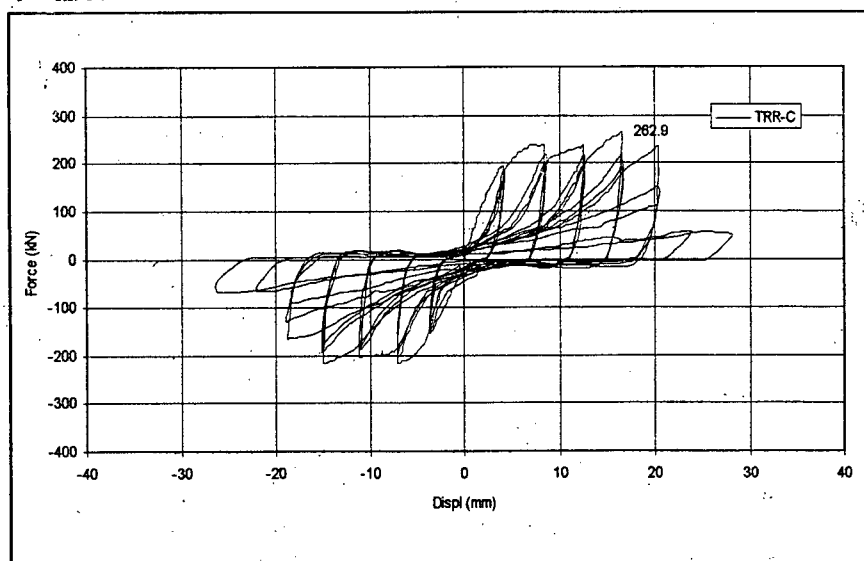


Figure 80. Cyclic behaviour of 3/8" 10 bolt lag screw PSL reinforced connections

The frequently observed second peak on the load-displacement envelope, caused by the contact of the bolts with the reinforcing screws, shifted the high strength capacity much further, compared to the truss plates. However, once the bolts contacted the lag screws, failure was typically initiated and the drop in the load was significantly faster. In spite of that, ductility of

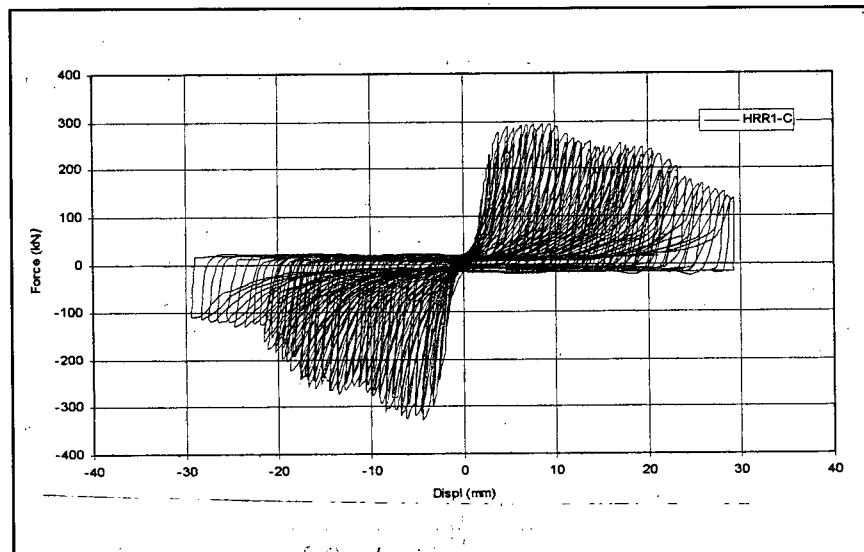


Figure 81. Cyclic behaviour of 1/2" 10 bolt lag screw PSL reinforced connections

the lag screw reinforced joints was satisfying, because the sudden drop occurred at very high displacements (around 20 mm in the 1/2" and 3/8" cases and 4mm in the 5/8" case).

Average energy dissipation after 100mm of cumulative cyclic displacement for 5/8", 1/2" and 3/8" lag screw reinforced connections in PSL was 1265, 1820 and 4784Nm respectively. The 3/8"-bolt lag screw reinforced connections in Glulam dissipated 3579Nm. These values were not compared to the energy dissipation of unreinforced connections, because it was not conclusive due to different displacement step in the loading protocol of each connection type (see Sec.7.2).

For the most slender bolts (3/8" in diameter) the failure mode was fully ductile consisting of significant wood crushing, while the bolts greatly contributed to the energy dissipation in bending (Fig. 83). No cracks were seen on the surface of either the glulam or PSL 3/8"-bolt specimens.

Thick and less pinched hysteresis loops were observed, with relatively higher loads in the zero displacement (slack) zone.

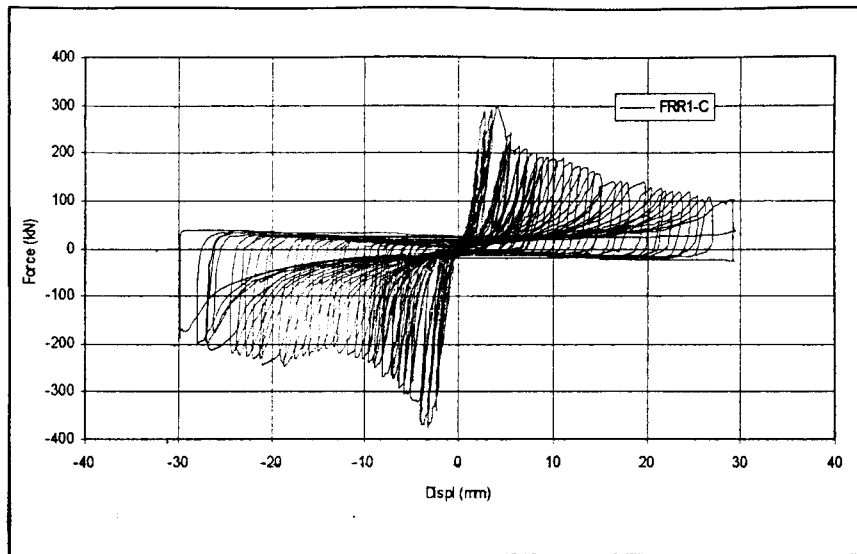


Figure 82. Cyclic behaviour of 5/8" 10 bolt lag screw PSL reinforced connections

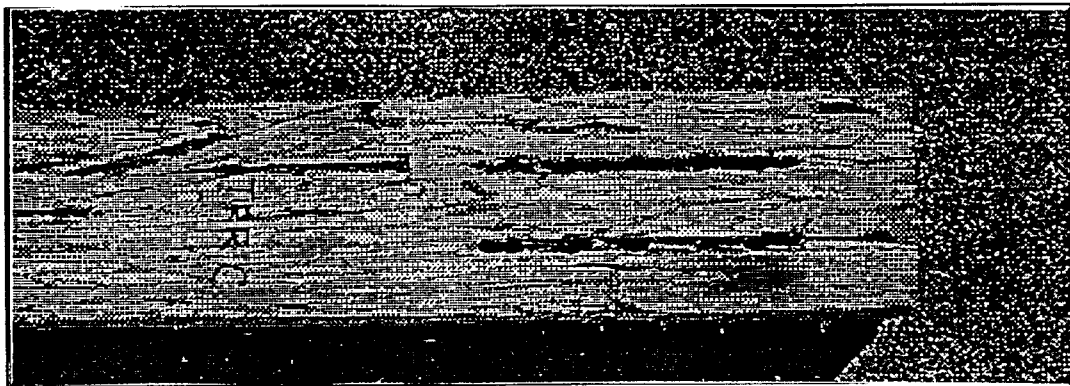


Figure 83. Row shear-out failure of 3/8" lag screw reinforced PSL specimen tested in reverse cyclic loading

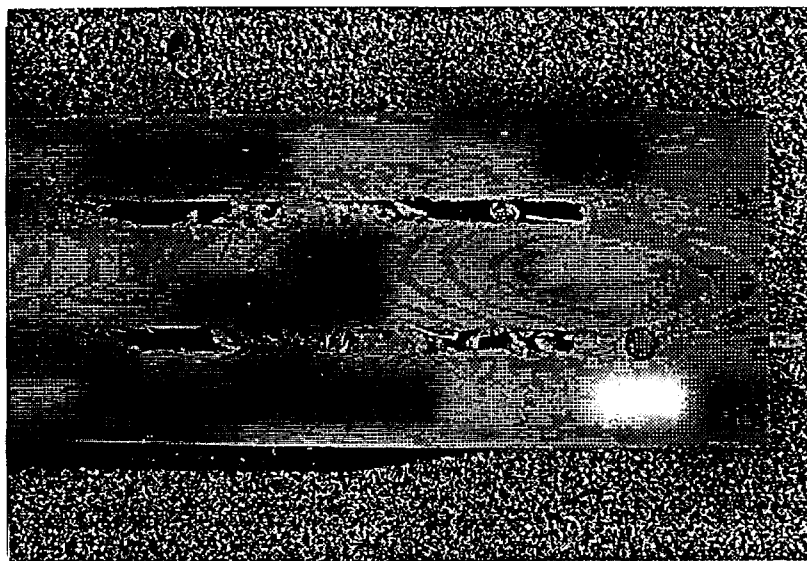


Figure 84. Failure of 3/8" lag screw reinforced Glulam specimens tested in reverse cyclic loading

The glulam connections (failure in Fig. 84) showed more strength and less ductility (P- Δ curve in Fig 85) than their PSL equivalents, which is similar to what was observed for the static tension tests. Another difference was observed. Due to the higher embedding strength of glulam (see embedding strength in Chap. 2.1.7.), the bolts in the connection GTRR-C (3/8") failed in low-cycle fatigue. This happened in stages: at the 22.5mm amplitude two end bolts broke, at 25mm all except two bolts in the bottom failed also in fatigue.

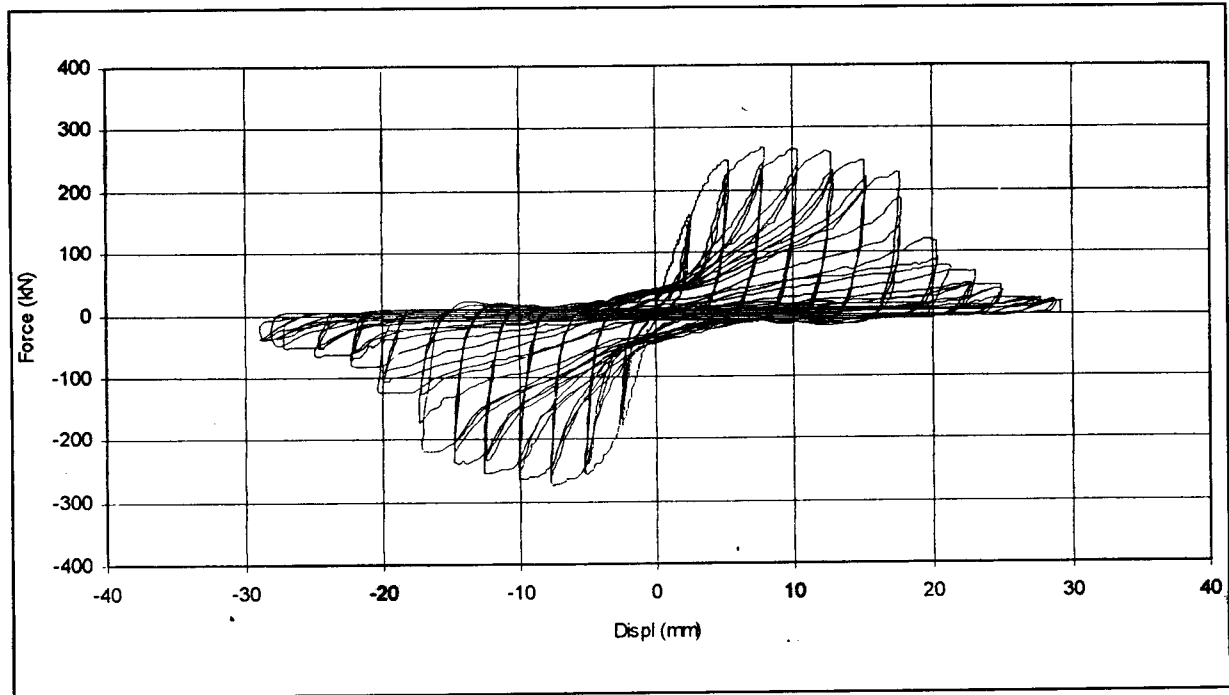


Figure 85. Lag screw reinforced; P- Δ curves of 3/8" Glulam specimens tested in reverse cyclic loading

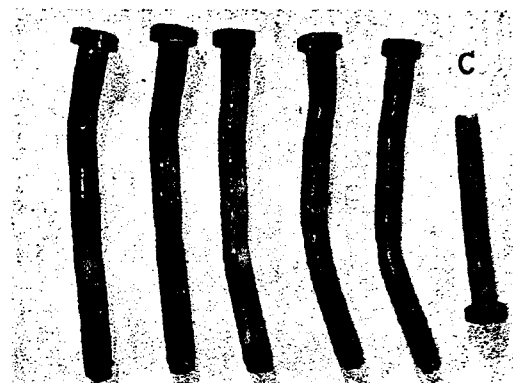
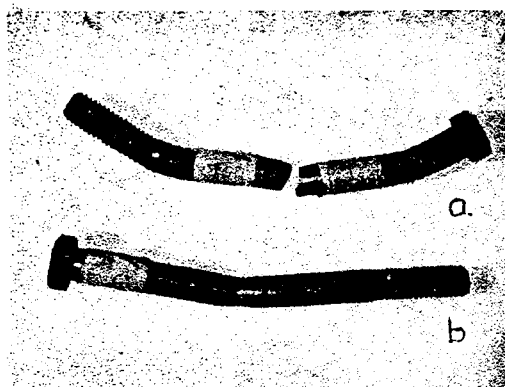


Figure 86. Fatigue failure of 3/8" bolts

- (a) broken bolt in one of the hinges
- (b) reduced cross section at hinge location

- (c) typical shape of 3/8" bolts after failure

Fig. 86 shows a typical fatigue failure of the 9.5mm (3/8") bolts. After creating three plastic hinges, one of the hinges narrowed down (b) and in its weakest cross section failed, breaking the bolt in two pieces (a).

7.2.4. Displacement-Stiffness Relation

After the cyclic tests, the relation between ultimate displacement and elastic stiffness was analyzed. Different symbols are assigned to different connection configurations. Unreinforced and lag screw reinforced connections were tested in three bolt diameters (5/8", 1/2" and 3/8"), whereas 3/8" truss plate reinforced connections were not tested in reverse cyclic loading.

In general, the less stiff the connection was (in its elastic stage), the higher ultimate displacement it could reach. This phenomenon was least significant in the brittle (unreinforced) joints, as can be recognized by the steep trend line in Fig. 87. In more ductile lag screw reinforced connections, the same increase of L/d ratio (or bolt diameter) causes higher maximum displacement (flatter trend line).

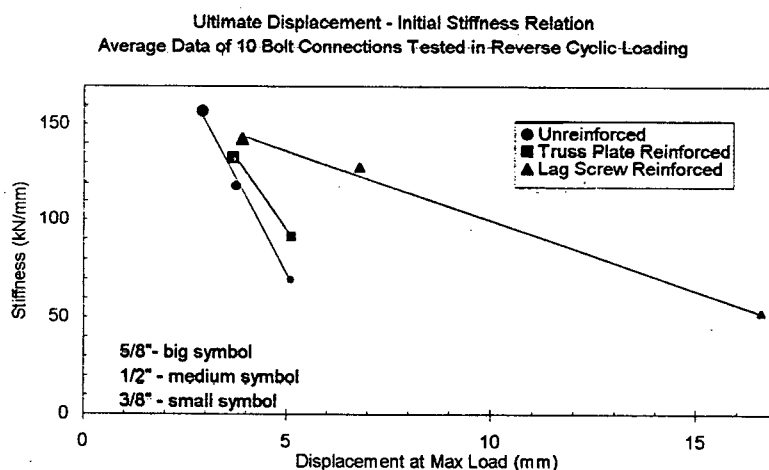


Figure 87. Relation between elastic stiffness and displacement at maximum load

8. SUMMARY, DISCUSSION

8.1. Static Tension Tests

REINFORCEMENT	Specimen Symbol	Bolt d. [in]	Force Ult. [kN]	Diff [%]	Stiffness [kN/m]	Diff [%]	Energy Dis [Nm]	Diff [%]	Ductility []	Diff [%]	Failure Mode
Unreinforced	FU-Avg	5/8"	373		275		4173		3.8		group shear, row shear
	HU-Avg	1/2"	288	-23	119	-57	5246	26	2.6	-31	row split, row shear
	TU-Avg	3/8"	175	-53	80	-71	3113	-25	4.9	28	row split, row shear
Threaded Rods	FRR-Avg	5/8"	346	-7	156	-43	6594	58	5.1	33	group shear
	FRRS-Avg	5/8"	389	4	120	-56	6781	62	4.3	12	group shear, net section
	FRRF-Avg	5/8"	373	0	93	-66	6242	50	4.7	25	group shear
	HRR-Avg	1/2"	357	24	125	5	7900	51	6.2	137	group shear, row shear
	HRRS-Avg	1/2"	341	18	128	7	8748	-67	12.5	378	group shear, row shear
	HRRSH-Avg	1/2"	363	26	110	-8	9990	90	8.8	236	group shear, row shear
	GHRR-Avg	1/2"	346	N/A	101	-13	6660	N/A	4.7	N/A	group shear, row split
	GHRRF-Avg	1/2"	338	N/A	90	-22	6447	N/A	6.1	N/A	group & row shear, split
	TRR-Avg	3/8"	325	86	87	9	9186	195	15.2	213	group shear, row shear
	GTRR-Avg	3/8"	354	N/A	75	-5	7532	N/A	8.8	N/A	row shear, row split
	HRT-Avg	1/2"	317	10	97	-19	7900	51	7.2	173	row shear
	FRT-Avg	5/8"	365	-2	179	-35	7130	71	4.0	5	group & row shear, split
Truss Plates	FRTT-Avg	5/8"	370	-1	93	-66	2491	-40	3.7	-3	group shear
	HRTW	1/2"	254	-12	62	-48	4931	-6	3.3	26	row shear
	HRN18	1/2"	393	36	135	13	3529	-33	3.0	-15	group shear
Nailed Plates	HRN26	1/2"	399	38	131	10	4195	-20	3.7	43	group shear
	FRN-I	5/8"	409	10	155	-44	5454	31	4.4	17	group shear
	FRN-II	5/8"	368	-1	270	-2	6645	59	3.3	-13	row shear
	FRN18	5/8"	445	N/A	113	N/A	N/A	N/A	N/A	N/A	not reached
	FRN26	5/8"	400	7	95	-65	6177	48	6.8	78	group shear
	FRE-Avg	5/8"	366	-2	130	-53	1713	-59	3.0	-22	group shear, row shear
Glued-on Plates	HRER-Avg	1/2"	381	32	97	-19	6372	21	4.1	55	group shear
Glued-in Rods	HRERE-Avg	1/2"	329	14	105	-12	4757	-9	4.2	61	group shear

Table 16. Total results of the joints tested in static tension

Table 16 summarizes the following mechanical properties of the PSL and glulam 10-bolt connections: ultimate force, elastic stiffness, ductility and energy dissipation, tested in static tension. The column labeled "diff" after each of the four properties shows the difference between unreinforced and reinforced joint expressed as the percentile improvement of the reinforced connection. In the three unreinforced cases, the number in the narrow column reflects the difference among the specimens with three different L/d ratios or bolt diameters (15.9, 12.7 and 9.5mm).

The average values of the elastic stiffness and the ultimate force are plotted together in Fig 88. The positive influence of the reinforcement on the connection strength behaviour is clearly recognized. When compared to the unreinforced joints, the reinforcement increased the ultimate force up around 380 kN in all reinforcement types and in all three bolt diameters. In the unreinforced connections the peak force values proportionally followed their bolt diameter values, as was observed in the code predictions. Because of this reinforcing equalizing- force influence it was hard to distinguish the behaviour of each particular reinforcement type. The ultimate force values of reinforced connections on average varied very little. Therefore, the other

quantities had to be considered as well. The positive aspect of this phenomenon was that the reinforced joints approached the net-area tension capacity, because some specimens failed in tension (e.g. FRRS-1). Hence the joints were very efficient and the cross-sectional area was chosen correctly.

As was observed previously with the elastic stiffness-displacement relation (Sec. 7.2.4), the ultimate force and the elastic stiffness values were related to each other.

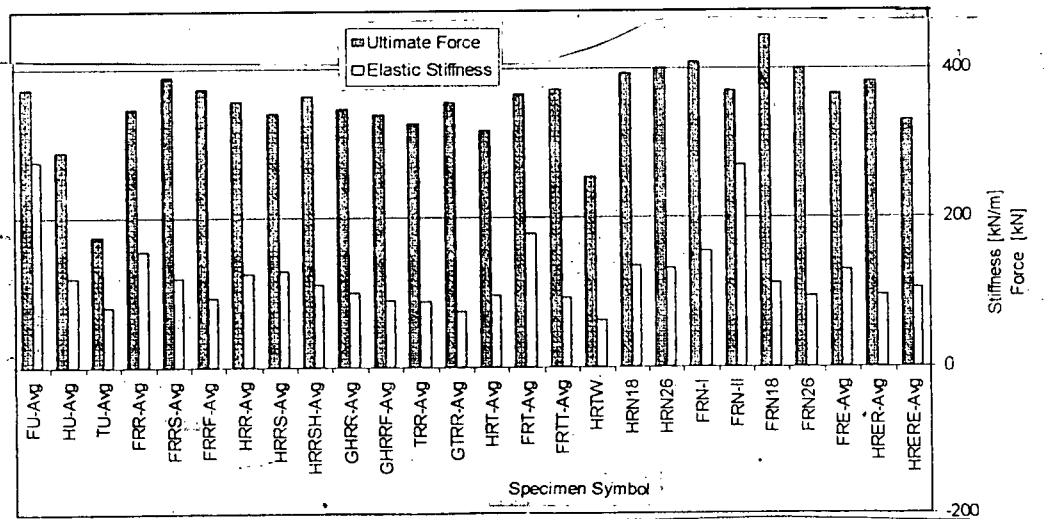


Figure 88. Elastic stiffness and the ultimate force average values – static tension

In static tension, the highest ratios of ductility (above 8) were obtained from the 12.7mm 10-bolt lag-screw reinforced specimens with offset lag screws (HRRSH), single lag screw at the end (HRRS) and from 9.5mm 10-bolt lag-screw reinforced glulam (GTRR) and PSL connections (TRR). The 12.7mm 10-bolt truss plate reinforced joints (HRT) reached ductility values of about 7.0, which is surprisingly similar to the 0.6mm nailed plate connections FRN26. The other following specimens all had ductility values around or below 4.0: unreinforced joints, nailed plate, glued-in lag screw and rebar, glued-on plate and stiff truss plate reinforced connections. Fig. 89 shows the ductility ratios of all the specimens tested in static tension.

Energy dissipation in most cases followed the same trend as the ductility. The coarse threaded rod again reached the highest values in all its configurations. The truss plate reinforced joints were similar to the lag screw joints (HRT, FRT around 8000 Nm). A somewhat lower energy dissipation was obtained from the brittle 15.9mm specimens, but still very high (6000 Nm). Since the energy dissipated was calculated as the area under the load-displacement curve, the 15.9mm connection values were greatly influenced by their high strength capacity. On the other hand, the connections with slender bolts reached lower ultimate force levels, but

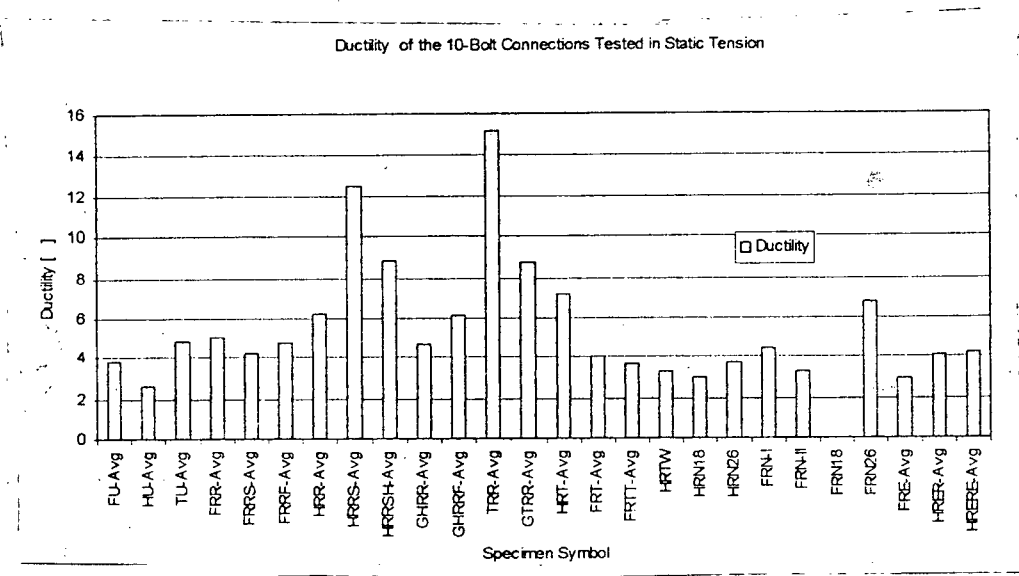


Figure 89. Ductility ratios of the connections tested in static tension

maintained a high strength to large displacement values. Therefore, when the total displacements were considered, the slender bolt joint results were more favourable, even though they reached similar energy dissipation values to those connections with low L/d ratios. The plot in Fig. 90 reflects the energy dissipation total values for joints tested in static tension.

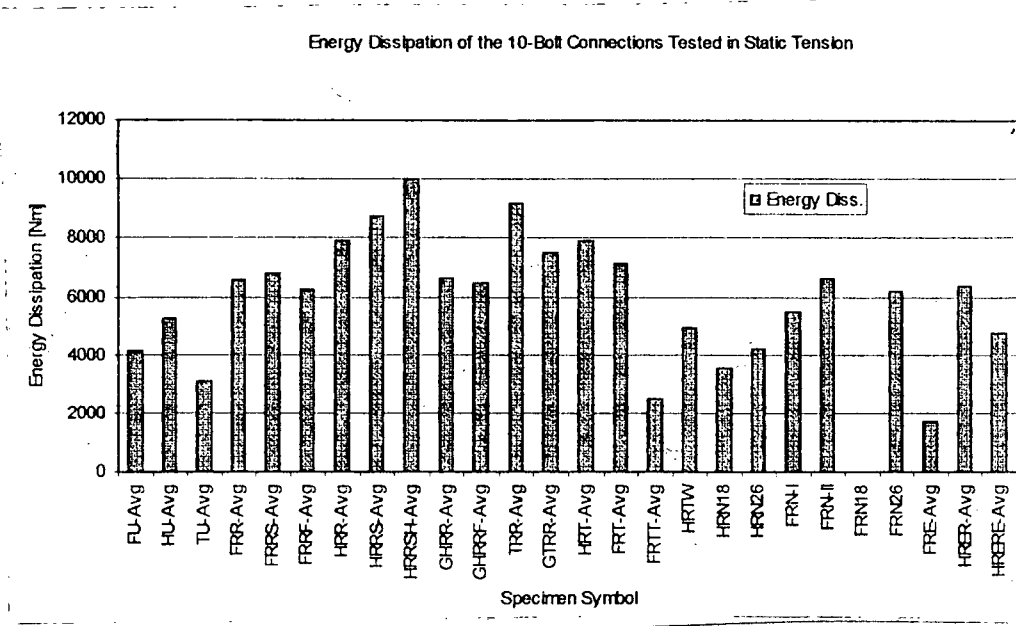


Figure 90. Energy dissipation of the connections tested in static tension

There were several differences observed, when the absolute values of ductility and energy dissipation were considered. It is interesting to compare both quantities in a relative way as a percentage value relative to the unreinforced connections. As shown in Fig. 91 only a few of the reinforcement techniques proved to be beneficial when considering this criterion. This time 12.7 and 9.5mm-bolt lag screw reinforcement and 12.7mm-bolt truss plate connections had an increase of close to 200%. Only the 3/8"(9.5mm) lag screw reinforced connections had their ductility and energy increase equally contributing to the total value, which was ideal.

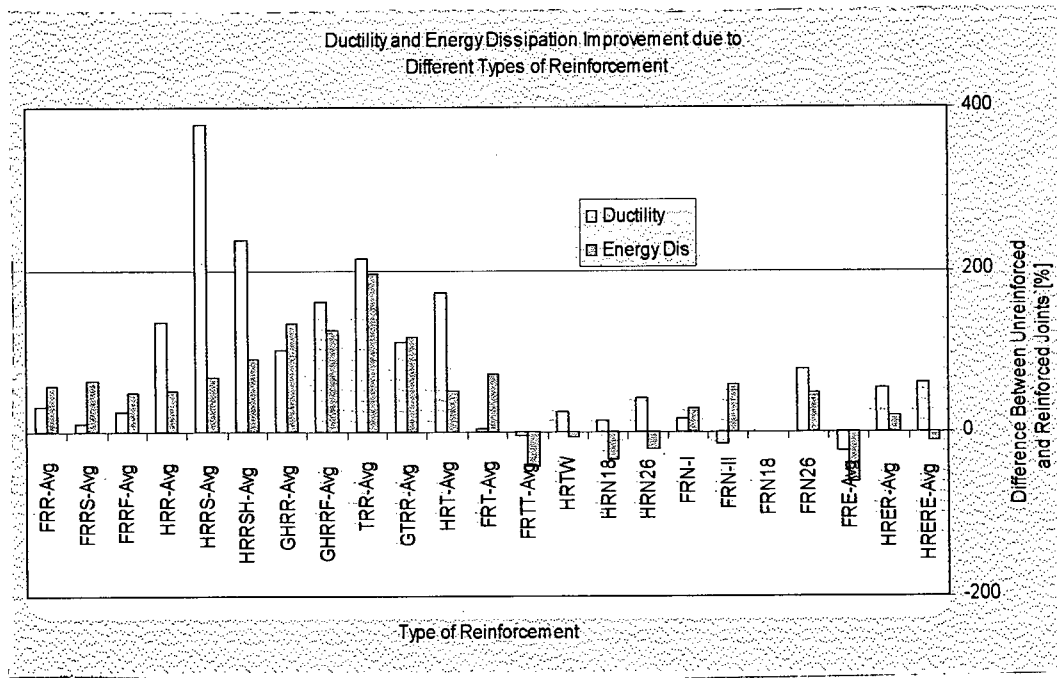


Figure 91. Ductility and energy dissipation improvement due to the reinforcement of the connections tested in static tension

8.2. Reverse Cyclic Tests

REINFORCEMENT	Specimen Symbol	Bolt d. [in]	Force Ult. [kN]	Diff [%]	Stiffness [kN/m]	Diff [%]	Energy Dis [Nm]	Diff [%]	Ductility []	Diff [%]	Failure Mode
Unreinforced	FU-C	5/8"	272		157		483		1.6		row split, row shear
	HU-C	1/2"	293	8	118	-25	2191	354	1.7	7	row split, row shear
	TU-C	3/8"	164	-40	69	-56	1580	227	5.4	237	wood crushing, row split
Threaded Rods	FRR-C	5/8"	309	14	142	-9	1265	162	4.9	201	row split, row shear
	HRR-C	1/2"	283	-4	128	8	1821	-17	8.3	382	wood crush, group shear
	TRR-C	3/8"	263	60	52	-25	4784	203	8.7	60	wood crushing
	GTRR-C	3/8"	268	N/A	64	N/A	3579	N/A	8.6	N/A	wood crushing
Truss Plates	FRT-C	5/8"	321	18	132	-16	2454	408	3.0	88	row split, row shear
	HRT-C	1/2"	278	-5	91	-22	2025	-8	3.4	96	row split, row shear

Table 17. Total results of the joints tested in reverse cyclic loading

In the reverse cyclic tests, similar to the static tension tests, the ultimate force and elastic stiffness were correlated. The ultimate strength capacity was 18.2% (mean) higher for the static tension in comparison to the cyclic tests. The reinforcement did not have such equalizing influence on the force as in the static tension tests. The joints in the cyclic tests underwent much higher cumulative displacements than their static tension equivalents. Even though the cyclic loading rate was eight times faster, the cycling significantly decreased the connection capacity. In total, more energy was dissipated by bolts bending and wood crushing. Also, in both unreinforced and reinforced cases the ultimate force was gradually dropping as the diameter of the bolts was decreasing. On average the highest ultimate force was observed in the 15.9mm-bolt truss plate connections (321 kN). The peak elastic stiffness was on average recorded with 15.9mm unreinforced joints (156.7 kN/m). Both quantities are plotted in Fig. 92.

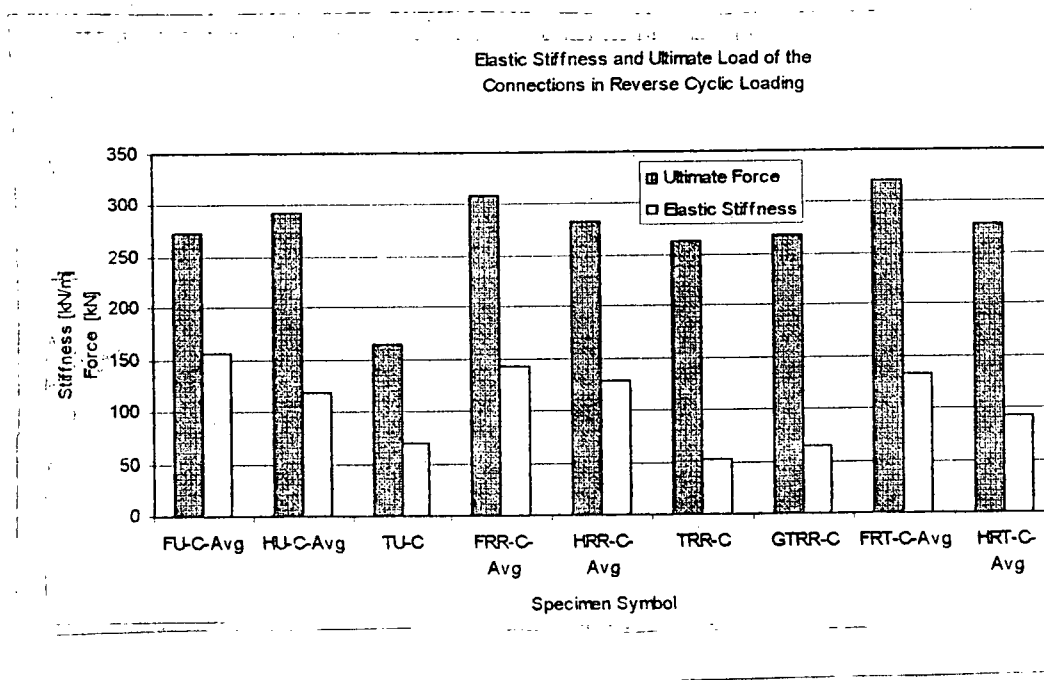


Figure 92. Elastic stiffness and the ultimate force average values – cyclic tests

When the percentage improvement values of the ductility and energy dissipation in cyclic tests are plotted together, the influence of the bolt slenderness on both quantities is emphasized (Fig. 93). Although the units were not consistent, again the graph reflects the gain of slender bolt (9.5mm) connections (TU, TRR) from both aspects. Significantly, the lag screw reinforced

(FRR) behaved better than the truss-plate ones (FRT). Mainly because of the lack of energy dissipation in the truss plate connections, the truss plates were carrying minimal loads after the connection failure. The truss-plate teeth pulled out of the wood and the whole connector simply fell off the specimen surface. The truss plate teeth were not long enough or they did not have enough friction to maintain their position in the wood fibers.

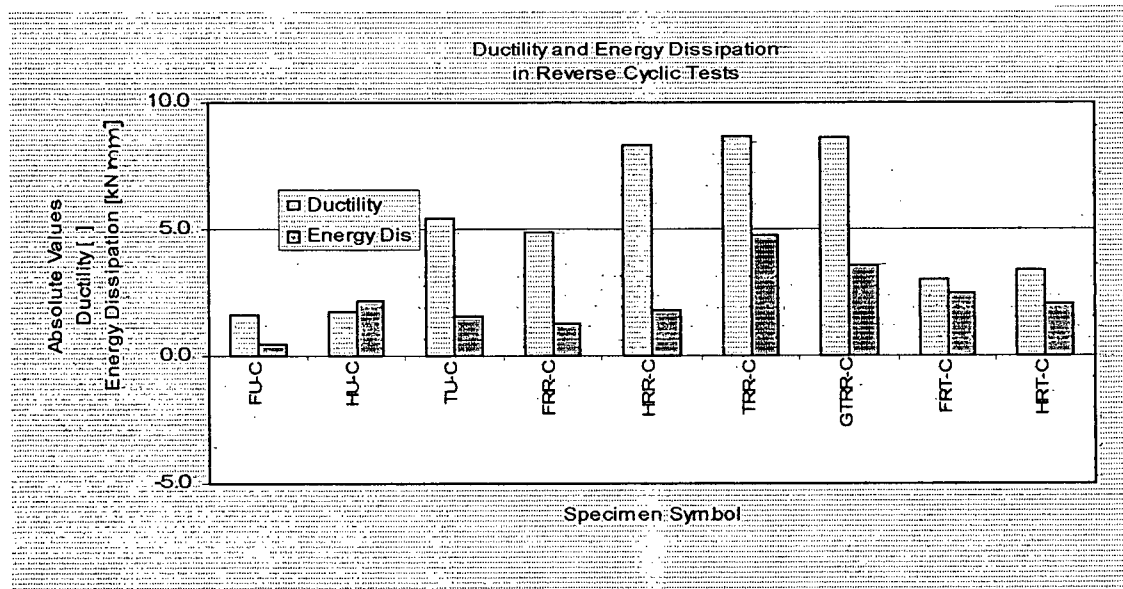


Figure 93. Summation of absolute values of ductility and energy dissipation – reverse cyclic tests

The main focus of this thesis was to investigate methods to enhance the ductility and the strength of multiple bolted connections in PSL and Glulam. Several reinforcement techniques were introduced to obtain the desired energy dissipation of these joints. The use of reinforcement in general increased these mechanical quantities.

The code design values appeared to be conservative when compared to the basic unreinforced connection test strength values. The comparisons were done with no safety factors in the code calculations, and the code values were expected to approach the test results. The European yield model of the code is based on rigid-plastic behaviour of all participating materials – the bolts and the wood, whereas in most cases the tests showed brittle failures and uneven distribution of the load among the bolts. Only the most slender - 3/8" (9.5mm) 10-bolt connections experienced failures in a ductile manner.

An important point can be brought up in the case of the higher diameter (1/2", 5/8") bolt lag screw and truss plate reinforced connections. Although brittle failure e.g. splitting or shear plug, was observed in these joints, the load-displacement curves were ductile. This means the cracking or the shear action can contribute to the global energy dissipation of the connection and it is not necessarily causing failure. The behaviour is similar in the case of reinforced concrete structural elements. After reaching the cracking load, part of the total capacity is taken by the reinforcement, and cracking is merely an intermediate process in the element or the connection behaviour.

The most promising reinforcement was apparently the lag screw (4mm thread) inserted perpendicular to the grain between each of the connection bolts.

Ready rod with its fine thread (1.8mm) could not prevent extensive perpendicular-to-grain splitting. In these cases the connections failed suddenly and in brittle failure modes.

The tests with truss plates as a surface reinforcement showed that the teeth of the truss plate were not long enough. Especially in the cyclic tests, the huge cumulative displacements caused the truss plates to prematurely pull out from the timber. Thus a more sudden drop in the strength and stiffness followed after the peak load was reached, compared to the lag screw reinforced cases.

The use of epoxy as a glue in different forms of reinforcement (glued-on plates, glued-in rods) increased the strength but caused sudden failure. Their behaviour was even worse than in the case of unreinforced specimens.

The nailed plate reinforcement showed promising improvement when finishing nails and thin plates (0.6mm) were used. Energy was mostly dissipated by crushing the thin plate in the location of bolts and also by bending the slender finishing nails. This was not true in the case of the thick 2"-long nails or in the 1.2 mm thick plate.

The stiff truss plate, or the transfer of the load through the reinforcement, did not appear to be a good connection design, because the entire load applied to the joint was concentrated in the truss plate teeth. This phenomenon caused the truss-plate to be pulled out off the wood, which caused brittle failure and low ductility values as was the case of regular truss plates.

In some tests, the two wood products were compared – PSL and Glulam. The Glulam connections were stronger than their PSL equivalents, but less ductile. This was in part caused by the different densities of the two materials. Also, very unpredictable cracking was observed in the Glulam connections. Sometimes the specimen cracked along its entire length. On the contrary PSL joints cracked in a very consistent way. The cracks never propagated very far (10-15cm from the last bolt) because of the random wood chip configuration in the Parallam® cross section.

From the experience of this study the following recommendations for further research can be made:

- To continue developing the nailed plate reinforcement with slender but flat headed nails
- To try using other types of truss plates; especially ones with long teeth, which are not bent
- To focus on finding the limit of the optimum bolt diameter used for multiple bolted connections
- To experiment with different lag screw positions and actually try to design a lag screw reinforced joint based on the modeling of unreinforced joints
- To conduct bending tests of the bolts prior to the connection tests in order to get realistic (performance) yield stress values

REFERENCES

- Augusti, G., Ceccotti, A., 1981. Antiseismic Rules for Timber Structures: An Italian Proposal. Symposium on Forest Products Research International. Dept. of Civil Engineering, Florence, Italy
- Brown, D.H., 1991. Performance of Low-Rise Wood Buildings in Recent Earthquakes. Intern. Timber Engineering Conference, London
- Buchanan, A., 1984. Wood Properties and Seismic Design of Timber Structures, Pacific Timber Engineering Conference, p.462-469, Auckland, New Zealand, U.S.A.
- Cruz, H., 1996. Behaviour of Structural Timber Joints Under Cyclic Loading, Lisboa, Portugal. International Wood Engineering Conference, New Orleans
- Deam, B.L., King, A.B., 1996, Building Research Association of New Zealand, Pseudo-Dynamic Testing of Structural Timber Elements. International Wood Engineering Conference, New Orleans, U.S.A.
- Deam, B., King, A. 1994. The Seismic Behaviour of Timber Structures. Pacific Timber Engineering Conference, Gold Coast, Australia
- Foschi, R.O., 7/1974. Load-Slip Characteristics of Nails, Wood Science, UBC, Vancouver, Canada
- Hirai, T., 10/1990. Some Considerations on Lateral Resistance of Mechanical Wood-Joints, Hokkaido University, International Timber Engineering Conference, Tokyo, Japan
- Hockey, B., 4/1999. Truss Plate Reinforced Bolted Connections in Parallel Strand Lumber. Thesis, UBC, Vancouver, BC, Canada
- Humphrey, P.E., Ostman, L.J., 5/1998. Bolted Timber Connections: Part II. Bolt Bending and Associated Wood Deformation, Oregon State University, U.S.A.
- Introduction to Wood Design, Canadian Wood Council, 1996. Ottawa, Ontario, Canada
- ISO Draft of Cyclic Protocol ISO TC 165/SC N, 07/1999. Timber structures – Joints made with mechanical fasteners - Quasi – static reversed cyclic test method
- Jorissen, A.J.M., 1998. Double Shear Connections with Dowel-Type Fasteners, Doctoral Dissertation, Delft, Netherlands
- Leijten, A.J.M., 1996. The Concept of the Prestressed DVW Reinforced Joint with Expanded Tubes, International Wood Engineering Conference, New Orleans, U.S.A.
- Masse, D.I., Salinas, J.J., Turnbull, J.E., 1988. Lateral Strength and Stiffness of Single and Multiple Bolts in Glue-Laminated Timber Loaded Parallel to Grain. Unpublished Contract No. C-029, Eng. and Stat. Research Centre, Research Branch, Agriculture, Ottawa, ON, Canada
- Mischler, A., 1998b. Design of Joints with Laterally Loaded Dowels, Paper CIB-W18131-7-2. Savonlinna, Finland
- Mischler, A., Prion, H.G.L., Lam, F., 7/2000. Load-Carrying Behaviour of Steel-To-Timber Dowel Connections, World Conference of Timber Engineering, Whistler, BC, Canada
- Moss, P.J., Carr, A.J., 9/1983. Earthquake Response of Low-Rise Timber Buildings. Bull.N.2. National Society for Earthquake Engineering Vol.19, No.3, pp 180-199, University of Canterbury, Christchurch, New Zealand
- Moss, P.J., 1997. Multiple Bolted Joints in Wood Members, a Literature Review. General Technical Report, FPL-GTR-97, United States Department of Agriculture, Forest Service, Christchurch, New Zealand

Ni, C., Chui, Y., 1994. Response of Nailed Wood Joints to Dynamic Loads, Pacific Timber Engineering Conference, Gold Coast, Australia

Prion, H.G.L., Foschi, R.O., 7/1994. Cyclic Behaviour of Dowel Type Connections, proc. of Pacific Timber Engineering Conference, Vol.2 (p.19), Vancouver, BC, Canada

Popovski, M., Prion, H.G.L., UBC, 1996. Karacabeyli, E., Forintek Canada Corp., Vancouver, Canada. Seismic Performance of Braced Timber Frames, proc. of Fourth Intern. Wood Engineering Conference 1:323-330, New Orleans, Louisiana, U.S.A.

Popovski, M., Prion, H.G.L., UBC 5/1998. Karacabeyli, E., Forintek Canada Corp., Vancouver, Canada., 1998. Seismic Behaviour of Braced Timber Frames, 6th National Conference on Earthquake Engineering, Seattle, Washington, U.S.A.

Rowlands, R.E., Rahman M.U., Wilkinson T.L., Chiang, Y.I., 1982. Single and Multiple Bolted Joints in Orthotropic Materials, University of Wisconsin, Composites 13(3):273-279, Wisconsin, U.S.A.

Schubert, Ch., 1998. Testing of Reinforced Bolted Connections of Parallel Strand Lumber Under Cyclic Loading, Research Report, Dept. of Wood Science, UBC, Vancouver, BC, Canada

Smith, I, Whale, L.R.J., Anderson, C., Hilson, B.O., Rodd, P.D., 2/1988. Design Properties of Laterally Loaded Nailed or Bolted Wood Joints, Can. Journal of Civ. Eng. Vol.15, Canada

Soltis L.A., Wilkinson T.L., Hubbard, F.K., 9/1986. Bearing Strength of Bolted Timber Joints, Forest Product Laboratory, Journal of Structural Eng., Vol.112, No.9 Madison, Wisconsin, U.S.A.

Soltis L.A., Wilkinson T.L., 8/1987. Timber Bolted Connection Design, Structures Congress, Orlando, NY, U.S.A.

Soltis L.A., Wilkinson T.L., 7/1987. Bolted Connection Design, Forest Product Laboratory, General Technical Report, FPL-GTR-54, Madison, Wisconsin, U.S.A.

Tan, D., Smith, I, 7/1999. Failure In-the-Row Model For Bolted Timber Connections, Journal of Structural Engineering, Vol.125, No.7

Touliatos, P.G., 1991. Design Problems of the Timber Construction in Seismic Zones, International Timber Engineering Conference, London

Yasumura, M., 1990. Seismic Behaviour of Arched Frames and Braced Frames, International Timber Engineering Conference, Tokyo, Japan

Wang, H., Sadakata, K., 1994. Ductility Evaluation of Wooden Structures, Pacific Timber Engineering Conference, Gold Coast, Australia

Walford, G.B., Earthquake Resistance of Timber Buildings. TEW/27. Forest Research Institute, Rotorua, New Zealand

Wilkinson, T.L., 5/1979. Analysis of Mechanical Joints in Wood, SESA Spring Meeting, May 20-25, 1979, San Francisco, CA, U.S.A.

Wilkinson T.L., Bolted Connection Strength and Bolt Hole Size, Forest Product Laboratory, General Technical Report, FPL-RP-524, Madison, Wisconsin, U.S.A.

Wilkinson T.L., 7/1993. Bolted Connection Design Values Based on European Yield Model, Forest Product Laboratory, Journal of Structural Engineering, Vol.119, No.7, Madison, Wisconsin, U.S.A.

Wilkinson T.L., 4/1986. Load Distribution Among Bolts Parallel to Load. Forest Product Laboratory, Journal of Structural Engineering, Vol.112, No.4, Madison, Wisconsin, U.S.A.

Wood Design Manual, Canadian Wood Council, 1995, Revised Oct. 1997. Ottawa, Ontario, Canada,

Yasumura, M, 4/1995. Failure of Timber Bolted Joints Subjected to Lateral Load Perpendicular to Grain, Building Research Institute Japan, Meeting 27, Copenhagen, Denmark

Yasumura, M., Murota, T., Sakai, H., 1987. Ultimate Properties of Bolted Joints in Glued-Laminated Timber, Summary of Technical Paper of Annual Meeting, Building Research Institute, Ministry of Construction, Tsukuba, Japan

APPENDICES

APPENDIX I

Specimen Configuration and Test Results

The following pages contain detailed information of the experimental tests.

For each specimen configuration the following is provided respectively:

- (i) Table of test results
- (ii) Specimen Configurations
- (iii) Load-displacement curves
- (iv) Specimen Photos

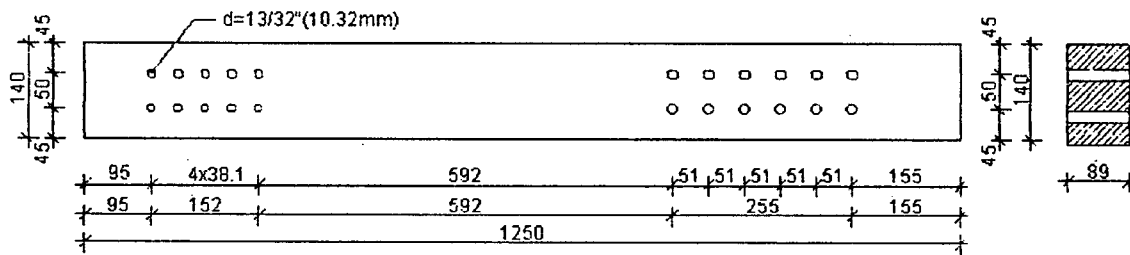
TU
10-3/8" Bolt Connection in PSL
Unreinforced

$L/d = 9.3$
 $e = 10d$
 $s = 4d$

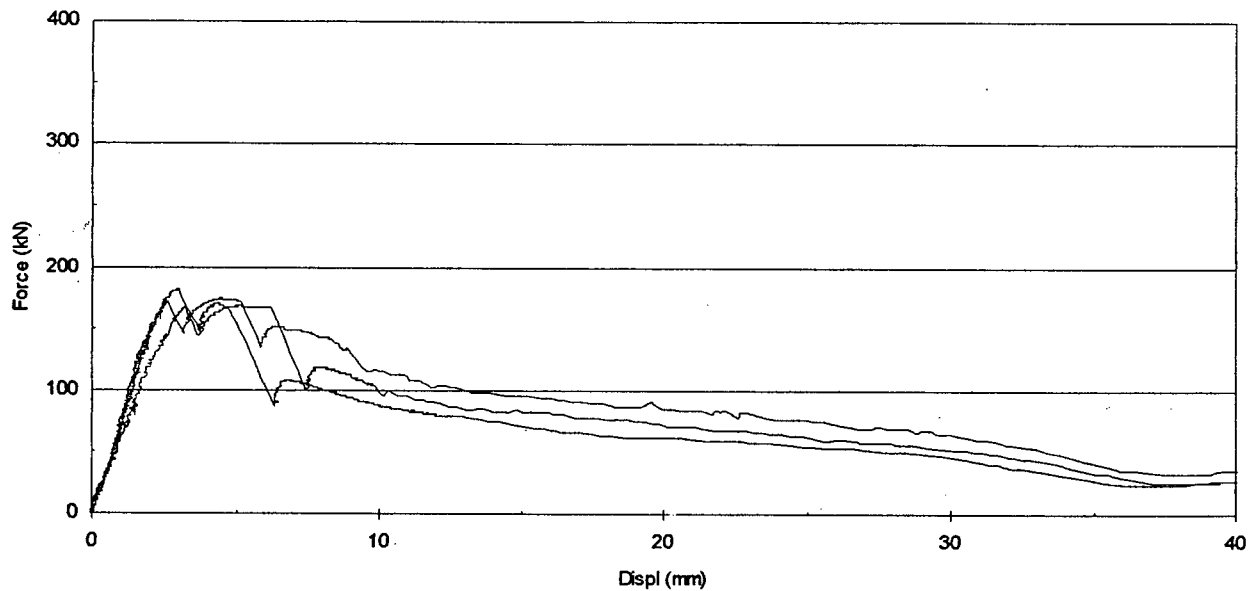
Quantity	Fult	D@Fult	80%Fult	D@80	D@50	Ductility
Specimen	[kN]	[mm]	[kN]	[mm]	[mm]	[]
TU-1	168.82	5.14	135.06	6.85	1.35	5.07
TU-2	174.69	4.48	139.75	5.70	1.15	4.96
TU-3	182.51	3.01	146.01	5.20	1.15	4.52

Quantity	Stiffness	Energy	Design F	Dens.green	Dens.dry	Moist.cnt.
Specimen	[kN/mm]	[Nm]	[kN]	[kg/m3]	[kg/m3]	[%]
TU-1	58.97	3070.92	100.90	619.71	599.61	8.96
TU-2	89.08	3523.98	100.90	629.04	592.86	9.14
TU-3	91.25	2744.76	100.90	694.22	628.78	8.91

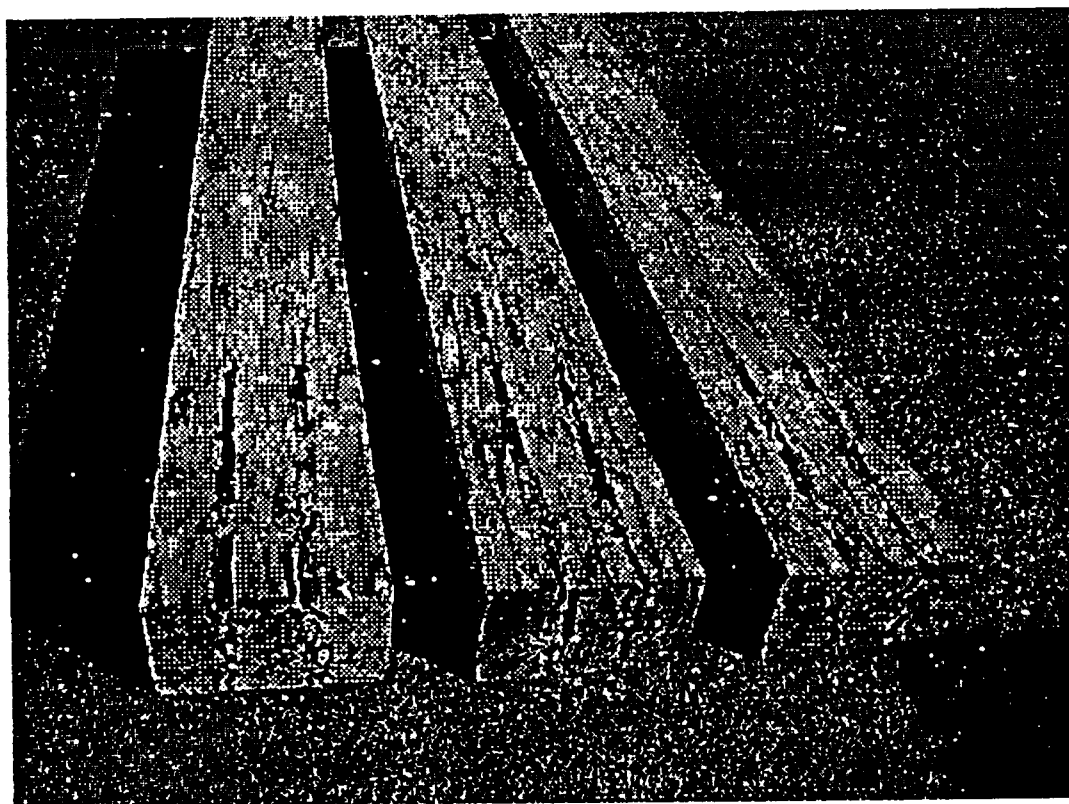
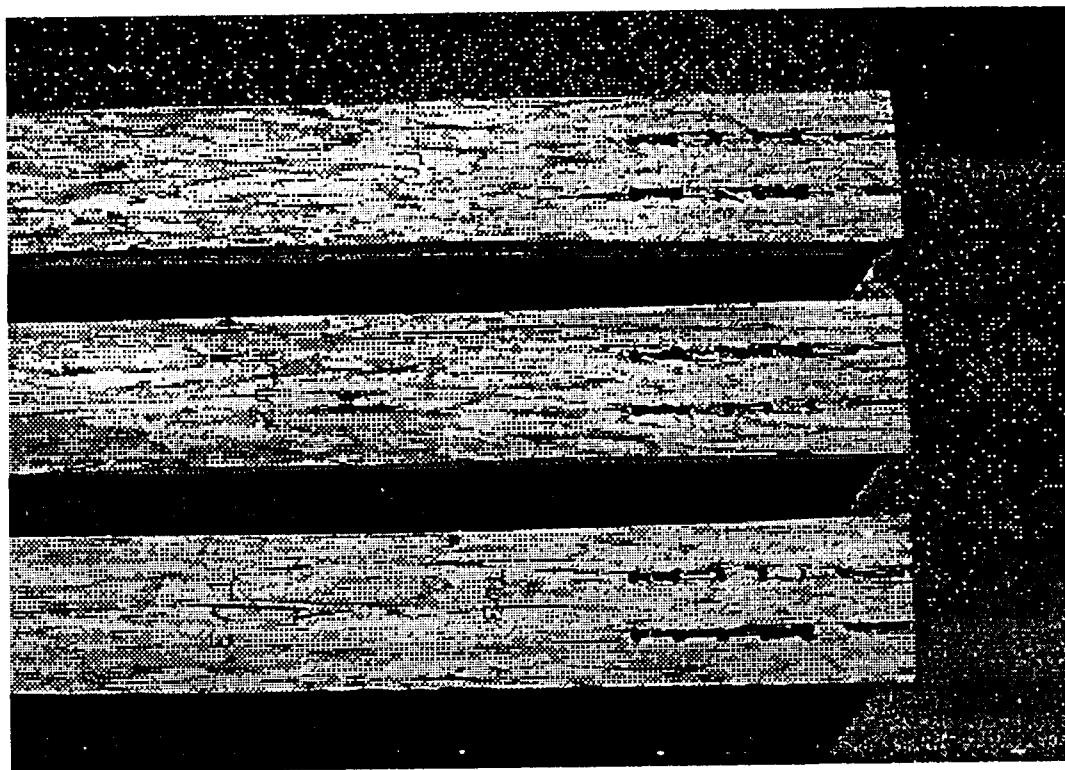
Failure mode: Row Tear –out, Row Splitting



Load-displacement Plot



TU

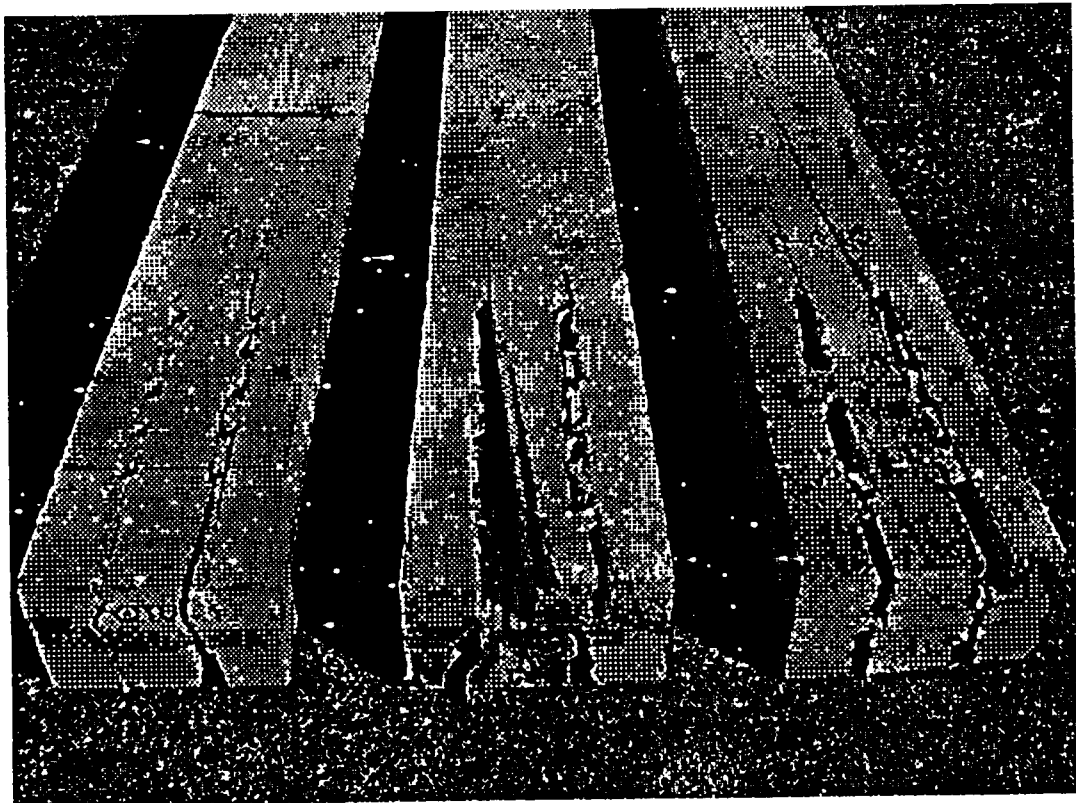
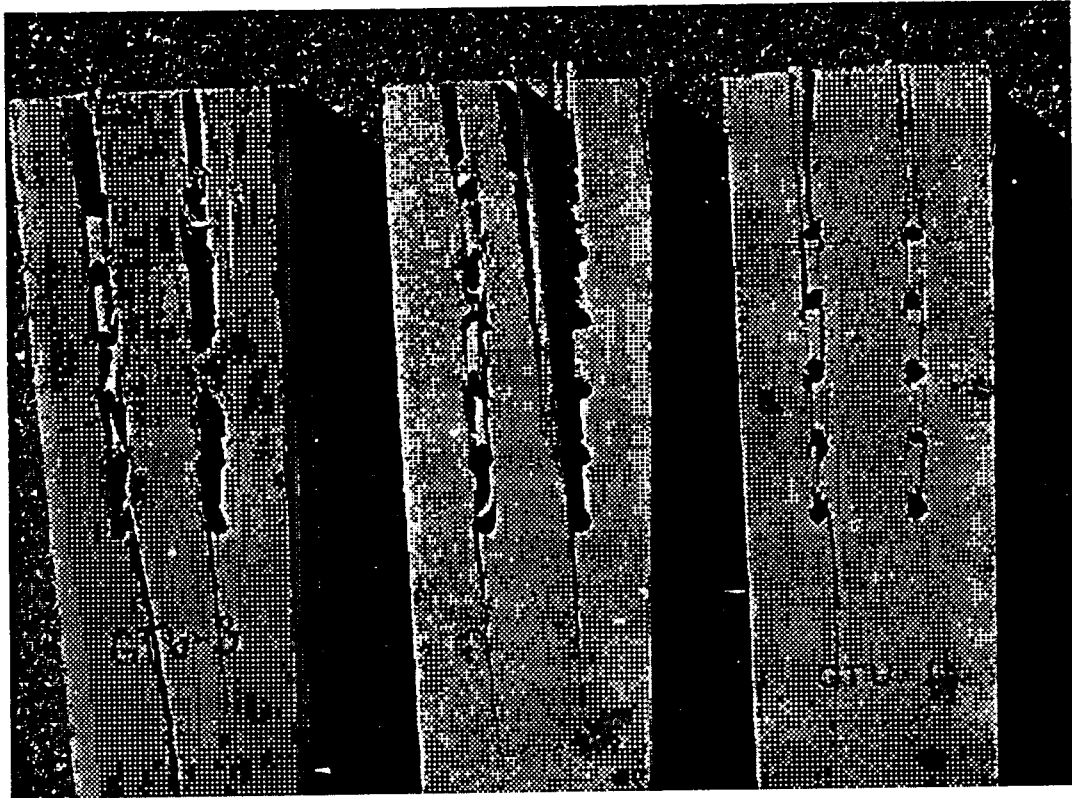


$$\begin{aligned} L/d &= 9.3 \\ e &= 10d \\ s &= 4d \end{aligned}$$

Quantity	Stiffness	Energy	Design F	Dens.green	Dens.dry	Moist.cnt.
Specimen	[kN/mm]	[Nm]	[kN]	[kg/m3]	[kg/m3]	[%]
GTU-1	83.13	1243.40	100.90	617.50	580.56	12.29
GTU-2	64.40	3684.79	100.90	622.23	584.14	12.46
GTU-3	88.05	5447.43	100.90	588.65	552.46	12.24

Technical drawing of a rectangular plate with dimensions and hole patterns. The plate has overall dimensions of 1250 mm by 130 mm. The thickness is 40 mm. The drawing shows two rows of holes, each with 5 holes. The distance between the two rows is 152 mm. The distance from the left edge to the first hole in each row is 95 mm. The distance between the holes in each row is 38.1 mm. The distance from the last hole in each row to the right edge is 155 mm. The diameter of the holes is $d = 13/32"$ (10.32 mm). The drawing also shows a side view of the plate with a width of 89 mm.

GTU



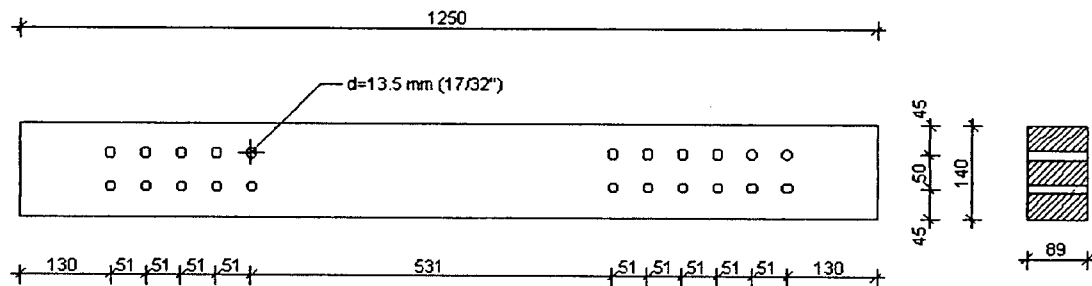
HU
10-1/2" Bolt Connection in PSL
Unreinforced

$L/d = 7.0$
$e = 10d$
$s = 4d$

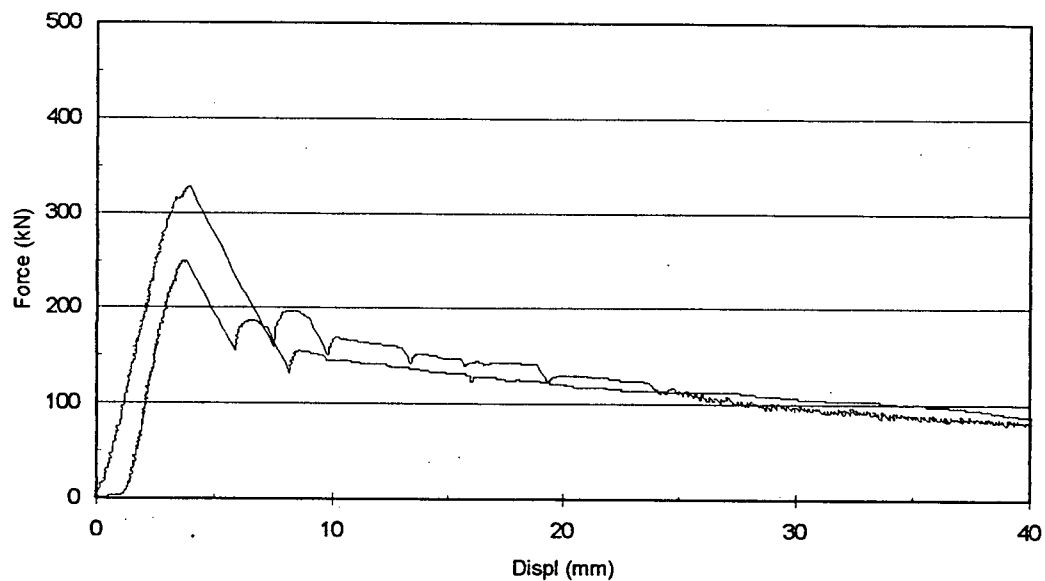
Quantity	Fult	D@Fult	80%Fult	D@80	D@50	Ductility
Specimen	[kN]	[mm]	[kN]	[mm]	[mm]	[]
HU1	328.08	3.96	262.46	5.33	1.74	3.06
HU2	248.56	3.77	198.85	4.9	2.25	2.18

Quantity	Stiffness	Energy	Design F	Dens.wet	Dens.dry	Moist.cnt.
Specimen	[kN/mm]	[Nm]	[kN]	[kg/m ³]	[kg/m ³]	[%]
HU1	110.36	5566	154.73	650.38	642.34	8.28
HU2	128.34	4925.9	154.73	671.45	648.01	8.32

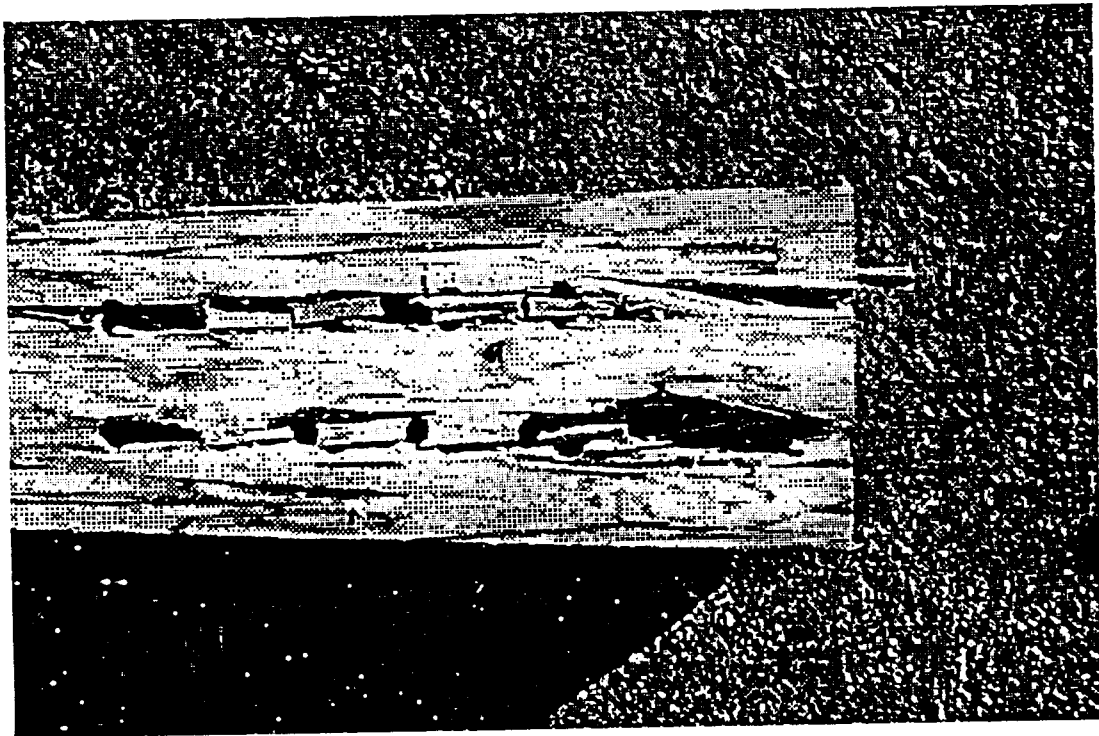
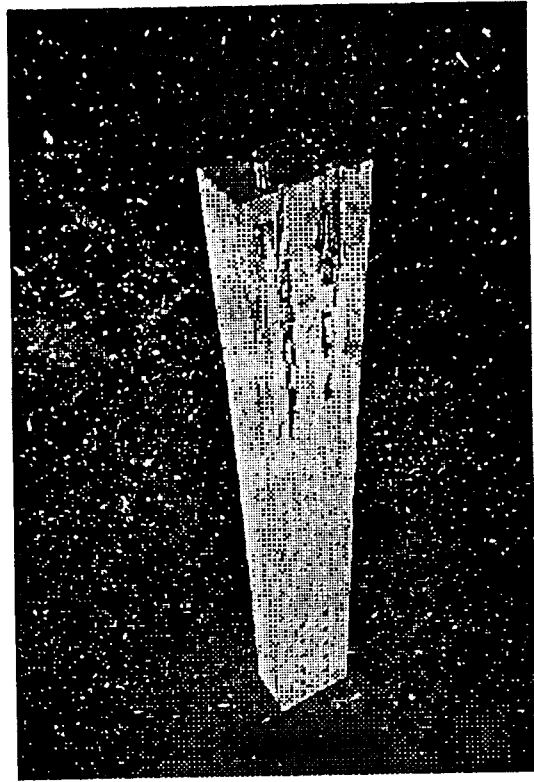
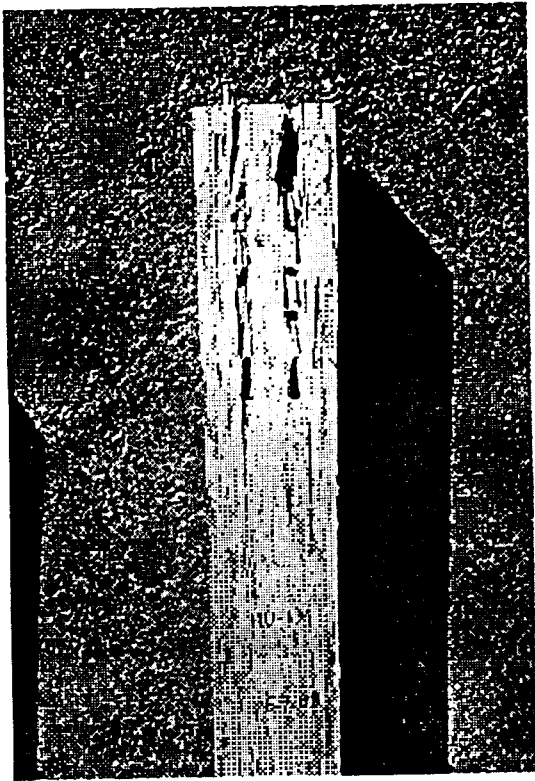
Failure mode: Row Splitting, Row Tear-out



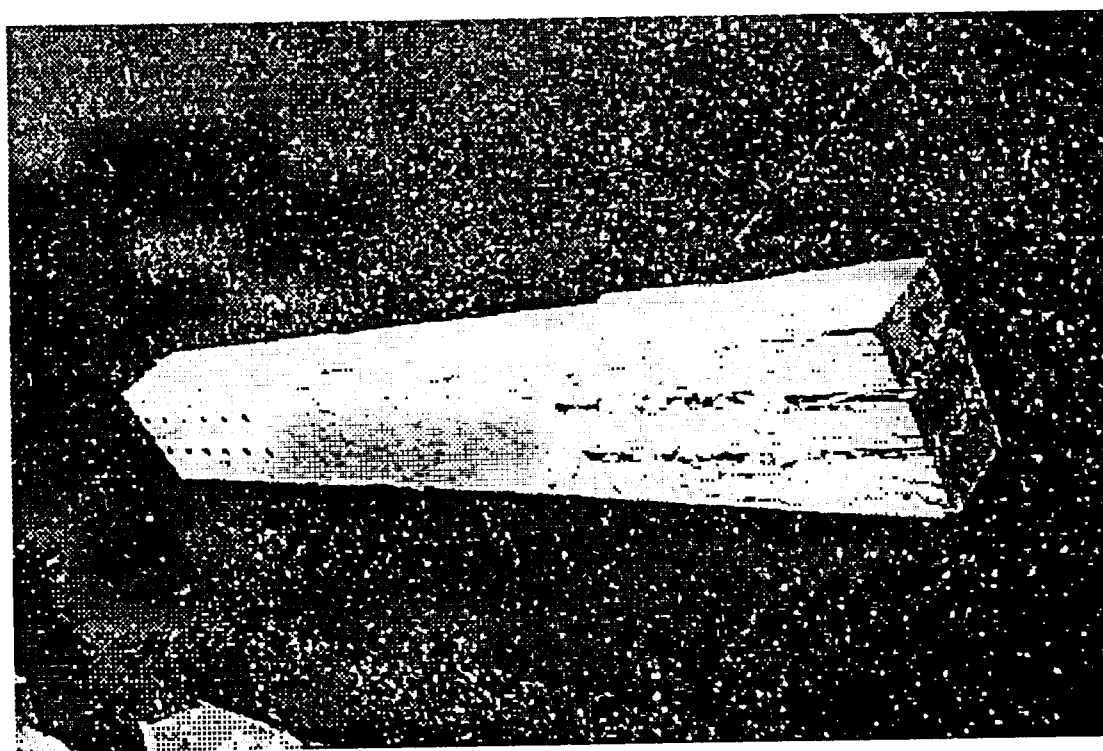
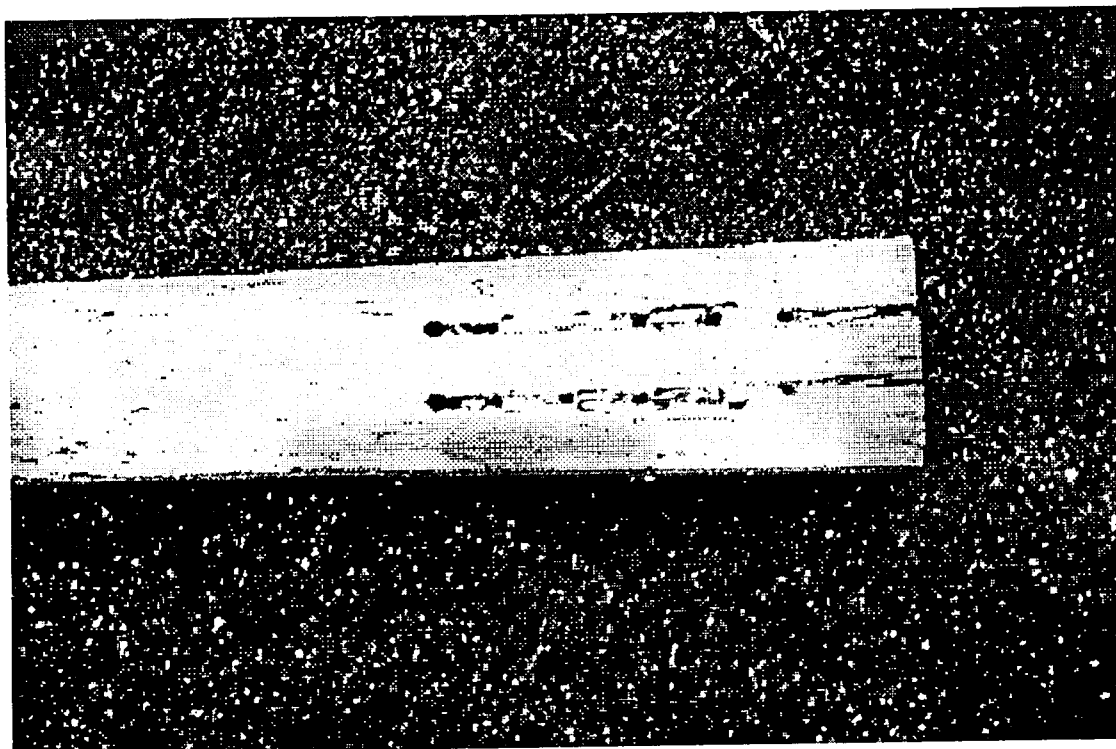
Load-displacement Plot



HU1



HU2



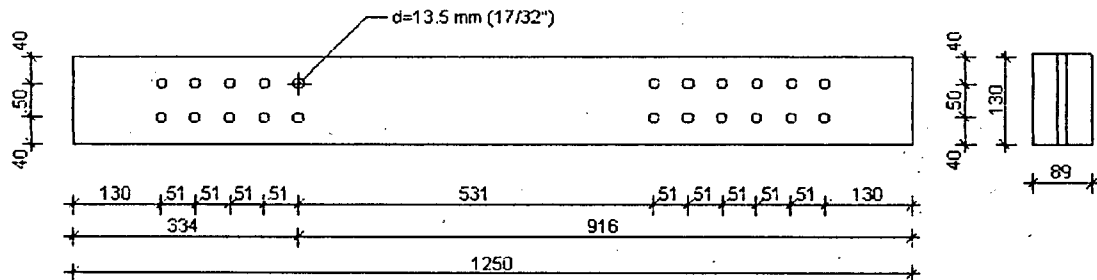
GHU
10-1/2" Bolt Connection in Glulam
Unreinforced

$L/d = 7.0$
$e = 10d$
$s = 4d$

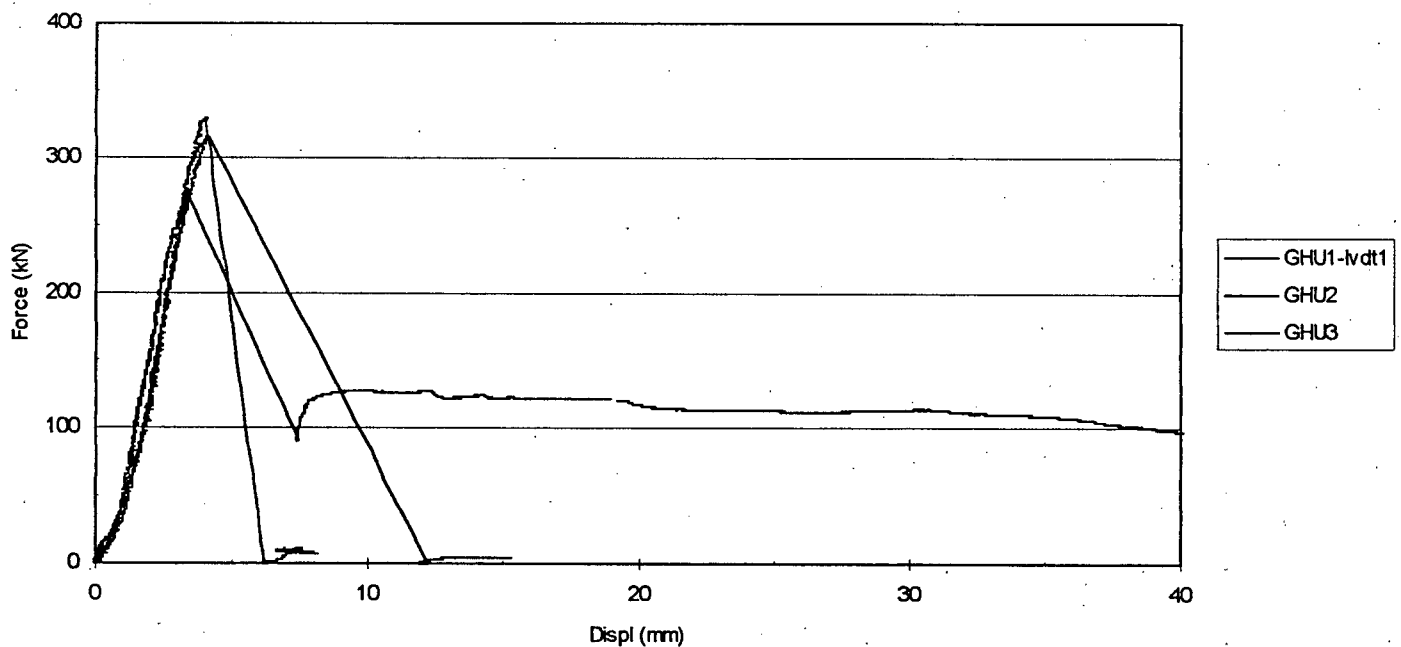
Quantity	Fult	D@Fult	80%Fult	D@80	D@50	Ductility
Specimen	[kN]	[mm]	[kN]	[mm]	[mm]	[]
GHU-1	330.04	3.98	264.03	4.40	2.31	1.90
GHU-2	274.63	3.30	219.70	4.46	1.80	2.48
GHU-3	315.05	4.11	252.04	5.80	2.20	2.64

Quantity	Stiffness	Energy	Design F	Dens.green	Dens.dry	Moist.cnt.
Specimen	[kN/mm]	[Nm]	[kN]	[kg/m ³]	[kg/m ³]	[%]
GHU-1	111.59	1724.09	154.73	588.37	560.08	11.47
GHU-2	116.82	4928.11	154.73	619.12	576.57	11.99
GHU-3	116.68	1871.75	154.73	583.78	560.73	11.95

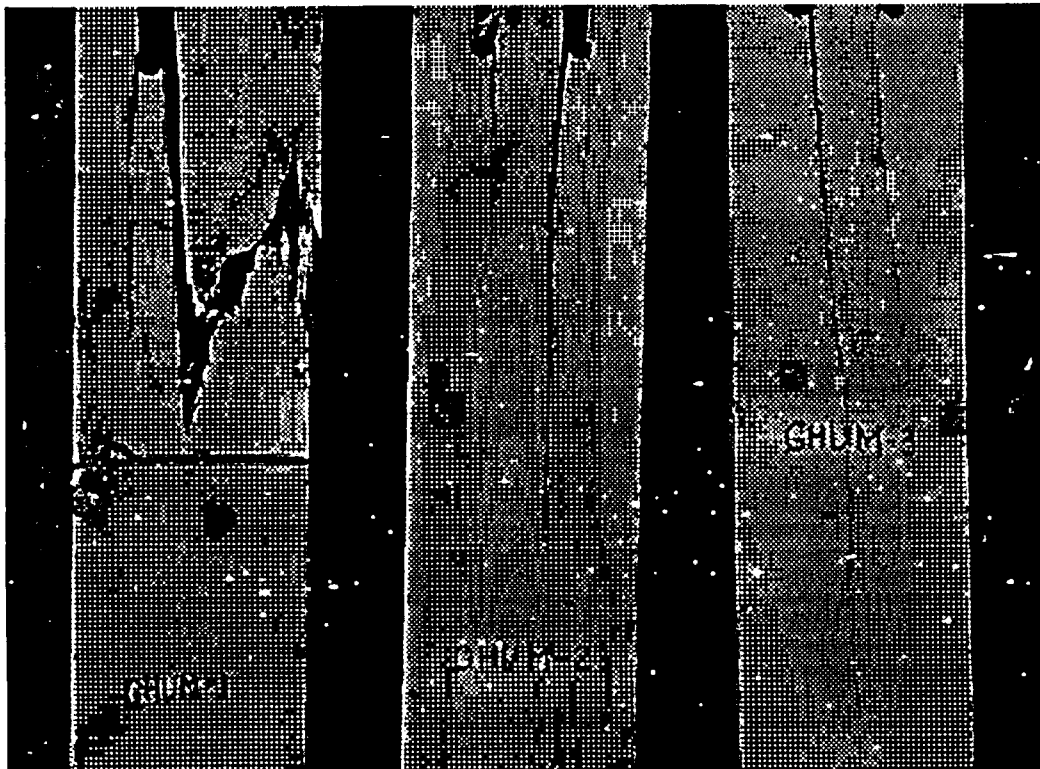
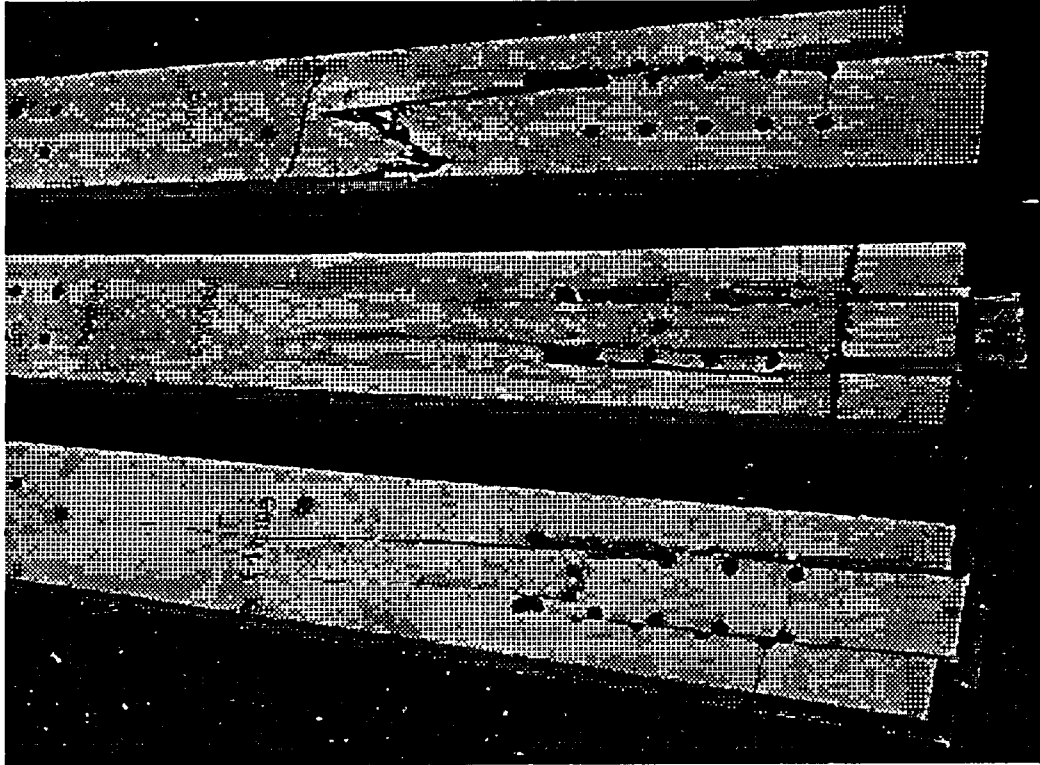
Failure mode: Shear Plug, Row tear-out



Load-displacement Plot



GHU



FU
10-5/8" Bolt Connection in PSL
Unreinforced

$L/d = 5.6$
 $e = 10d$
 $s = 4d$

Quantity	Fult	D@Fult	80%Fult	D@80	D@50	Ductility
Specimen	[kN]	[mm]	[kN]	[mm]	[mm]	[]
FU1	339.21	1.71	271.37	3.13	0.85	3.7
FU2	352.36	1.92	281.89	3.33	0.98	3.4
FU3	383.88	1.95	307.1	3.56	0.9	4
FU4	381.39	1.8	305.11	3.39	0.95	3.6
FU5	327.64	1.89	262.11	3.53	0.85	4.2
FU6	388.87	1.9	311.1	3.57	1.06	3.4
FU7	390.68	2.11	312.54	4.2	0.96	4.4
FU8	391.81	2.39	313.45	3.96	1.08	3.7
FU9	360.07	1.84	288.06	3.63	0.95	3.8
FU10	409.04	1.65	327.23	3.39	0.78	4.3
Avg	372.495	1.916	297.996	3.569	0.936	3.85

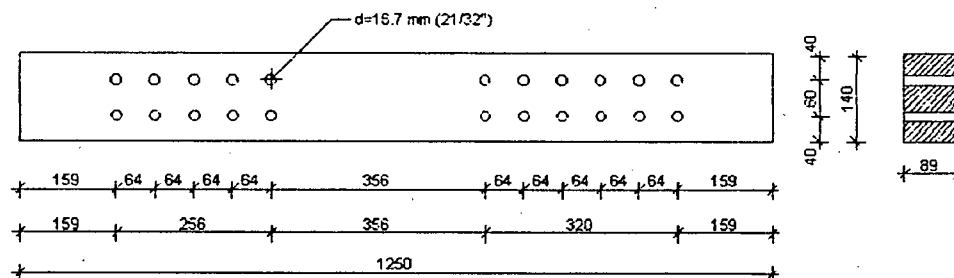
Code Ultimate Force = 181.79 kN

Stiffness (avg) = 275.29 kN/mm

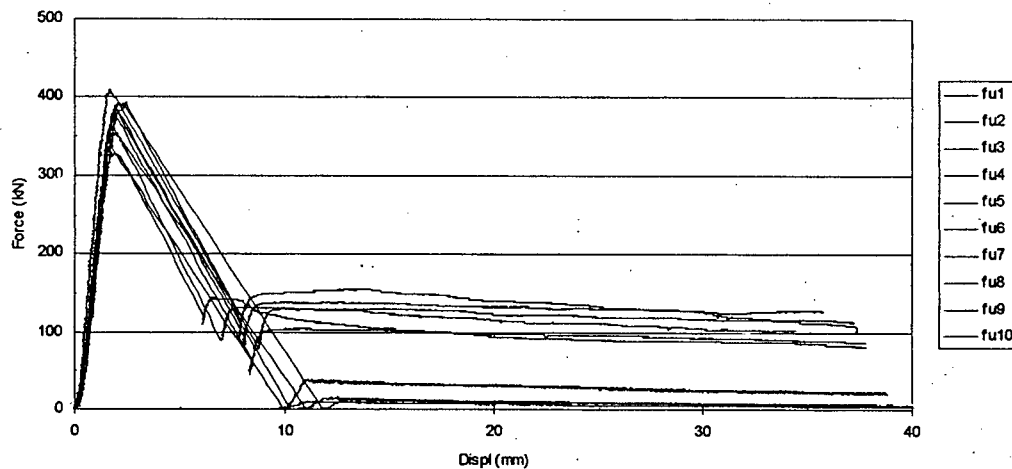
Energy Dissipated (avg) = 4170.78 kNmm

Moisture Content was not Measured

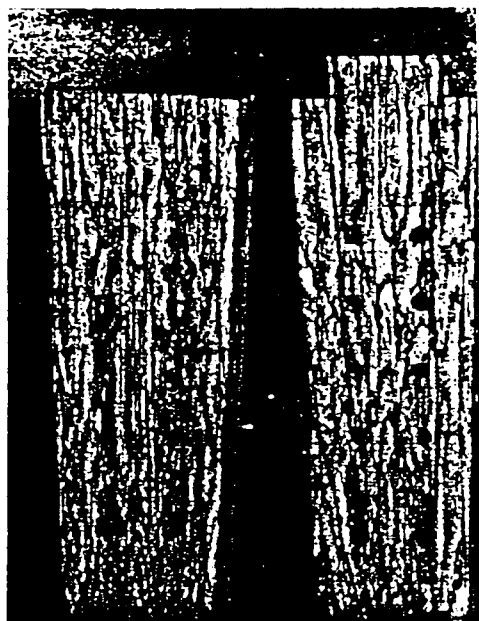
Failure mode: Group Shear, Row Tear-out (Row Shear)



Load-displacement Plot



FU



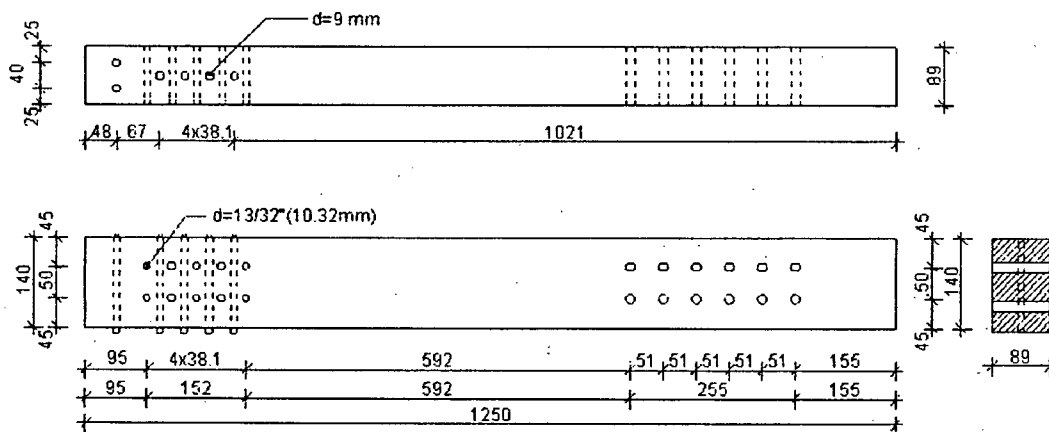
TRR
10-3/8" Bolt Connection in PSL
Lag Screw Reinforced

L/d = 9.3
e = 10d
s = 4d

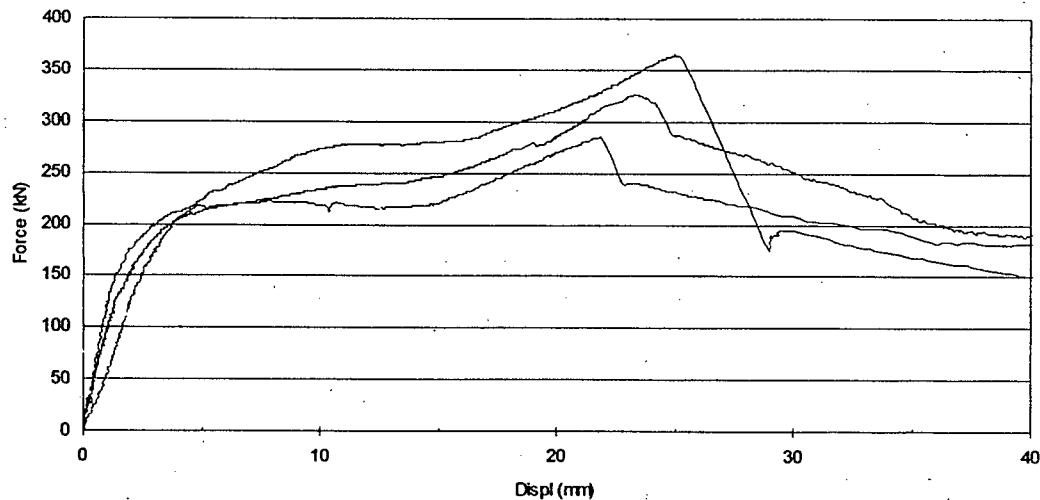
Quantity	Fult	D@Fult	80%Fult	D@80	D@50	Ductility
Specimen	[kN]	[mm]	[kN]	[mm]	[mm]	[]
TRR-1	365.02	24.97	292.02	26.60	3.20	8.31
TRR-2	284.41	21.72	227.53	26.50	1.10	24.09
TRR-3	326.35	23.42	261.08	28.90	2.20	13.14

Quantity	Stiffness	Energy	Design F	Dens.green	Dens.dry	Moist.cnt.
Specimen	[kN/mm]	[Nm]	[kN]	[kg/m3]	[kg/m3]	[%]
TRR-1	72.37	9491.67	N/A	676.34	635.72	8.44
TRR-2	106.13	8636.06	N/A	593.70	561.07	7.53
TRR-3	83.54	9431.28	N/A	640.64	616.65	8.21

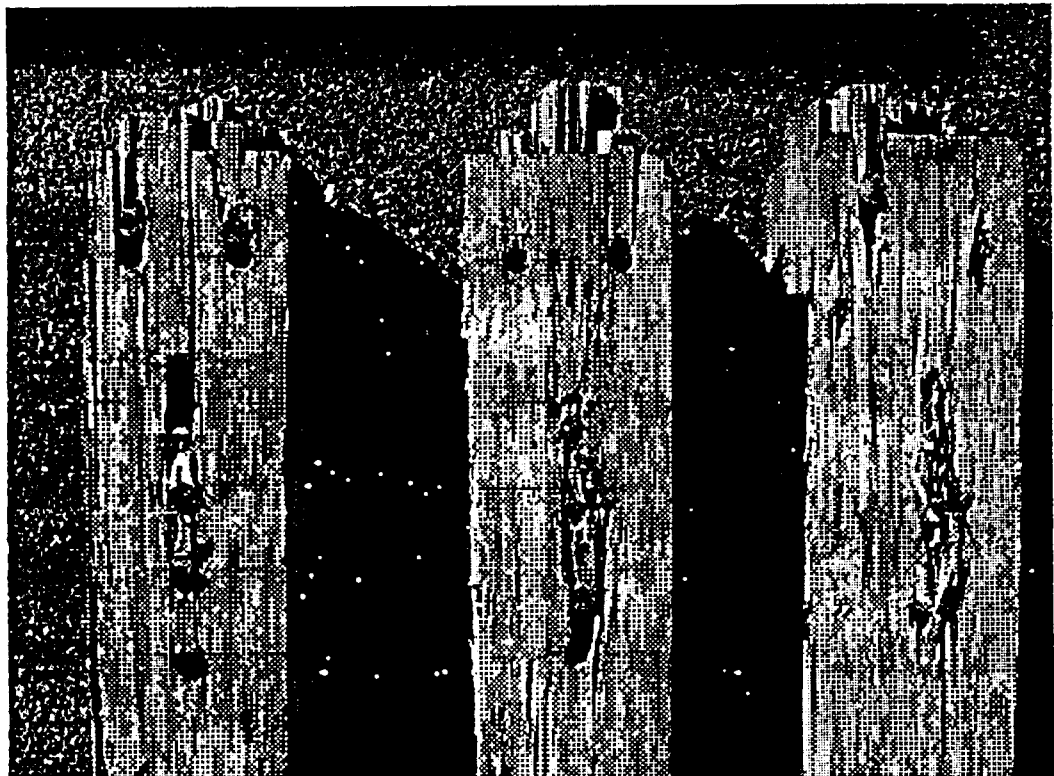
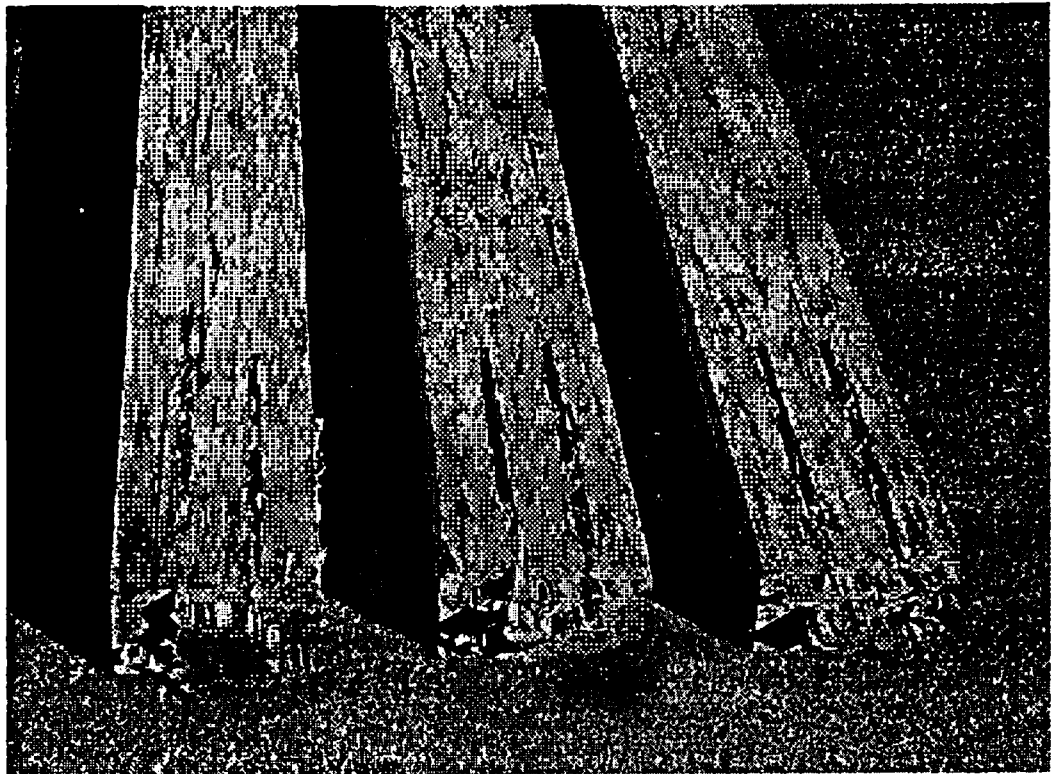
Failure mode: Biaxial Shear Plug, Row Tear -out



Load-displacement Plot



TRR



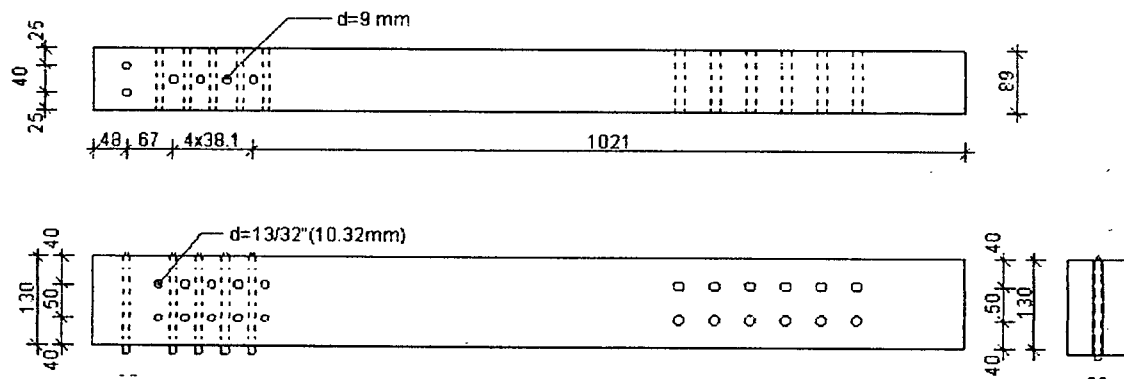
GTRR
10-3/8" Bolt Connection in Glulam
Lag Screw Reinforced

$L/d = 9.3$
 $e = 10d$
 $s = 4d$

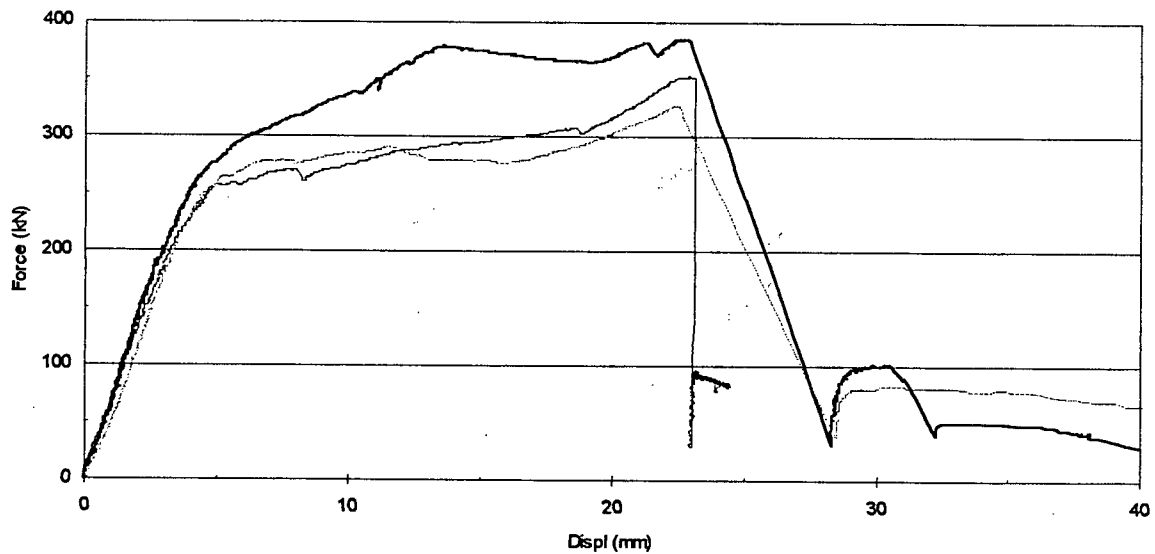
Quantity	Fult	D@Fult	80%Fult	D@80	D@50	Ductility
Specimen	[kN]	[mm]	[kN]	[mm]	[mm]	[]
GTRR-1	384.14	22.88	307.31	24.10	2.70	8.93
GTRR-2	326.13	22.50	260.90	23.70	2.70	8.77
GTRR-3	352.50	23.10	282.00	23.10	2.70	8.55

Quantity	Stiffness	Energy	Design F	Dens.green	Dens.dry	Moist.cnt.
Specimen	[kN/mm]	[Nm]	[kN]	[kg/m ³]	[kg/m ³]	[%]
GTRR-1	88.05	8850.07	N/A	616.04	588.15	11.84
GTRR-2	64.92	7663.35	N/A	613.05	572.92	13.02
GTRR-3	70.82	6081.70	N/A	617.76	587.70	10.96

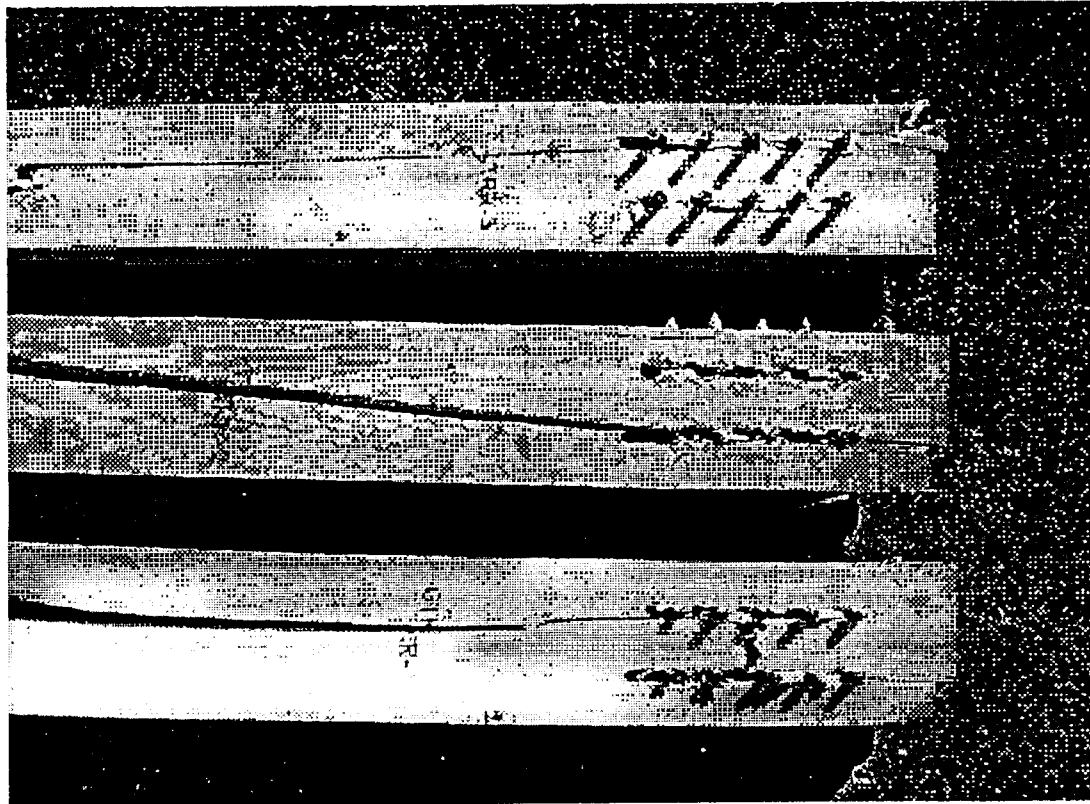
Failure mode: Row Tear –out, Row Splitting



Load-displacement Plot



GTRR



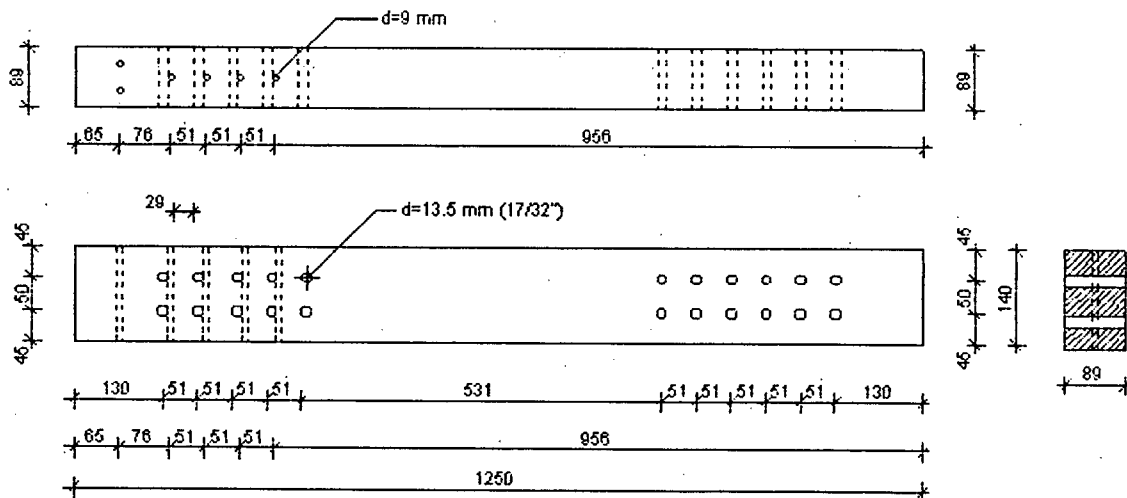
HRRSH
10-1/2" Bolt Connection in PSL
Lag Screw Reinforced-Offset Position

$L/d = 7.0$
$e = 10d$
$s = 4d$

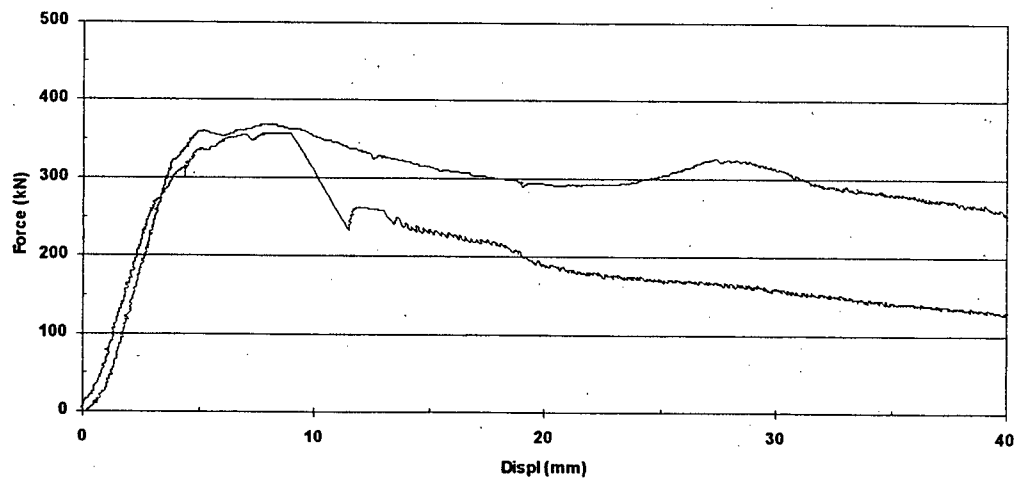
Quantity	Fult	D@Fult	80%Fult	D@80	D@50	Ductility
Specimen	[kN]	[mm]	[kN]	[mm]	[mm]	[]
HRRSH1	368.5	8.16	294.8	31.7	2.52	12.58
HRRSH2	357.6	8.5	286.08	10.4	2.06	5.05

Quantity	Stiffness	Energy	Design F	Dens.wet	Dens.dry	Moist.cnt.
Specimen	[kN/mm]	[Nm]	[kN]	[kg/m3]	[kg/m3]	[%]
HRRSH1	123.35	11781.4	N/A	634.78	607.19	8.53
HRRSH2	96.99	8199.41	N/A	608.07	586.99	8.72

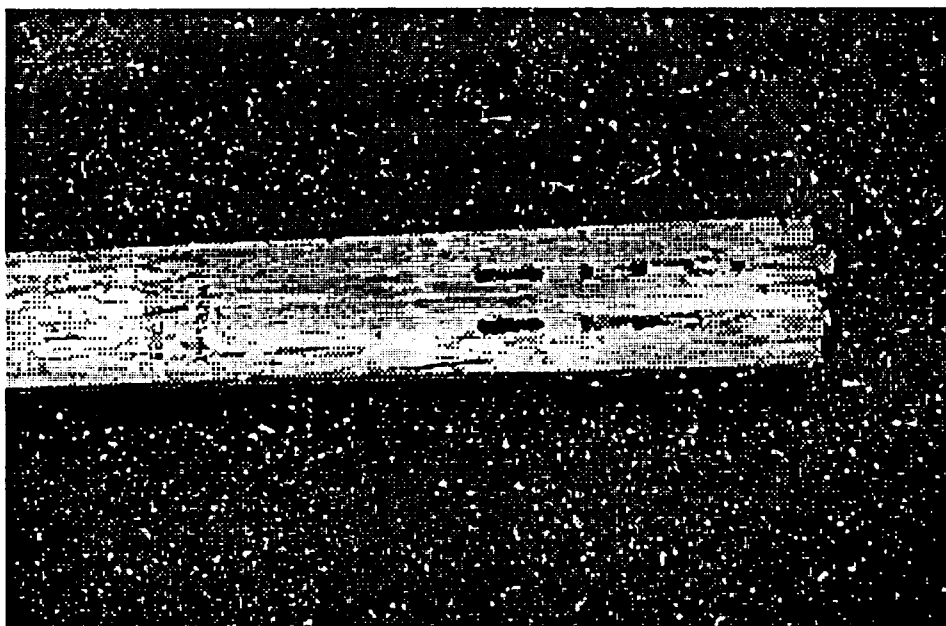
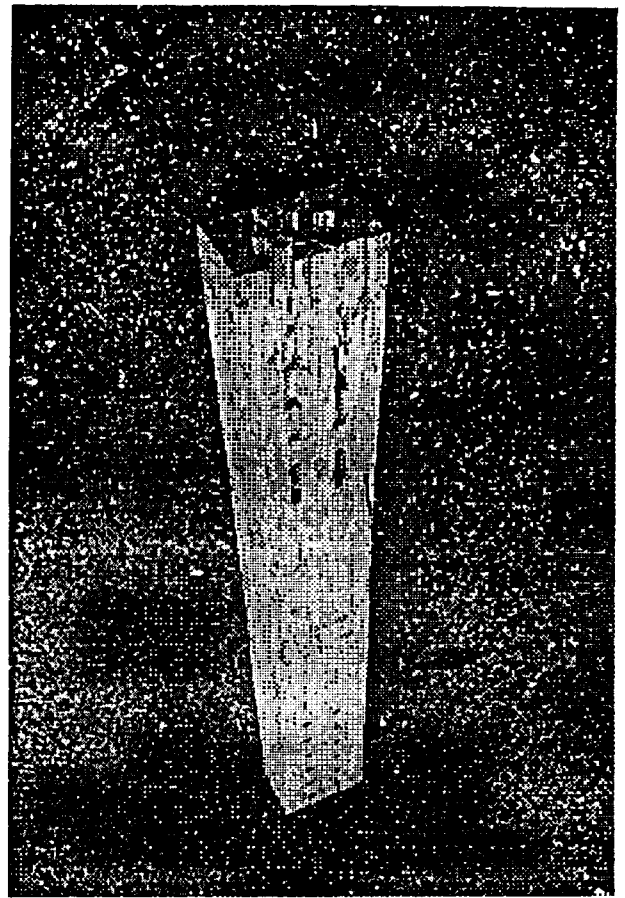
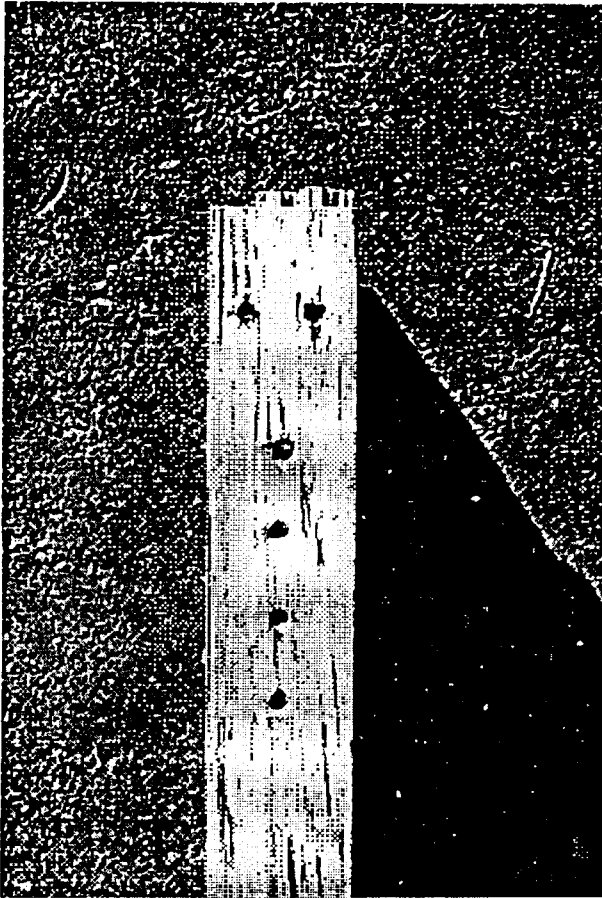
Failure mode: Bi-axial shear plug, row tear-out



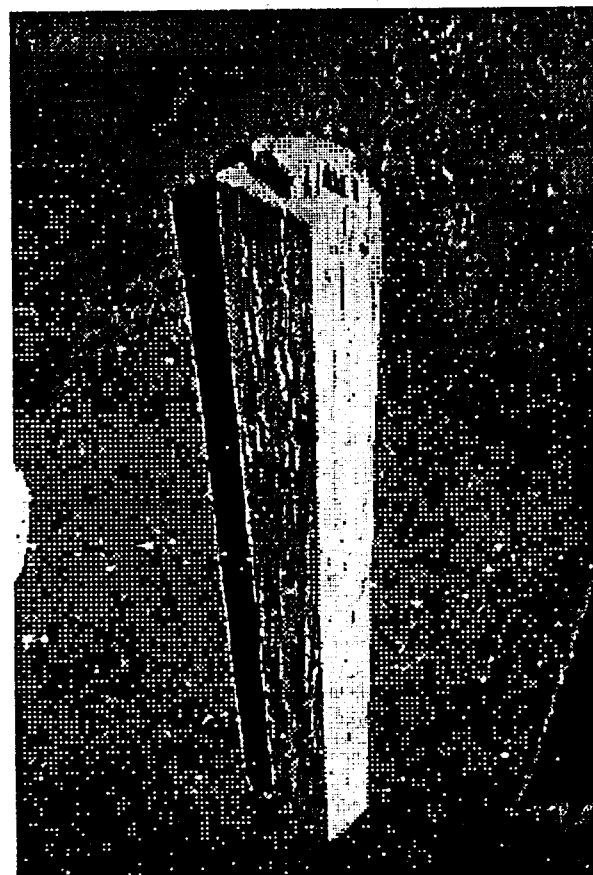
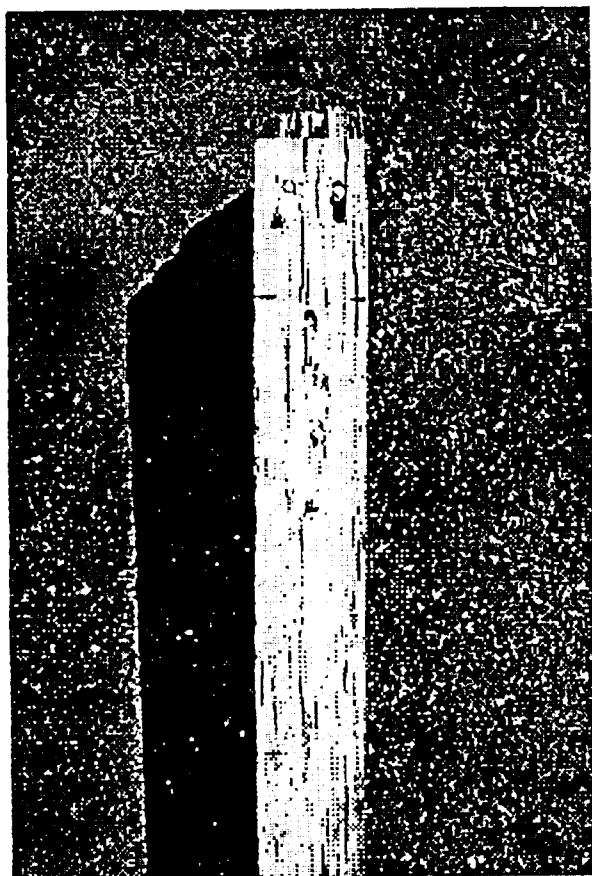
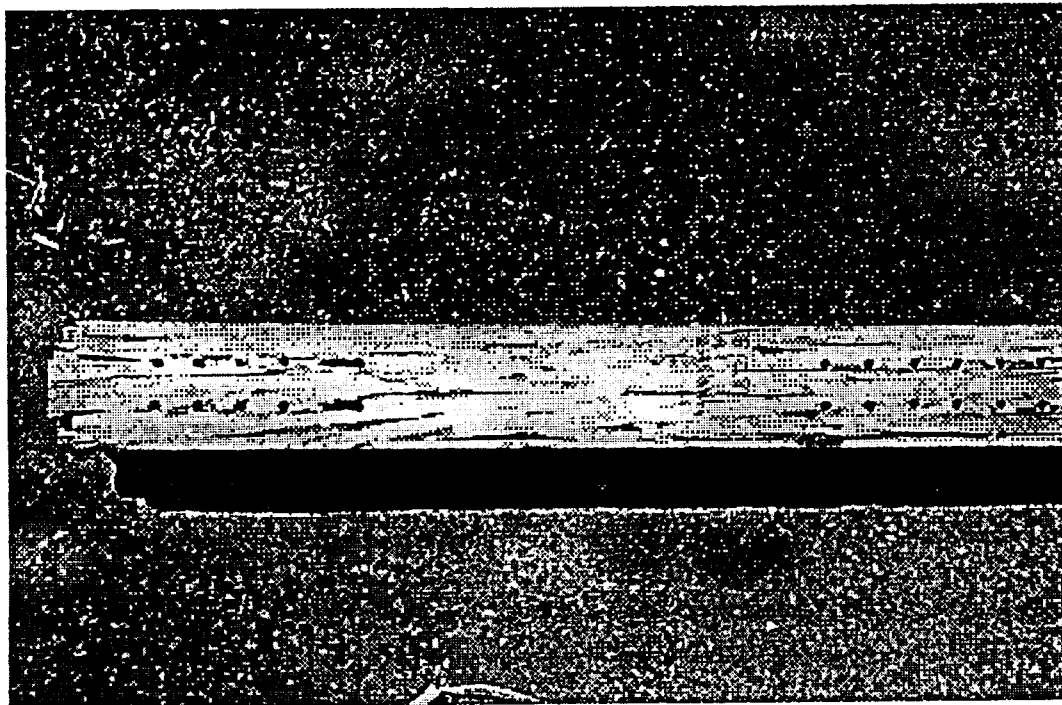
Load-displacement Plot



HRRSH1



HRRSH2



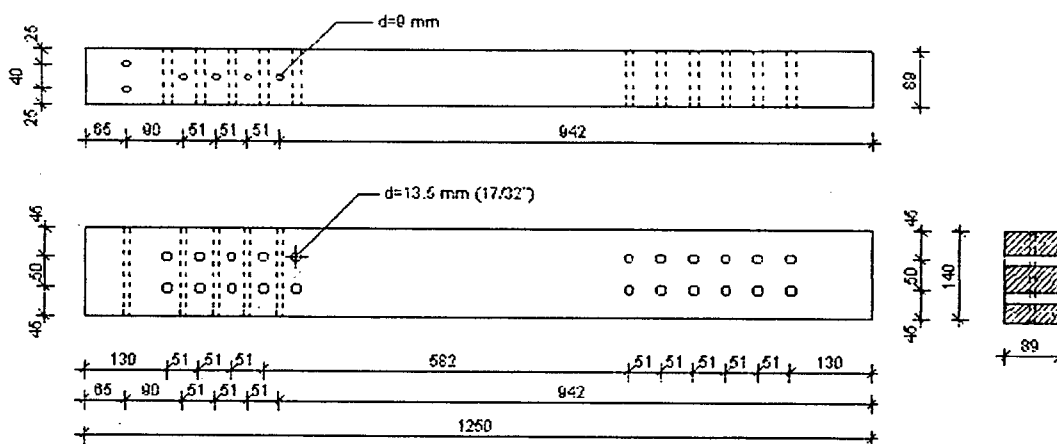
HRR
10-1/2" Bolt Connection in PSL
Lag Screw Reinforced

$L/d = 7.0$
 $e = 10d$
 $s = 4d$

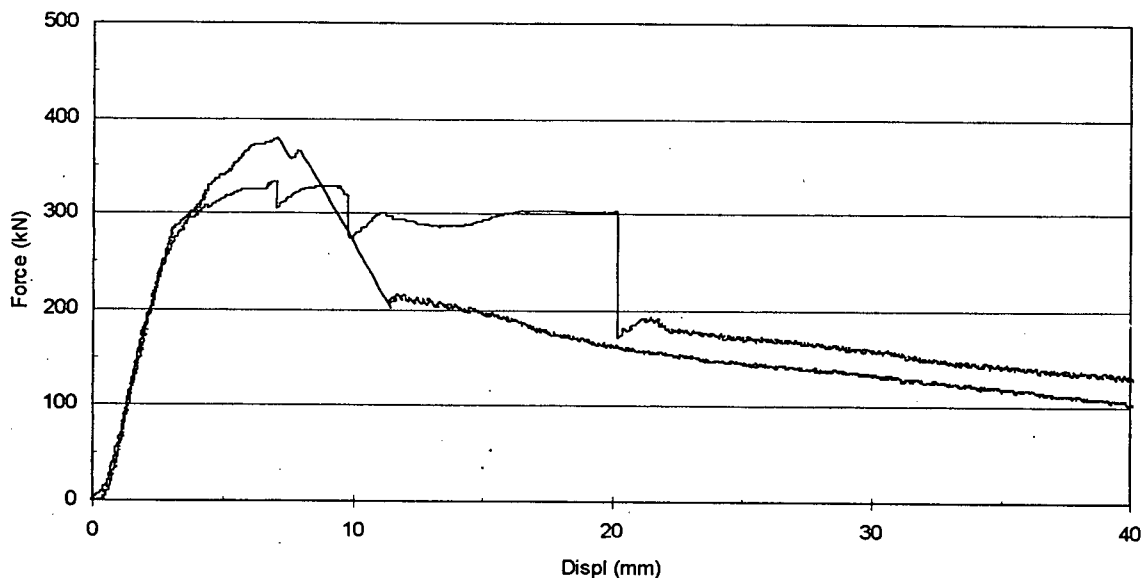
Quantity	Fult	D@Fult	80%Fult	D@80	D@50	Ductility
Specimen	[kN]	[mm]	[kN]	[mm]	[mm]	[]
HRR1	380.01	7.1	304.01	3.9	2.05	1.9
HRR2	333.95	5.77	267.16	17.58	1.67	10.53

Quantity	Stiffness	Energy	Design F	Dens.wet	Dens.dry	Moist.cnt.
Specimen	[kN/mm]	[Nm]	[kN]	[kg/m ³]	[kg/m ³]	[%]
HRR1	130.36	7333.04	N/A	652.1	592.58	8.2
HRR2	119.5	8467.43	N/A	653.36	642.06	8.01

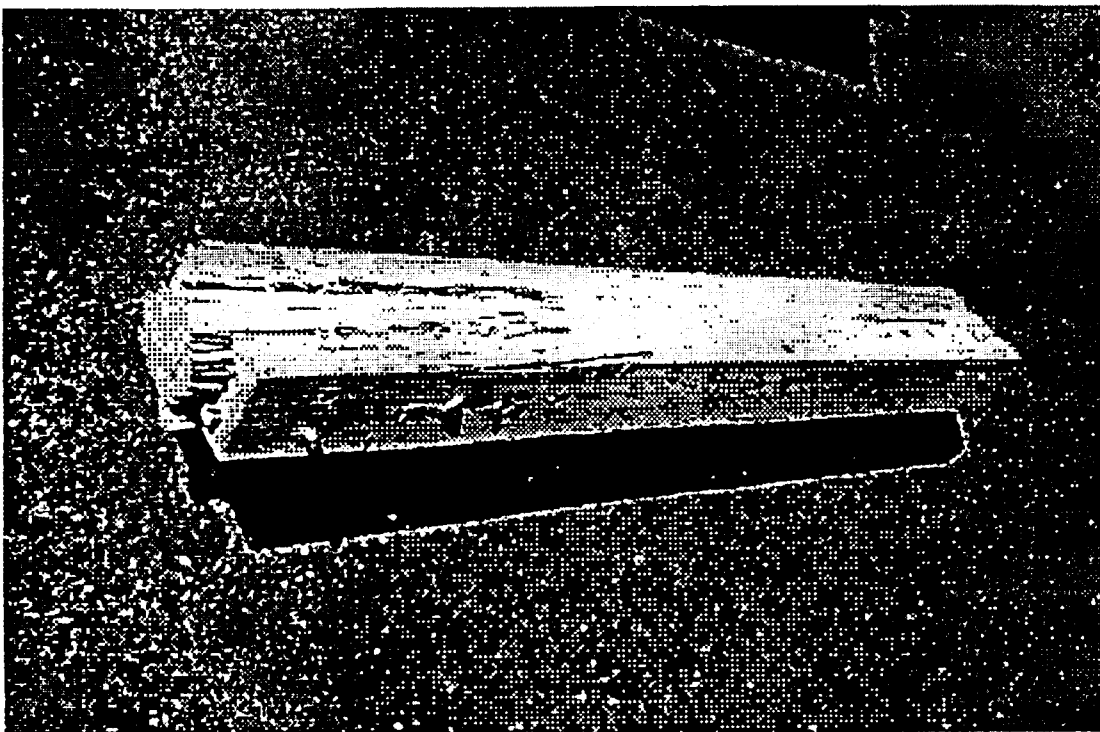
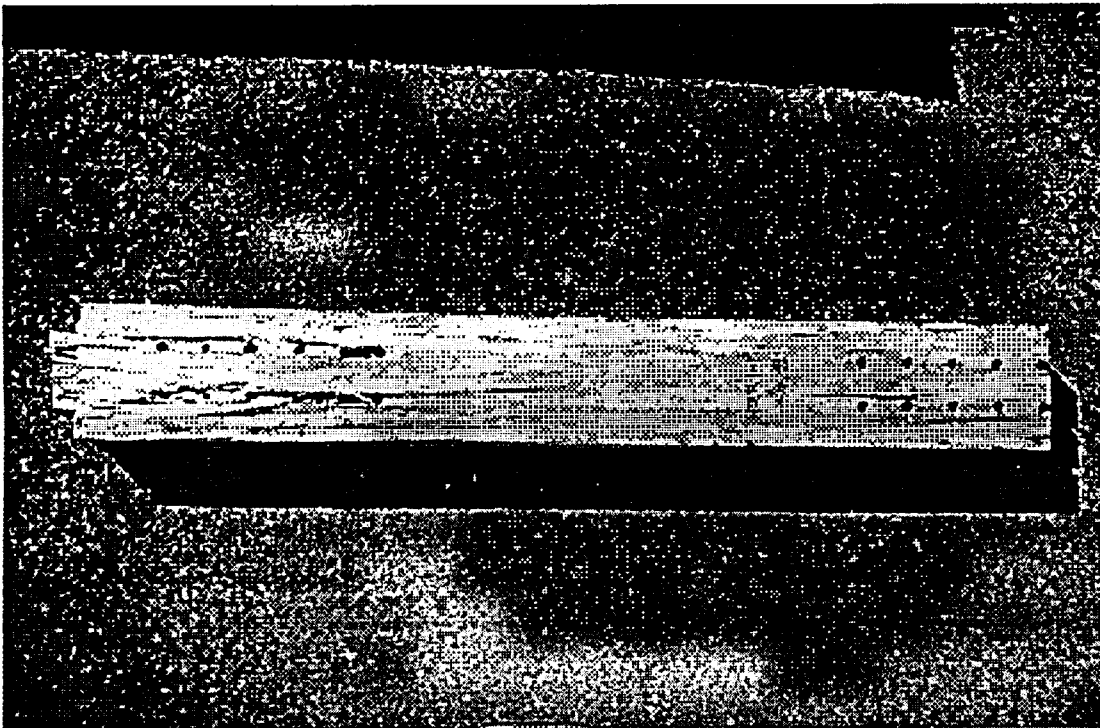
Failure mode: Bi-axial shear plug, row tear-out



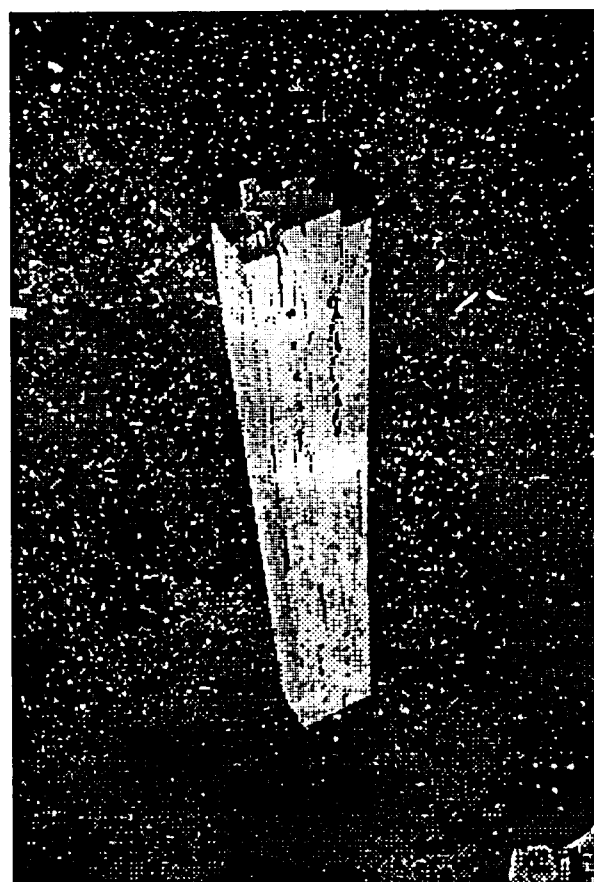
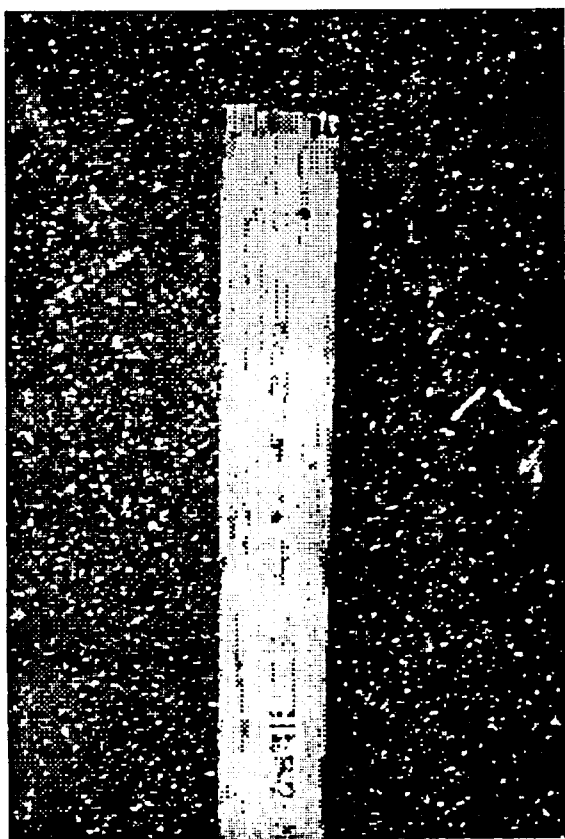
Load-displacement Plot



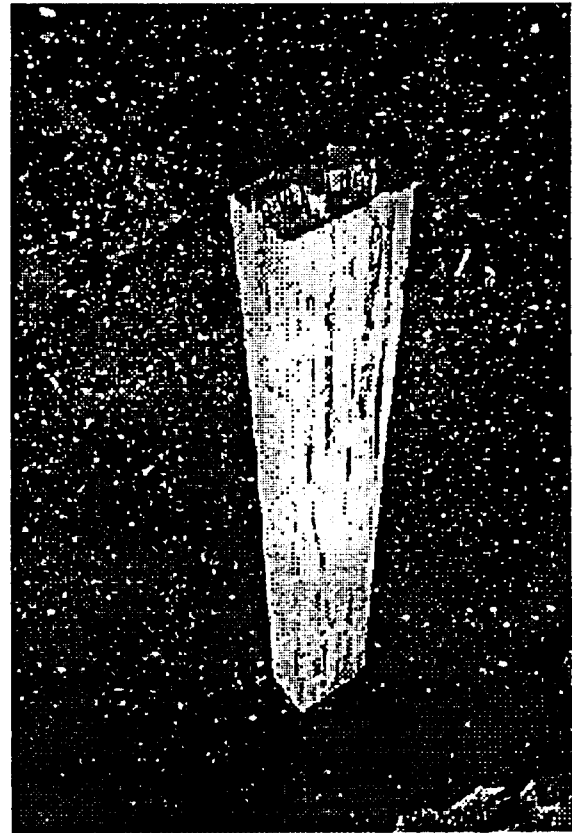
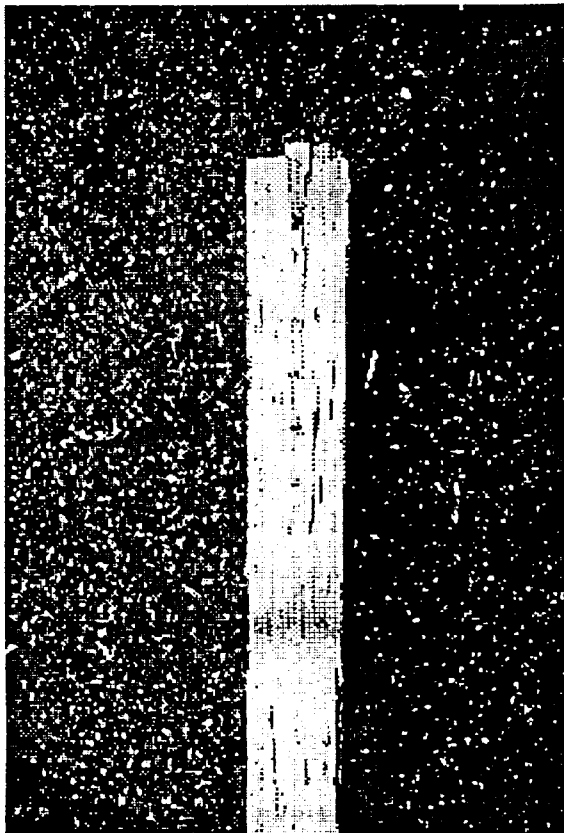
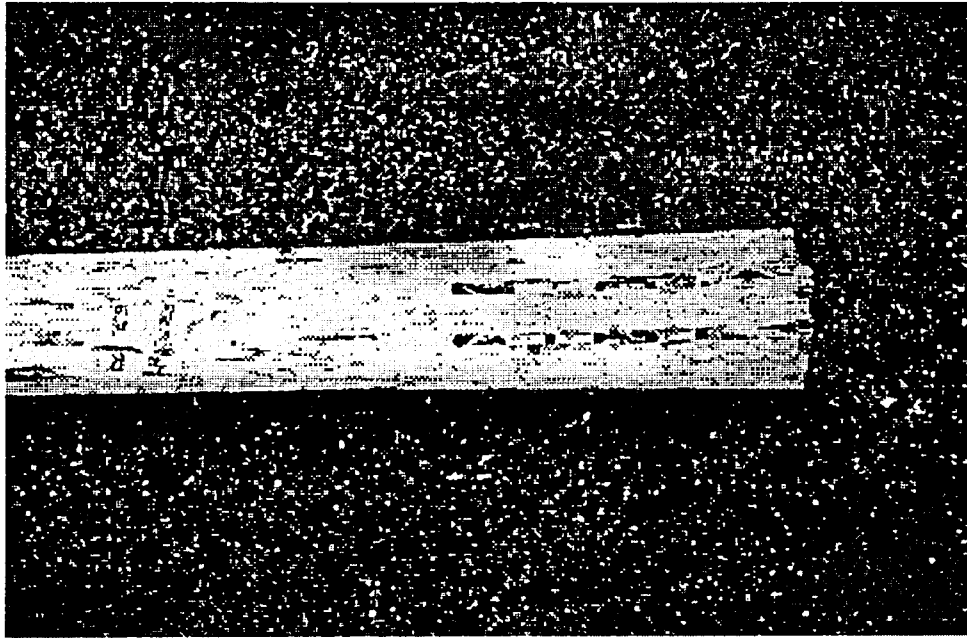
HRR1



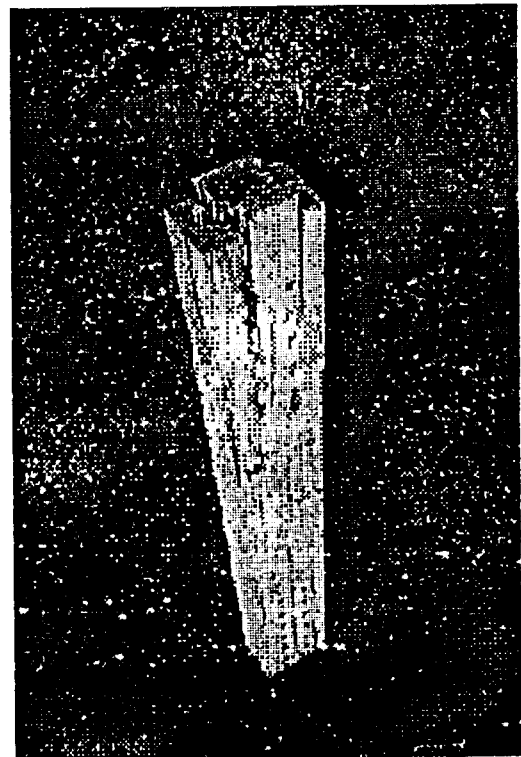
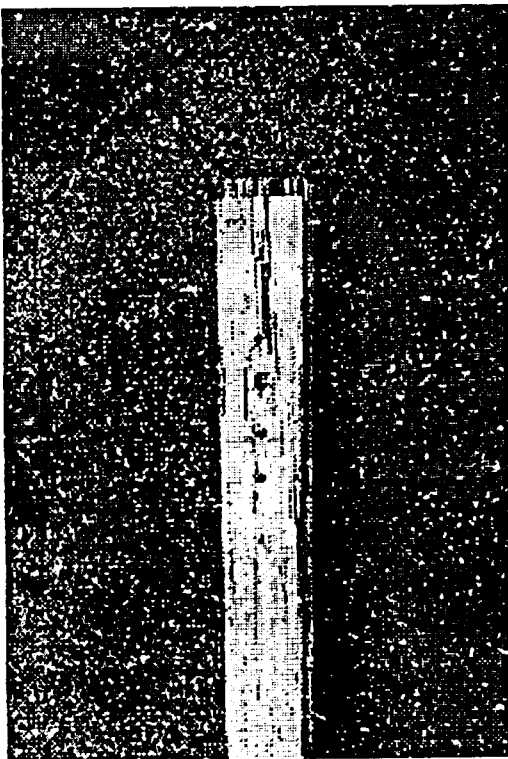
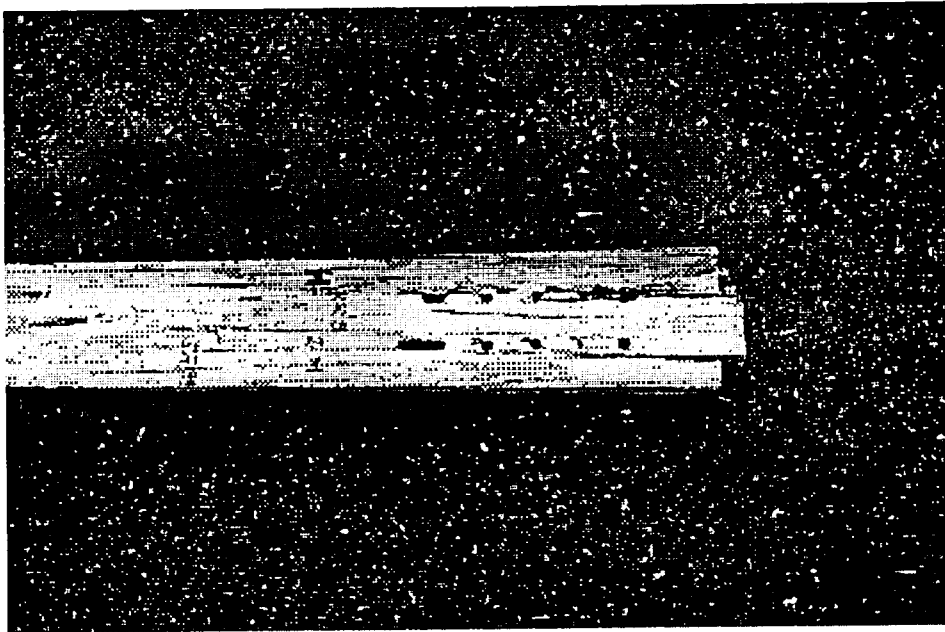
HRR2



HRRS1



HRRS2



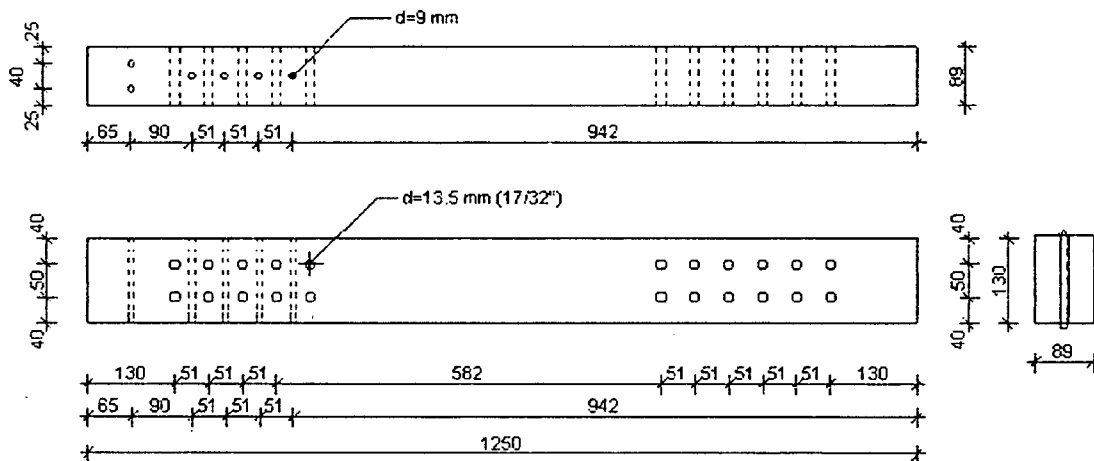
GHRR
10-1/2" Bolt Connection in Glulam
Lag Screw Reinforced

L/d = 7.0
e = 10d
s = 4d

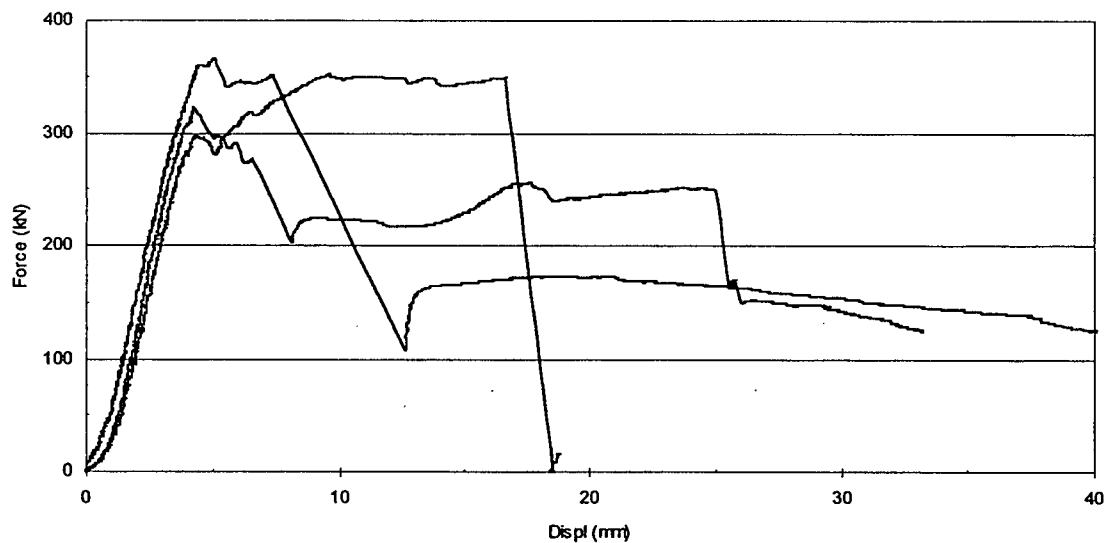
Quantity	Fult	D@Fult	80%Fult	D@80	D@50	Ductility
Specimen	[kN]	[mm]	[kN]	[mm]	[mm]	[]
GHRR-1	350.25	9.67	280.20	17.00	2.10	8.10
GHRR-2	366.32	5.06	293.06	8.60	2.80	3.07
GHRR-3	322.44	4.25	257.95	7.00	2.40	2.92

Quantity	Stiffness	Energy	Design F	Dens.green	Dens.dry	Moist.cnt.
Specimen	[kN/mm]	[Nm]	[kN]	[kg/m3]	[kg/m3]	[%]
GHRR-1	95.23	5040.38	N/A	574.78	541.63	12.06
GHRR-2	98.15	7308.52	N/A	573.60	544.63	12.08
GHRR-3	108.39	7630.08	N/A	615.68	546.48	11.14

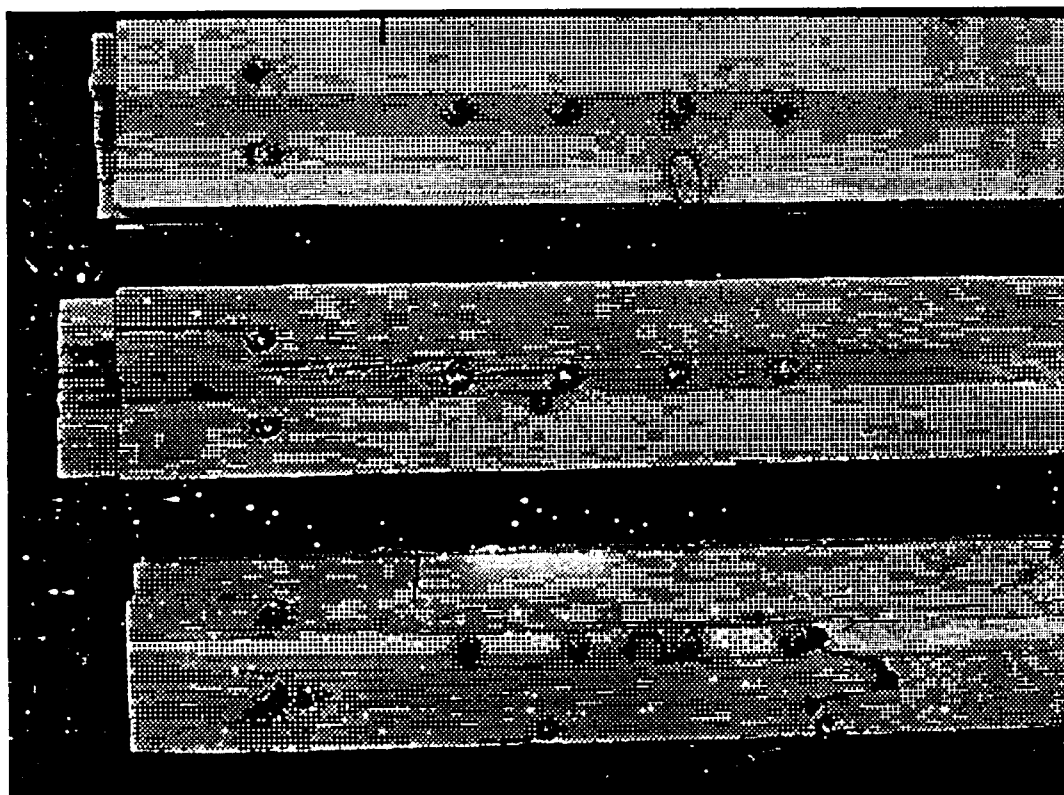
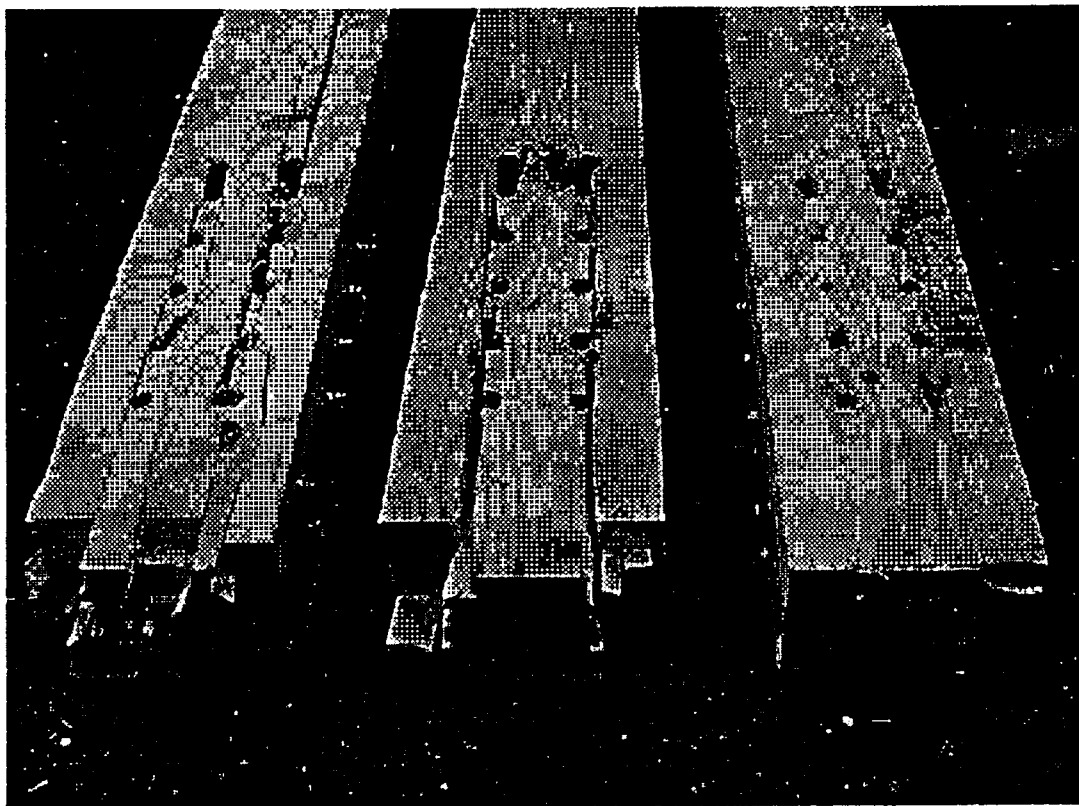
Failure mode: Shear Plug, Row Splitting



Load-displacement Plot



GHRR



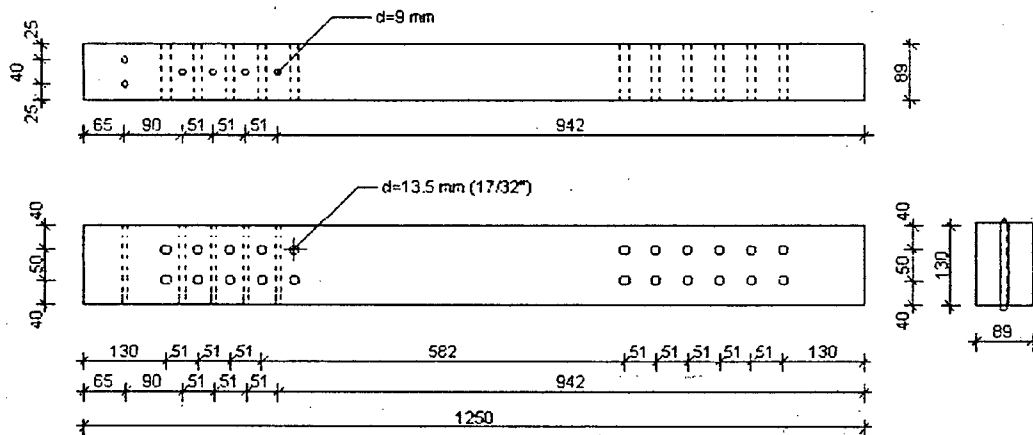
GHRRF
10-1/2" Bolt Connection in Glulam
Ready Rod (Fine Thread) Reinforced

$L/d = 7.0$
 $e = 10d$
 $s = 4d$

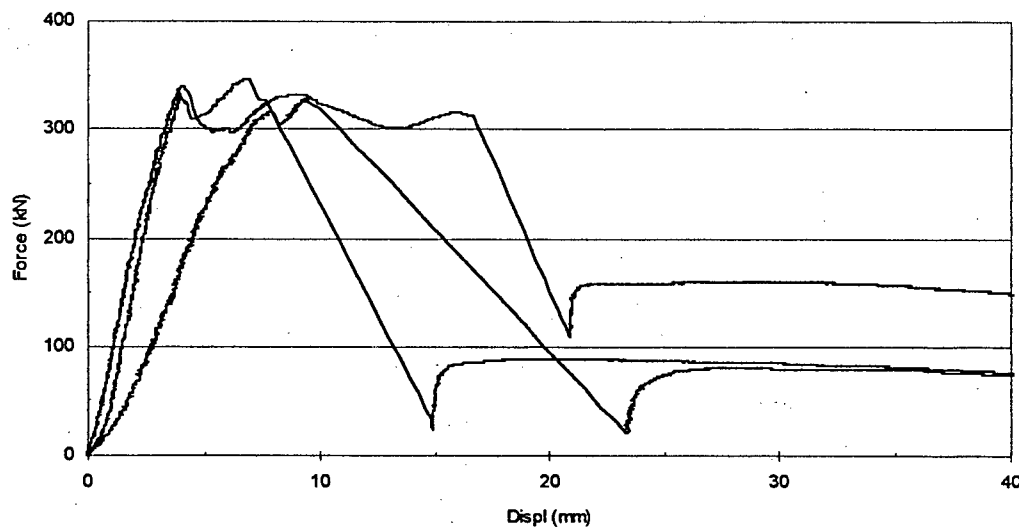
Quantity	Fult	D@Fult	80%Fult	D@80	D@50	Ductility
Specimen	[kN]	[mm]	[kN]	[mm]	[mm]	[]
GHRRF-1	346.68	6.96	277.34	8.90	2.10	4.24
GHRRF-2	338.30	4.20	270.64	17.60	1.60	11.00
GHRRF-3	327.65	9.42	262.12	12.50	4.00	3.13

Quantity	Stiffness	Energy	Design F	Dens.green	Dens.dry	Moist.cnt.
Specimen	[kN/mm]	[Nm]	[kN]	[kg/m ³]	[kg/m ³]	[%]
GHRRF-1	96.92	5233.51	N/A	622.93	611.50	11.91
GHRRF-2	108.36	8606.69	N/A	586.04	573.21	11.96
GHRRF-3	63.60	5500.00	N/A	575.84	555.14	12.00

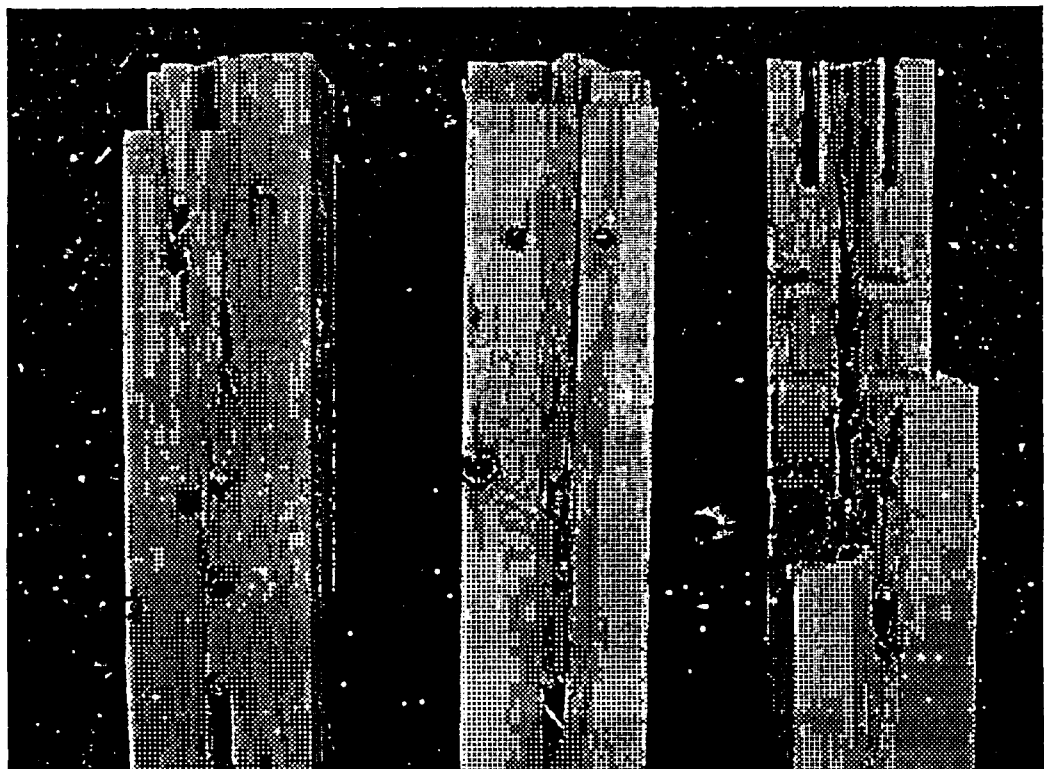
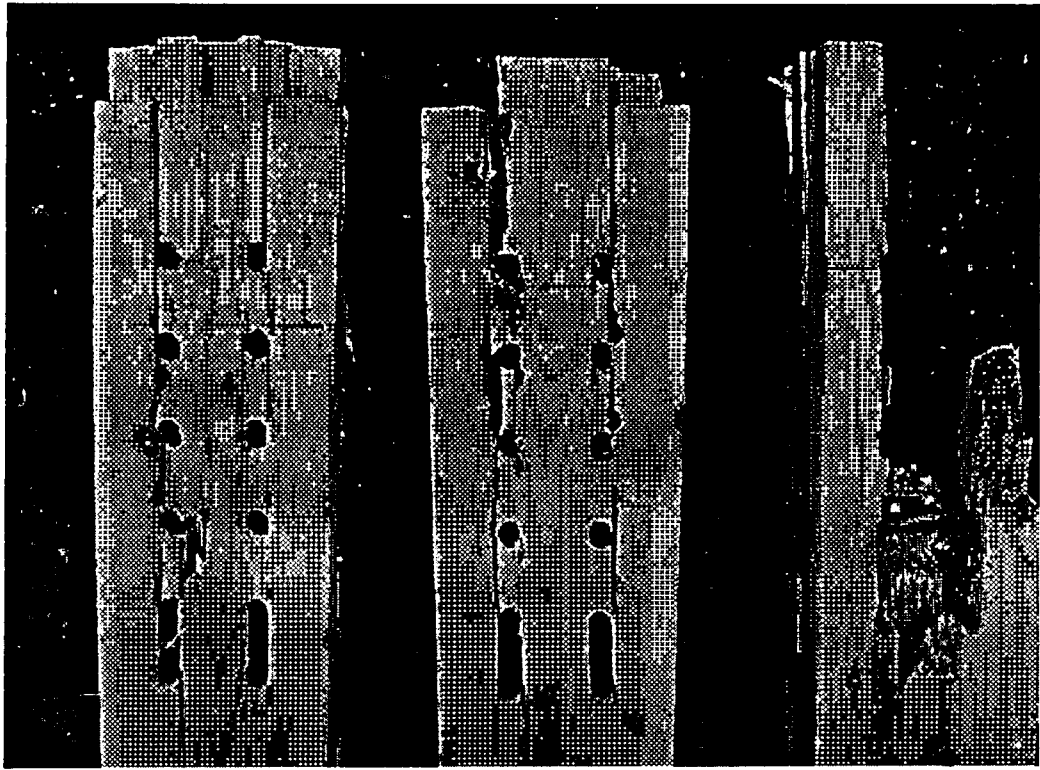
Failure mode: Shear Plug, Row Tear -out, Row Splitting



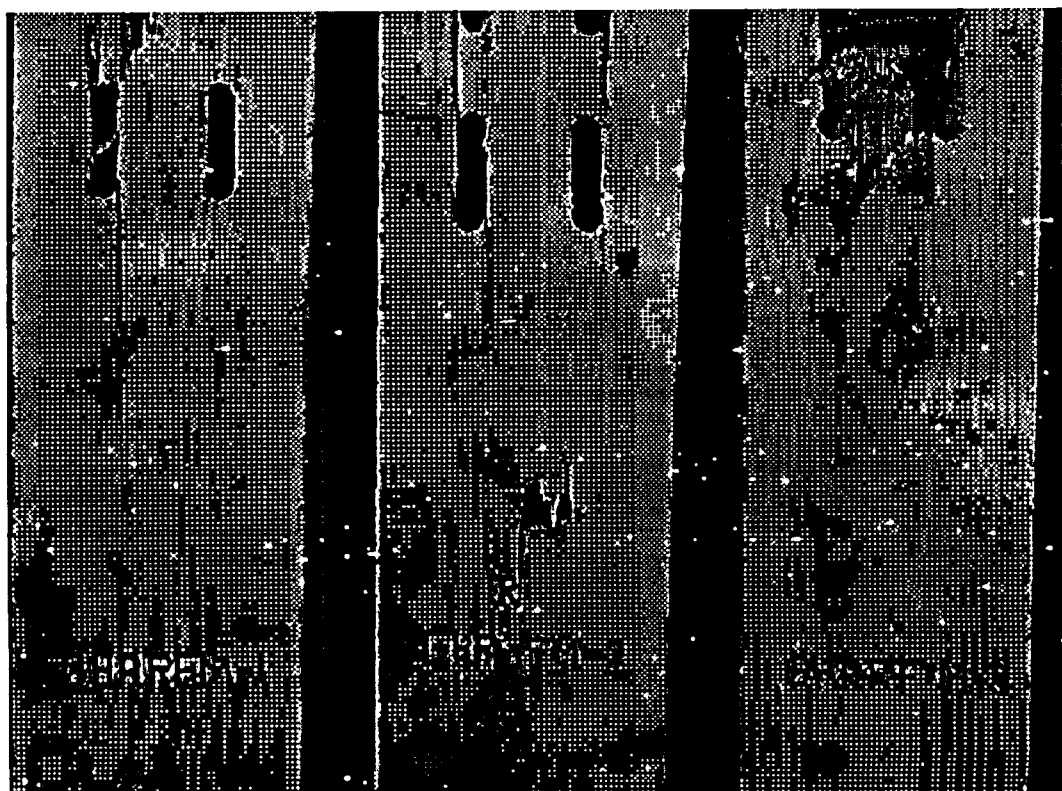
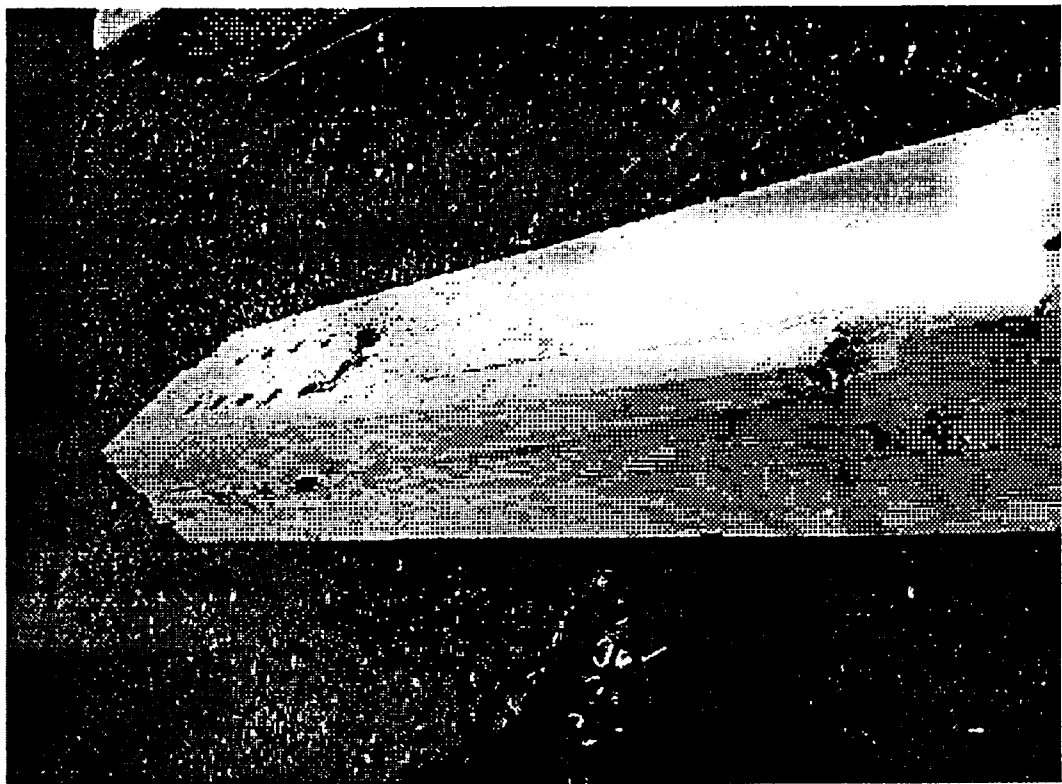
Load-displacement Plot



GHRRF



GHRRF



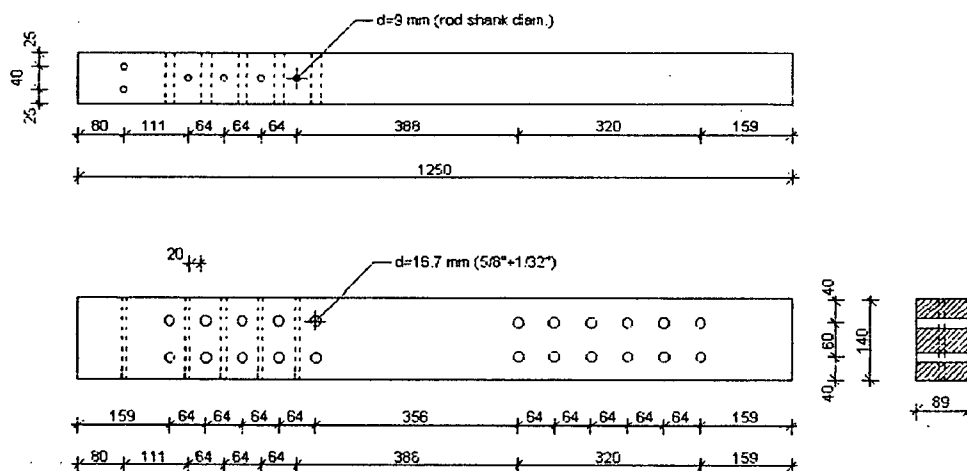
FRR
10-5/8" Bolt Connection in PSL
Lag Screw Reinforced

L/d = 5.6
e = 10d
s = 4d

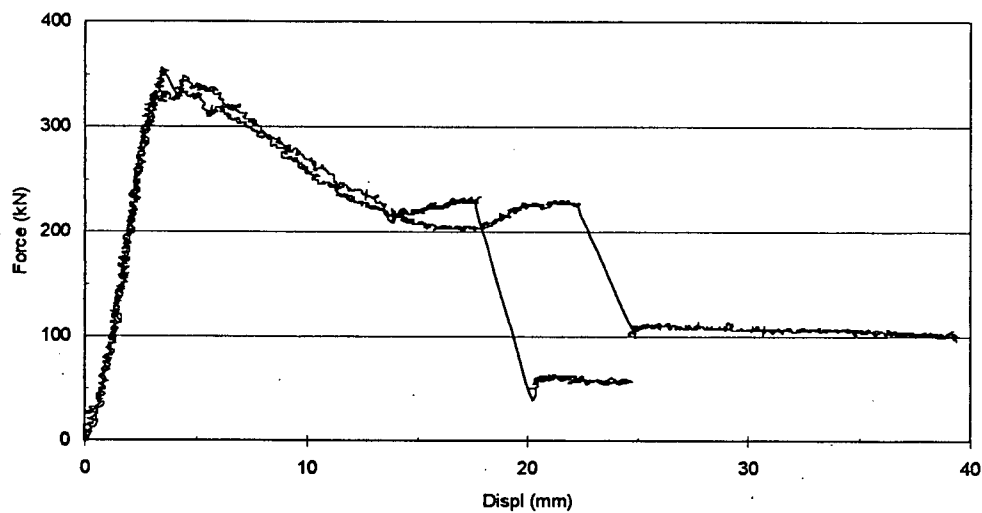
Quantity	Fult	D@Fult	80%Fult	D@80	D@50	Ductility
Specimen	[kN]	[mm]	[kN]	[mm]	[mm]	[]
FRR1	336.22	4.31	268.98	9.46	1.79	5.28
FRR2	356.42	3.41	285.14	8.7	1.8	4.83

Quantity	Stiffness	Energy	Design F	Dens.green	Dens.dry	Moist.cnt.
Specimen	[kN/mm]	[Nm]	[kN]	[kg/m3]	[kg/m3]	[%]
FRR1	160.57	7300.94	N/A	663.82	625.47	9.7
FRR2	151.43	5887.54	N/A	677.48	652.66	9.34

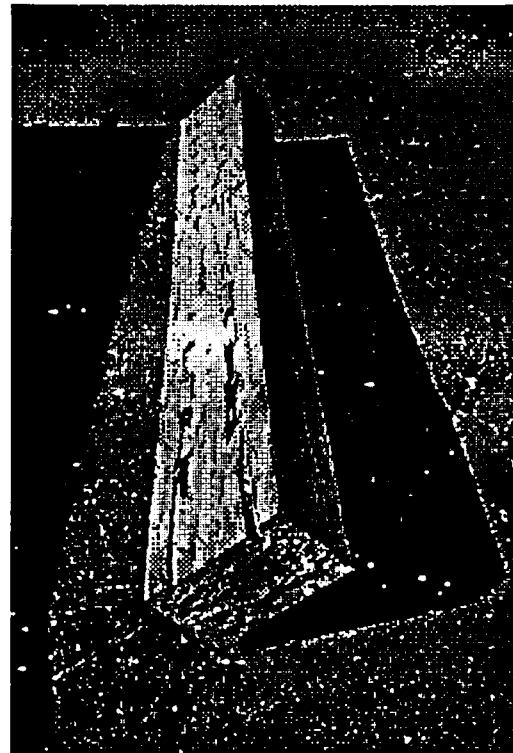
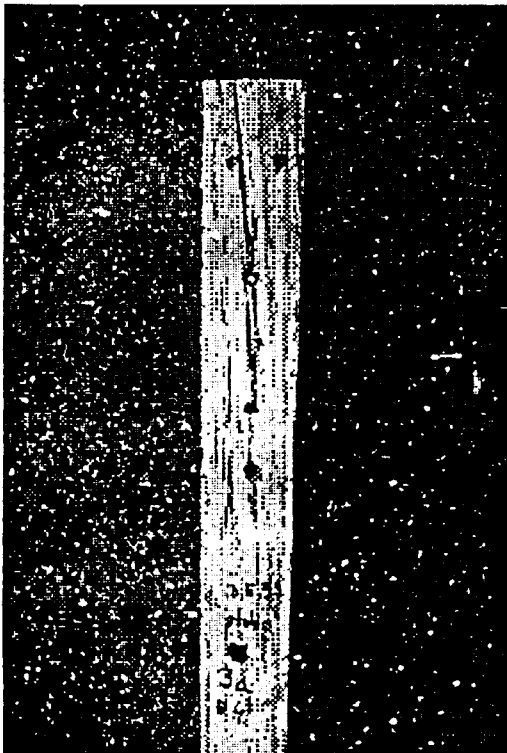
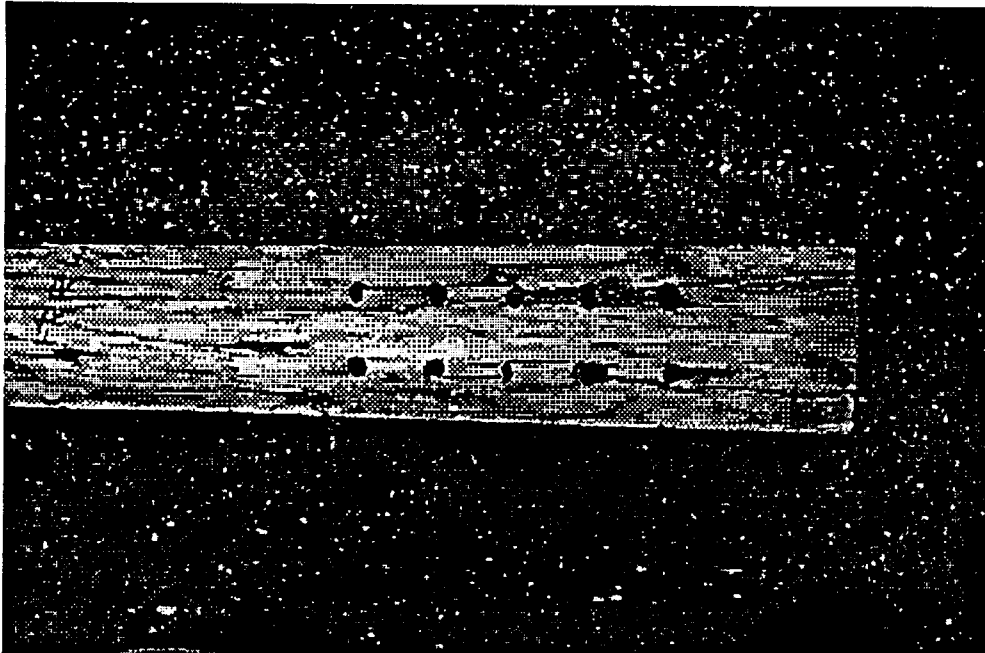
Failure mode: Biaxial shear plug



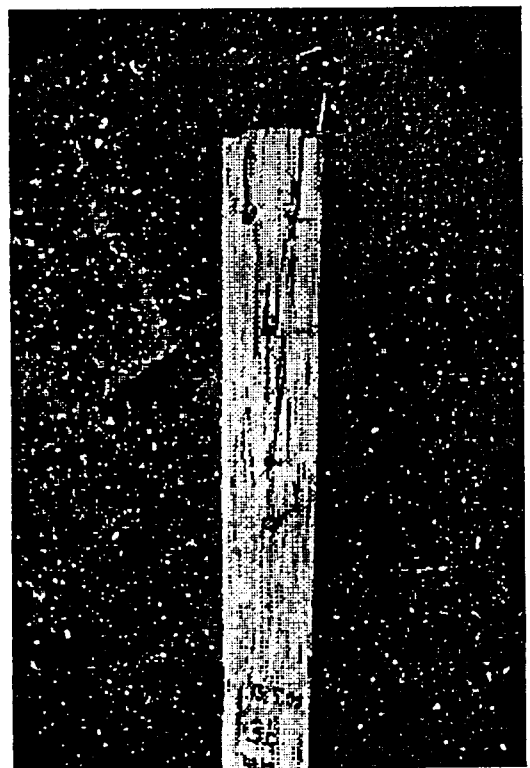
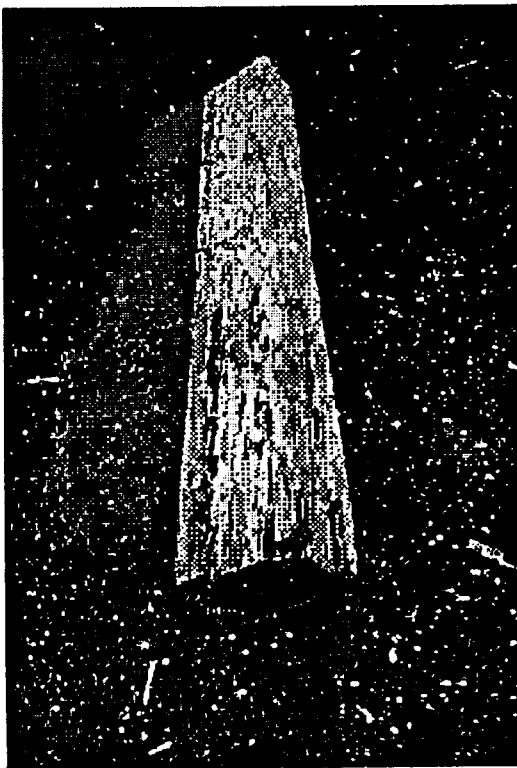
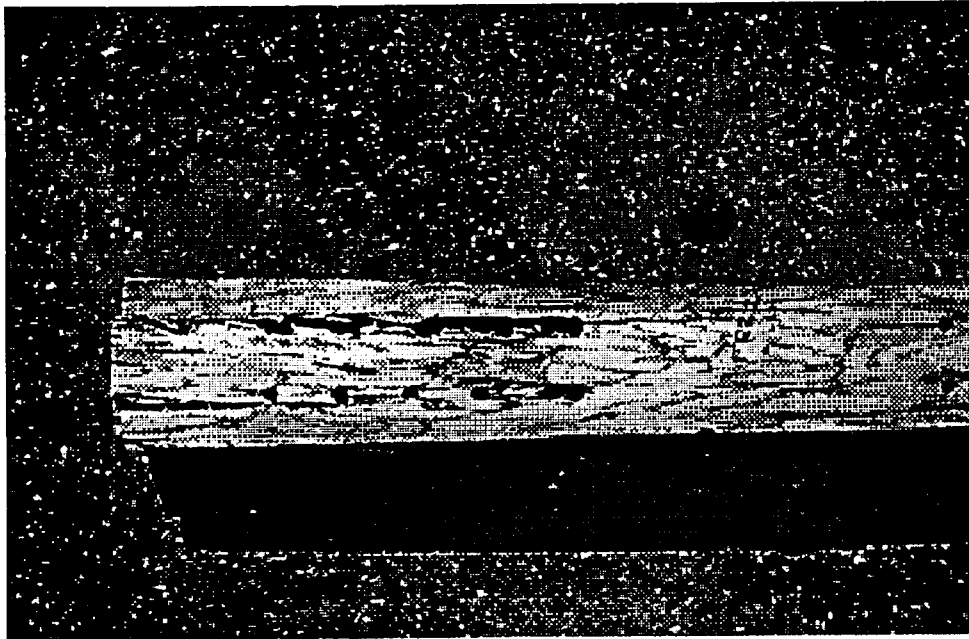
Load-displacement plot



FRR1



FRR2



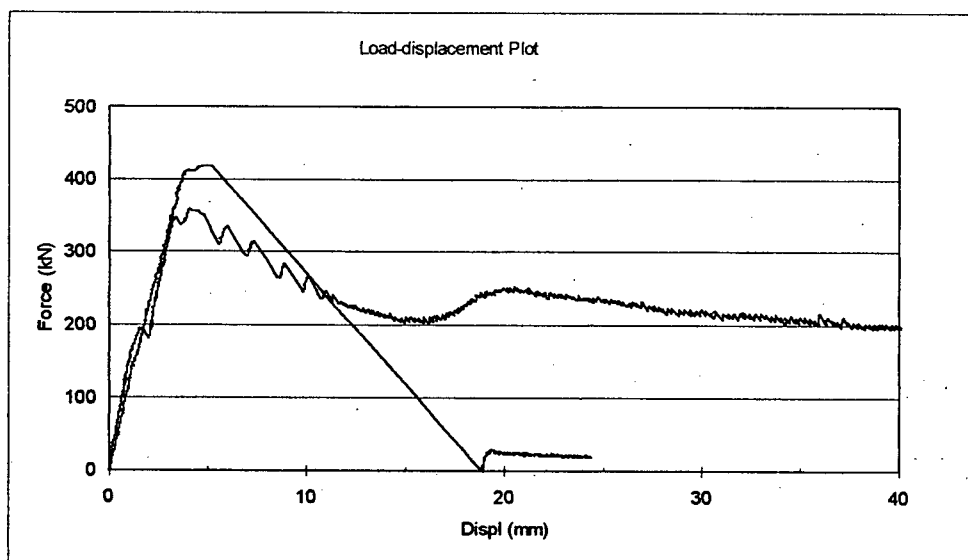
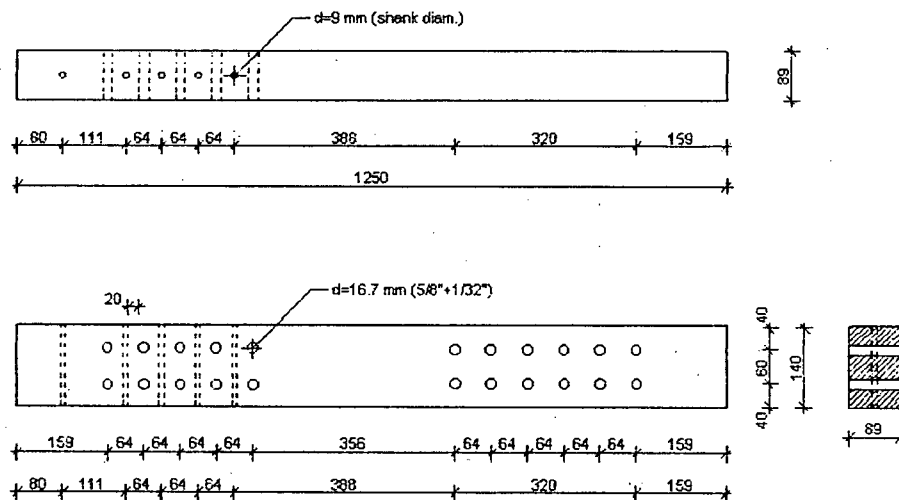
FRRS
10-5/8" Bolt Connection in PSL
Lag Screw Reinforced-Single End Rod

$L/d = 5.6$
 $e = 10d$
 $s = 4d$

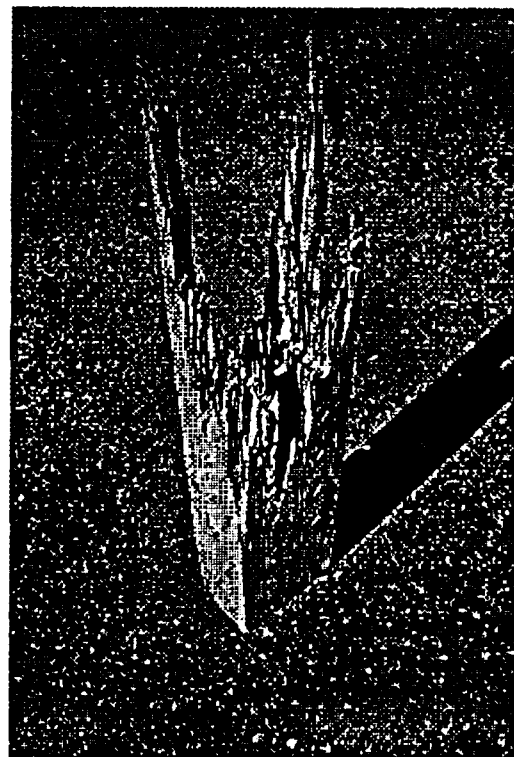
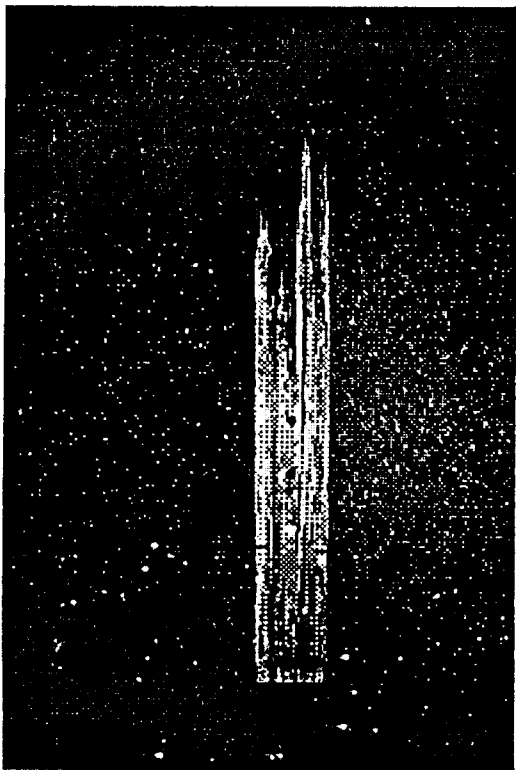
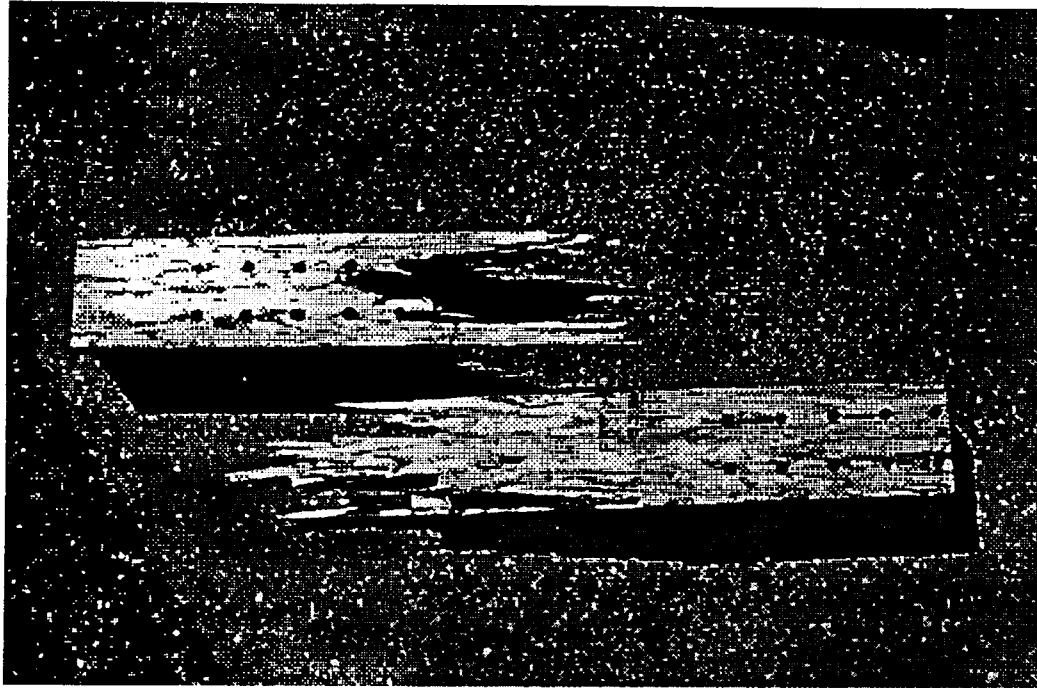
Quantity	Fult	D@Fult	80%Fult	D@80	D@50	Ductility
Specimen	[kN]	[mm]	[kN]	[mm]	[mm]	[]
FRRS1	418.47	5	334.78	7.89	1.84	4.29
FRRS2	360.02	4.09	288.02	7.99	1.9	4.21

Quantity	Stiffness	Energy	Design F	Dens.green	Dens.dry	Moist.cnt.
Specimen	[kN/mm]	[Nm]	[kN]	[kg/m ³]	[kg/m ³]	[%]
FRRS1	111.5	4231.22	N/A	651.69	586.99	9.69
FRRS2	128.31	9330.75	N/A	602.28	588.7	7.42

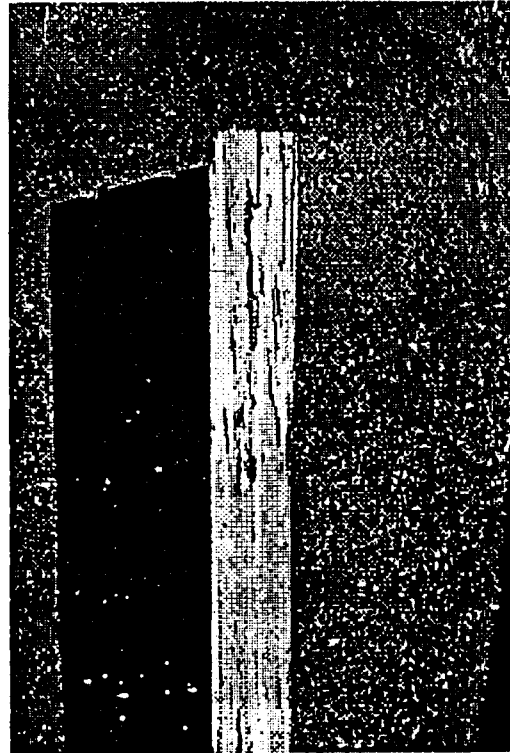
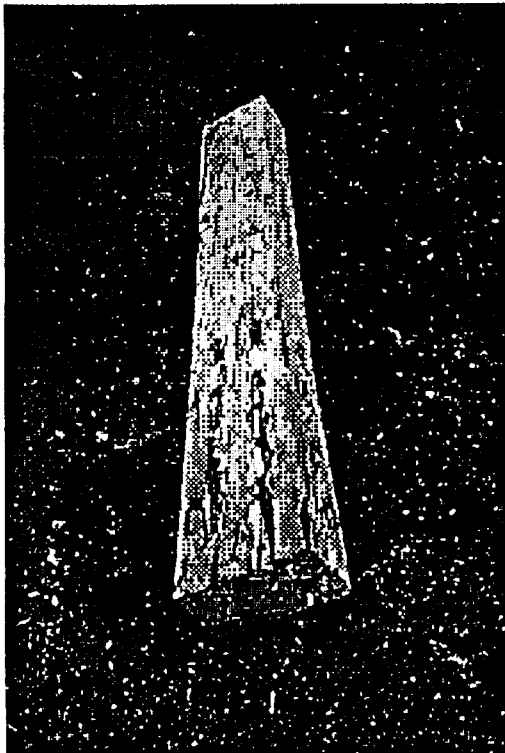
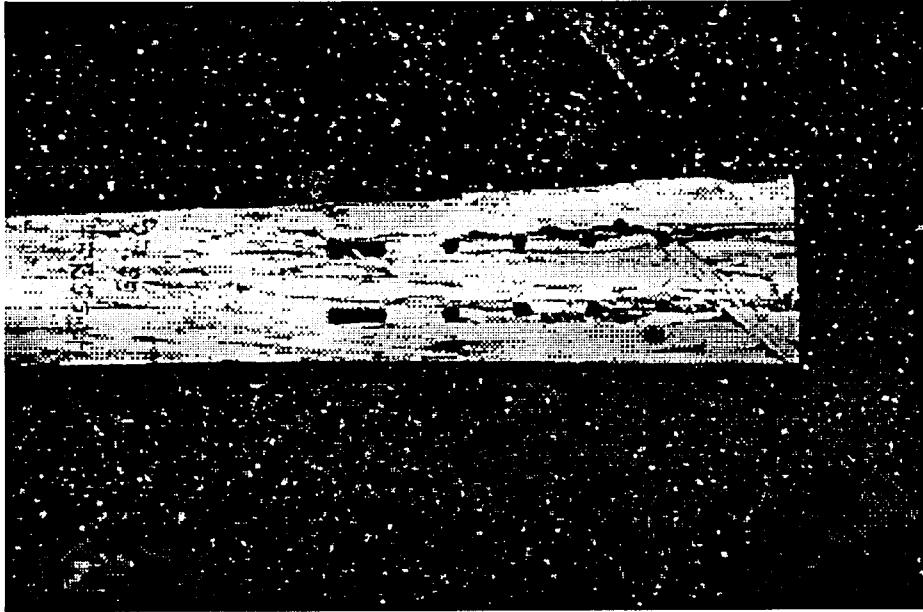
Failure mode: FRRS1- Net section failure (rupture)
FRRS2- Row tear-out



FRRS1



FRRS2



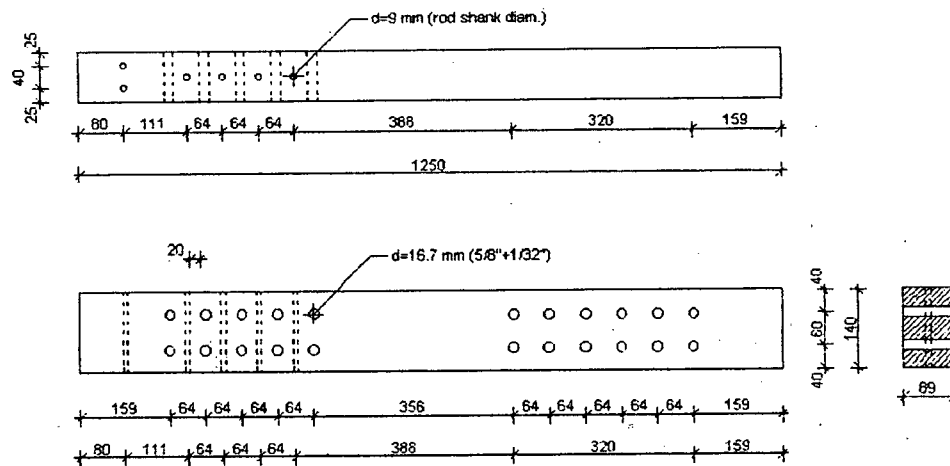
FRRF
10-5/8" Bolt Connection in PSL
Ready Rod Reinforced

$L/d = 5.6$
 $e = 10d$
 $s = 4d$

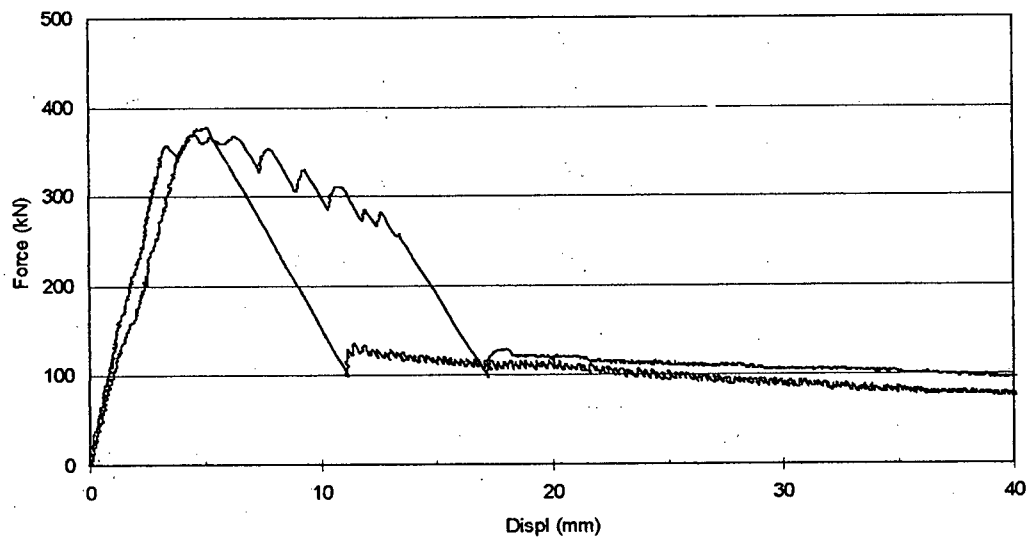
Quantity	Fult	D@Fult	80%Fult	D@80	D@50	Ductility
Specimen	[kN]	[mm]	[kN]	[mm]	[mm]	[]
FRRF1	376.97	5.12	301.58	6.76	1.6	4.23
FRRF2	369.37	4.63	295.50	11.3	2.15	5.26

Quantity	Stiffness	Energy	Design F	Dens.wet	Dens.dry	Moist.cnt.
Specimen	[kN/mm]	[Nm]	[kN]	[kg/m ³]	[kg/m ³]	[%]
FRRF1	98.5	5569.01	N/A	671.77	641.42	9.09
FRRF2	86.74	6914.85	N/A	592.44	567.37	9.2

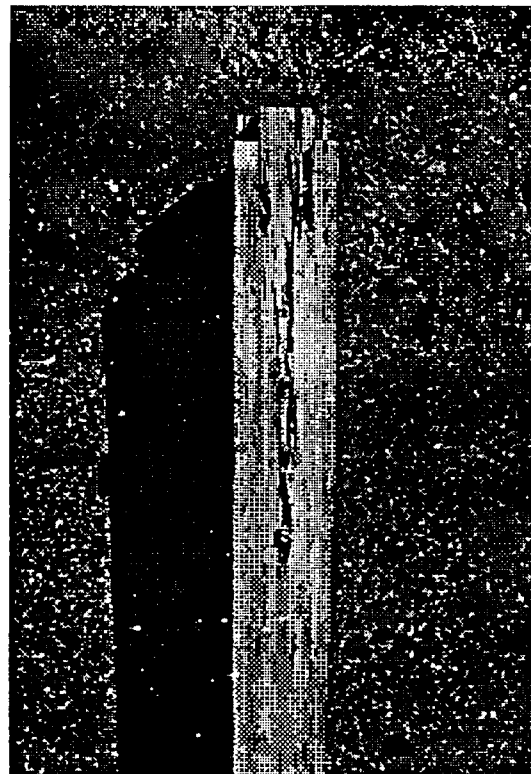
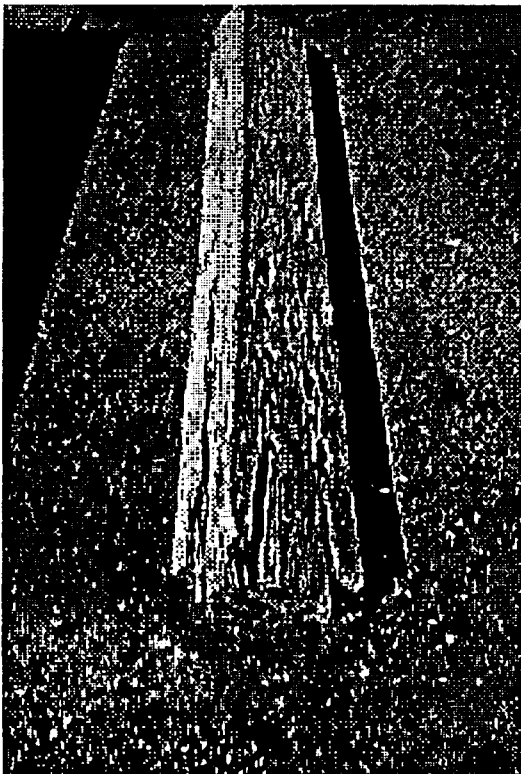
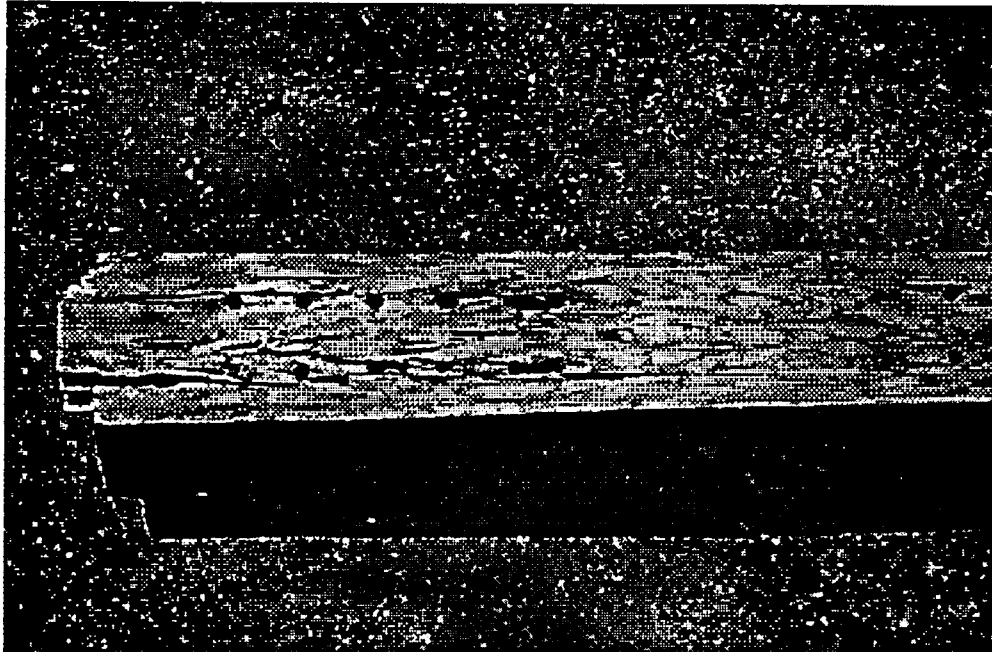
Failure mode: Bi-axial shear plug



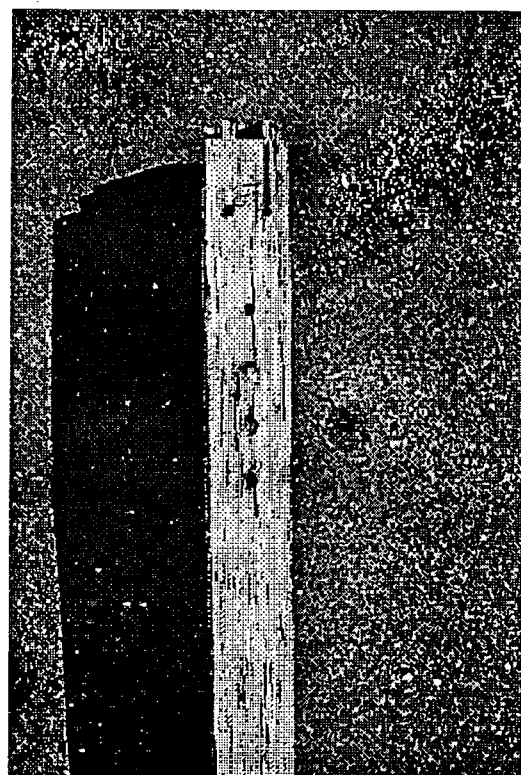
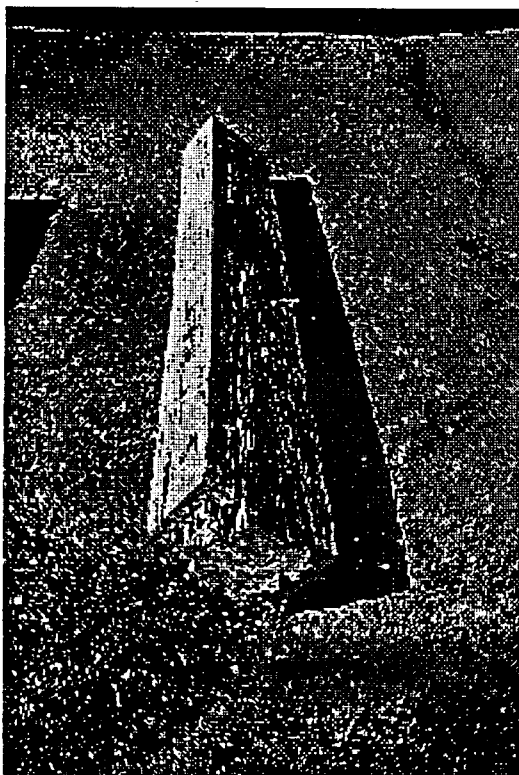
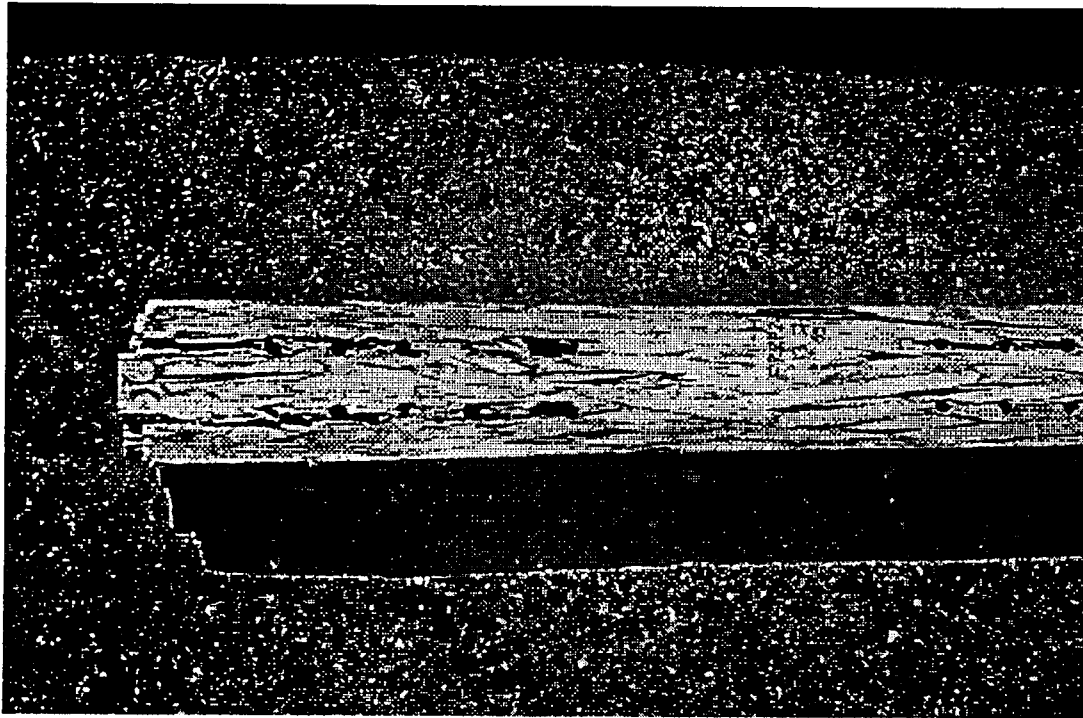
Load-displacement Plot



FRRF1



FRRF2



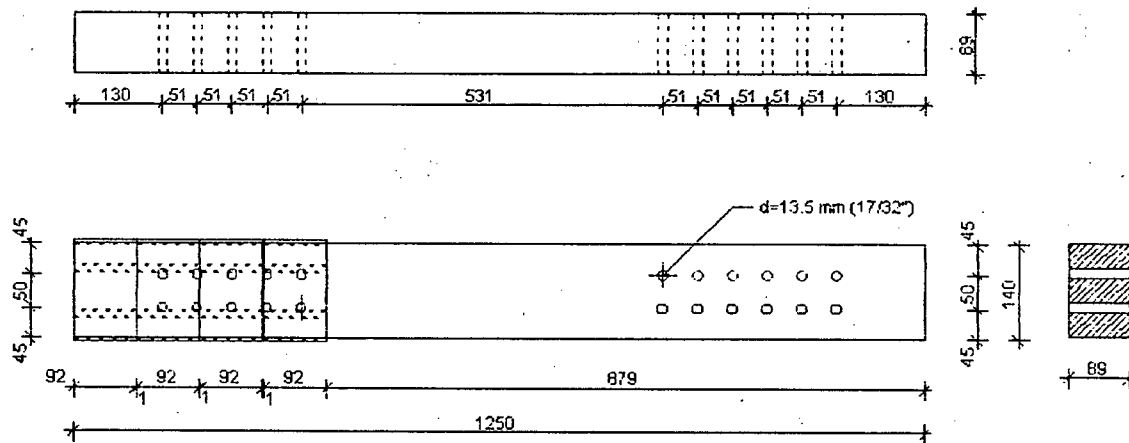
HRT
10-1/2" Bolt Connection in PSL
Truss Plate Reinforced

L/d = 7.0
e = 10d
s = 4d

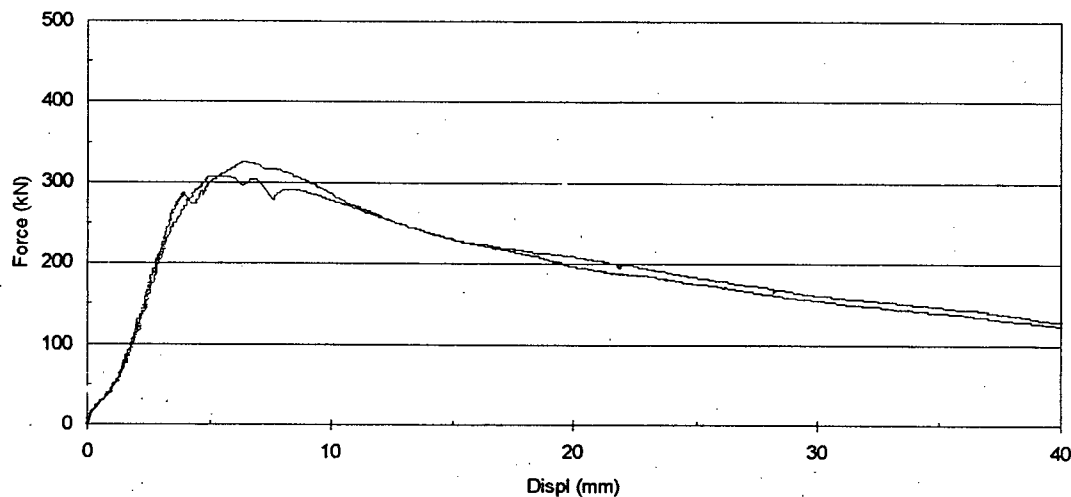
Quantity	Fult	D@Fult	80%Fult	D@80	D@50	Ductility
Specimen	[kN]	[mm]	[kN]	[mm]	[mm]	[]
HRT1	325.48	6.52	260.38	11.9	2.41	4.94
HRT2	307.88	5.34	246.3	13.13	2.45	5.36

Quantity	Stiffness	Energy	Design F	Dens.wet	Dens.dry	Moist.cnt.
Specimen	[kN/mm]	[Nm]	[kN]	[kg/m ³]	[kg/m ³]	[%]
HRT1	104.94	7863.95	N/A	674.86	647.7	8.94
HRT2	89.16	7936.32	N/A	653.8	626.77	9.09

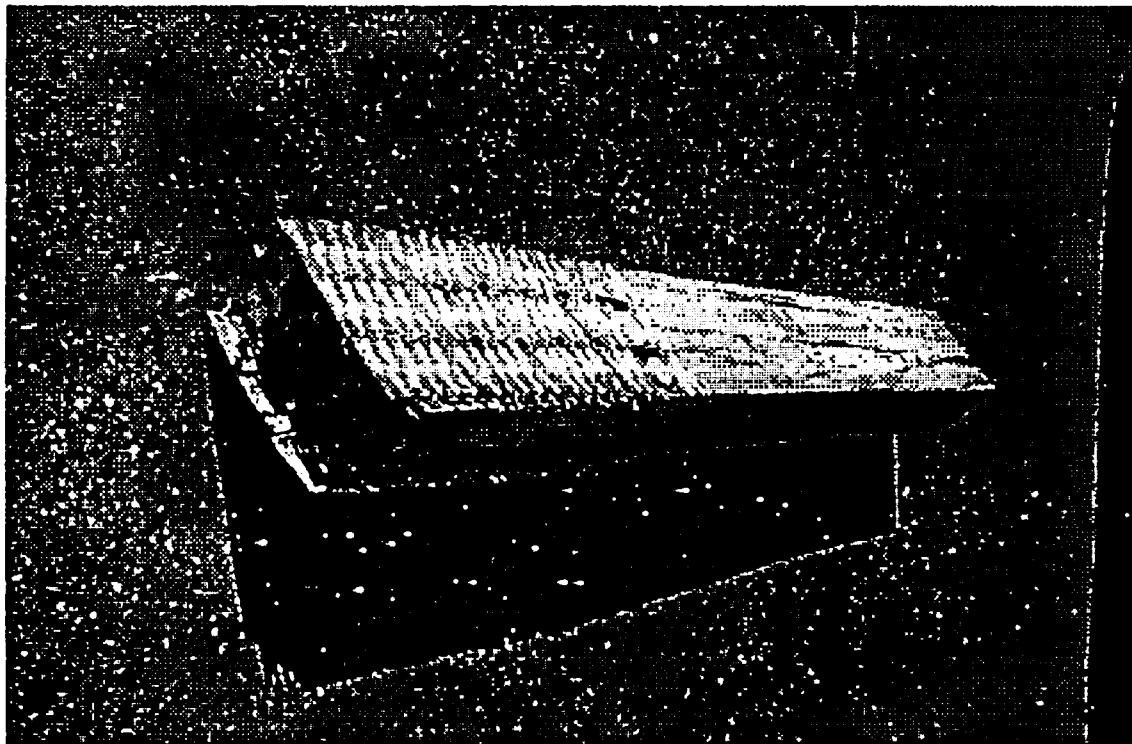
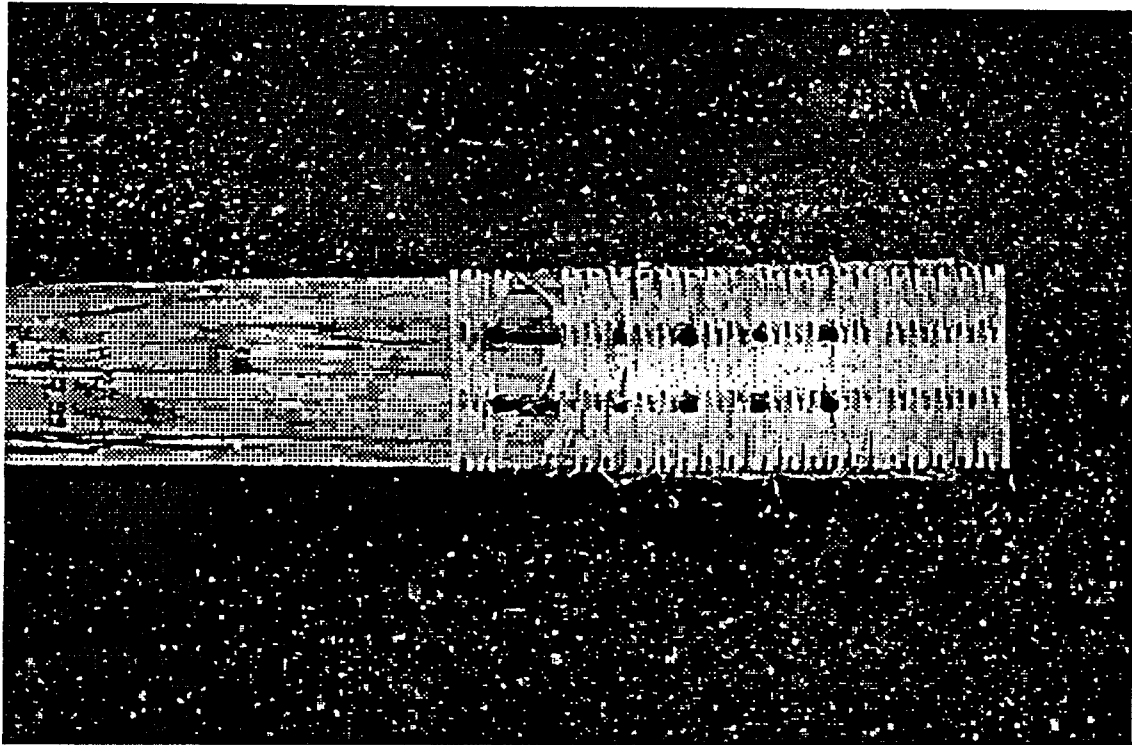
Failure mode: Row Tear-out



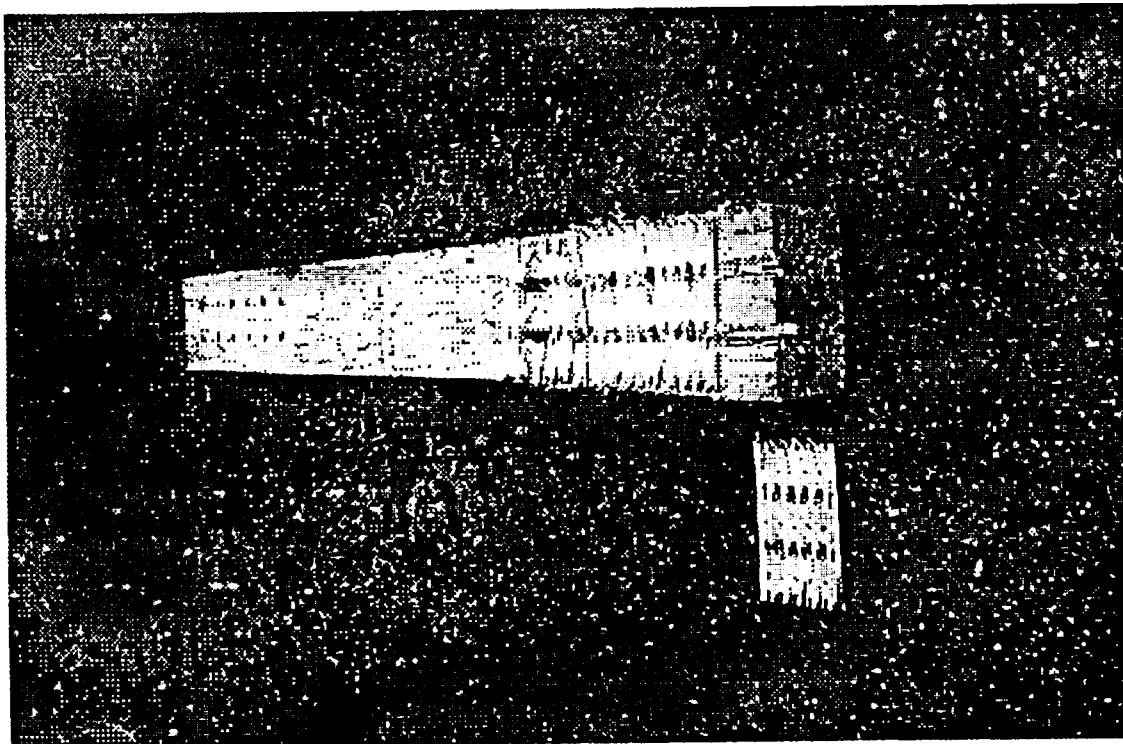
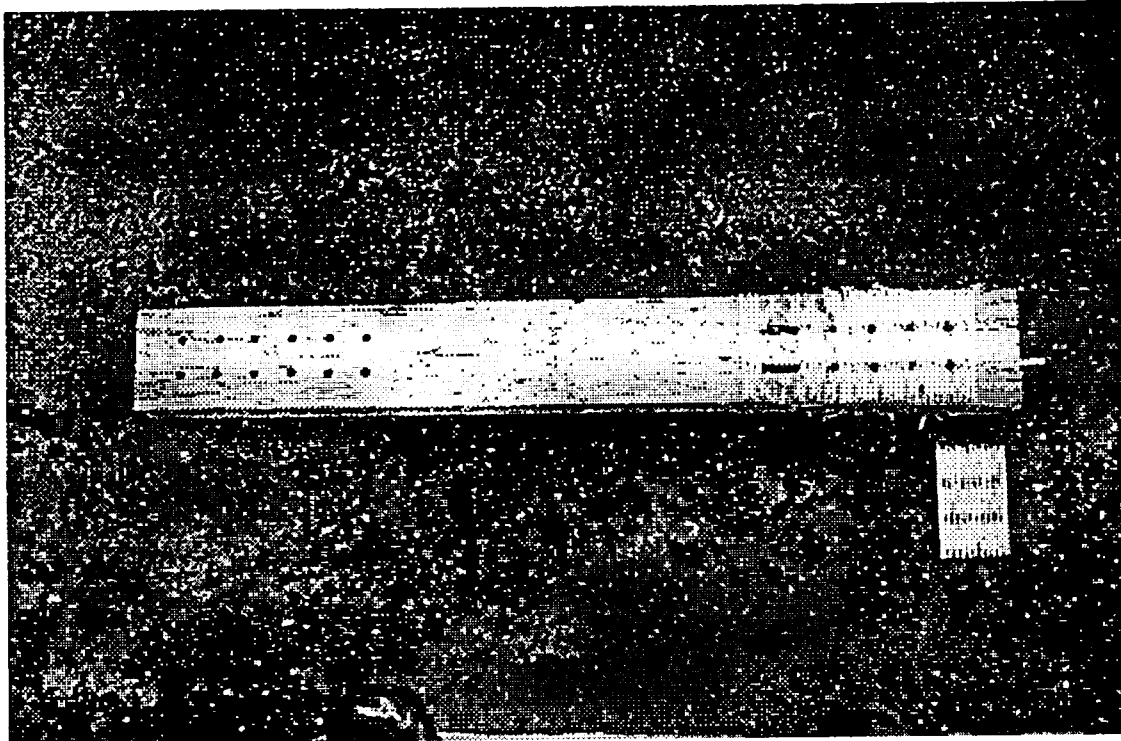
Load-displacement Plot



HRT1



HRT2



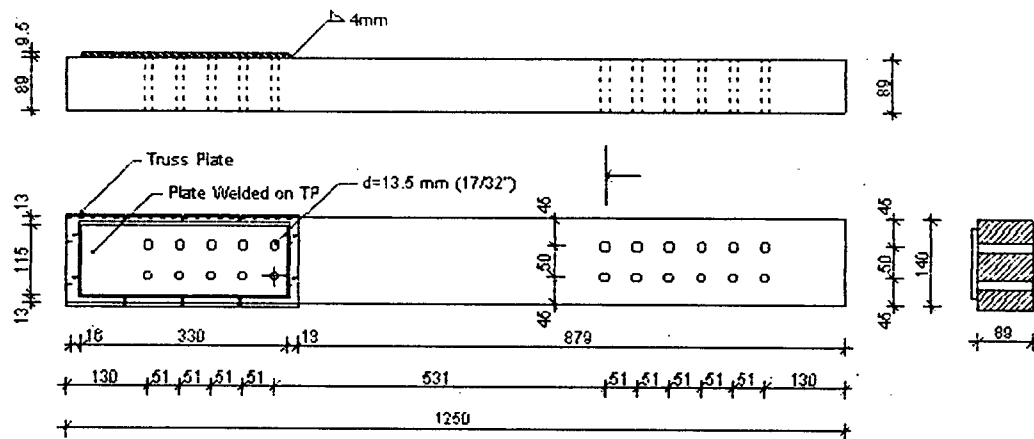
HRTW
10-1/2" Bolt Connection in PSL
Stiff Truss Plate Reinforced

$L/d = 7.0$
$e = 10d$
$s = 4d$

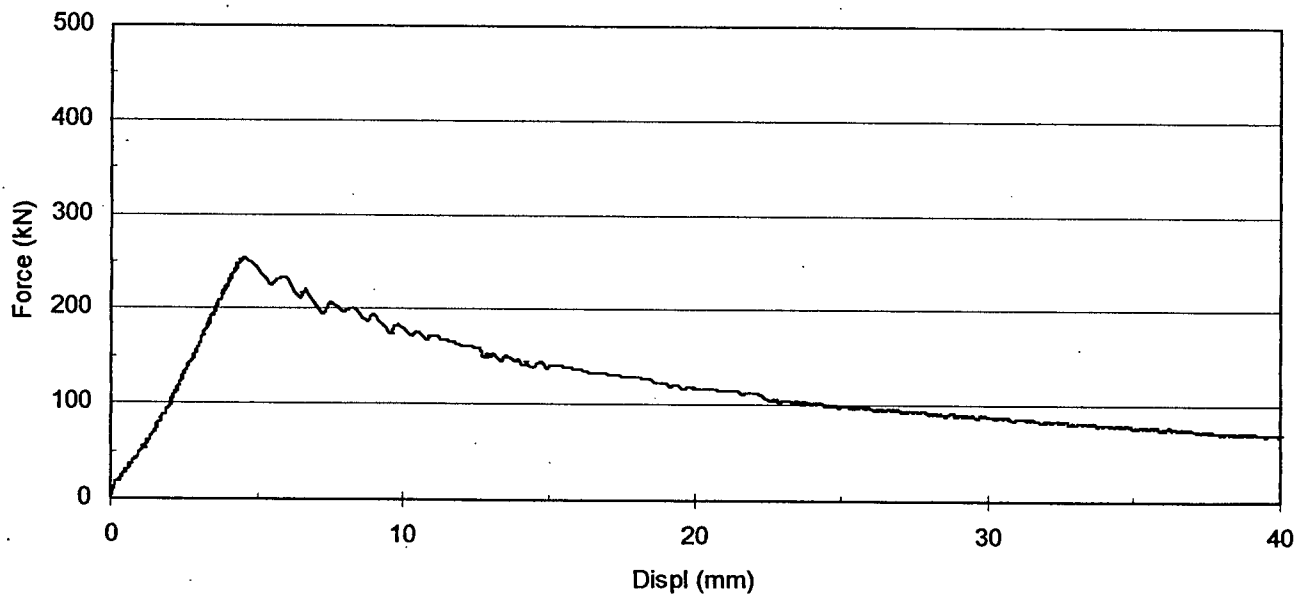
Quantity	Fult	D@Fult	80%Fult	D@80	D@50	Ductility
Specimen	[kN]	[mm]	[kN]	[mm]	[mm]	[]
HRTW	254.21	4.505	203.37	7.76	2.35	3.3

Quantity	Stiffness	Energy	Design F	Dens.green	Dens.dry	Moist.cnt.
Specimen	[kN/mm]	[Nm]	[kN]	[kg/m ³]	[kg/m ³]	[%]
HRTW	62.02	4930.5	N/A	641.52	609.05	9.71

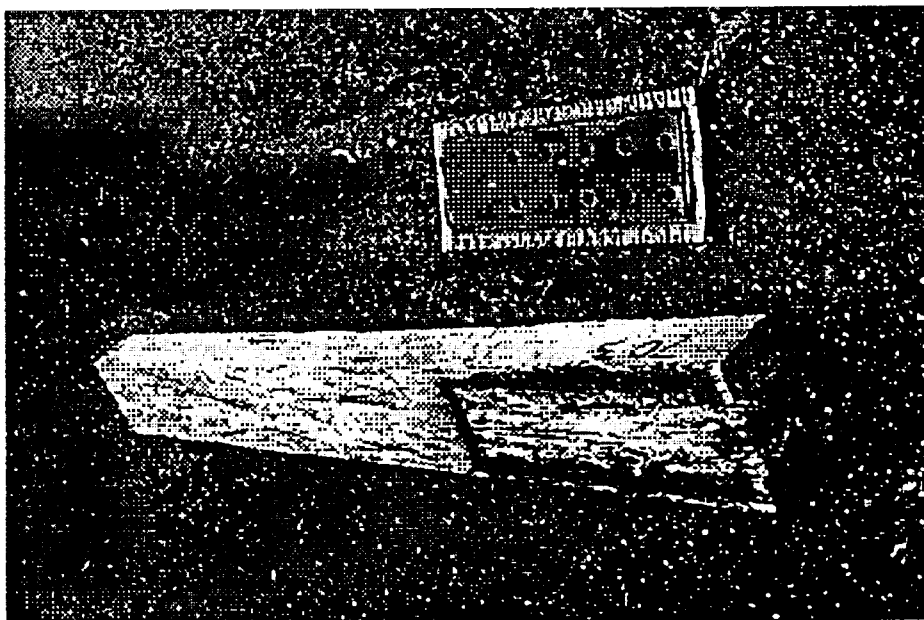
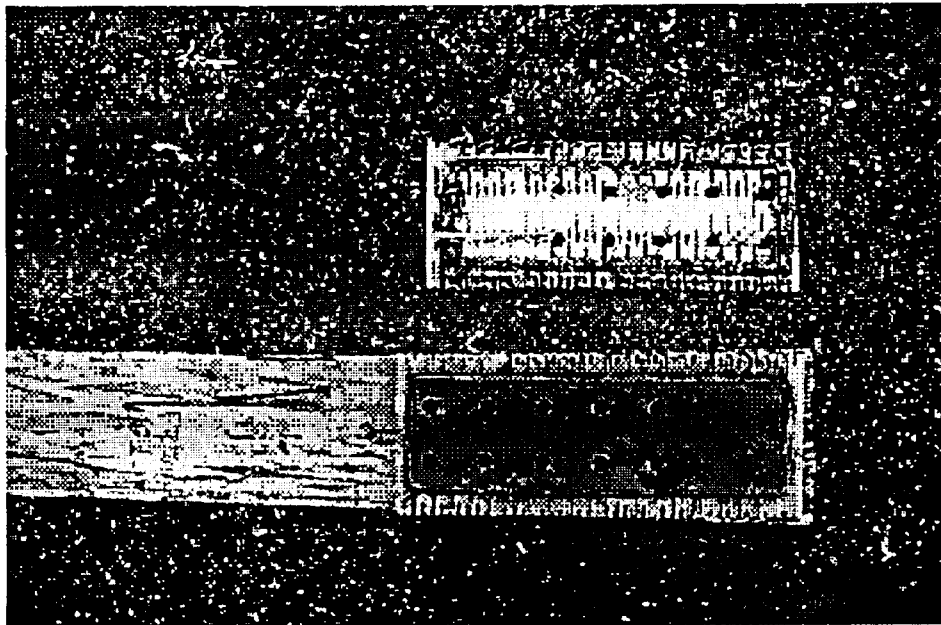
Failure mode: Row tear-out



Load-displacement Plot



HRTW1



FRT
10-5/8" Bolt Connection in PSL
Truss Plate Reinforced

L/d = 5.6
e = 10d
s = 4d

Quantity	Fult	D@Fult	80%Fult	D@80	D@50	Ductility
Specimen	[kN]	[mm]	[kN]	[mm]	[mm]	[]
FRT1	337.4	3.6	269.92	11.34	1.31	8.7
FRT2	361.88	2.18	289.5	3.88	1.2	3.2
FRT3	346.69	2.37	277.35	3.7	1.32	2.8
FRT4	325.6	3.24	260.48	5.85	1.39	4.2
FRT5	347.82	2.38	278.25	3.84	1.25	3.1
FRT6	447.59	3.01	358.07	4.76	1.6	3
FRT8	394.31	2.76	315.44	4.99	1.41	3.5
FRT9	374.58	2.33	299.66	3.57	1.2	3
FRT10	348.5	3.98	278.8	6.43	1.32	4.9
Avg	364.93	2.87	291.94	5.37	1.33	4.04

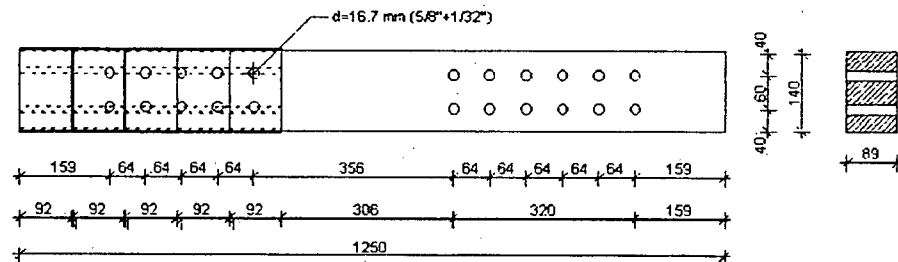
Design Force = N/A

Stiffness (avg) = 179.15 kN/mm

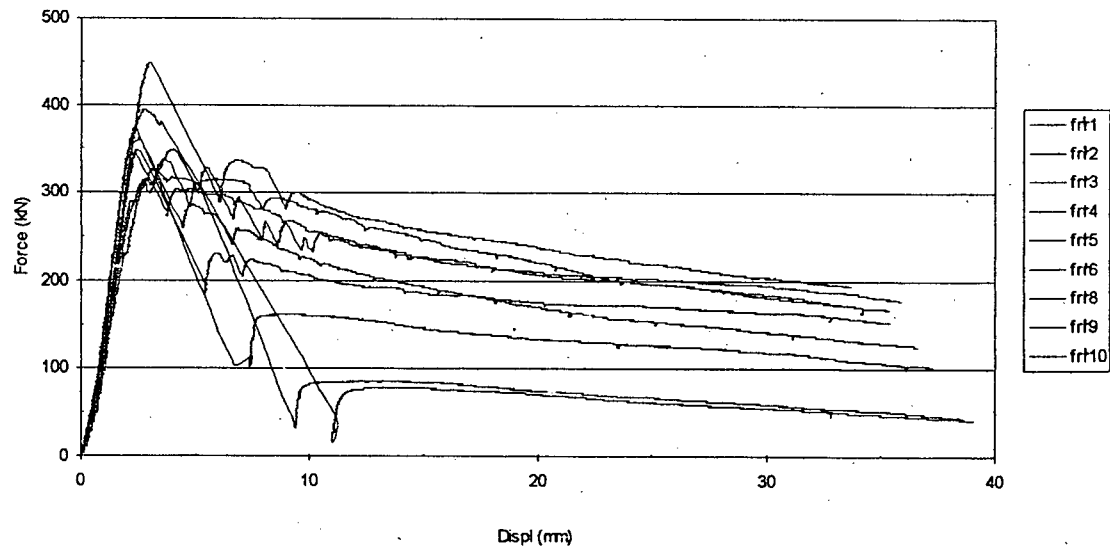
Energy Dissipated (avg) = 7165.1 kNmm

Moisture Content was not Measured

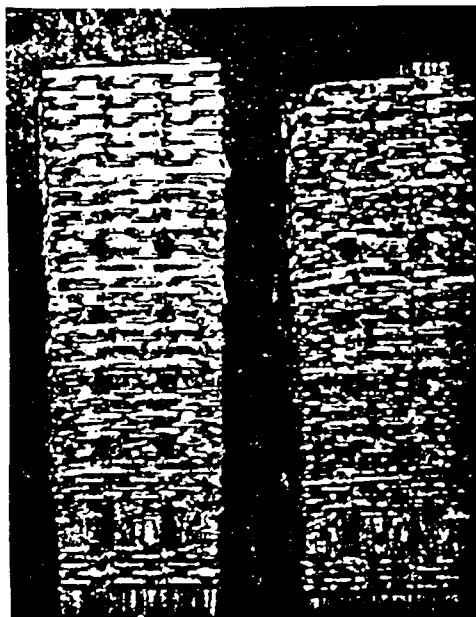
Failure mode: Group Shear, Row Tear-out, Row Splitting



Load-displacement Plot



FRT



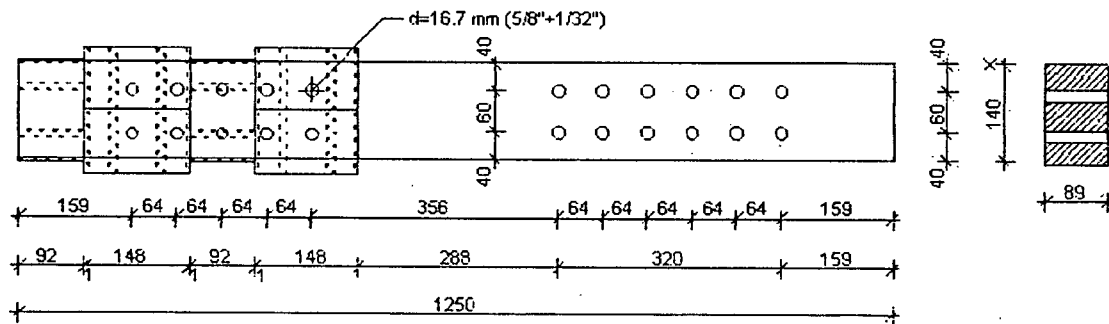
FRTT
10-5/8" Bolt Connection in PSL
Transversely Rotated Truss Plate Reinforced

L/d = 5.6
e = 10d
s = 4d

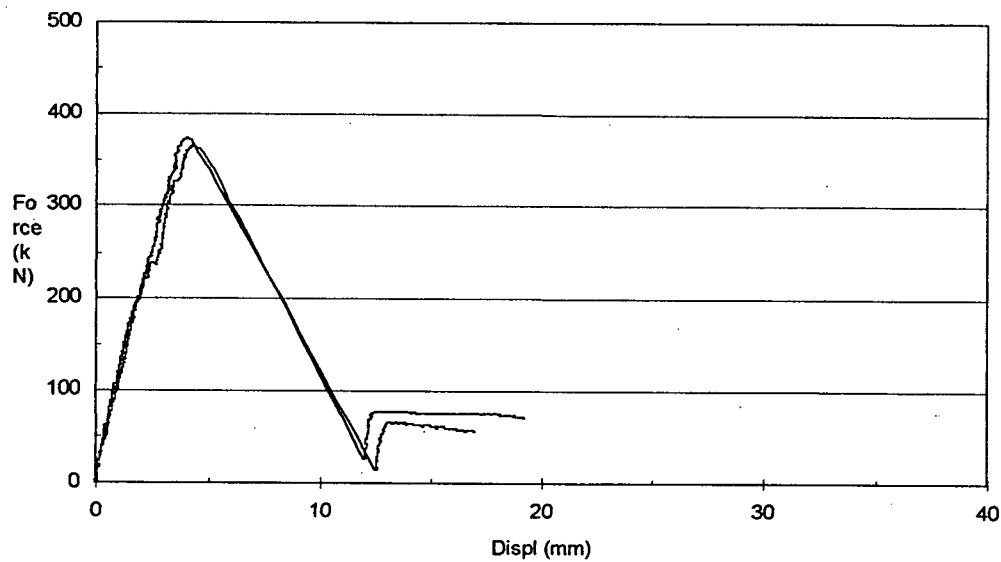
Quantity	Fult	D@Fult	80%Fult	D@80	D@50	Ductility
Specimen	[kN]	[mm]	[kN]	[mm]	[mm]	[]
FRTT1	374.36	3.98	299.48	5.91	1.71	3.45
FRTT2	366.54	4.36	293.23	6.2	1.54	3.9

Quantity	Stiffness	Energy	Design F	Dens.green	Dens.dry	Moist.cnt.
Specimen	[kN/mm]	[Nm]	[kN]	[kg/m ³]	[kg/m ³]	[%]
FRTT1	101.82	2510.05	N/A	642.03	618.34	8.62
FRTT2	84.55	2472.5	N/A	632.85	604.8	8.99

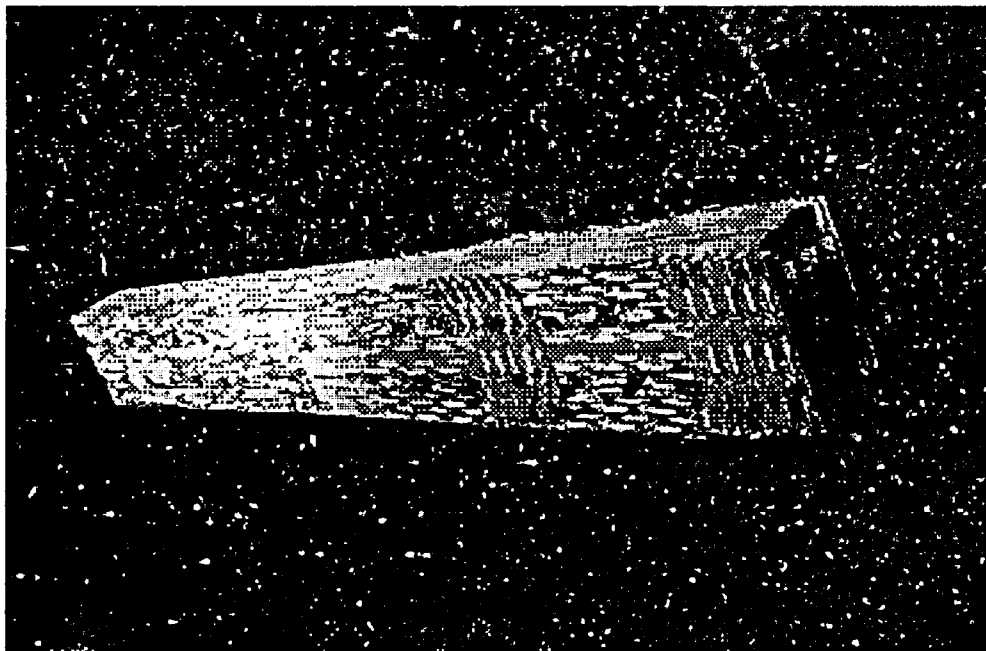
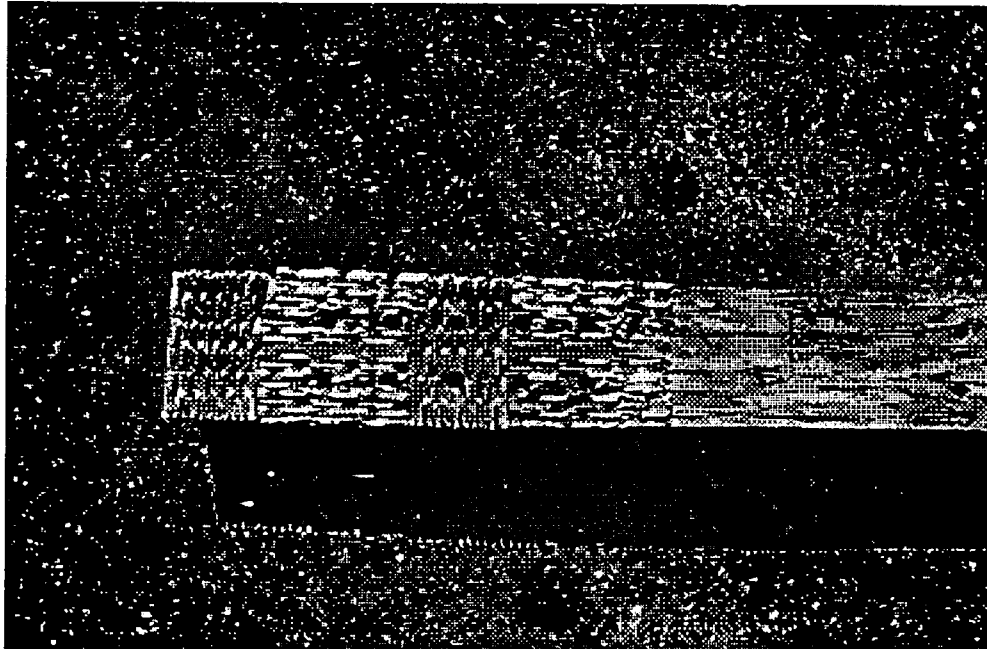
Failure mode: Shear plug



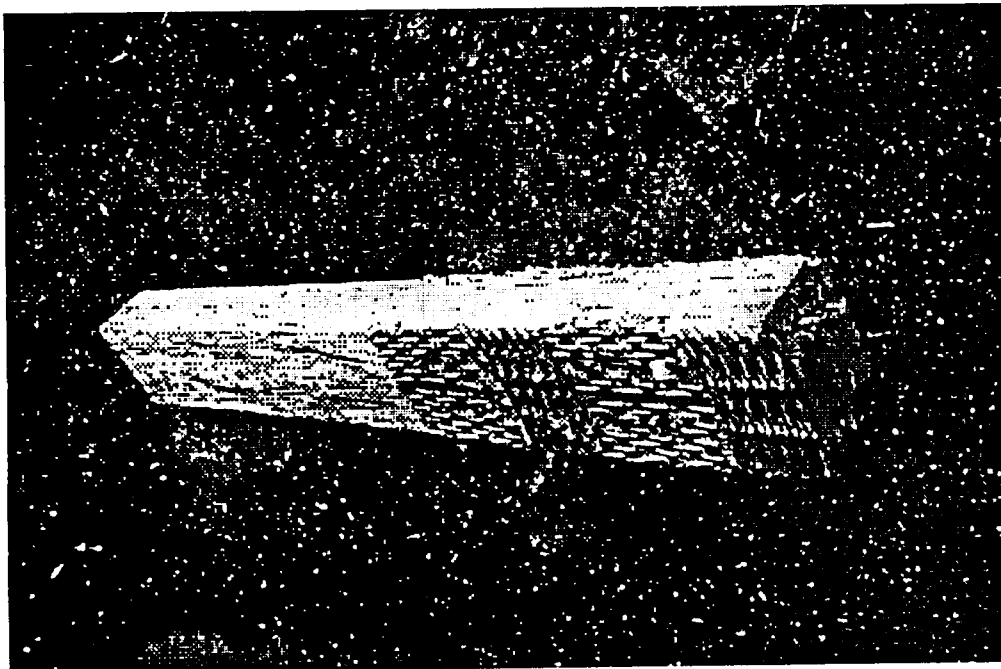
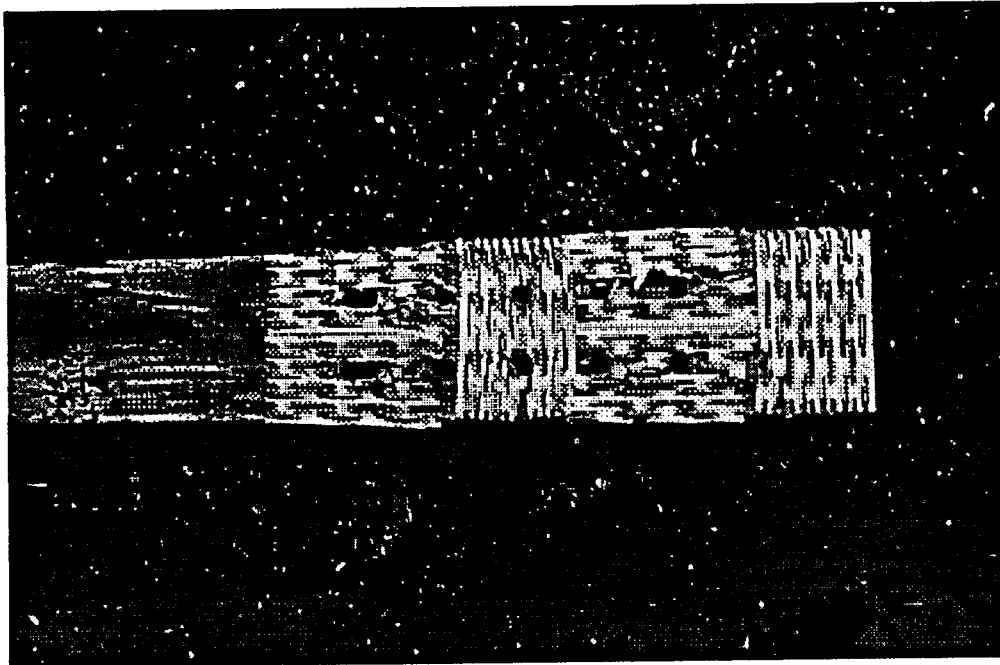
Load-displacement Plot



FRTT1



FRTT2



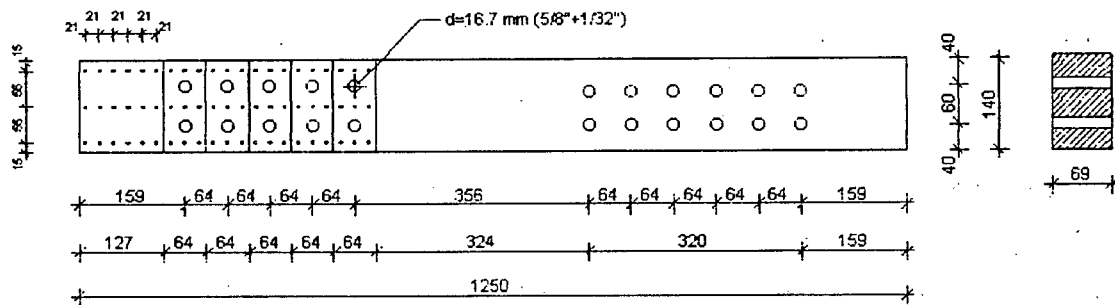
FRN-type I
 10-5/8" Bolt Connection in PSL
 Separate Nailed Plates Reinforced
 Galvanized Plate Gauge 18 (1.2mm)
 Spiral Nail – Length 2", Gauge 12-1/2

$L/d = 5.6$
 $e = 10d$
 $s = 4d$

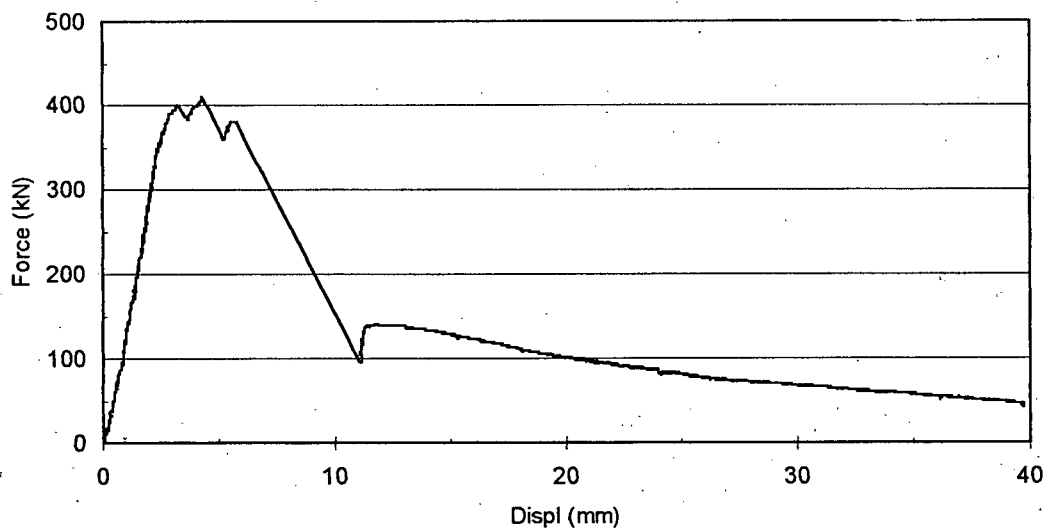
Quantity	Fult	D@Fult	80%Fult	D@80	D@50	Ductility
Specimen	[kN]	[mm]	[kN]	[mm]	[mm]	[]
FRNtype1	409.27	4.31	327.42	6.74	1.52	4.43

Quantity	Stiffness	Energy	Design F	Dens.green	Dens.dry	Moist.cnt.
Specimen	[kN/mm]	[Nm]	[kN]	[kg/m3]	[kg/m3]	[%]
FRNtype1	154.65	5454.49	N/A	662.8	644.94	8.67

Failure mode: Shear plug



Load-displacement Plot



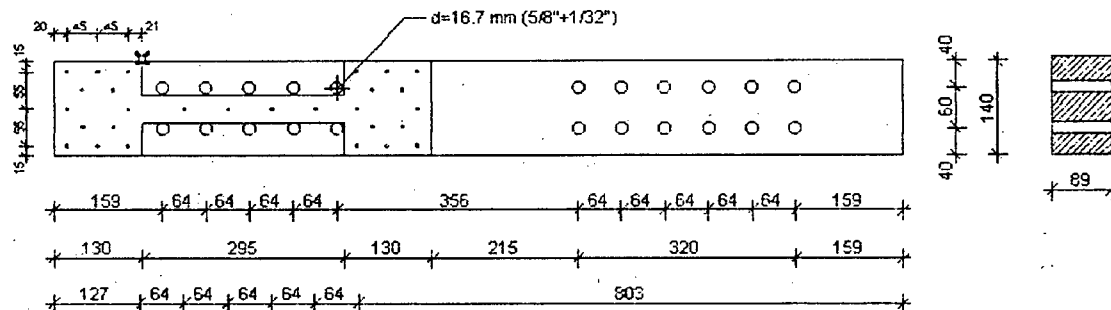
FRN-type 2
 10-5/8" Bolt Connection in PSL
 I-Shape Nailed Plate Reinforced
 Galvanized Plate Gauge 18 (1.2mm)
 Spiral Nail – Length 2", Gauge 12-1/2

$L/d = 5.6$
 $e = 10d$
 $s = 4d$

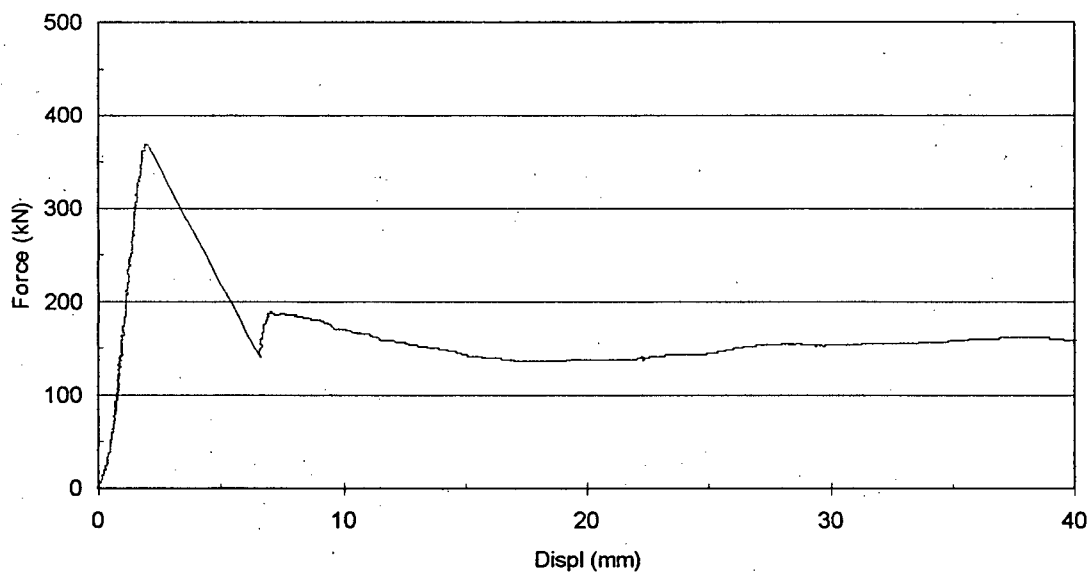
Quantity	Fult	D@Fult	80%Fult	D@80	D@50	Ductility
Specimen	[kN]	[mm]	[kN]	[mm]	[mm]	[]
FRNtype2	368.23	1.98	294.58	3.48	1.05	3.31

Quantity	Stiffness	Energy	Design F	Dens.green	Dens.dry	Moist.cnt.
Specimen	[kN/mm]	[Nm]	[kN]	[kg/m3]	[kg/m3]	[%]
FRNtype2	270.33	6645	N/A	664.42	647.25	8.56

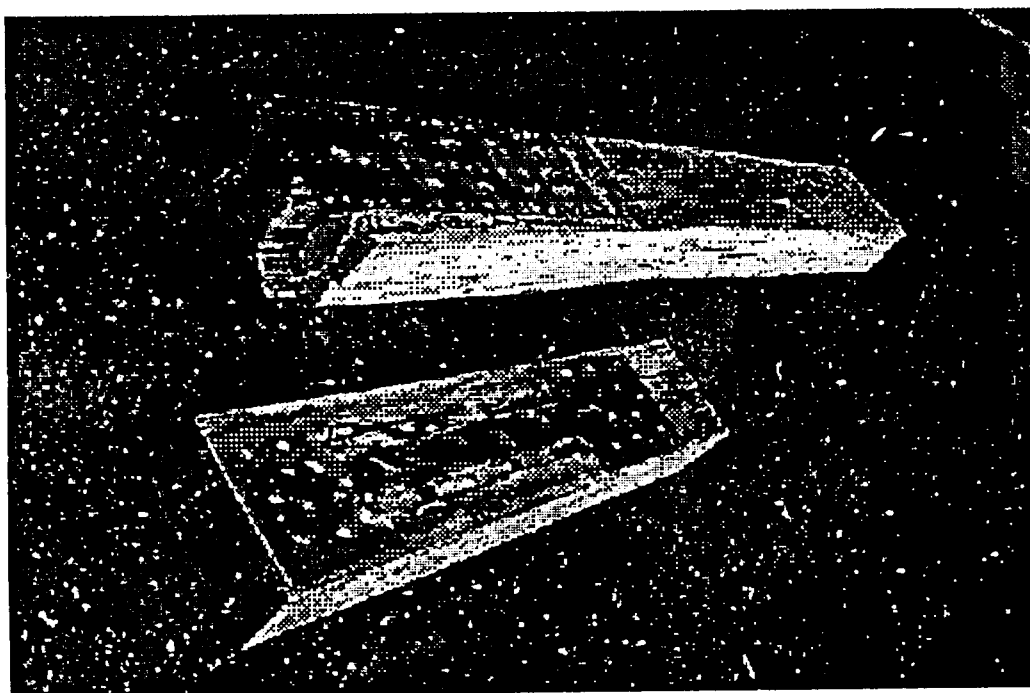
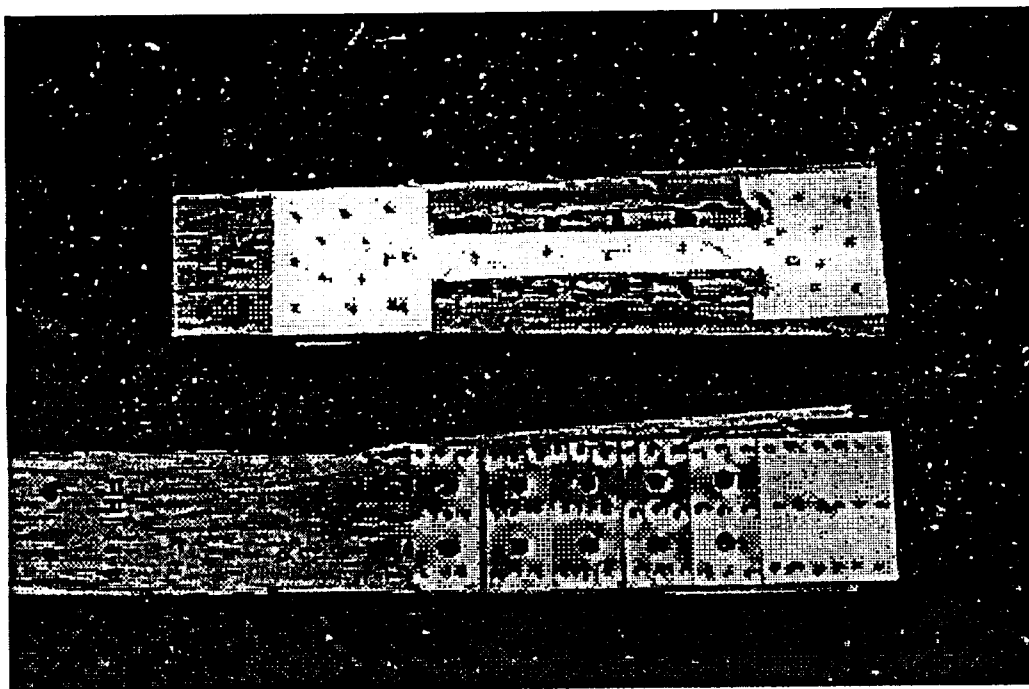
Failure mode: Row shear-out



Load-displacement Plot



FRN1,2



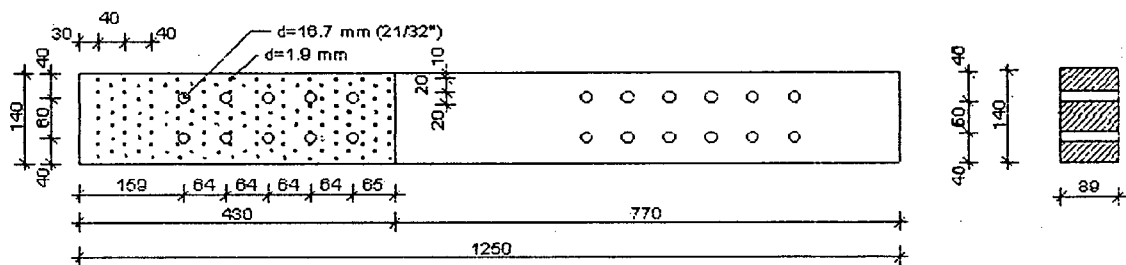
FRN-18, FRN-26
 10-5/8" Bolt Connection in PSL
 Nailed Plate Reinforced
 Galvanized Plate - Gauge 26 (0.6mm), 18 (1.2mm)
 Finishing Nails

$L/d = 5.6$
 $e = 10d$
 $s = 4d$

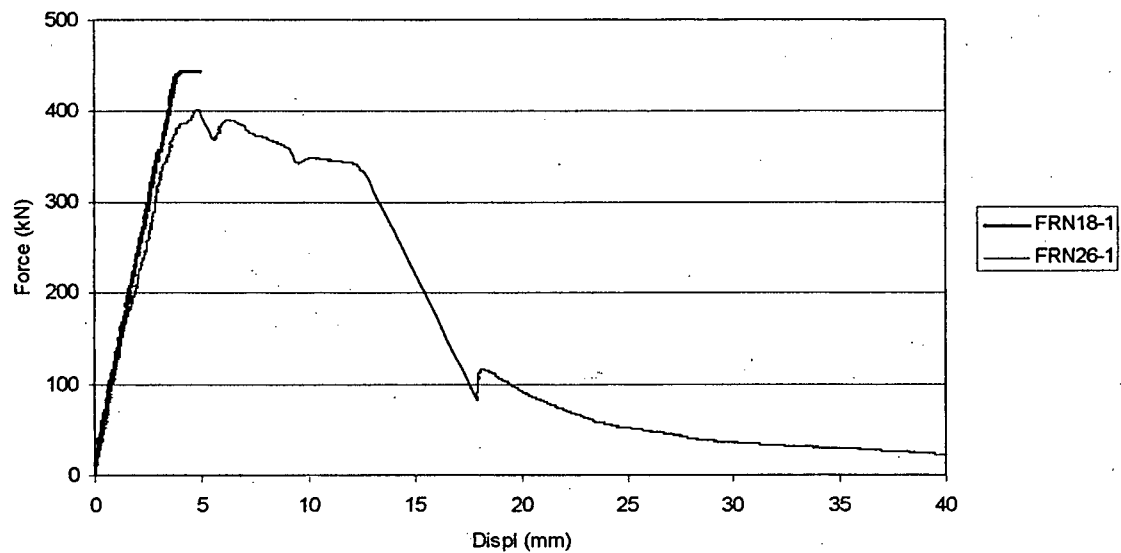
Quantity	Fult	D@Fult	80%Fult	D@80	D@50	Ductility
Specimen	[kN]	[mm]	[kN]	[mm]	[mm]	[]
FRN18	>445	N/A	N/A	N/A	N/A	N/A
FRN26	400.22	4.875	320.18	13	1.92	6.77

Quantity	Stiffness	Energy	Design F	Dens.green	Dens.dry	Moist.cnt.
Specimen	[kN/mm]	[Nm]	[kN]	[kg/m3]	[kg/m3]	[%]
FRN18	N/A	N/A	N/A	680.59	661.39	10.5
FRN26	95.07	6176.65	N/A	670.35	651.16	10.5

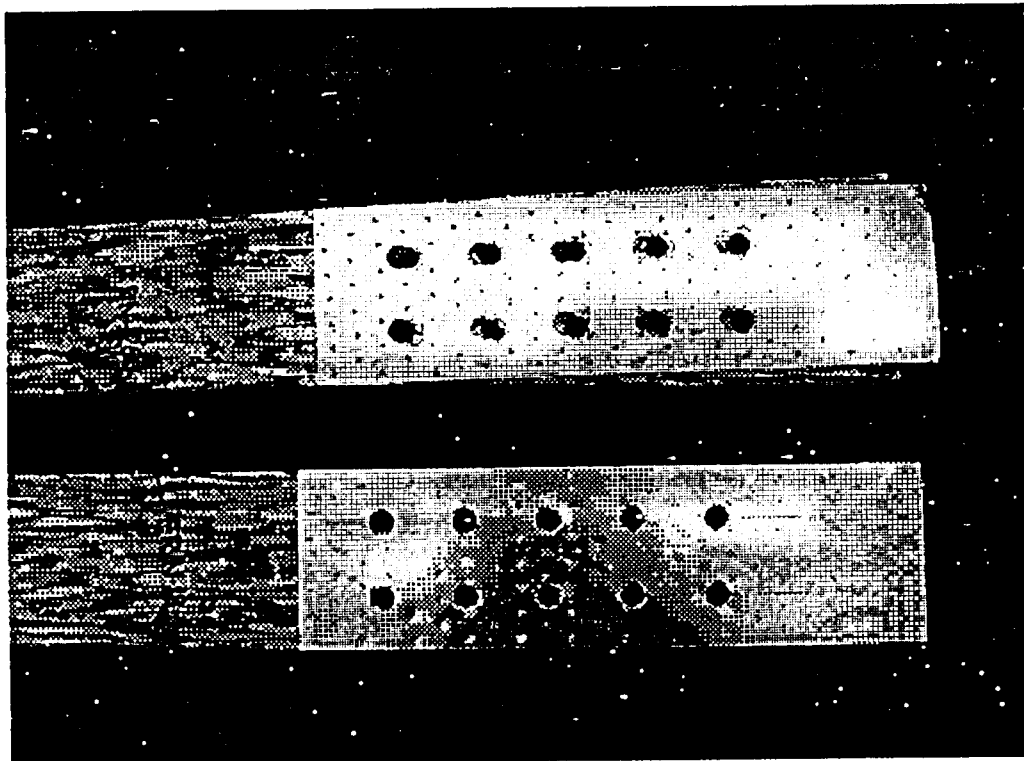
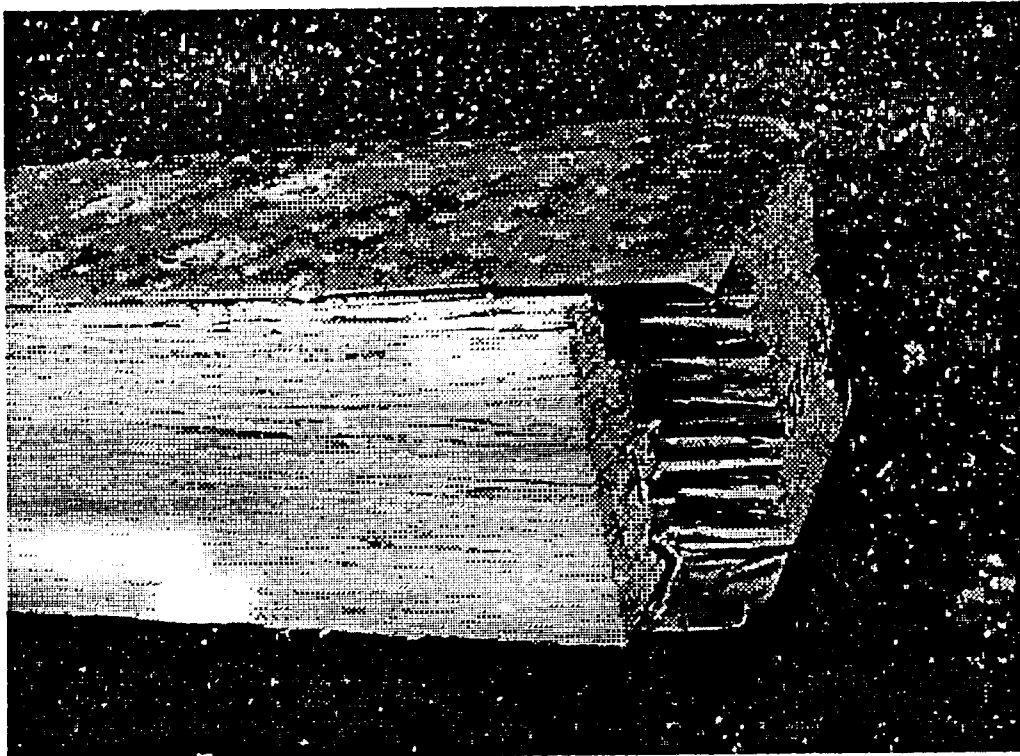
Failure mode: FRN-18 - N/A (reached the jack limit)
 FRN-26 - Shear plug



Load-displacement Plot



FRN18, FRN26



HRN-18, HRN-26
10-1/2" Bolt Connection in PSL

Nailed Plate Reinforced

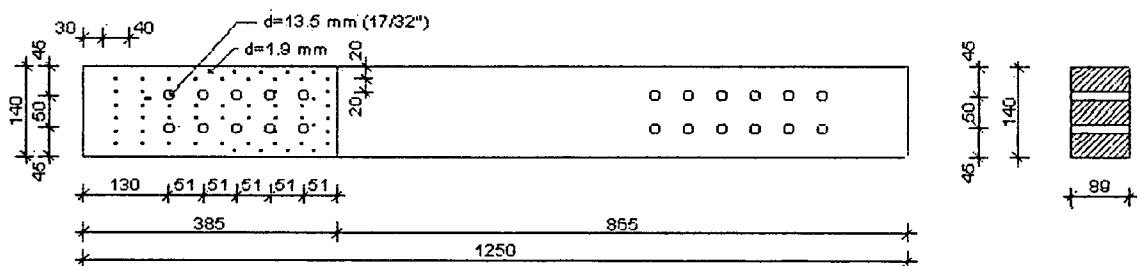
Galvanized Plate - Gauge 26 (0.6mm), 18 (1.2mm)
Finishing Nail

$L/d = 7.0$
 $e = 10d$
 $s = 4d$

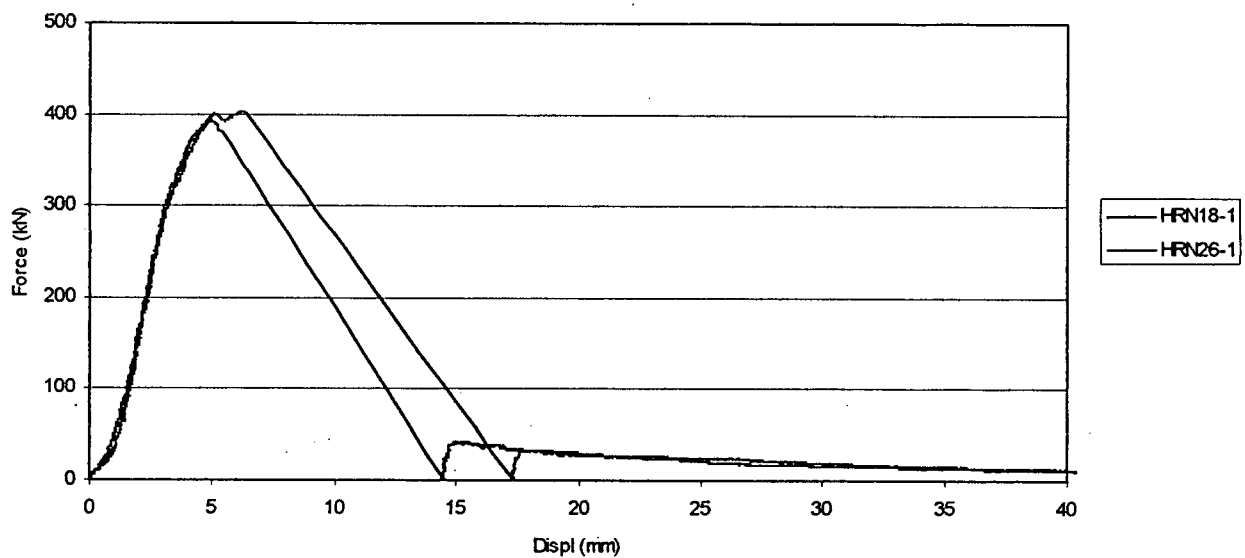
Quantity	Fult	D@Fult	80%Fult	D@80	D@50	Ductility
Specimen	[kN]	[mm]	[kN]	[mm]	[mm]	[]
HRN18	392.80	5.00	314.24	7.00	2.32	3.02
HRN26	398.92	6.39	319.14	8.60	2.30	3.74

Quantity	Stiffness	Energy	Design F	Dens.green	Dens.dry	Moist.cnt.
Specimen	[kN/mm]	[Nm]	[kN]	[kg/m3]	[kg/m3]	[%]
HRN18	134.92	3529.22	N/A	633.50	631.15	9.14
HRN26	131.28	4195.35	N/A	609.16	593.98	8.99

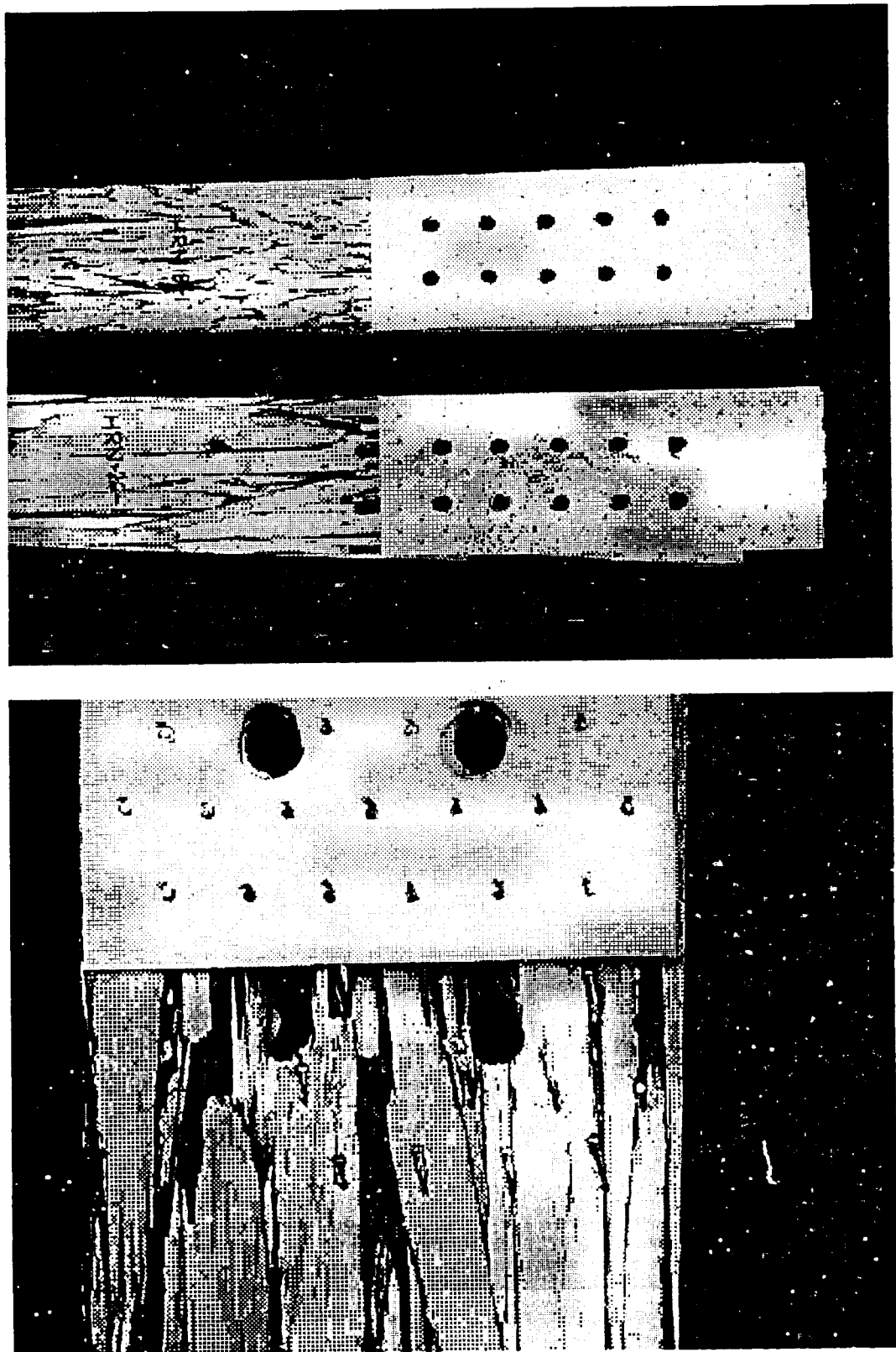
Failure mode: Group Shear

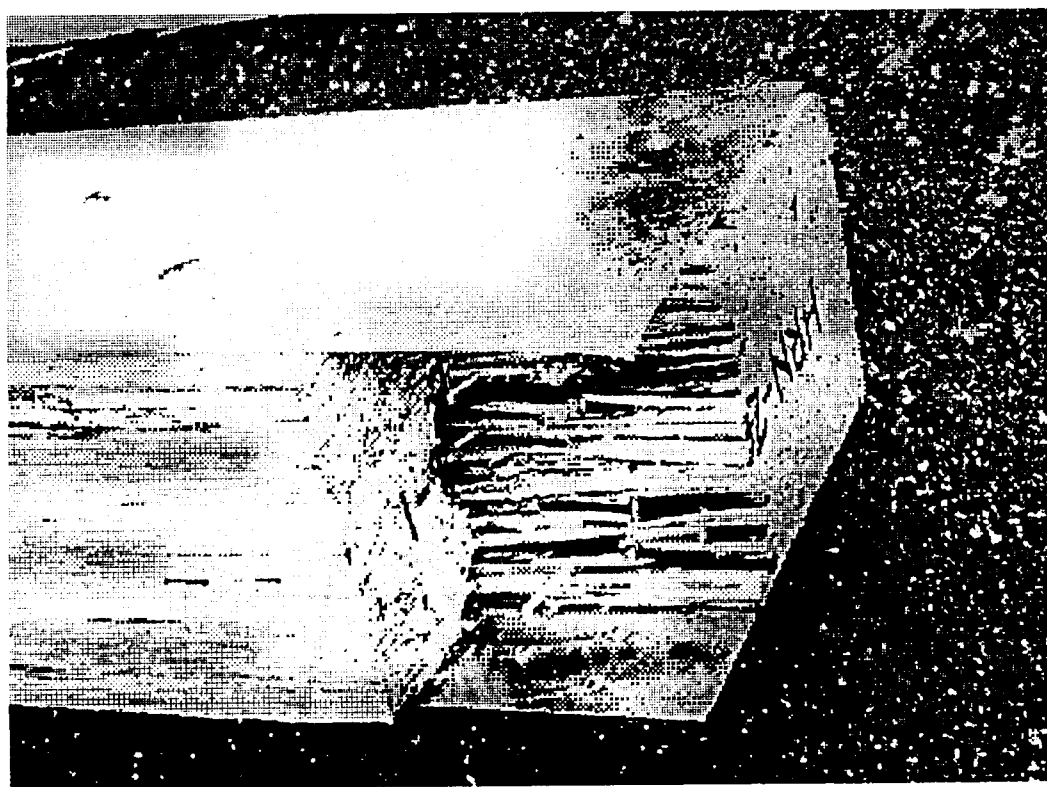
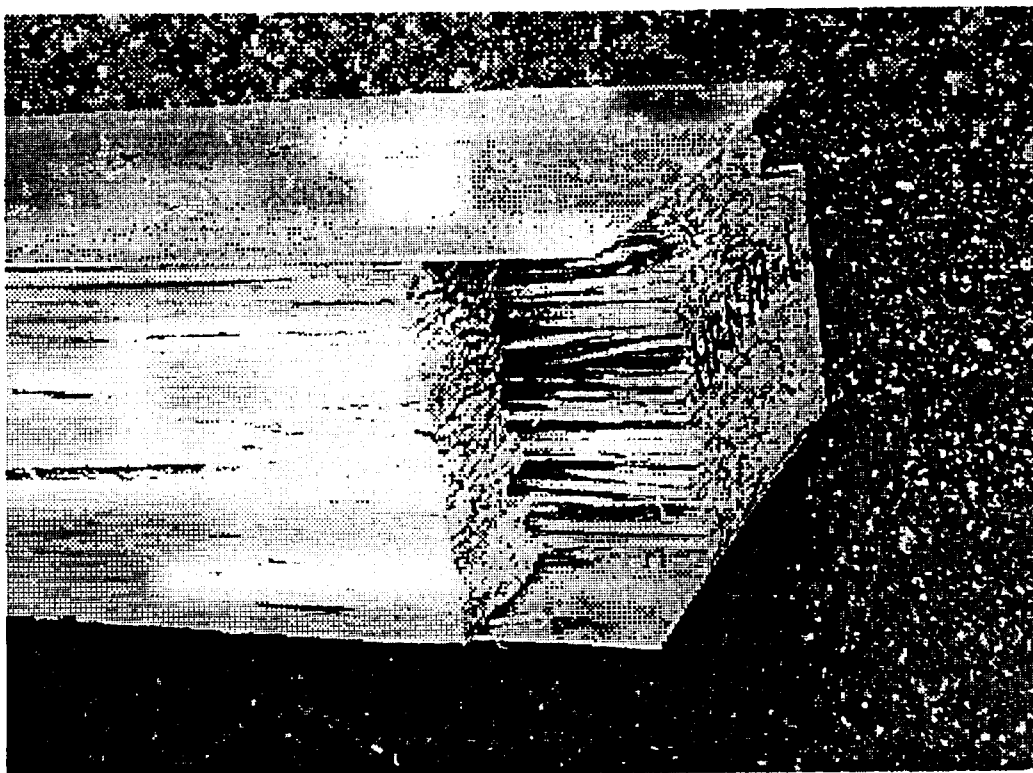


Load-displacement Plot



HRN18-26





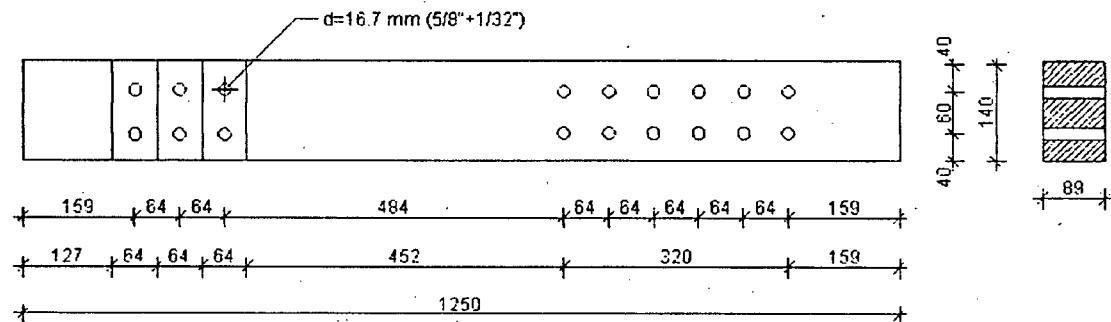
FRE
6-5/8" Bolt Connection in PSL
Epoxy Glued Plates Reinforced

$$\begin{aligned} L/d &= 5.6 \\ e &= 10d \\ s &= 4d \end{aligned}$$

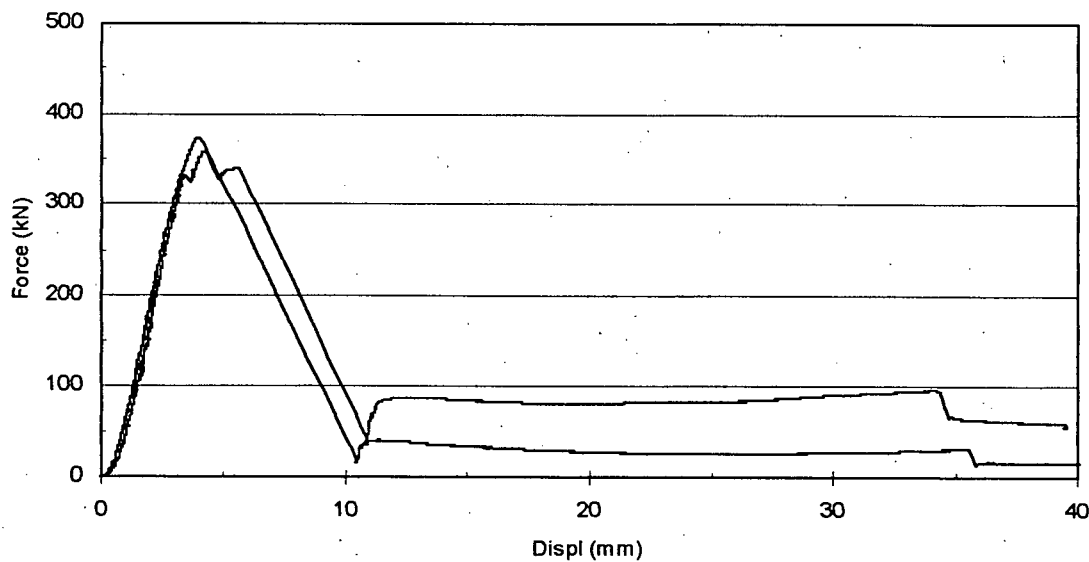
Quantity	Fult	D@Fult	80%Fult	D@80	D@50	Ductility
Specimen	[kN]	[mm]	[kN]	[mm]	[mm]	[]
FRE1(6bolt)	358.48	4.15	286.78	6.54	2.07	3.16
FRE2(6bolt)	373.67	3.92	298.94	5.38	1.96	2.74

Quantity	Stiffness	Energy	Design F	Dens.green	Dens.dry	Moist.cnt.
Specimen	[kN/mm]	[Nm]	[kN]	[kg/m3]	[kg/m3]	[%]
FRE1(6bolt)	131.52	1416.03	N/A	657.33	632.43	8.64
FRE2(6bolt)	127.87	2009.8	N/A	637.88	611.43	9.82

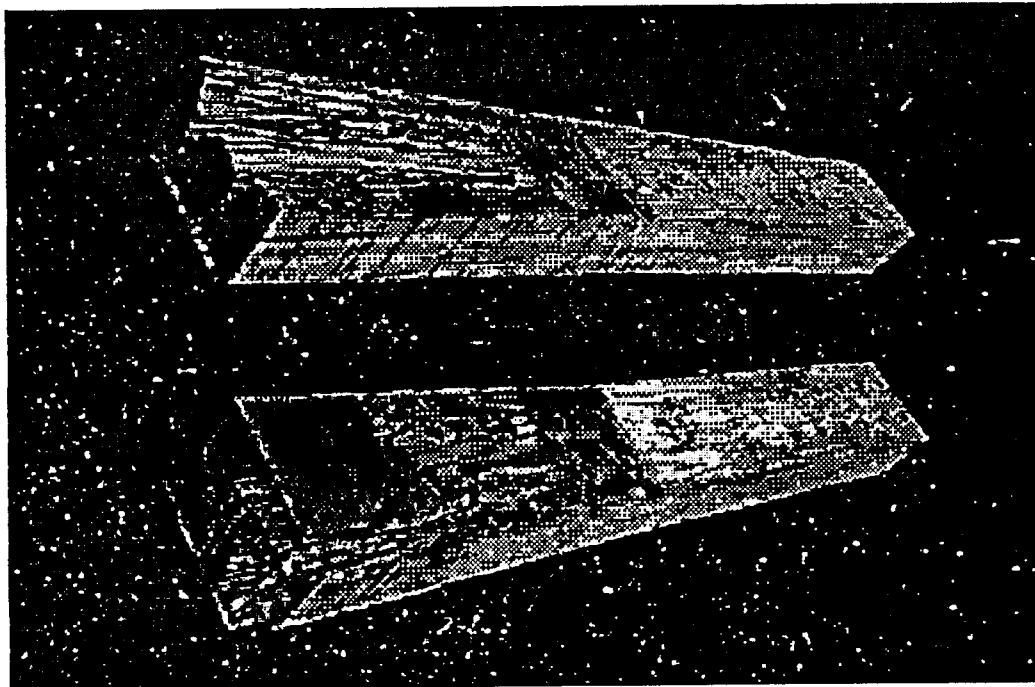
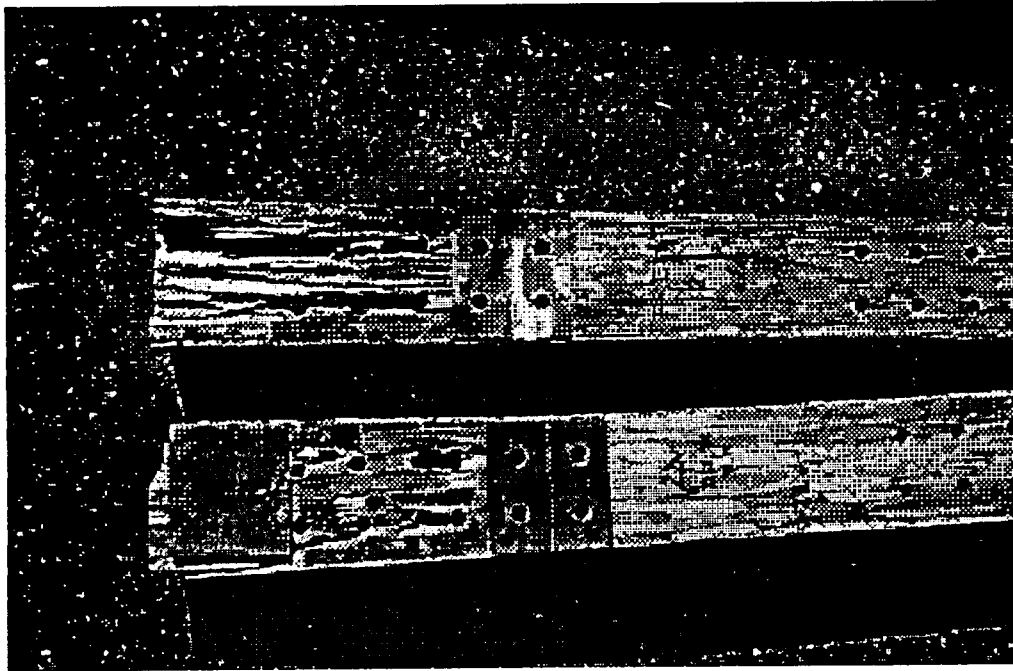
Failure mode: Shear plug, Row shear-out



Load-displacement Plot



FRE1,2



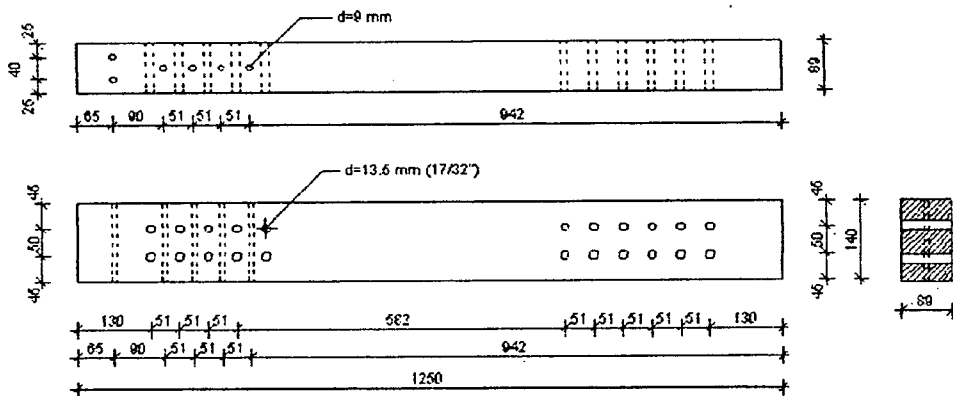
HRER
10-1/2" Bolt Connection in PSL
Epoxy Glued Lag Screw Reinforced

$L/d = 7.0$
 $e = 10d$
 $s = 4d$

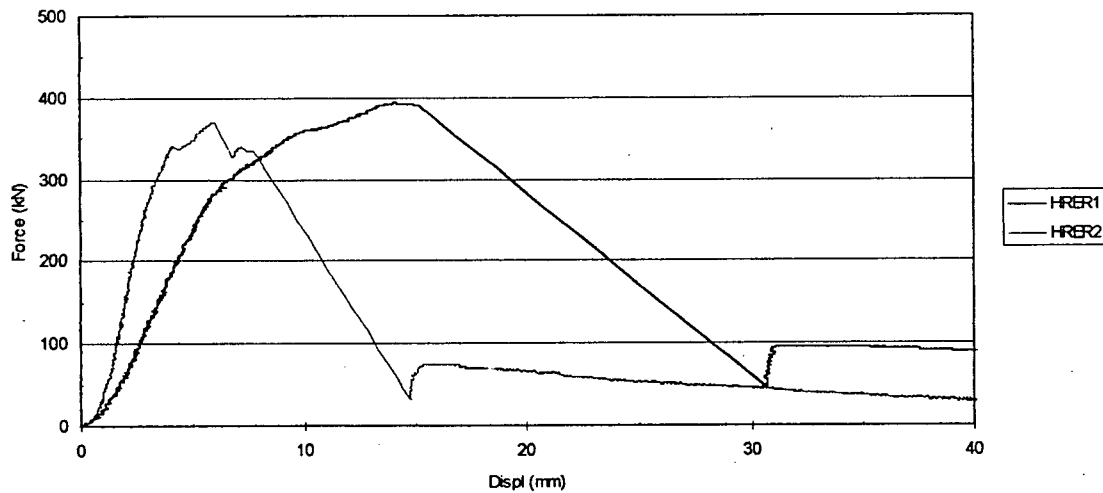
Quantity	Fult	D@Fult	80%Fult	D@80	D@50	Ductility
Specimen	[kN]	[mm]	[kN]	[mm]	[mm]	[]
HRER-1	393.05	14.08	314.44	18.50	4.28	4.32
HRER-2	368.71	5.93	294.97	8.60	2.25	3.82

Quantity	Stiffness	Energy	Design F	Dens.green	Dens.dry	Moist.cnt.
Specimen	[kN/mm]	[Nm]	[kN]	[kg/m3]	[kg/m3]	[%]
HRER-1	58.33	8271.60	N/A	622.60	606.17	9.08
HRER-2	135.51	4473.36	N/A	649.28	645.02	9.45

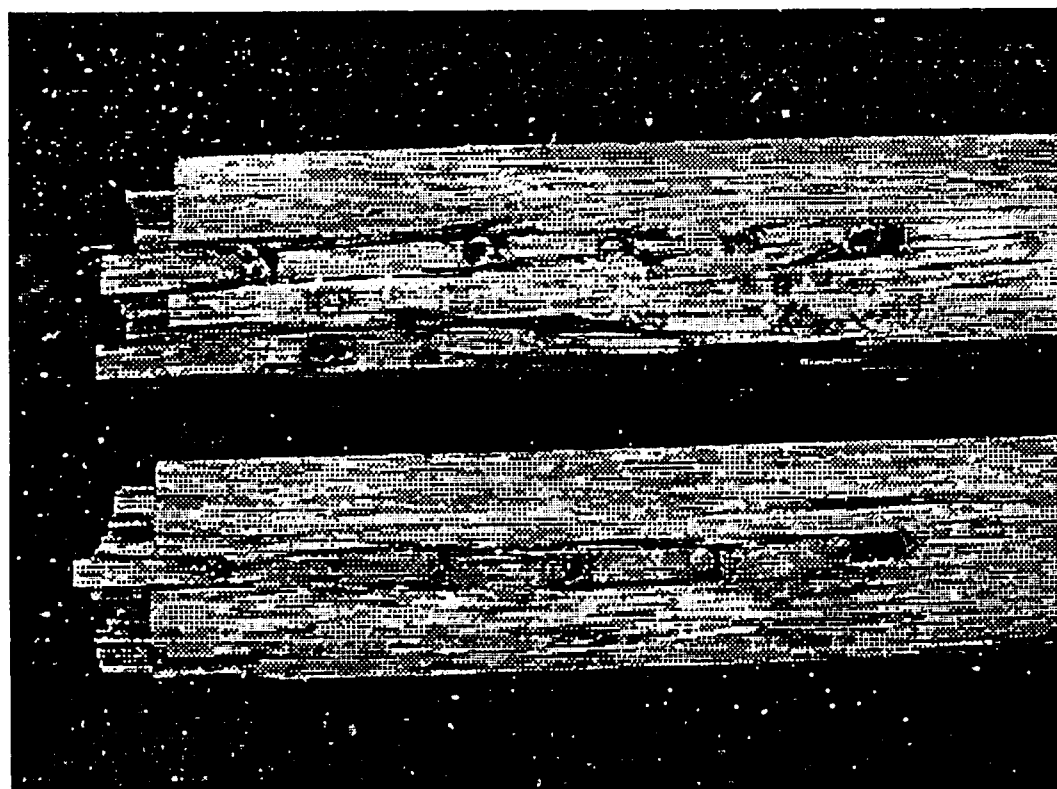
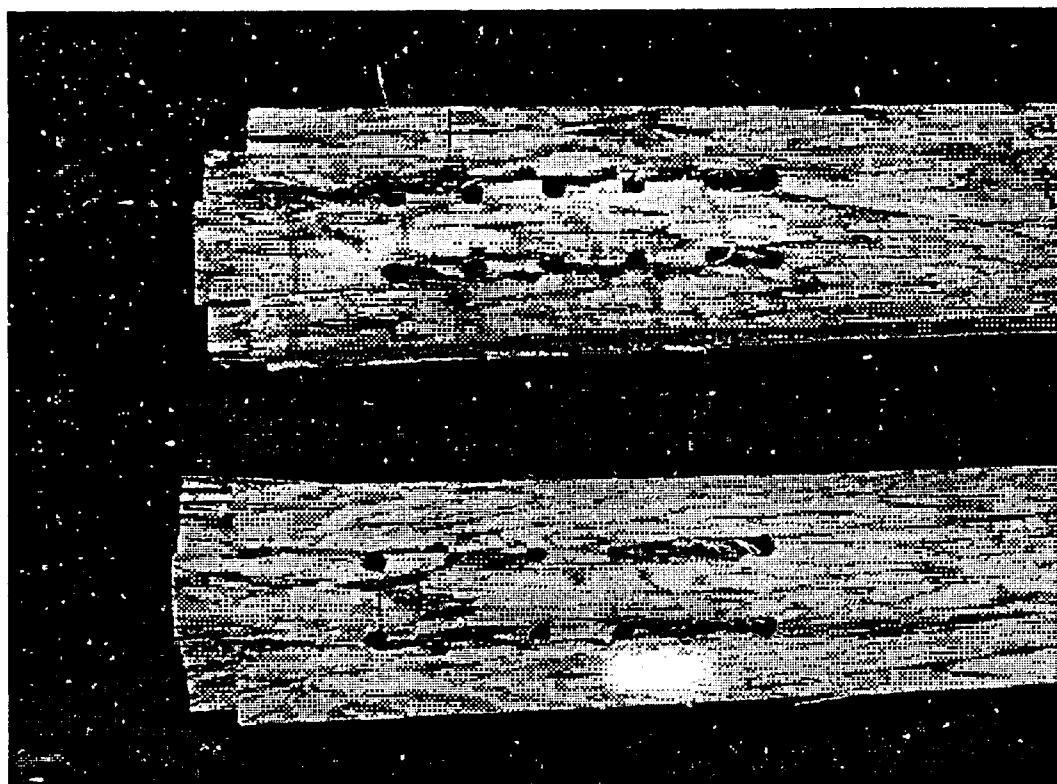
Failure mode: Bi-axial Shear Plug



Load-displacement Plot



HRER



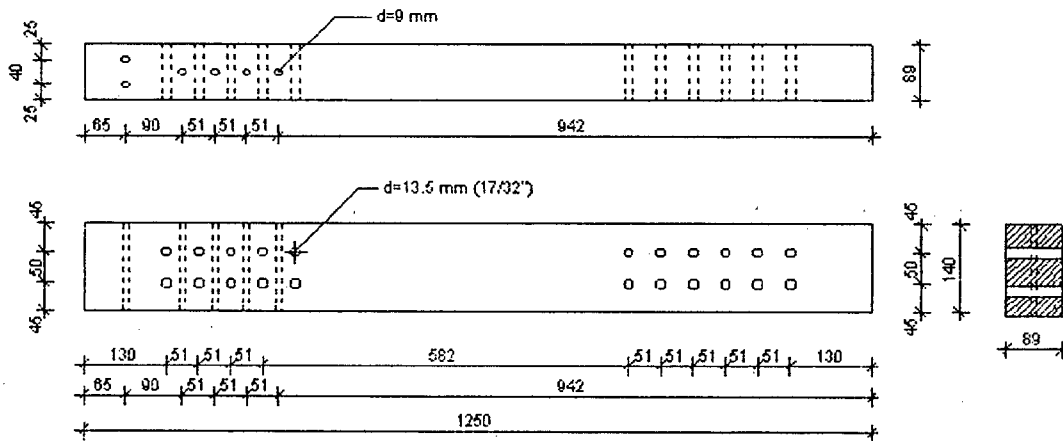
HRERe
10-1/2" Bolt Connection in PSL
Epoxy Glued Rebar Reinforced

$L/d = 7.0$
 $e = 10d$
 $s = 4d$

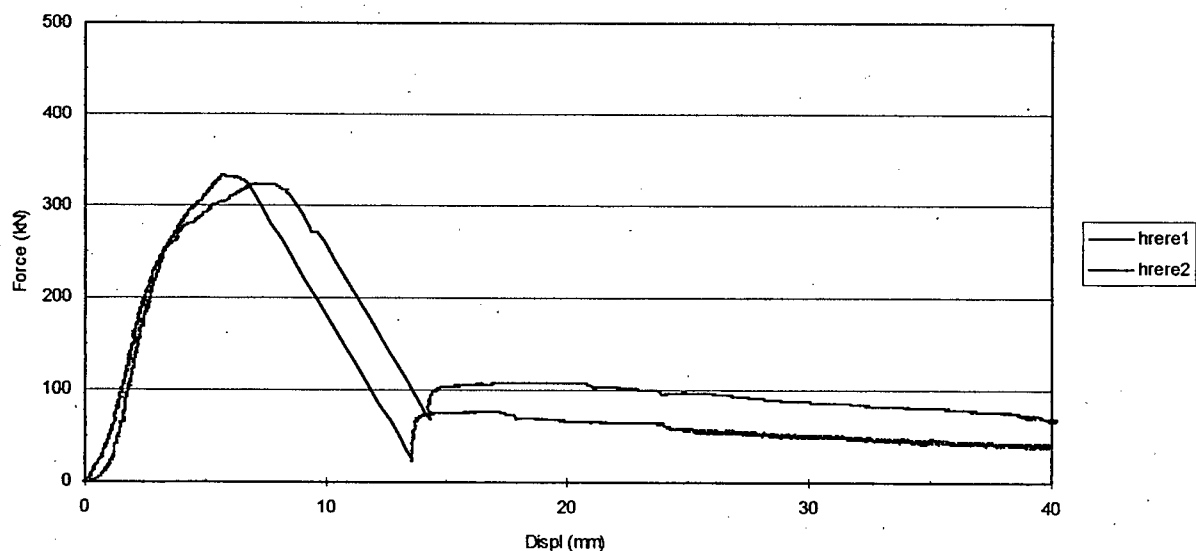
Quantity	Fult	D@Fult	80%Fult	D@80	D@50	Ductility
Specimen	[kN]	[mm]	[kN]	[mm]	[mm]	[]
HRERe-1	324.61	6.69	259.69	9.80	2.00	4.90
HRERe-2	332.86	5.93	266.29	8.00	2.25	3.56

Quantity	Stiffness	Energy	Design F	Dens.green	Dens.dry	Moist.cnt.
Specimen	[kN/mm]	[Nm]	[kN]	[kg/m3]	[kg/m3]	[%]
HRERe-1	105.38	5443.99	N/A	626.71	637.26	9.12
HRERe-2	105.51	4069.97	N/A	639.95	628.42	9.08

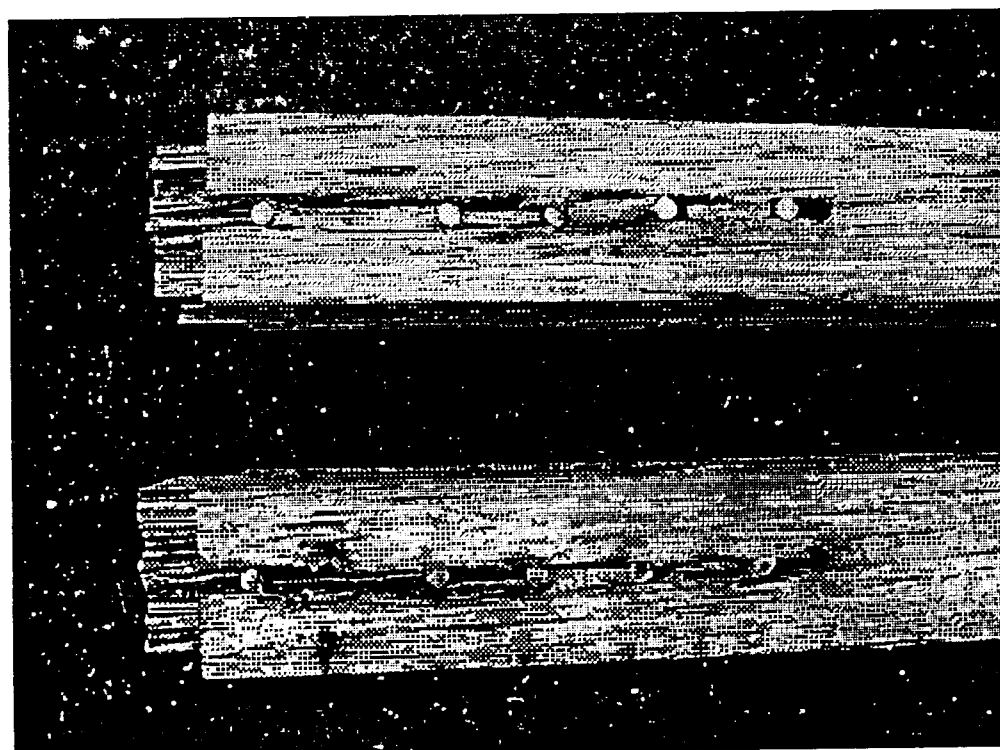
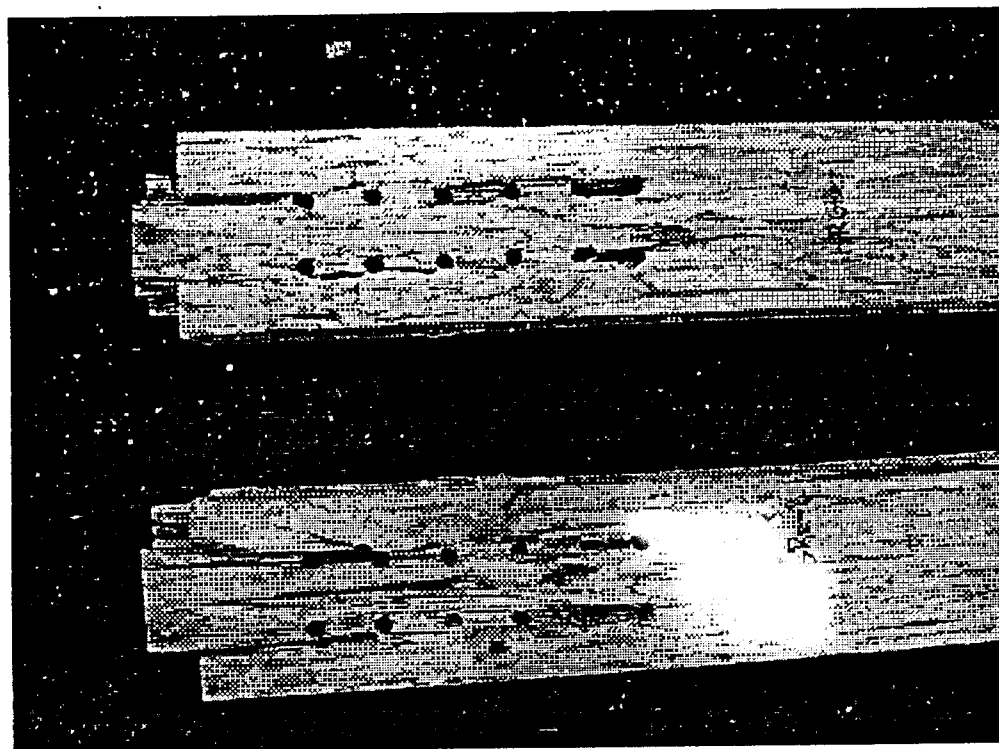
Failure mode: Bi-axial Shear Plug



Load-displacement Plot



HRERE



TU-C
10-3/8" Bolt Connection in PSL
Unreinforced

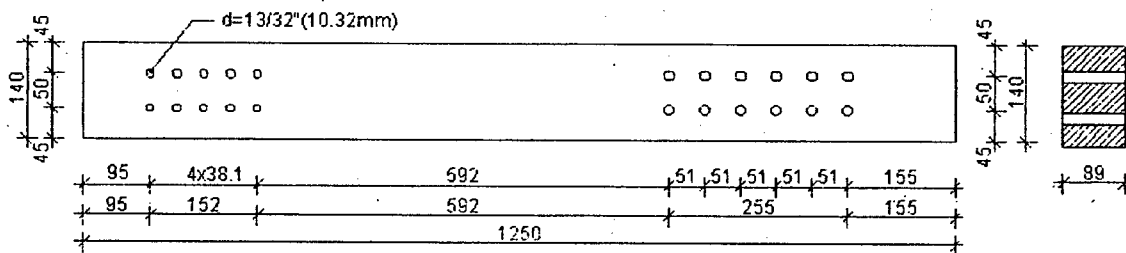
L/d = 9.3
e = 10d
s = 4d

Quantity	Fult	D@Fult	Cycle	80%Fult	D@80	Cycle	D@50
Specimen	[kN]	[mm]	Nr.	[kN]	[mm]	Nr.	[mm]
TU-C	164.04	5.12	13.00	131.23	7.50	19.00	1.38

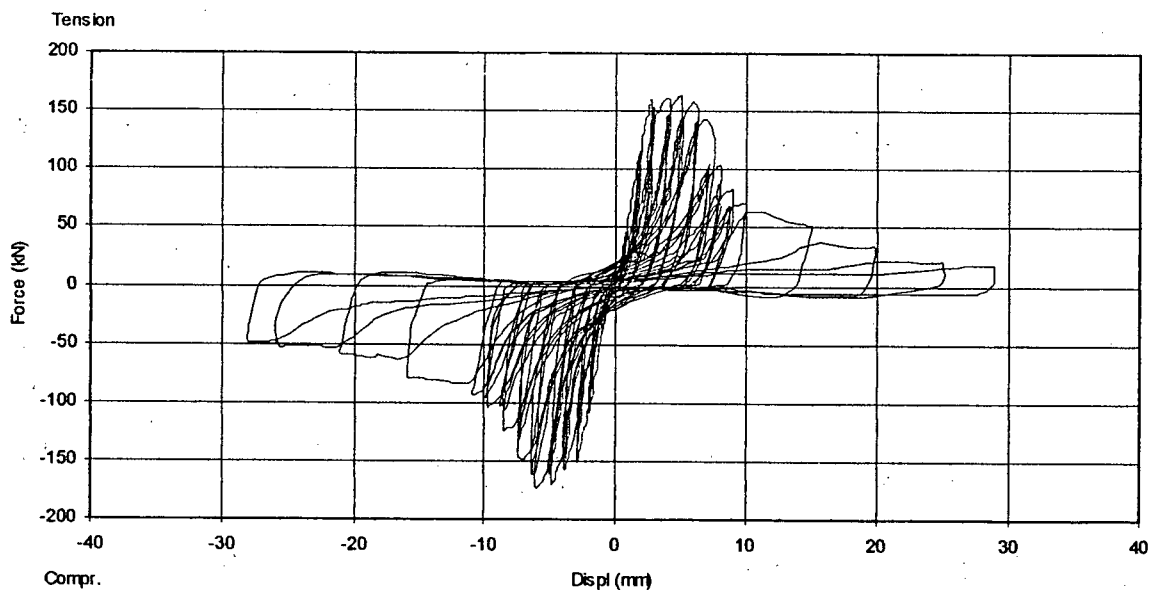
Specimen	Ductility	Elast.Stiff.	Ener.Diss.*	Step	Dens.green	Dens.dry	Moist.cnt.
symbol	[]	[kN/mm]	[Nm]	[mm]	[kg/m ³]	[kg/m ³]	[%]
TU-C	5.43	69.26	1580	0.80	676.01	643.24	9.02

*Calculated after 100 mm of Cumulative Cyclic Displacement

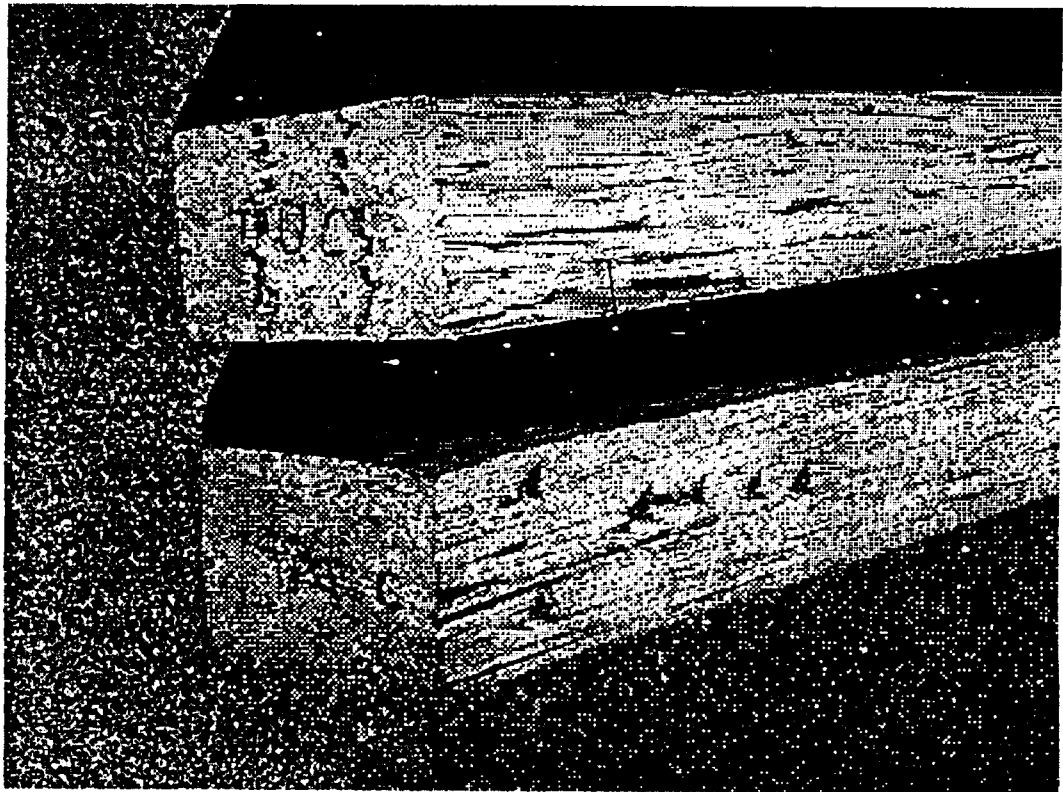
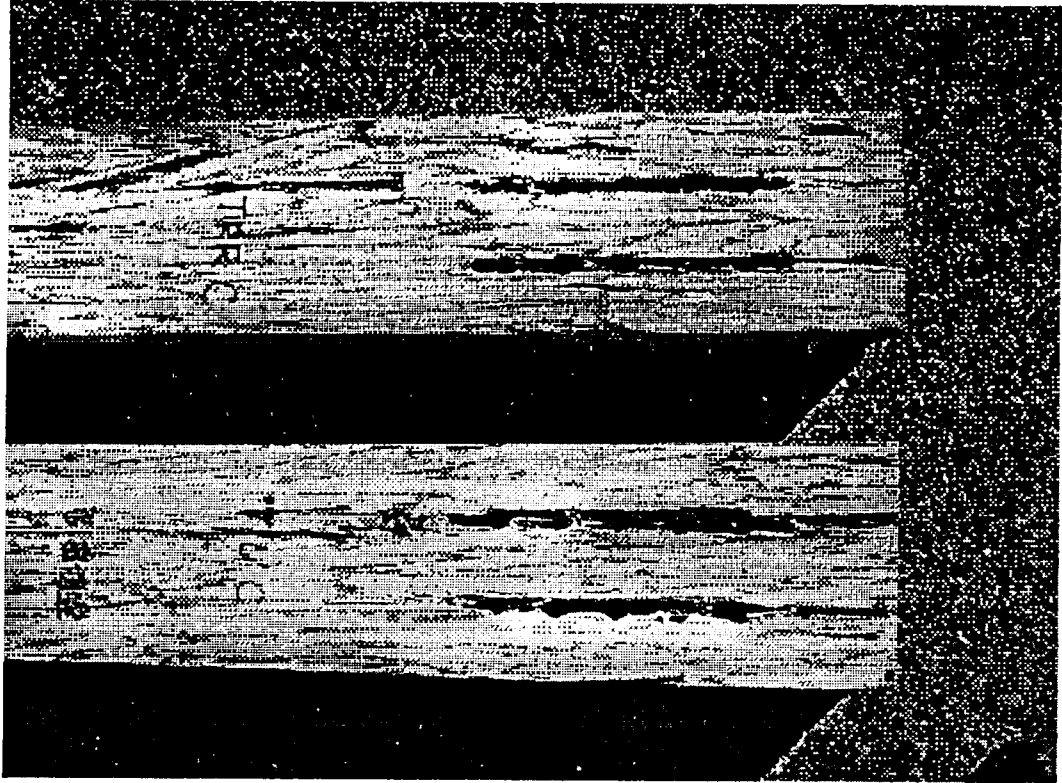
Failure mode: Wood Crushing (Bearing), Row Splitting



Load-displacement Plot



TRR-C, TU-C



HU-C
10-1/2" Bolt Connection in PSL
Unreinforced

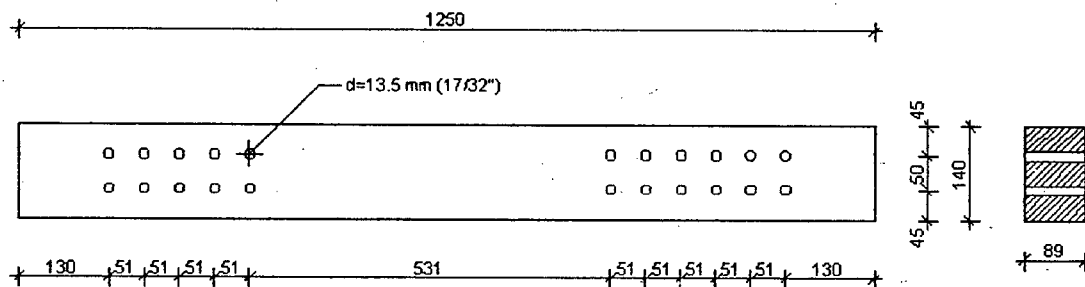
L/d = 7.0
e = 10d
s = 4d

Quantity	Fult	D@Fult	Cycle	80%Fult	D@80	Cycle	D@50
Specimen	[kN]	[mm]	Nr.	[kN]	[mm]	Nr.	[mm]
HU-1-C	298.97	4.12	7.00	239.18	5.40	7.00	1.77
HU-2-C	282.02	3.44	10.00	225.62	4.10	13.00	1.70
HU-3-C	297.67	3.70	10.00	238.14	5.20	10.00	1.70

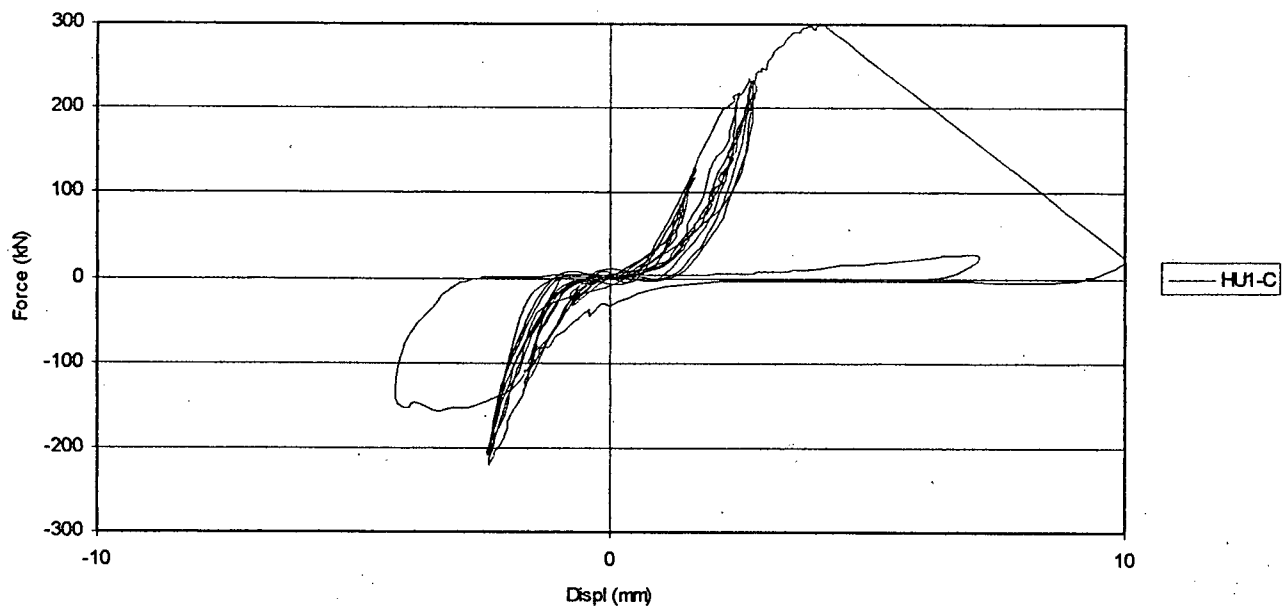
Specimen	Ductility	Elast.Stiff.	Ener.Diss.*	Step	Dens.green	Dens.dry	Moist.cnt.
symbol	[]	[kN/mm]	[Nm]	[mm]	[kg/m3]	[kg/m3]	[%]
HU-1-C	3.05	108.84	2420.00	0.80	667.94	639.52	9.54
HU-2-C	2.41	130.96	2044.00	0.80	654.30	627.29	9.22
HU-3-C	3.06	113.32	2110.00	0.80	656.95	630.43	8.94

*Calculated after 100 mm of Cumulative Cyclic Displacement

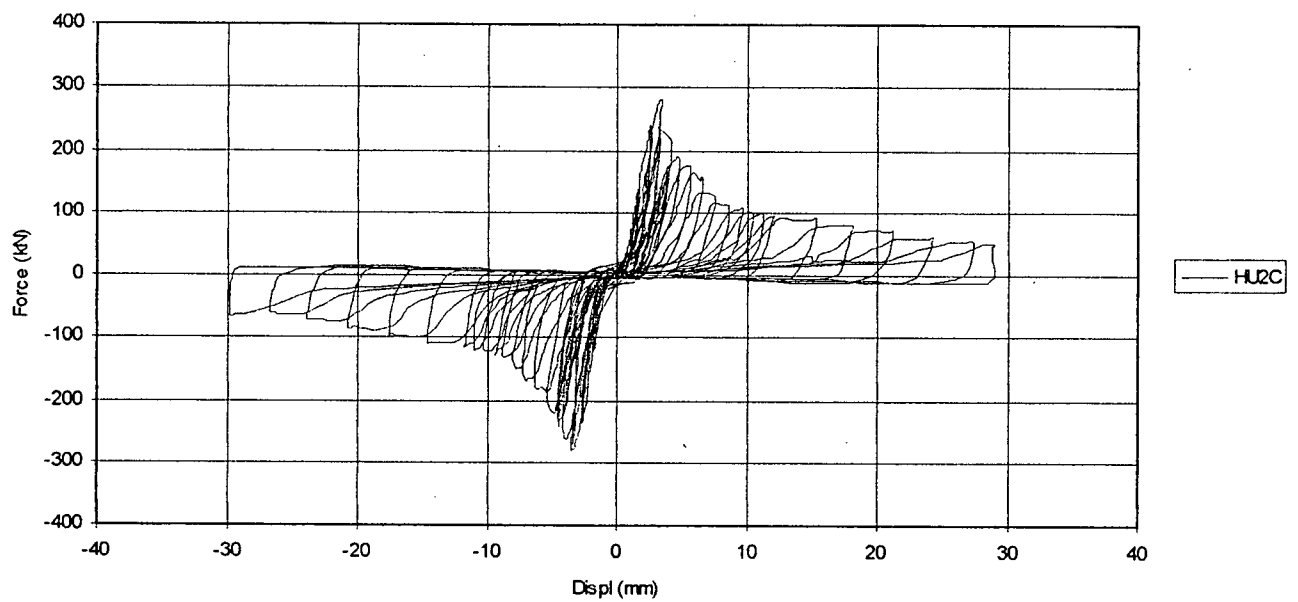
Failure mode: Row Shear, Row Splitting



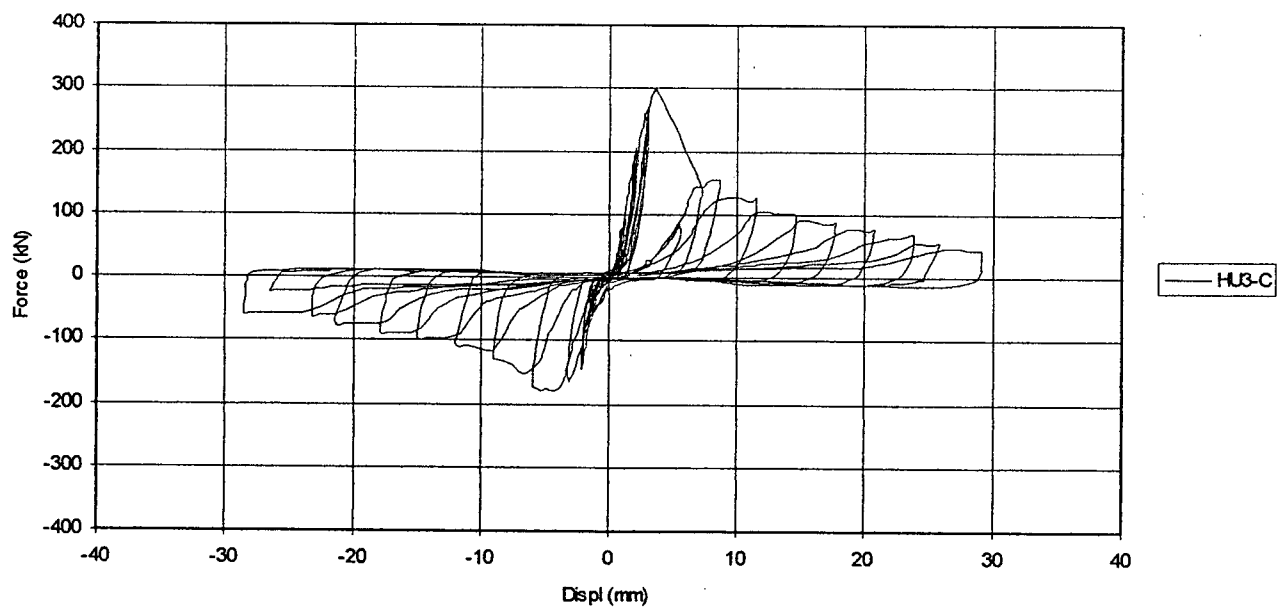
1/2"-10 BOLT PSL CONNECTION
UNREINFORCED



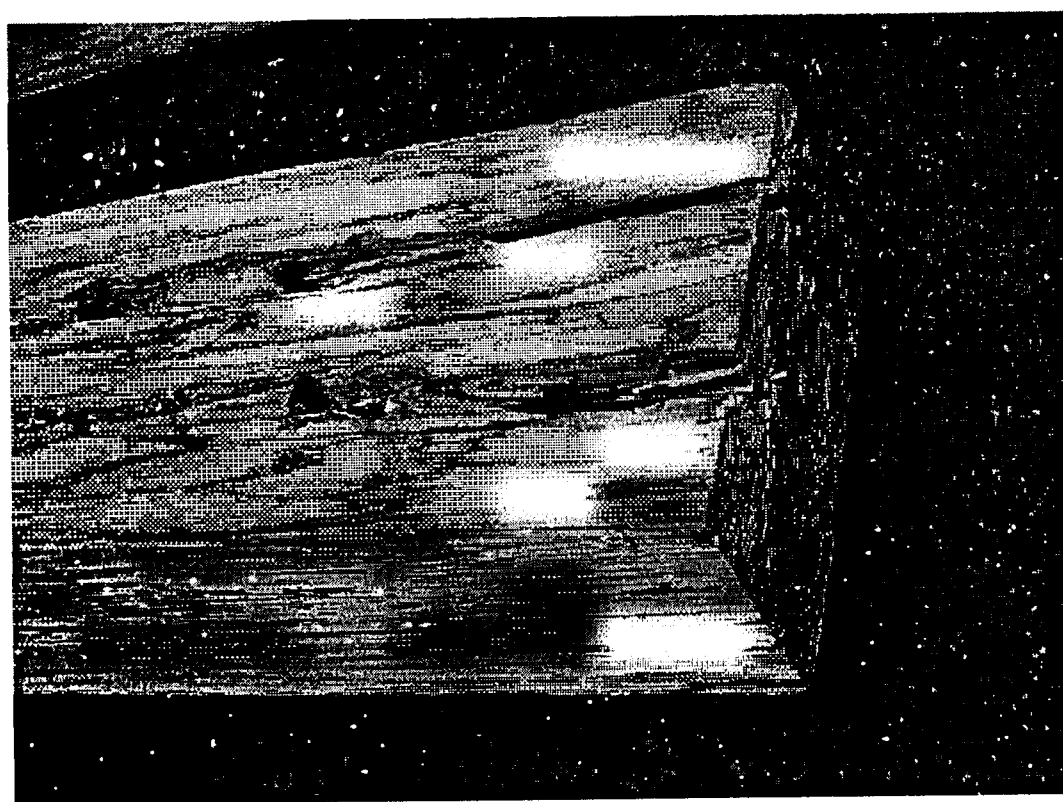
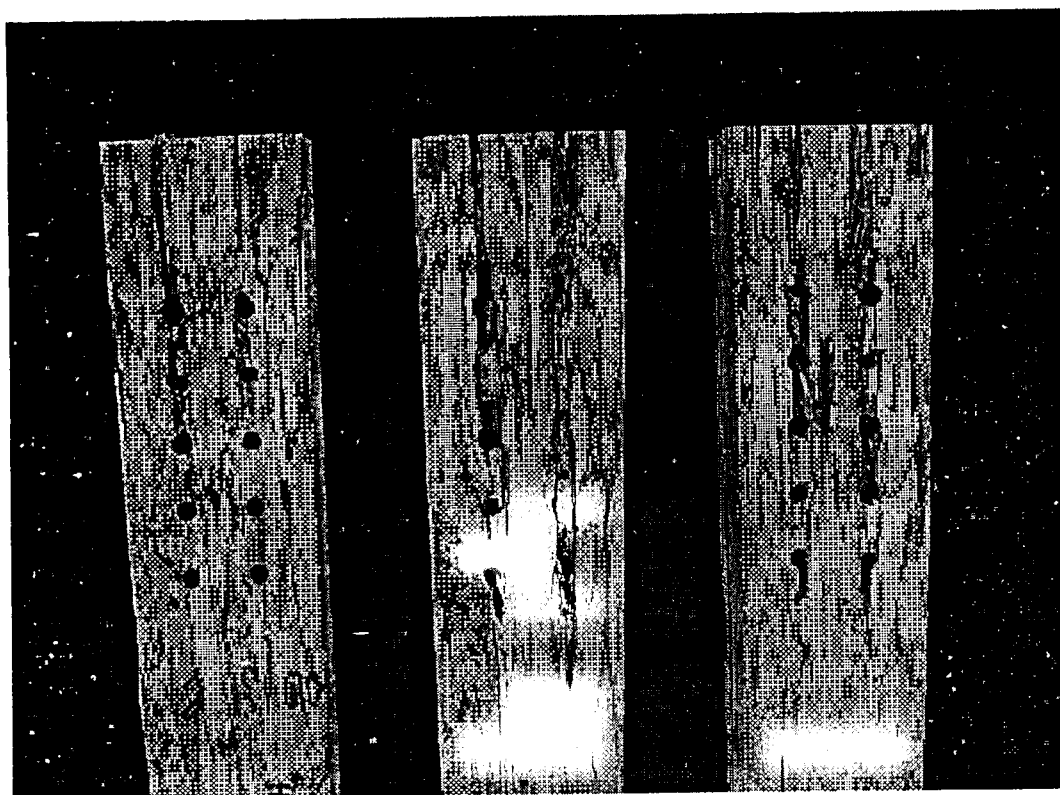
1/2"-10 BOLT PSL CONNECTION
UNREINFORCED



1/2"-10 BOLT PSL CONNECTION
UNREINFORCED



HU-C



FU-C
10-5/8" Bolt Connection in PSL
Unreinforced

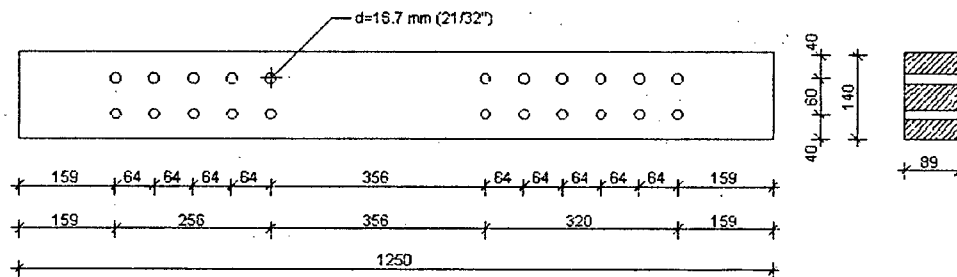
L/d = 5.6
e = 10d
s = 4d

Quantity	Fult	D@Fult	Cycle	80%Fult	D@80	Cycle	D@50
Specimen	[kN]	[mm]	Nr.	[kN]	[mm]	Nr.	[mm]
FU-1-C	290.50	2.82	23.00	232.40	4.20	31.00	1.62
FU-2-C	244.43	2.87	21.00	195.54	4.12	29.00	1.62
FU-3-C	282.24	3.09	23.00	225.79	4.60	25.00	1.58

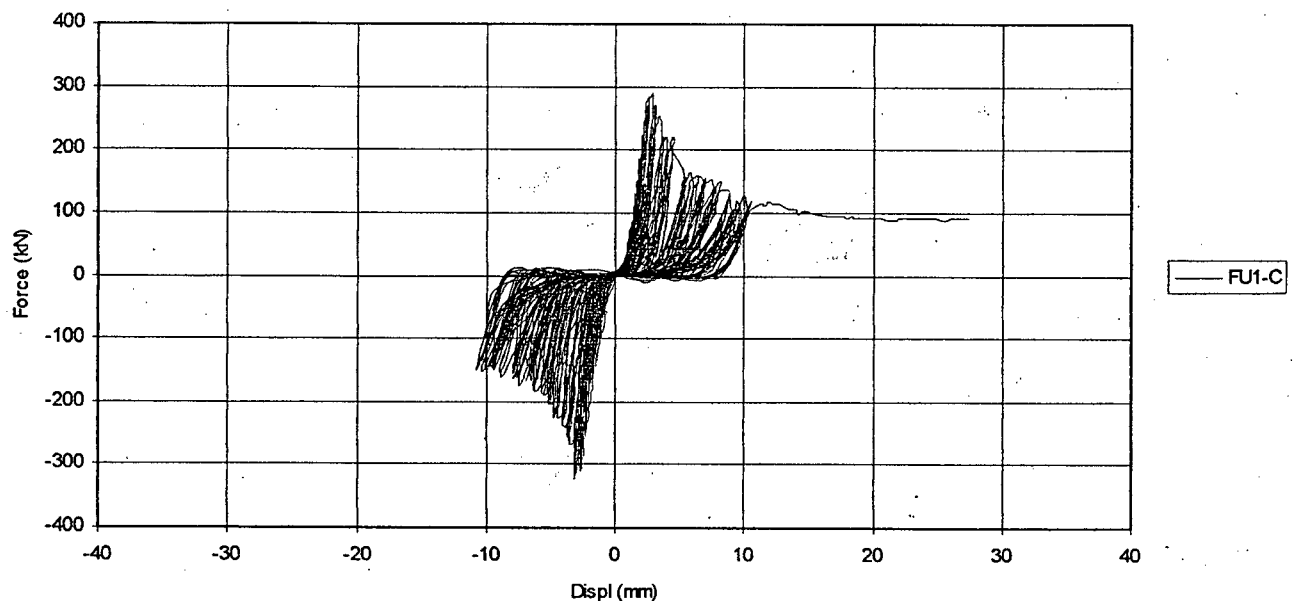
Specimen	Ductility	Elast.Stiff.	Ener.Diss.*	Step	Dens.green	Dens.dry	Moist.cnt.
symbol	[]	[kN/mm]	[Nm]	[mm]	[kg/m3]	[kg/m3]	[%]
FU-1-C	2.59	171.43	398.00	0.40	634.53	610.09	8.73
FU-2-C	2.54	138.67	288.00	0.40	615.23	587.42	8.71
FU-3-C	2.91	160.00	762.00	0.40	664.35	635.68	9.27

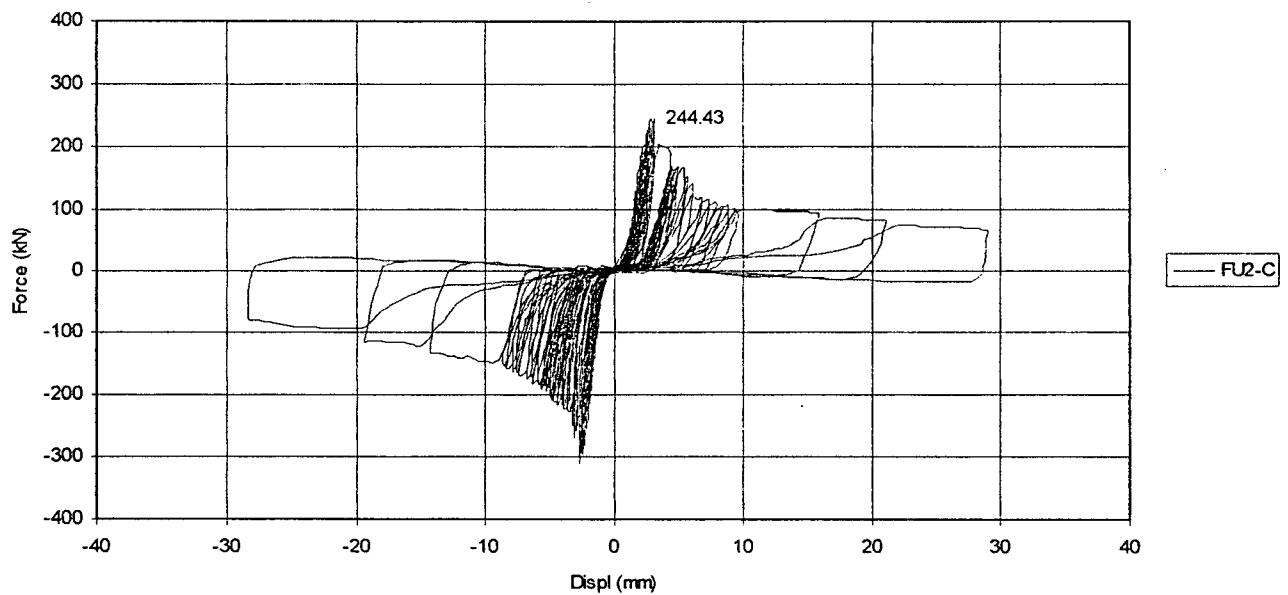
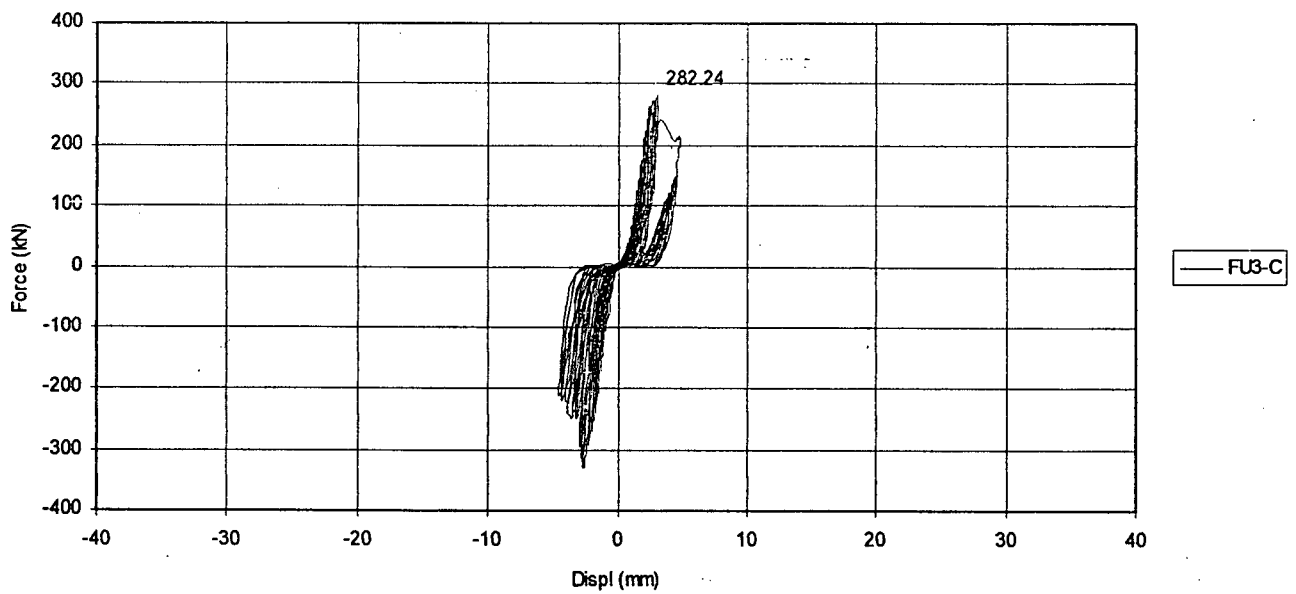
*Calculated after 100 mm of Cumulative Cyclic Displacement

Failure mode: Row Shear, Row Splitting

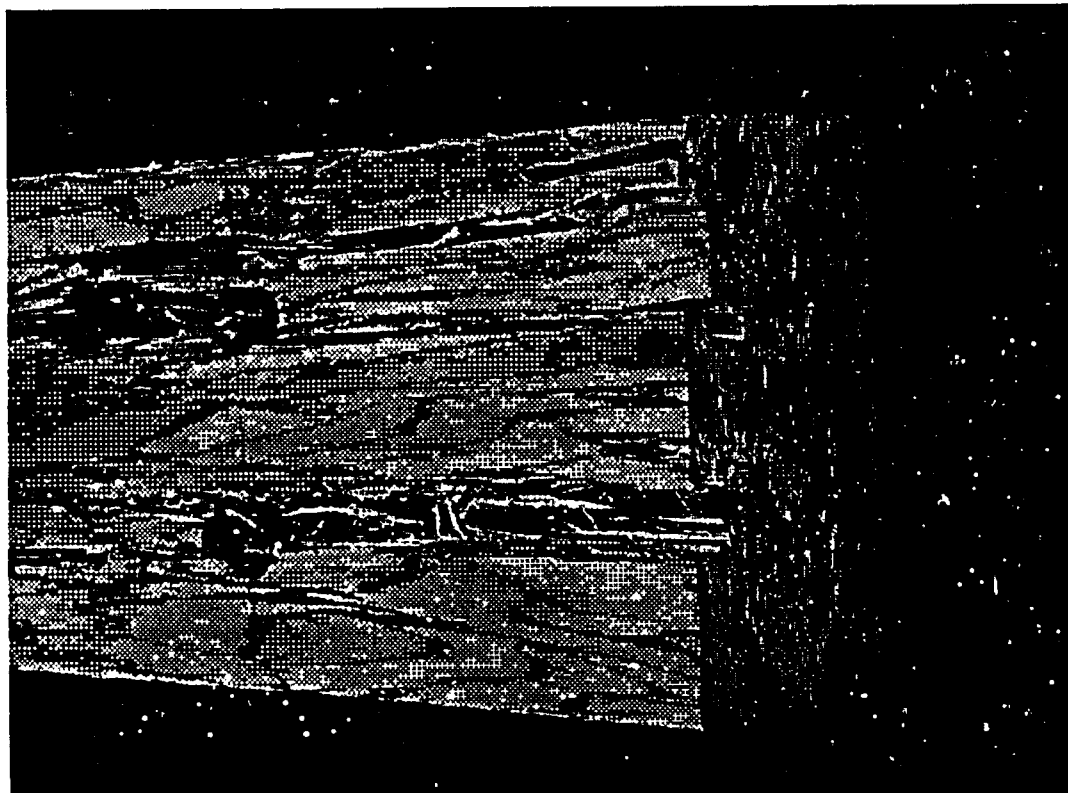
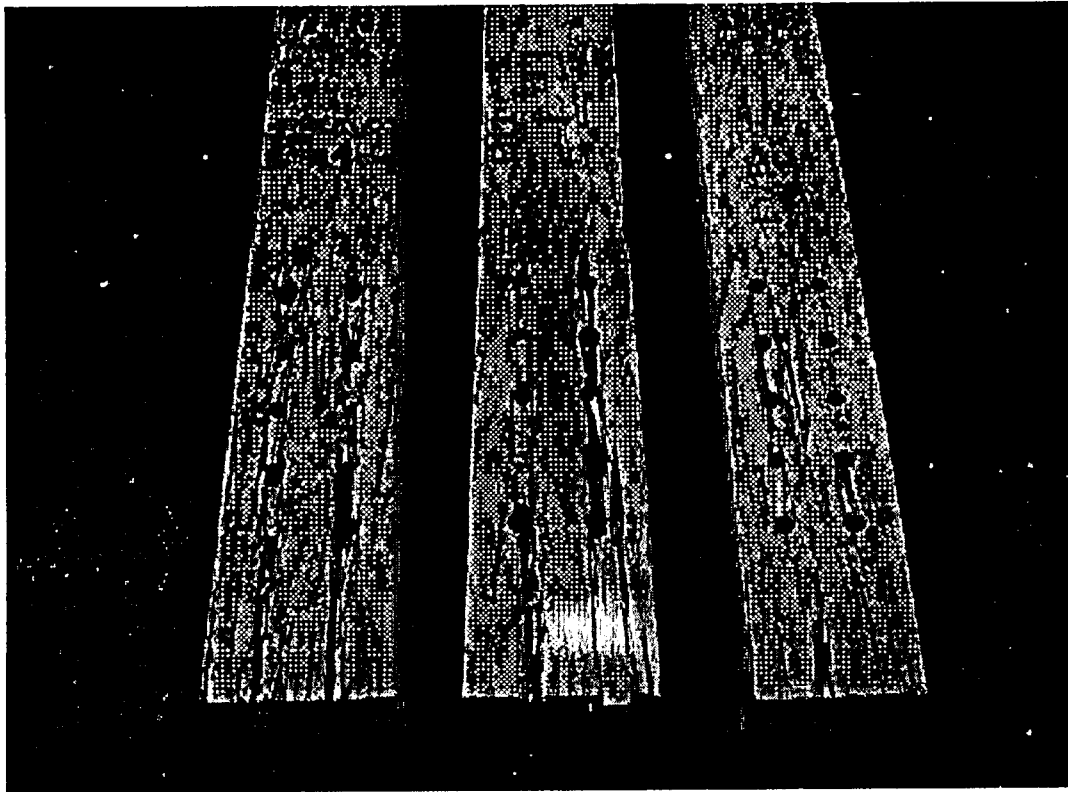


5/8"-10 BOLT PSL CONNECTION
UNREINFORCED



5/8"-10 BOLT PSL CONNECTION
UNREINFORCED5/8"-10 BOLT PSL CONNECTION
UNREINFORCED

FU-C



TRR-C
10-3/8" Bolt Connection in PSL
Lag Screw Reinforced

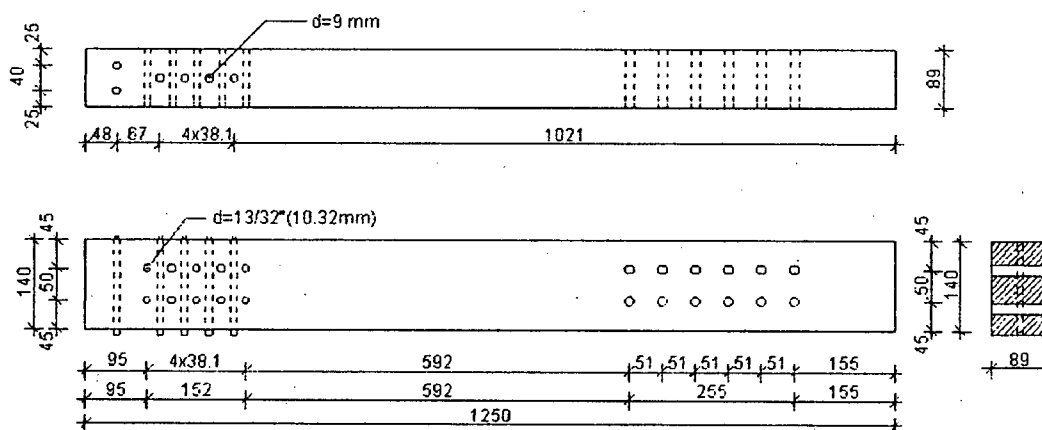
$$\begin{aligned} L/d &= 9.3 \\ e &= 10d \\ s &= 4d \end{aligned}$$

Quantity	Fult	D@Fult	Cycle	80%Fult	D@80	Cycle	D@50
Specimen	[kN]	[mm]	Nr.	[kN]	[mm]	Nr.	[mm]
TRR-C	262.90	16.60	13.00	210.32	20.45	16.00	2.36

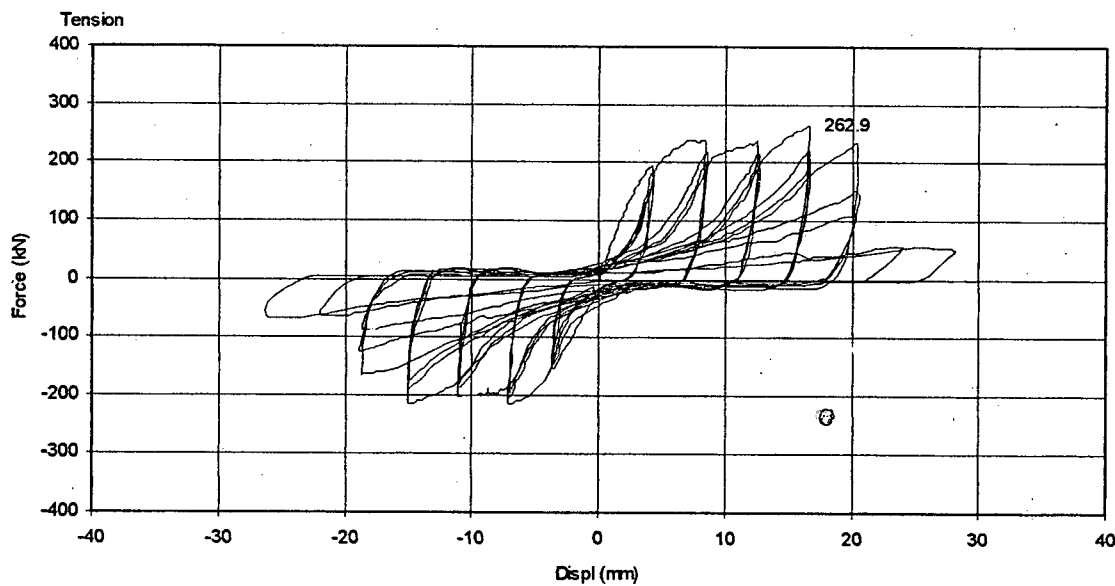
Specimen	Ductility	Elast.Stiff.	Ener.Diss.*	Step	Dens.greer	Dens.dry	Moist.cnt.
symbol	[]	[kN/mm]	[Nm]	[mm]	[kg/m3]	[kg/m3]	[%]
TRR-C	8.67	52.23	4784.00	4.00	576.86	547.25	8.12

*Calculated after 100 mm of Cumulative Cyclic Displacement

Failure mode: Ductile-Wood Crushing (Bearing)



Load-displacement Plot



GTRR-C
10-3/8" Bolt Connection in Glulam
Lag Screw Reinforced

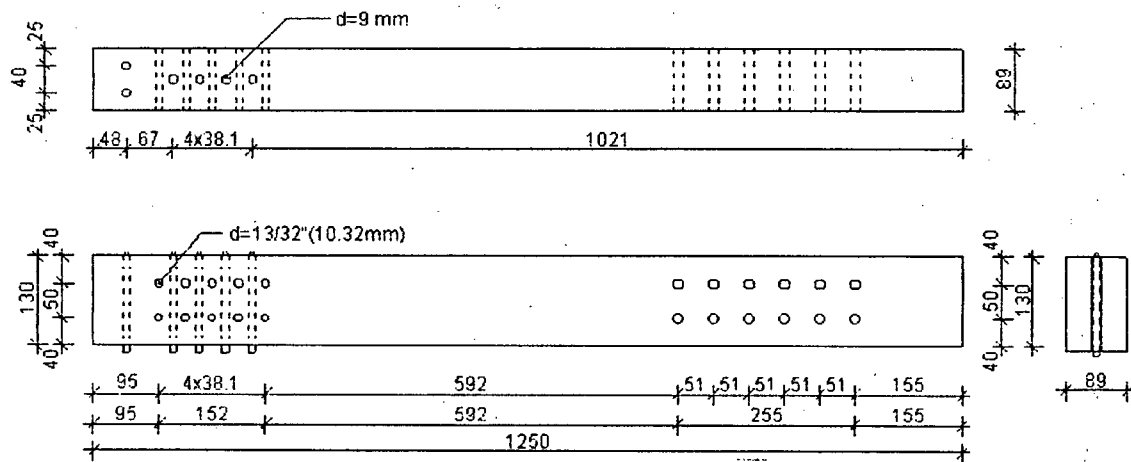
L/d = 9.3
e = 10d
s = 4d

Quantity	Fult	D@Fult	Cycle	80%Fult	D@80	Cycle	D@50
Specimen	[kN]	[mm]	Nr.	[kN]	[mm]	Nr.	[mm]
GTRR-C	267.70	7.90	7.00	214.16	17.68	19.00	2.05

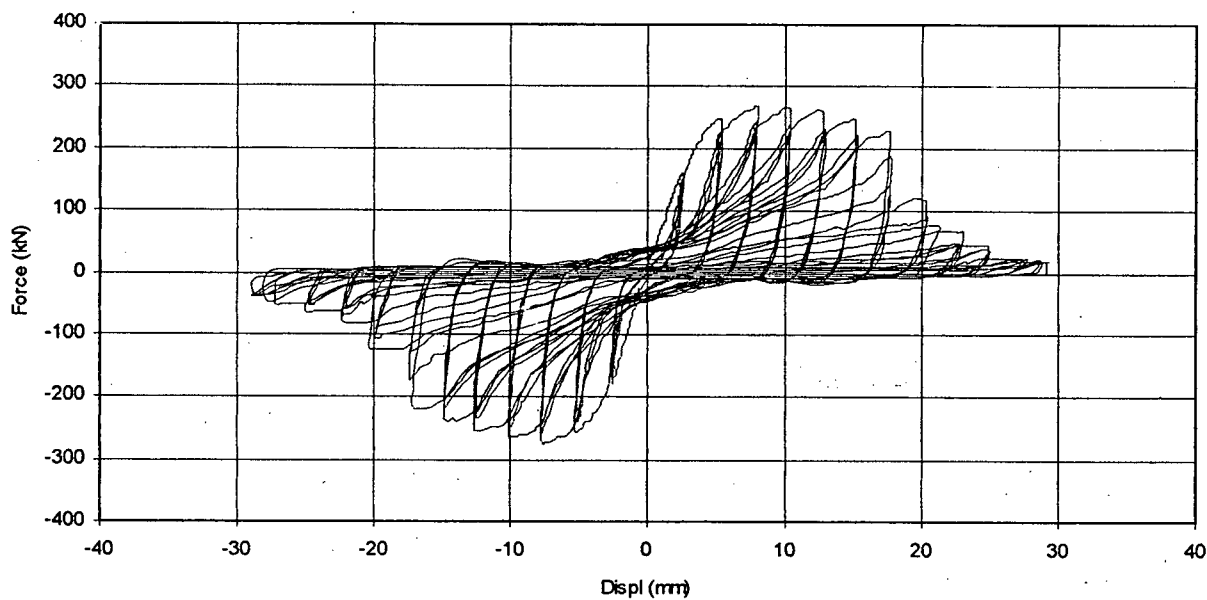
Specimen	Ductility	Elast.Stiff.	Ener.Diss.*	Step	Dens.green	Dens.dry	Moist.cnt.
symbol	[]	[kN/mm]	[Nm]	[mm]	[kg/m3]	[kg/m3]	[%]
GTRR-C	8.62	64.46	3579.00	2.50	638.65	610.51	12.19

*Calculated after 100 mm of Cumulative Cyclic Displacement

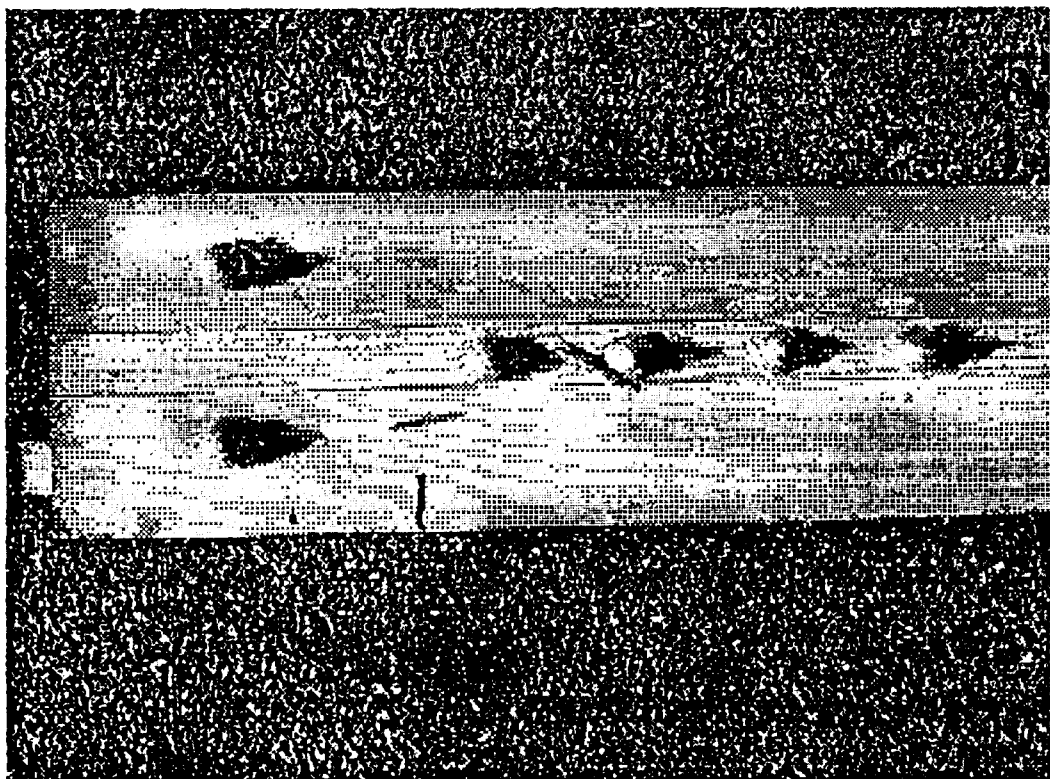
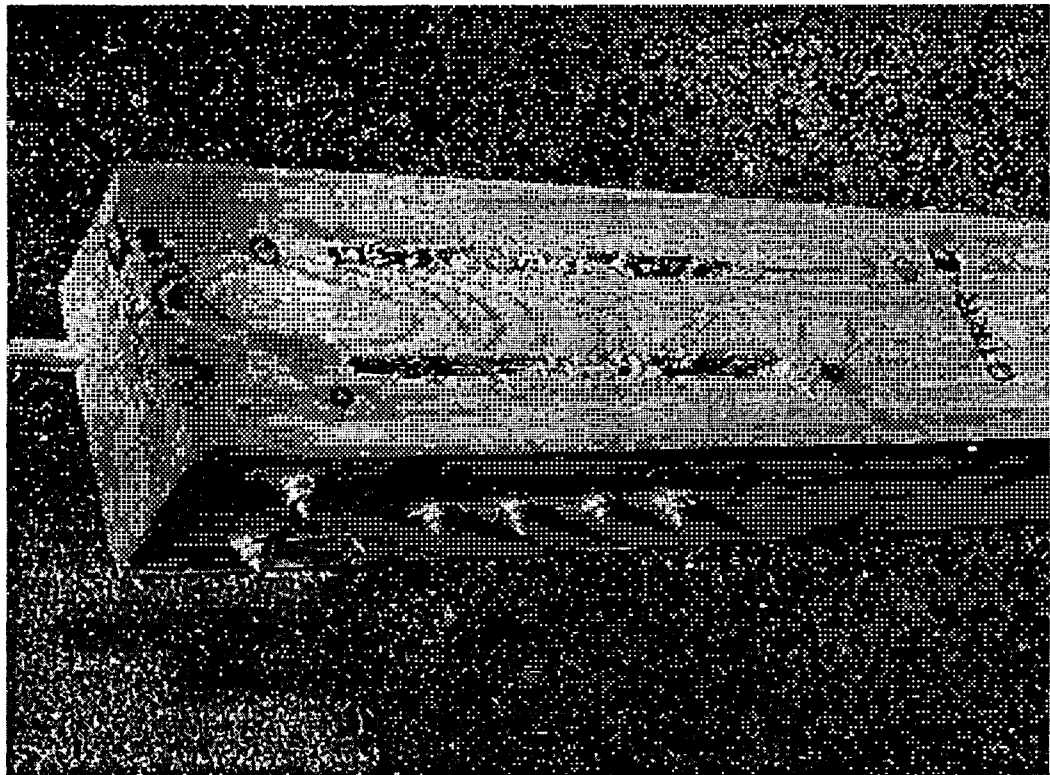
Failure mode: Ductile-Wood Crushing (Bearing)

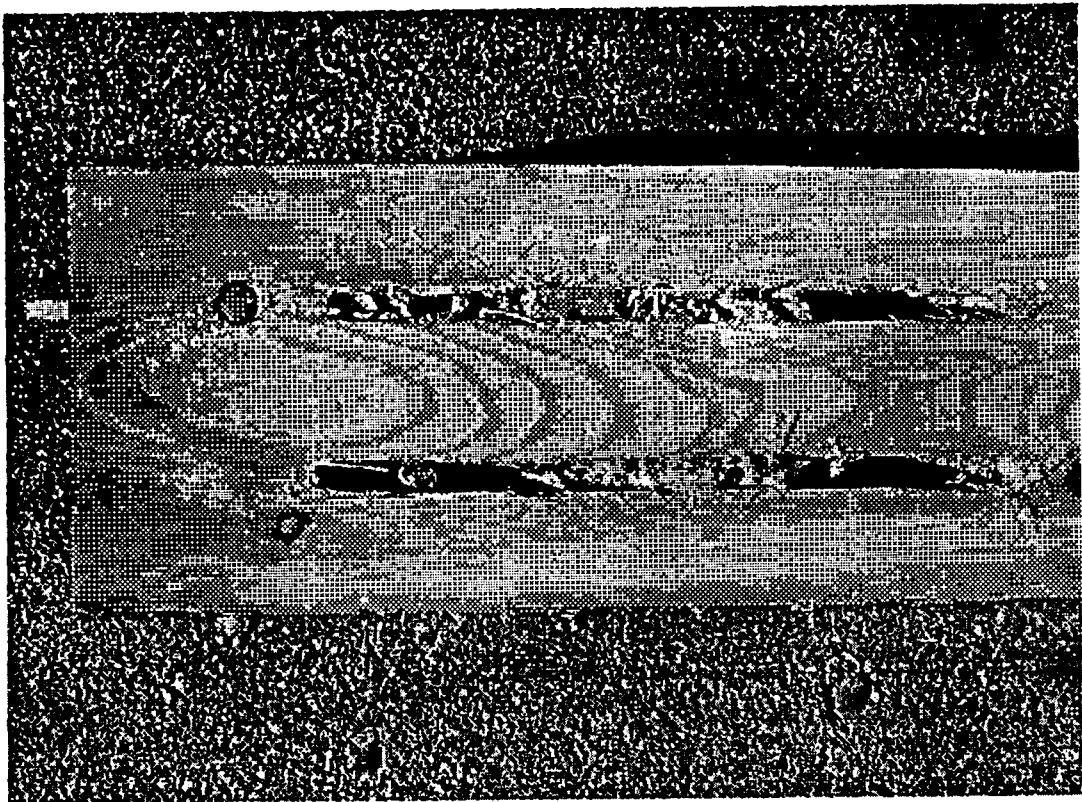


Load-displacement Plot



GTRR-C





69

HRR-C
10-1/2" Bolt Connection in PSL
Lag Screw Reinforced

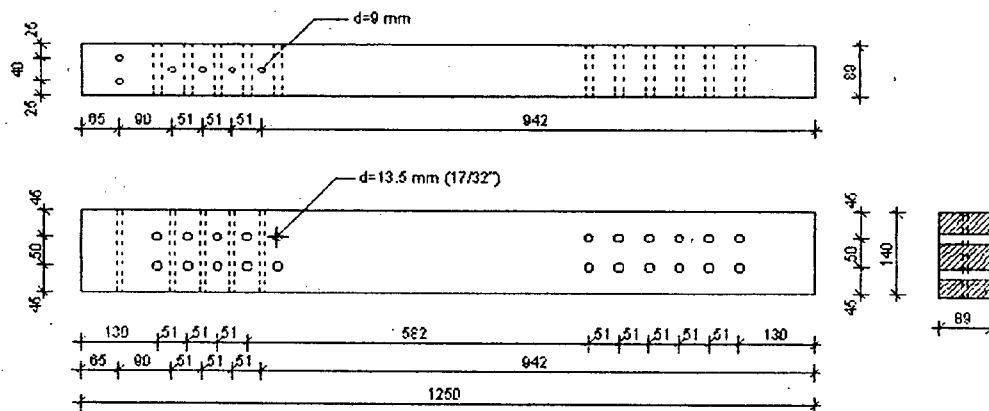
L/d = 7.0
e = 10d
s = 4d

Quantity	Fult	D@Fult	Cycle	80%Fult	D@80	Cycle	D@50
Specimen	[kN]	[mm]	Nr.	[kN]	[mm]	Nr.	[mm]
HRR-1-C	295.28	7.82	28.00	236.22	21.28	73.00	2.20
HRR-2-C	262.25	5.50	19.00	209.80	18.60	67.00	1.98
HRR-3-C	290.06	7.09	25.00	232.05	12.20	46.00	2.10

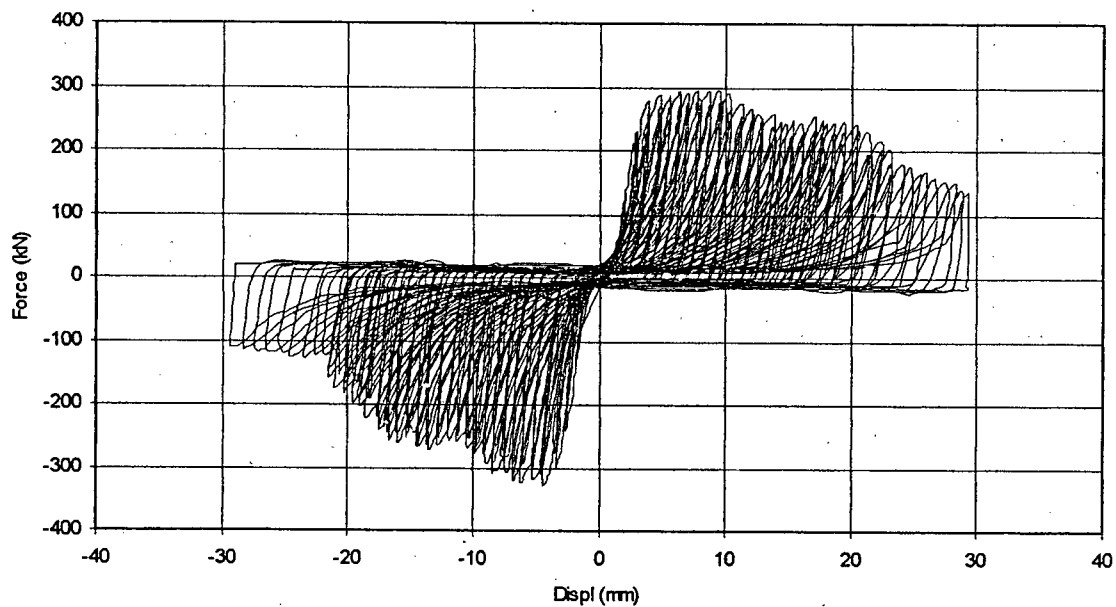
Specimen	Ductility	Elast. Stiff.	Ener. Diss.*	Step	Dens. greer	Dens. dry	Moist. cnt.
symbol	[]	[kN/mm]	[Nm]	[mm]	[kg/m3]	[kg/m3]	[%]
HRR-1-C	9.67	118.41	1743.00	0.80	652.34	645.91	8.95
HRR-2-C	9.39	134.28	1833.00	0.80	675.77	652.41	8.61
HRR-3-C	5.81	130.00	1886.00	0.80	674.16	646.83	8.56

*Calculated after 100 mm of Cumulative Cyclic Displacement

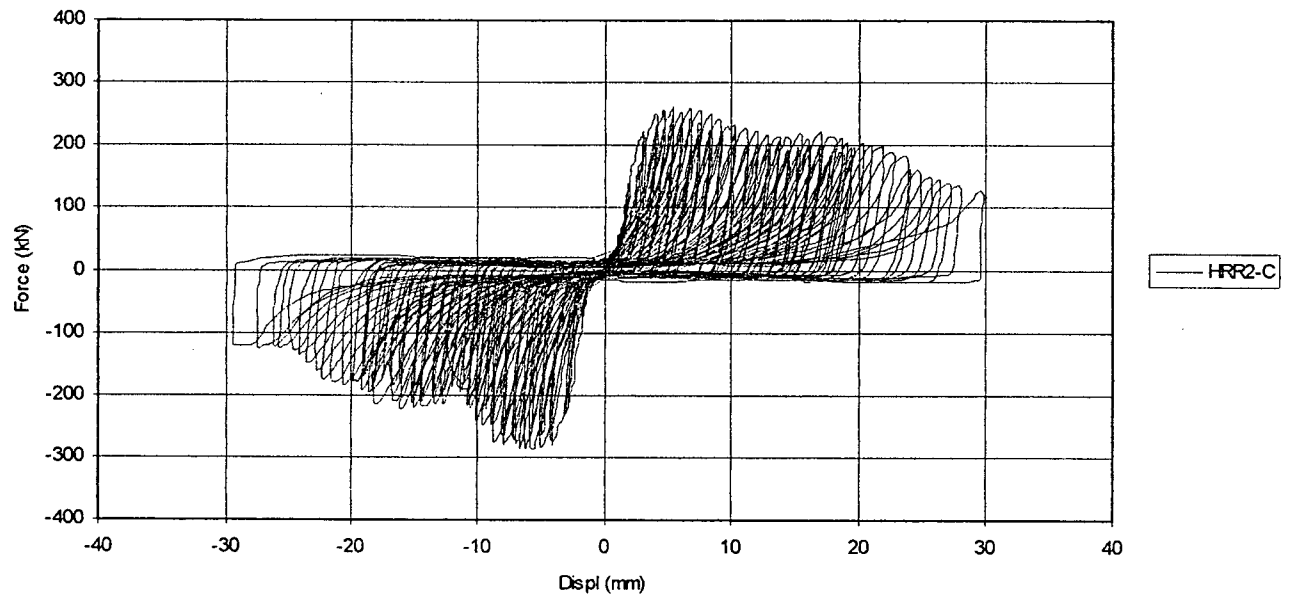
Failure mode: Wood Crushing, Shear Plug



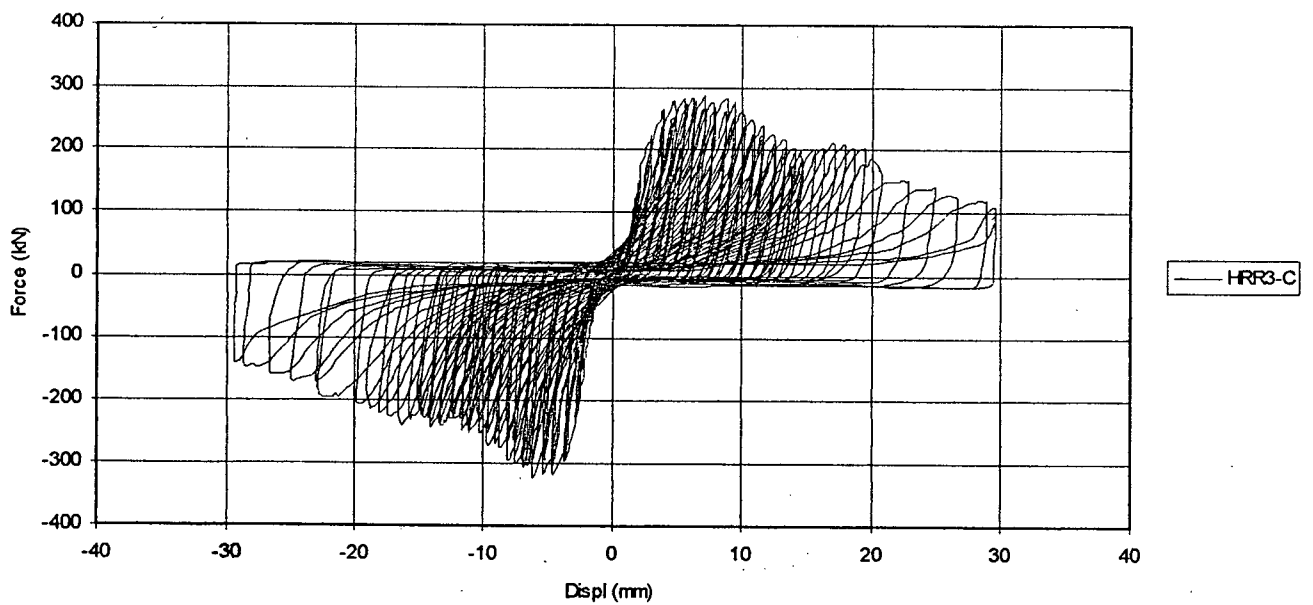
1/2"-10 BOLT PSL CONNECTION
LAG SCREW REINFORCED



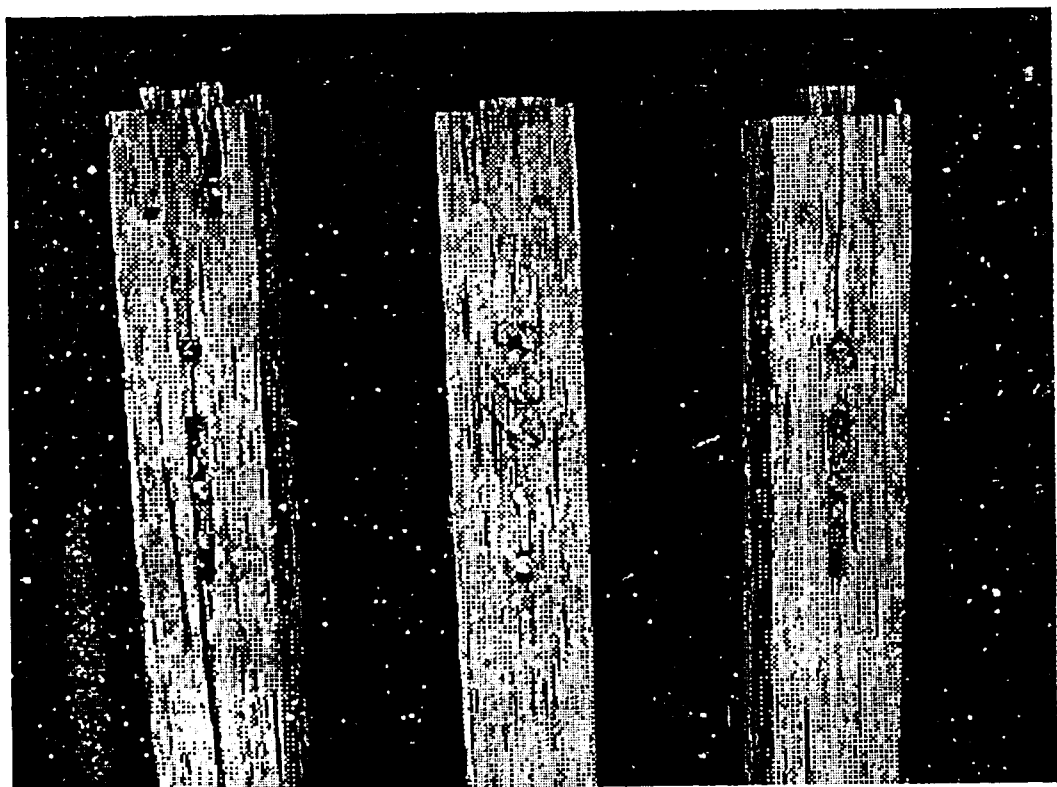
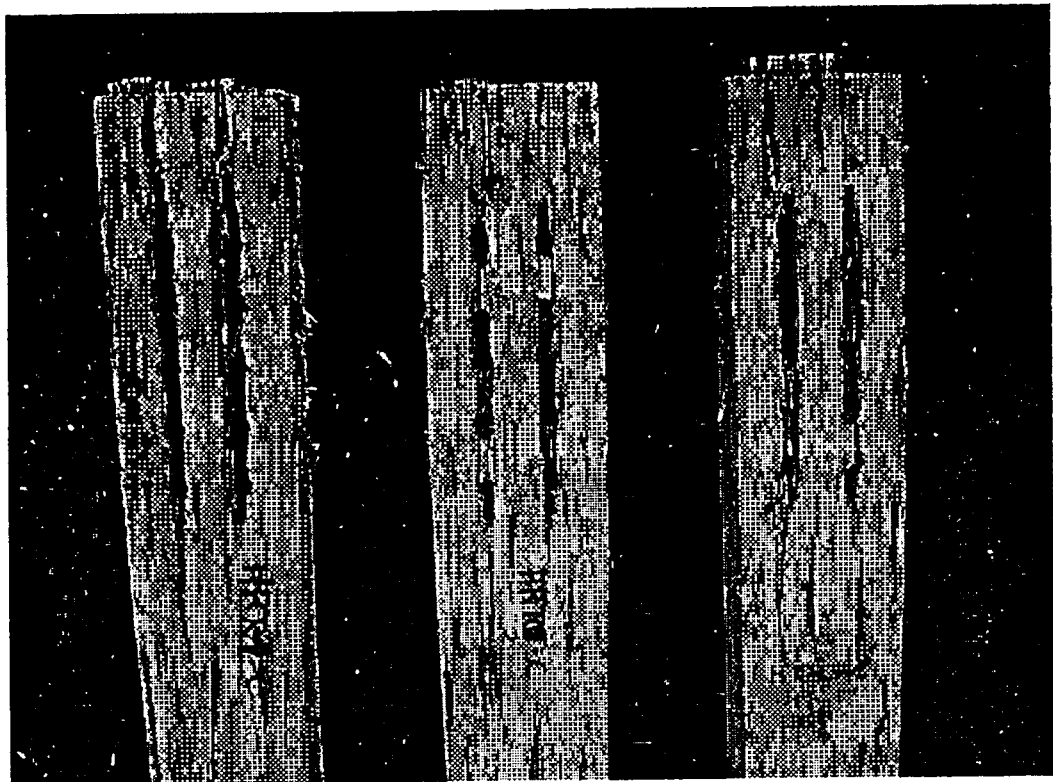
1/2"-10 BOLT PSL CONNECTION
LAG SCREW REINFORCED



1/2"-10 BOLT PSL CONNECTION
LAG SCREW REINFORCED



HRRC



FRR-C
10-5/8" Bolt Connection in PSL
Lag Screw Reinforced

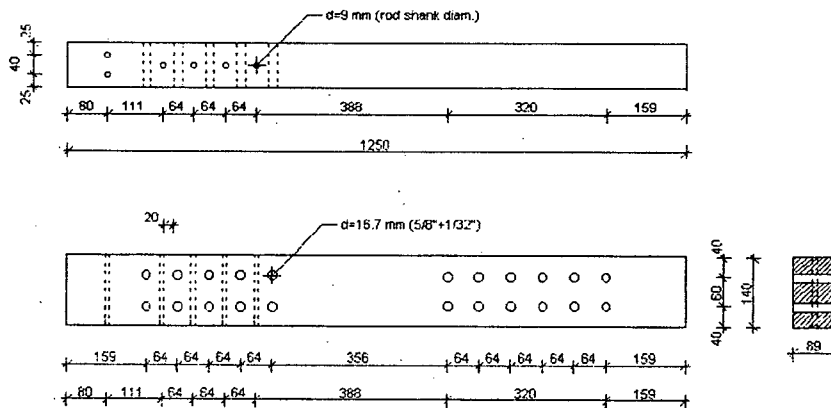
L/d = 5.6
e = 10d
s = 4d

Quantity	Fult	D@Fult	Cycle	80%Fult	D@80	Cycle	D@50
Specimen	[kN]	[mm]	Nr.	[kN]	[mm]	Nr.	[mm]
FRR-1-C	298.75	4.07	17.00	239.00	5.35	23.00	1.70
FRR-2-C	336.99	2.55	11.00	269.59	6.20	21.00	1.24
FRR-3-C	292.45	5.07	16.00	233.96	11.50	37.00	1.80

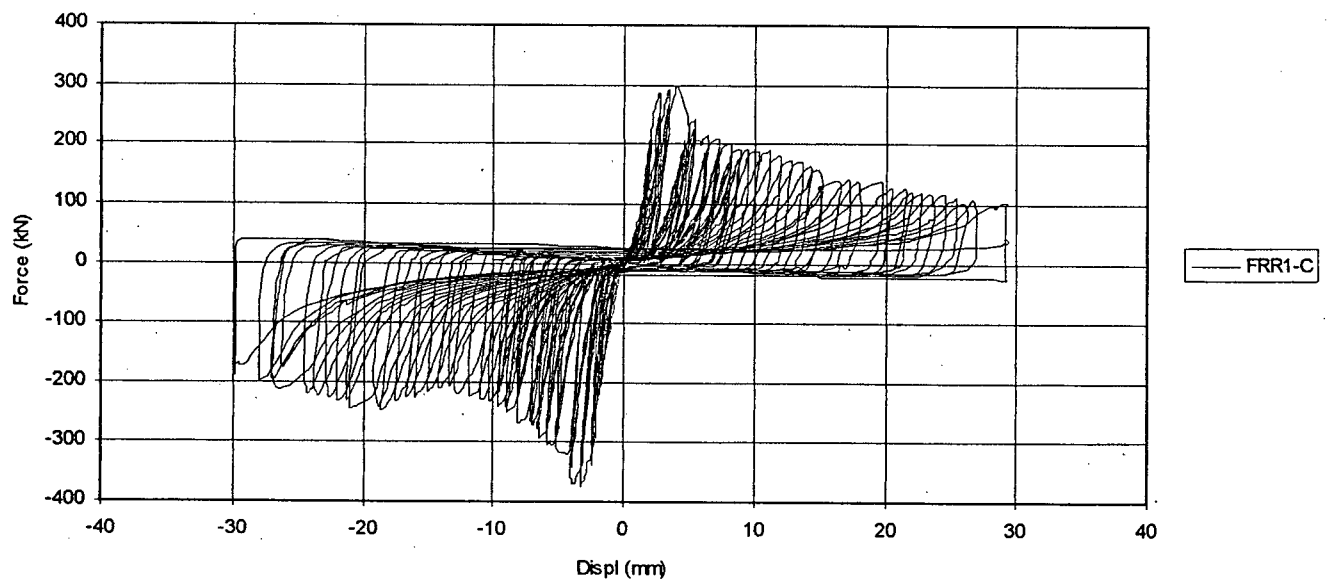
Specimen	Ductility	Elast.Stiff.	Ener.Diss.*	Step	Dens.greer	Dens.dry	Moist.cnt.
symbol	[]	[kN/mm]	[Nm]	[mm]	[kg/m3]	[kg/m3]	[%]
FRR-1-C	3.15	160.71	1080.00	0.80	639.68	628.27	9.28
FRR-2-C	5.00	168.00	1375.00	0.80	623.85	616.72	9.09
FRR-3-C	6.39	97.78	1340.00	0.80	635.81	627.39	9.38

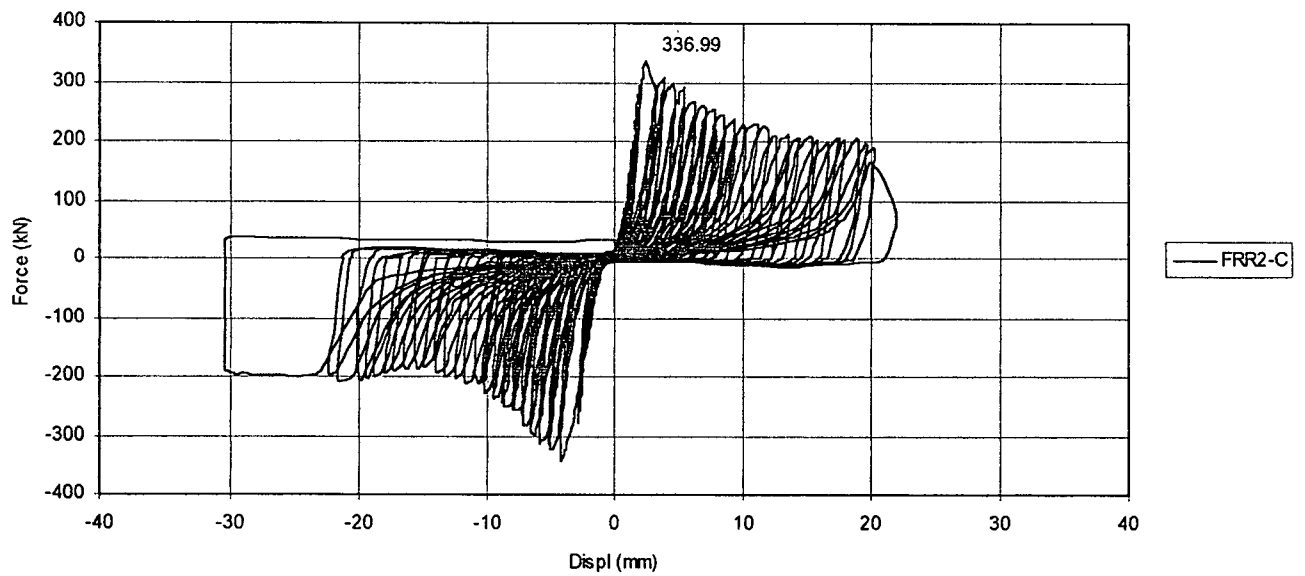
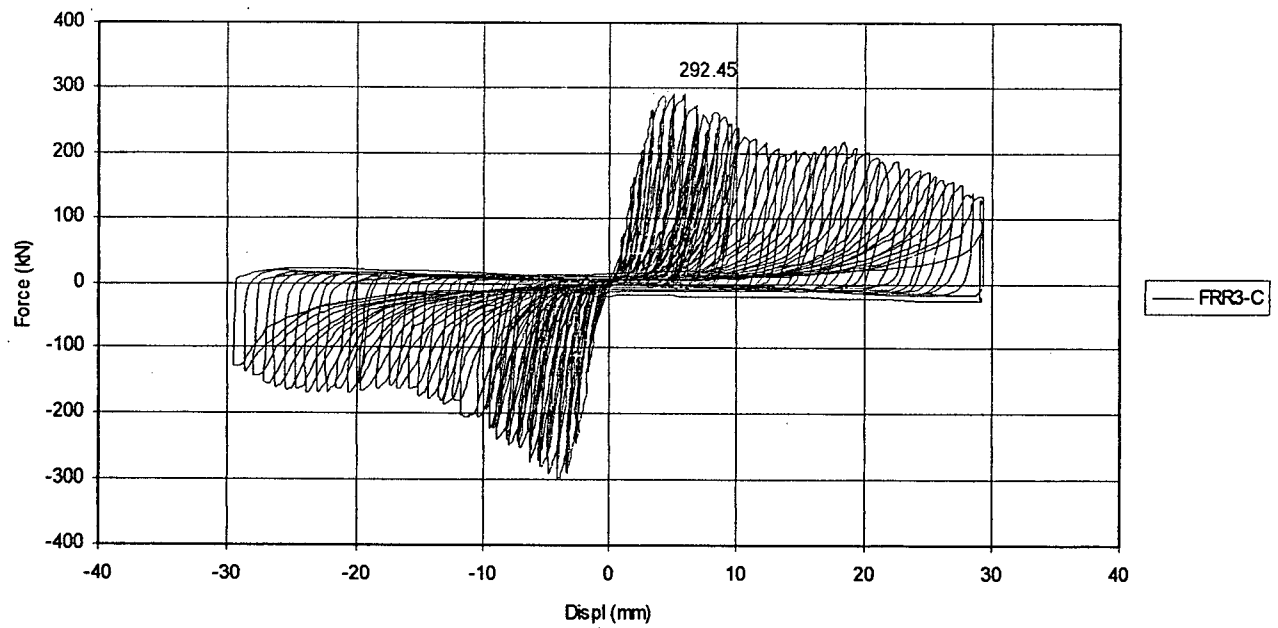
*Calculated after 100 mm of Cumulative Cyclic Displacement

Failure mode: Row Shear, Row Splitting

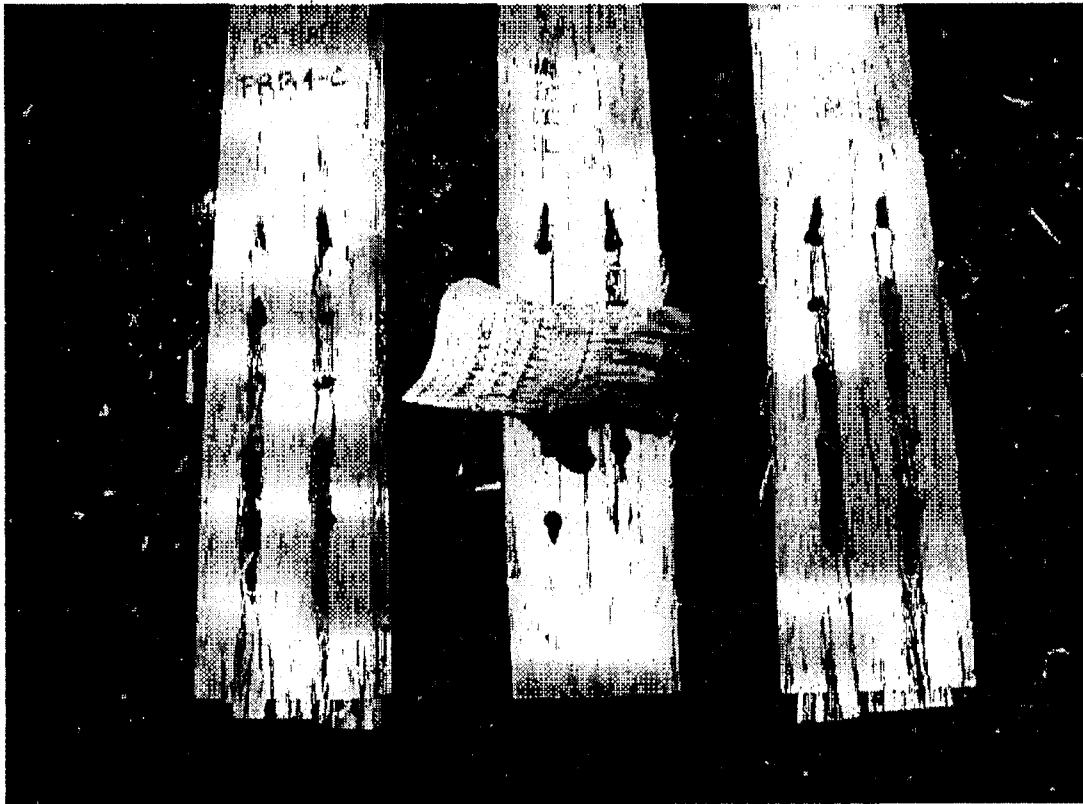


5/8"-10 Bolt Connection in PSL
Lag Screw Reinforced



5/8"-10 BOLT PSL CONNECTION
LAG SCREW REINFORCED5/8"-10 BOLT PSL CONNECTION
LAG SCREW REINFORCED

FRR-C



HRT-C
10-1/2" Bolt Connection in PSL
Truss Plate Reinforced

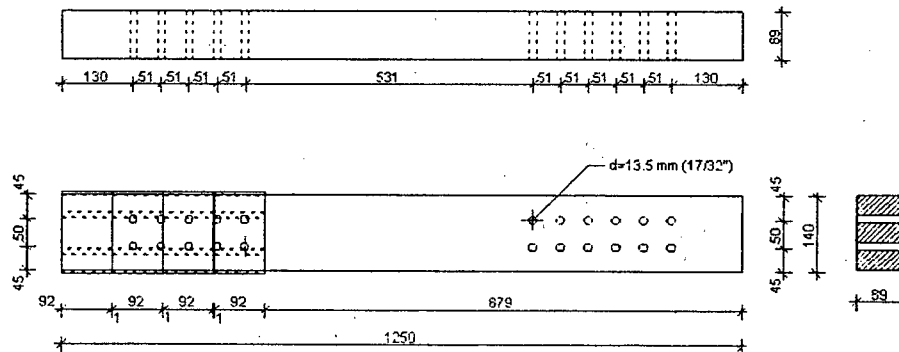
$L/d = 7.0$
 $e = 10d$
 $s = 4d$

Quantity	Fult	D@Fult	Cycle	80%Fult	D@80	Cycle	D@50
Specimen	[kN]	[mm]	Nr.	[kN]	[mm]	Nr.	[mm]
HRT1-C	263.99	4.71	13.00	211.19	6.96	22.00	2.24
HRT2-C	290.06	4.58	13.00	232.05	6.50	19.00	1.90
HRT3-C	280.72	6.09	19.00	224.58	10.42	34.00	2.90

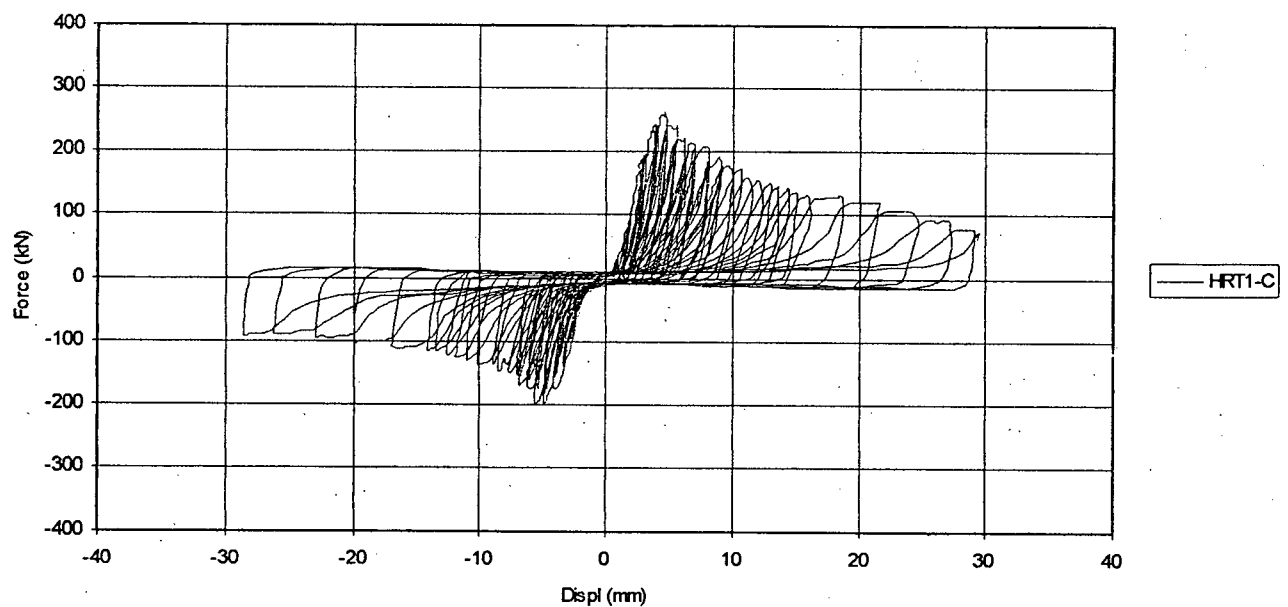
Specimen	Ductility	Elast.Stiff.	Ener.Diss.*	Step	Dens.greer	Dens.dry	Moist.cnt.
symbol	[]	[kN/mm]	[Nm]	[mm]	[kg/m3]	[kg/m3]	[%]
HRT1-C	3.10	99.22	1569.00	0.80	701.34	673.81	8.60
HRT2-C	3.42	89.87	2503.00	0.80	679.54	658.85	10.38
HRT3-C	3.59	84.85	2003.00	0.80	715.42	686.97	10.56

*Calculated after 100 mm of Cumulative Cyclic Displacement

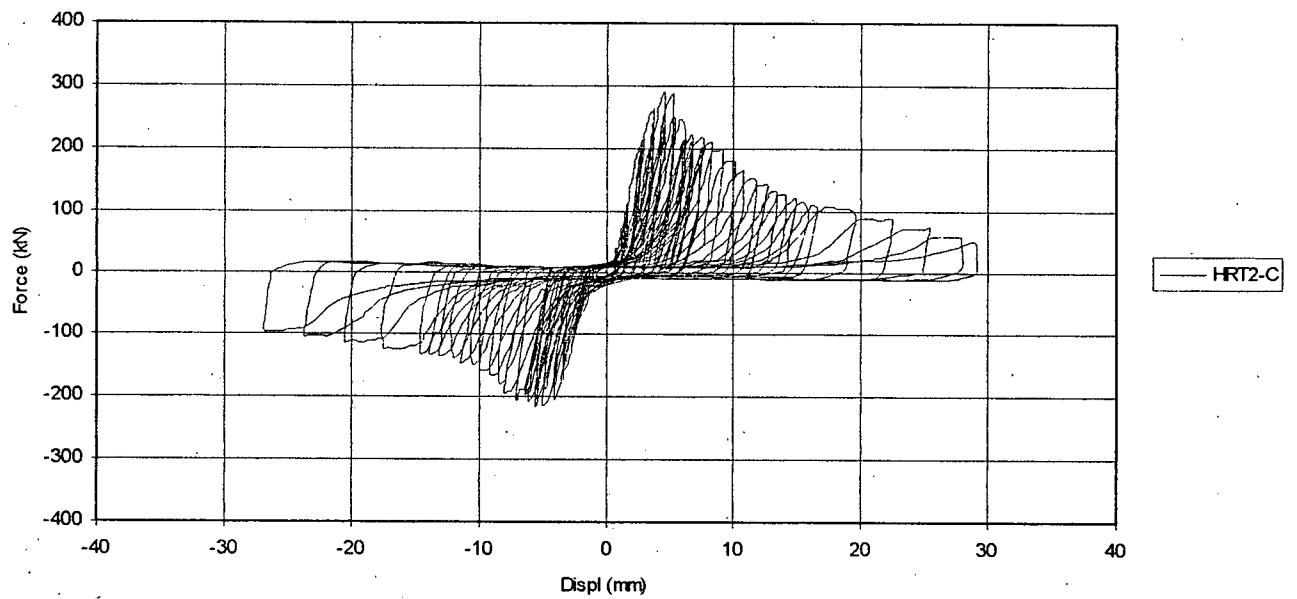
Failure mode: Row Shear, Row Splitting



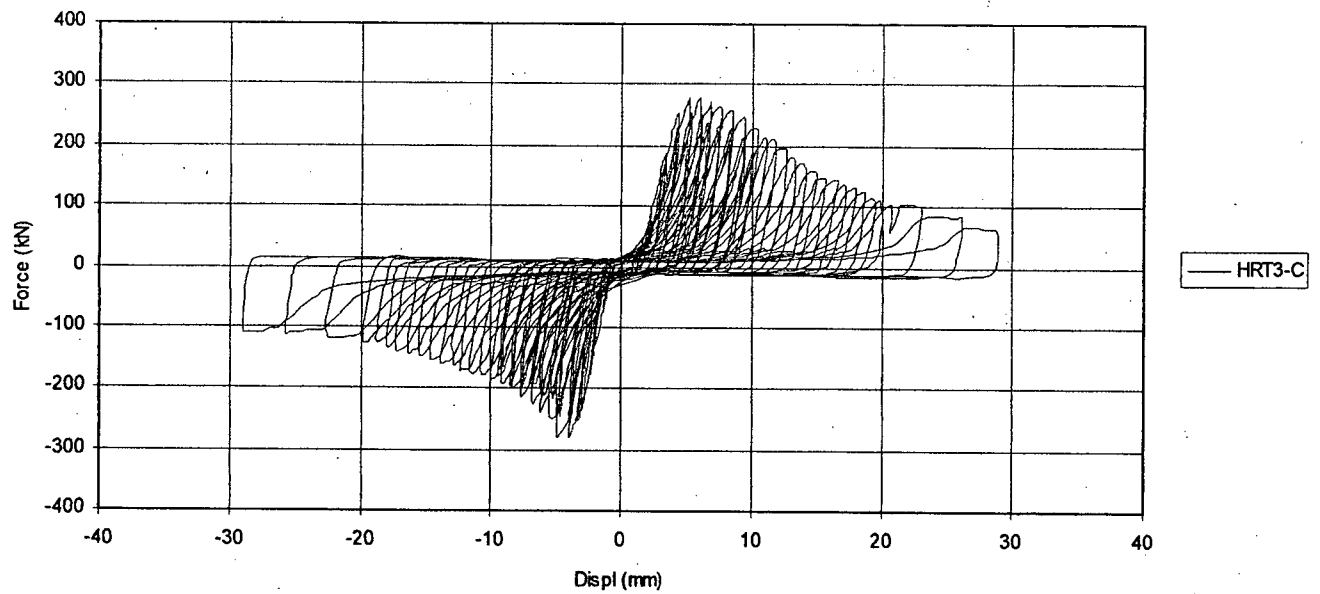
1/2"-10 BOLT PSL CONNECTION
TRUSS PLATE REINFORCED



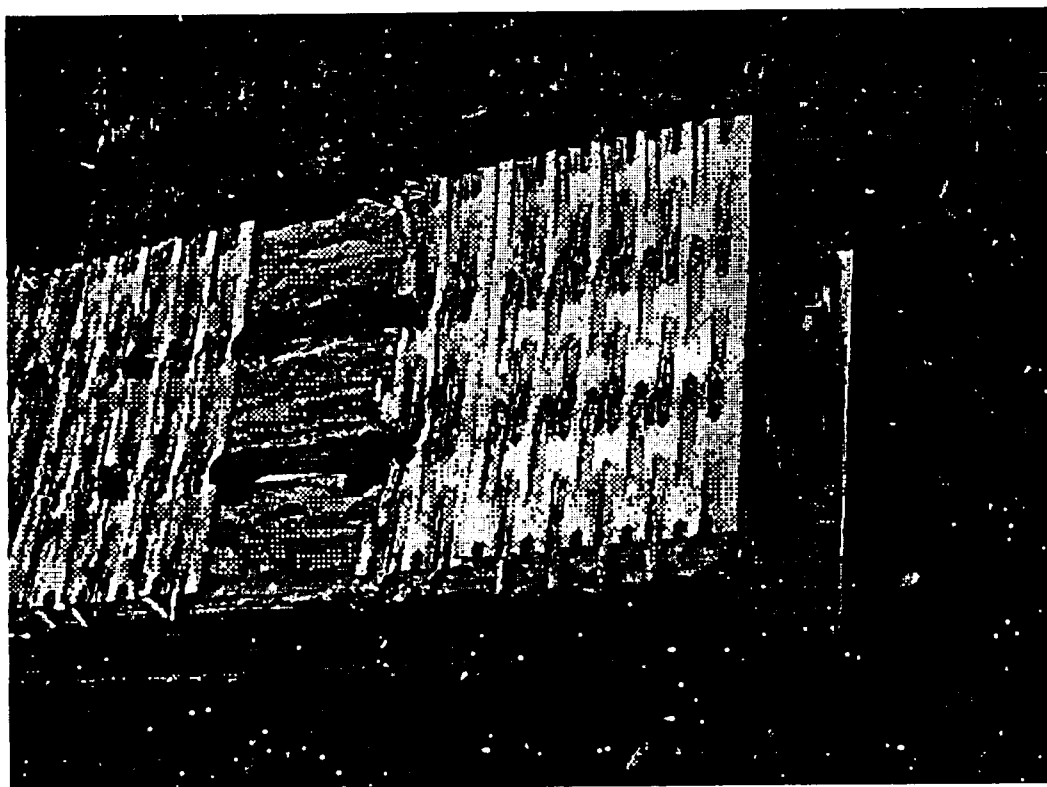
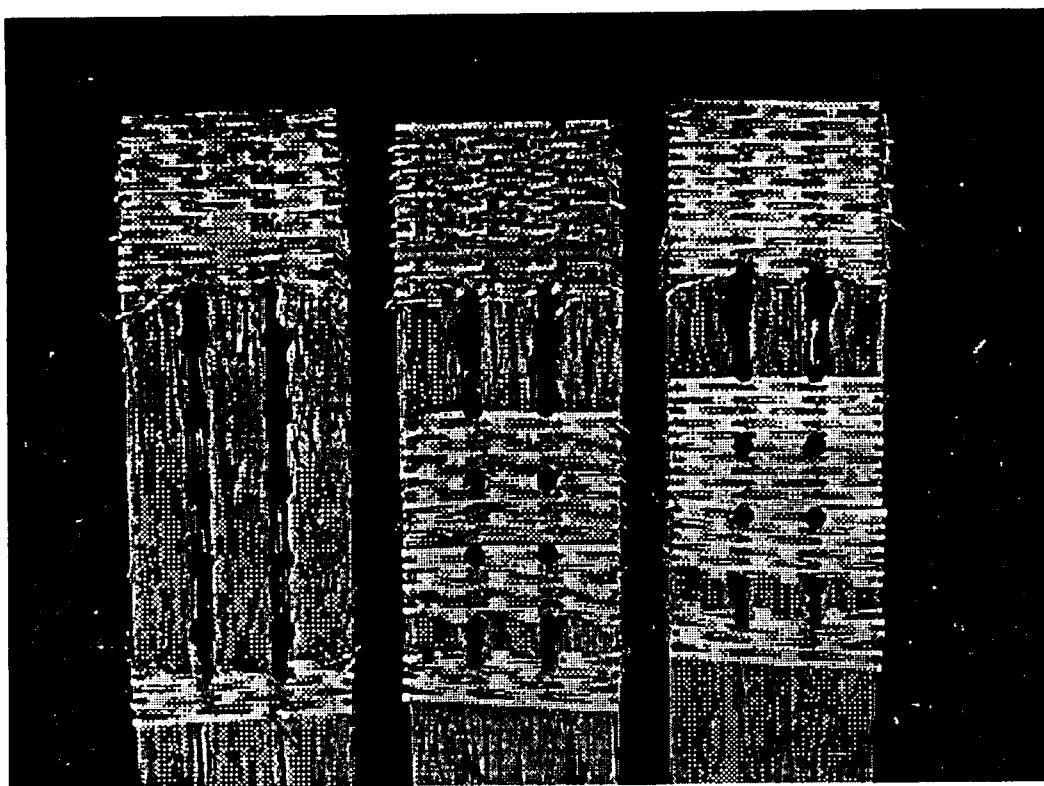
1/2"-10 BOLT PSL CONNECTION
TRUSS PLATE REINFORCED



1/2"-10 Bolt Connection in PSL
Truss Plate Reinforced



HRT-C



FRT-C
10-5/8" Bolt Connection in PSL
Truss Plate Reinforced

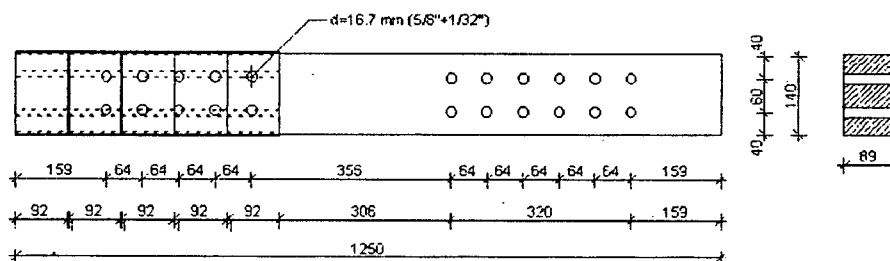
L/d = 5.6
e = 10d
s = 4d

Quantity	Fult	D@Fult	Cycle	80%Fult	D@80	Cycle	D@50
Specimen	[kN]	[mm]	Nr.	[kN]	[mm]	Nr.	[mm]
FRT-1-C	326.35	3.64	13.00	261.08	6.10	22.00	2.40
FRT-2-C	287.24	3.44	10.00	229.79	7.40	25.00	2.20
FRT-3-C	350.03	3.98	15.00	280.02	6.40	22.00	2.02

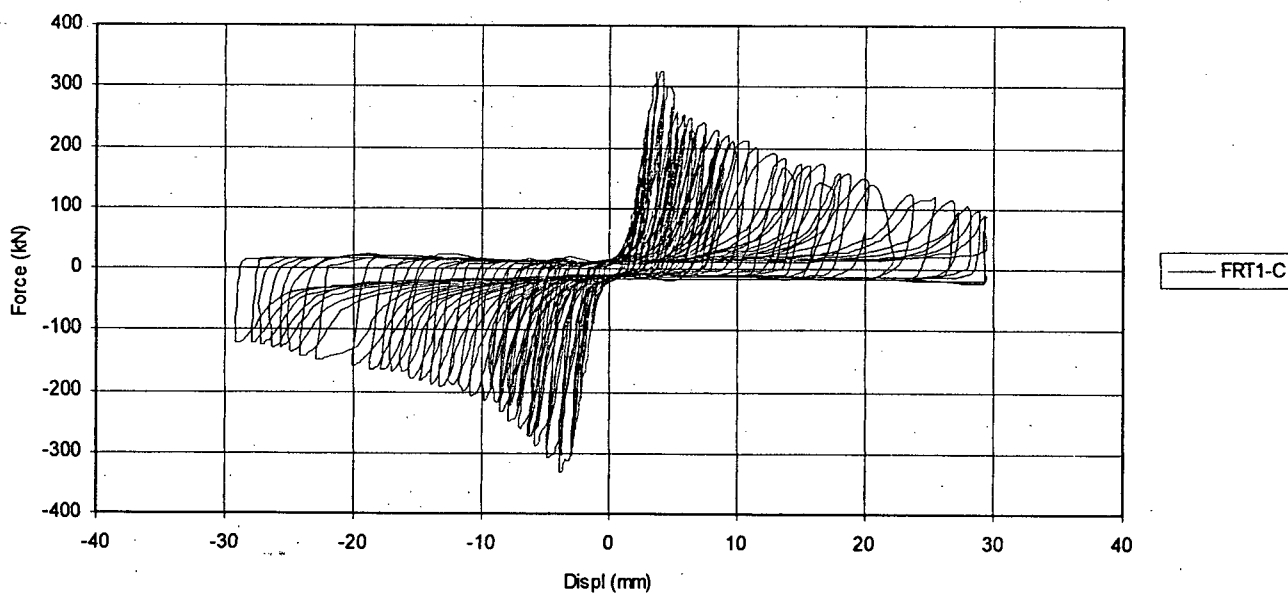
Specimen	Ductility	Elast.Stiff.	Ener.Diss.*	Step	Dens.green	Dens.dry	Moist.cnt.
symbol	[]	[kN/mm]	[Nm]	[mm]	[kg/m3]	[kg/m3]	[%]
FRT-1-C	2.54	141.46	2546.00	0.80	590.23	582.98	8.84
FRT-2-C	3.36	123.81	2079.00	0.80	658.29	628.83	9.48
FRT-3-C	3.17	131.88	2737.00	0.80	695.75	675.59	8.45

*Calculated after 100 mm of Cumulative Cyclic Displacement

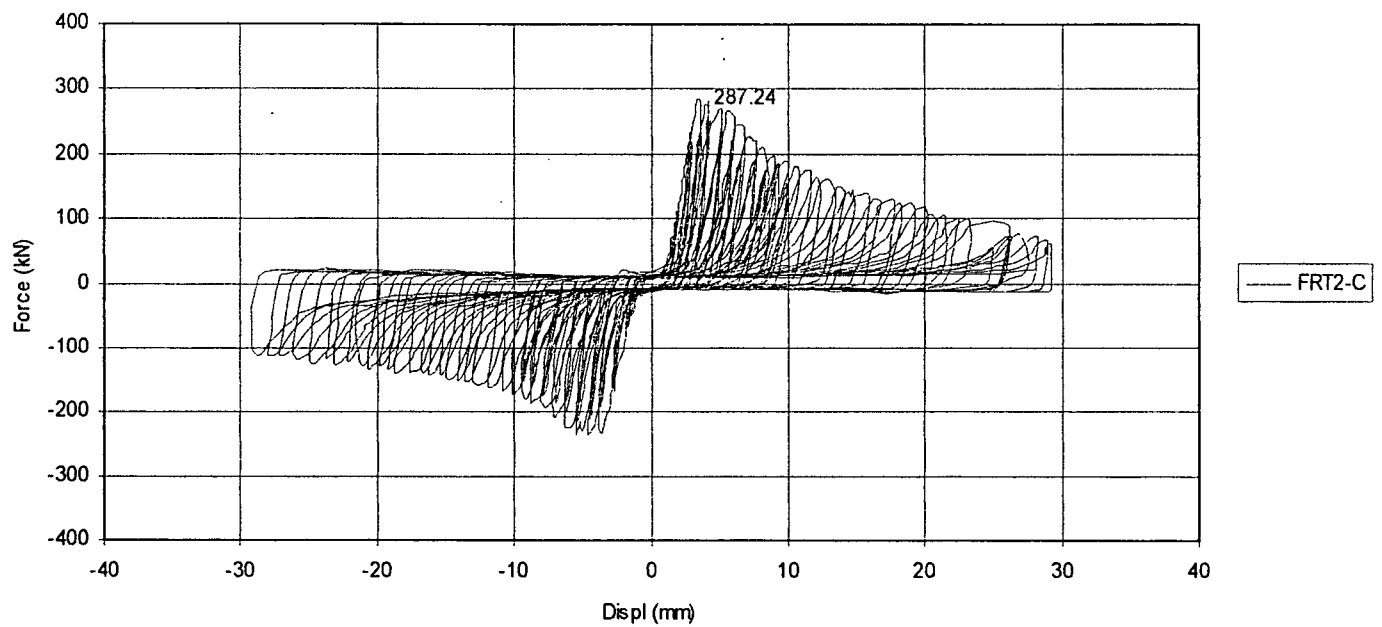
Failure mode: Row Shear, Row Splitting



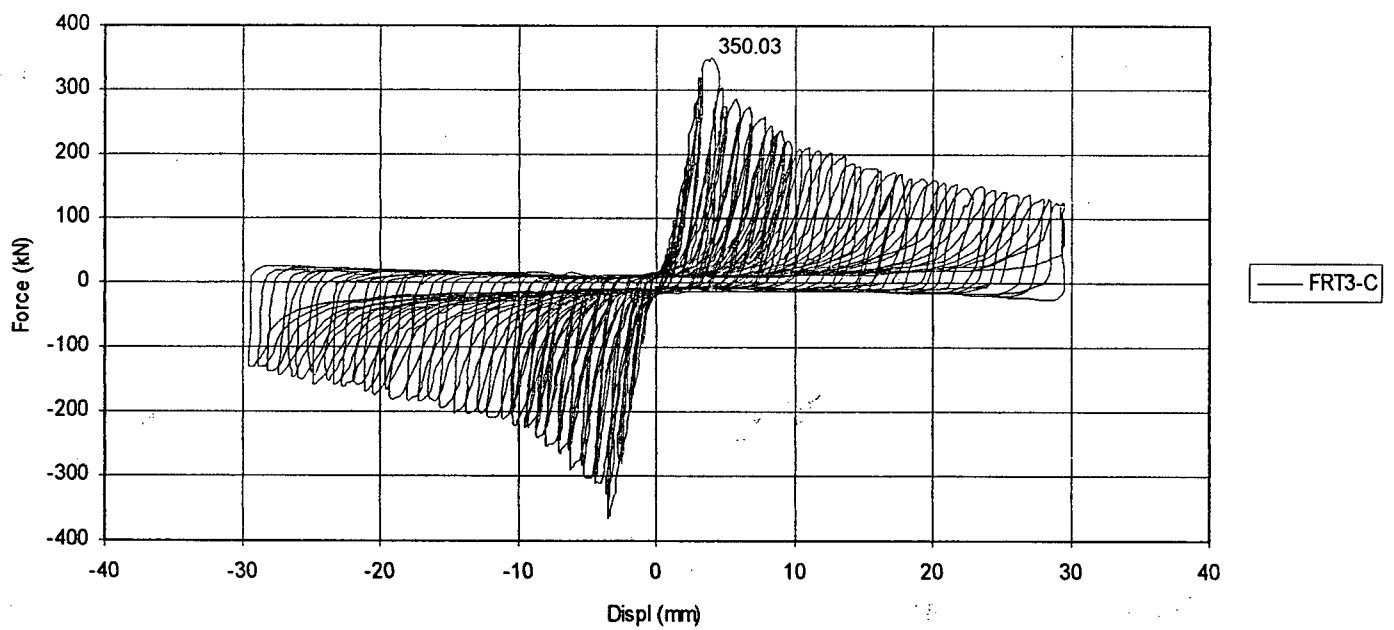
5/8"-10 BOLT PSL CONNECTION
TRUSS PLATE REINFORCED



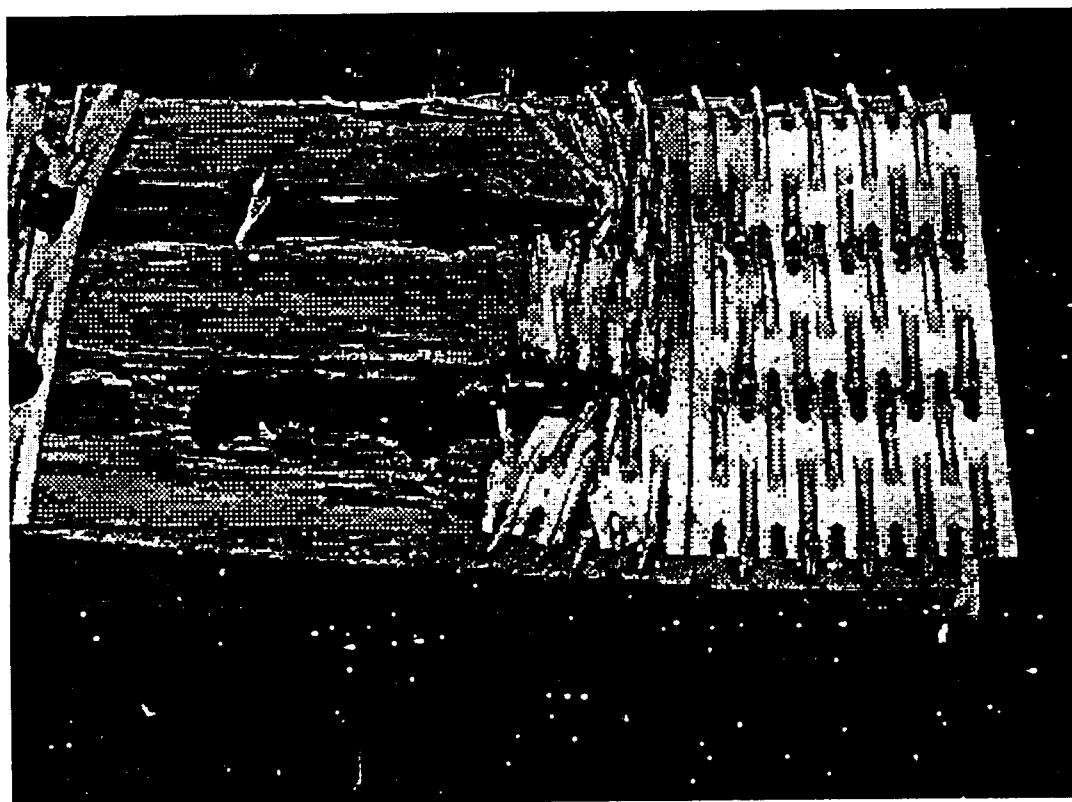
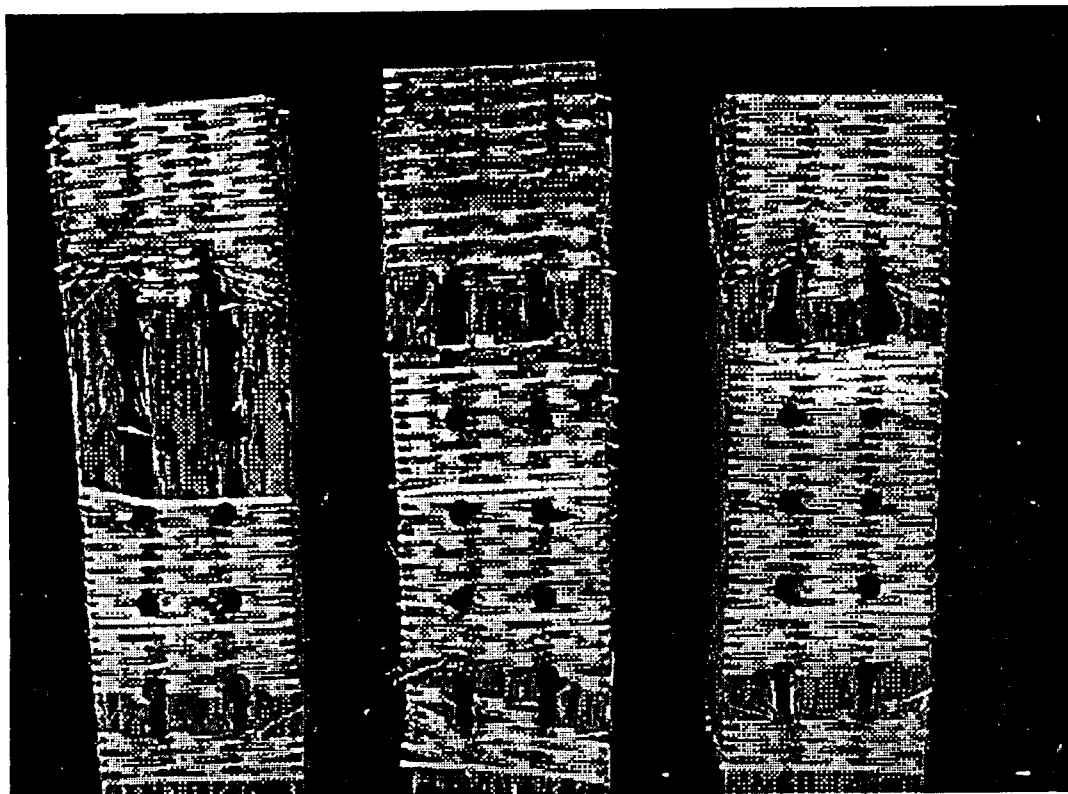
5/8"-10 BOLT PSL CONNECTION
TRUSS PLATE REINFORCED



5/8"-10 BOLT PSL CONNECTION
TRUSS PLATE REINFORCED



FRT-C

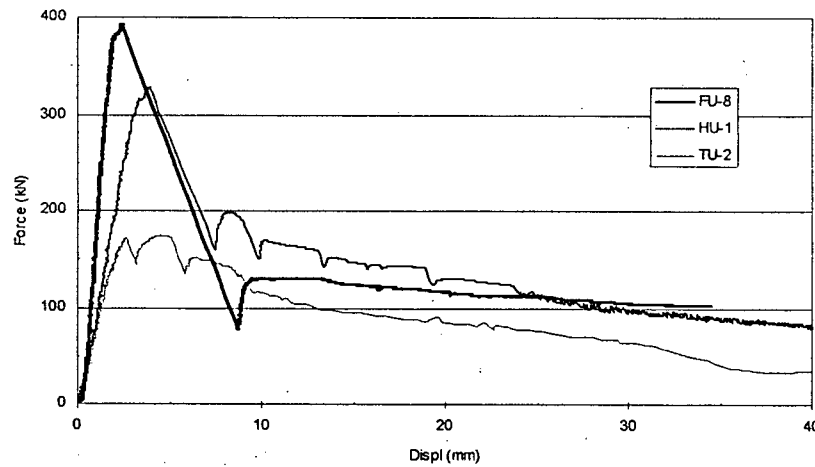


APPENDIX II

Static Test Comparisons in Size and Material

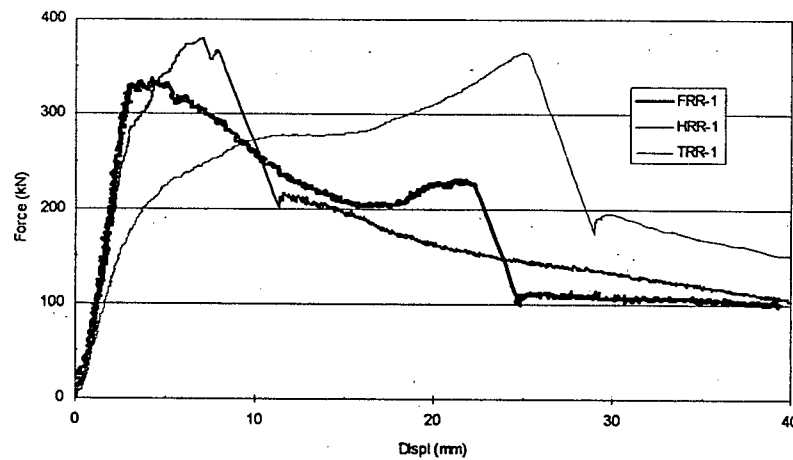
Influence of L/d Ratio
5/8", 1/2", 3/8" 10-Bolt Connection in PSL
Unreinforced, Lag Screw Reinforced

Unreinforced



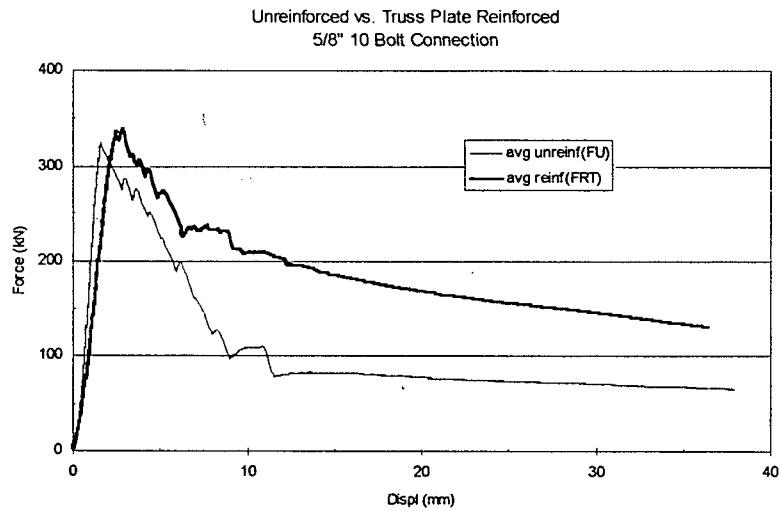
Quantity	Fult	D@Fult	El.stiffness	Ductility	Energy dis
Specimen	[kN]	[mm]	[kN/mm]	[]	[Nm]
FU-8	391.81	2.39	267.54	3.7	5514.48
HU-1	328.08	3.96	110.36	3.06	5566
TU-2	174.69	4.48	89.08	4.96	3600.64

Lag Screw Reinforced

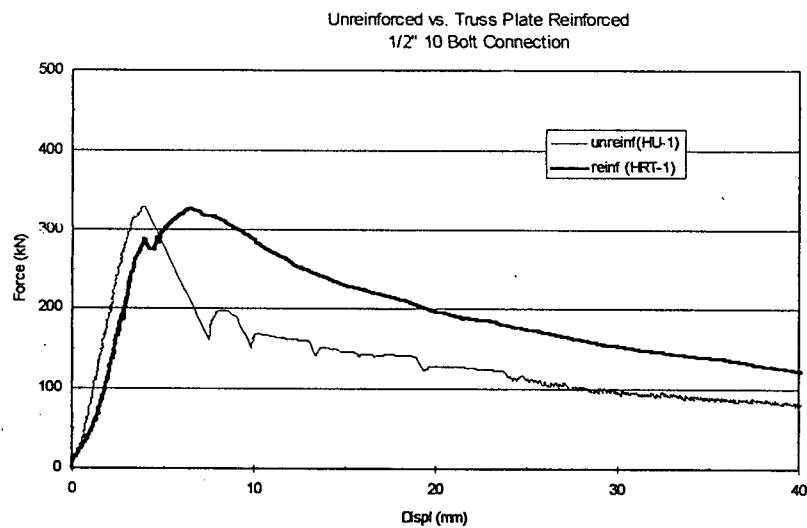


Quantity	Fult	D@Fult	El.stiffness	Ductility	Energy dis
Specimen	[kN]	[mm]	[kN/mm]	[]	[Nm]
FRR-1	336.22	4.31	160.57	5.28	7300.94
HRR-1	380.01	7.1	130.36	1.9	73333.04
TRR-1	365.02	24.97	72.37	8.31	9447.35

Influence of Reinforcement
5/8", 1/2" 10-Bolt Connection in PSL
Unreinforced, Truss Plate Reinforced

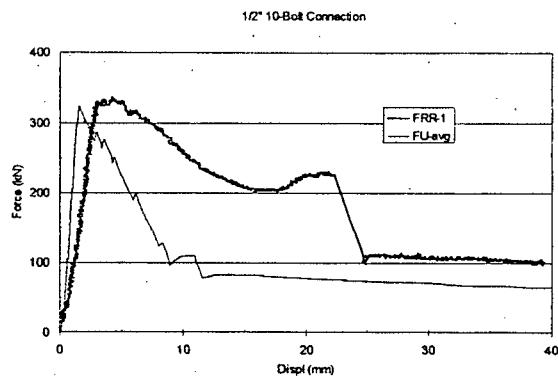


Quantity	Fult	D@Fult	El.stiffness	Ductility	Energy dis
Specimen	[kN]	[mm]	[kN/mm]	[]	[Nm]
FU-avg	372.5	1.92	275.29	3.8	4173.15
FRT-avg	364.93	2.87	179.15	4	7129.89

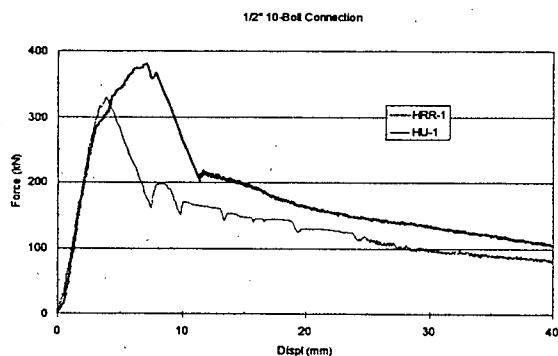


Quantity	Fult	D@Fult	El.stiffness	Ductility	Energy dis
Specimen	[kN]	[mm]	[kN/mm]	[]	[Nm]
HU-1	328.08	3.96	110.36	3.06	5566
HRT-1	325.48	6.52	104.94	8.94	7863.95

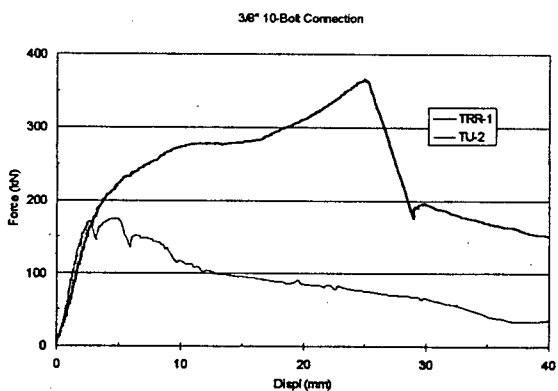
Influence of Reinforcement
5/8", 1/2", 3/8" 10-Bolt Connection in PSL
Unreinforced, Lag Screw Reinforced



Quantity	F _{ult}	D@F _{ult}	E _i stiffness	Ductility	Energy diss
Specimen	[kN]	[mm]	[kN/mm]	[]	[Nm]
FU-avg	372.5	1.92	275.29	3.8	4173.15
FRR-1	336.22	4.31	160.57	5.28	7300.94



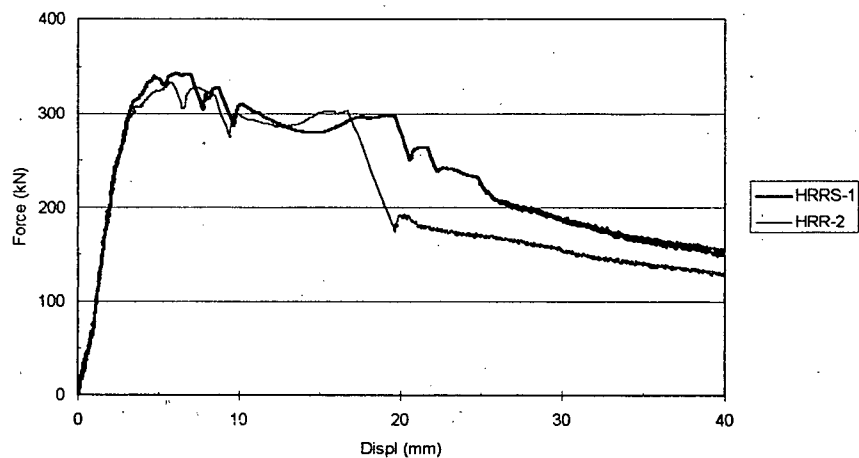
Quantity	F _{ult}	D@F _{ult}	E _i stiffness	Ductility	Energy diss
Specimen	[kN]	[mm]	[kN/mm]	[]	[Nm]
HU-1	328.08	3.96	110.36	3.06	5566
HRR-1	360.01	7.1	130.36	1.9	7333.04



Quantity	F _{ult}	D@F _{ult}	E _i stiffness	Ductility	Energy diss
Specimen	[kN]	[mm]	[kN/mm]	[]	[Nm]
TU-2	174.69	4.48	89.08	4.96	3523.98
TRR-1	365.02	24.97	72.37	8.31	9491.67

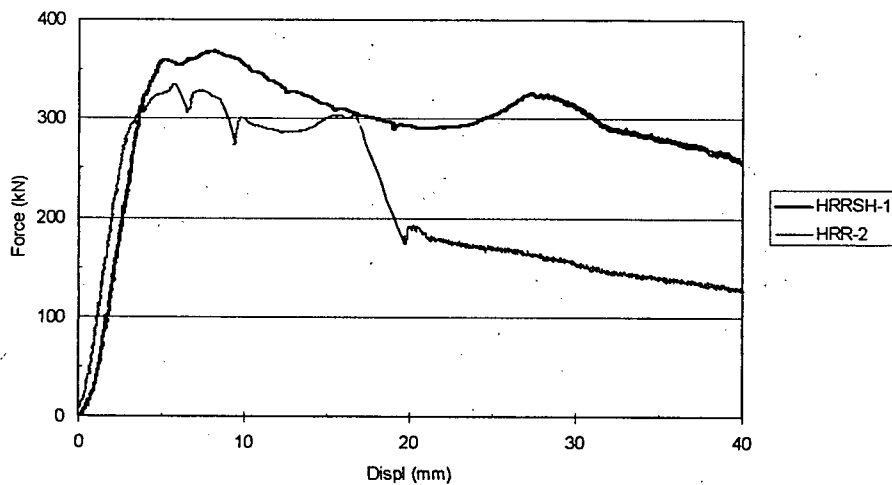
Influence of Rod Configuration
 1/2" 10-Bolt Connection in PSL- Lag Screw Reinforced
 Rods Shifted away from the Bolts, Two End Rods (HRRSH),
 Rods with Centr. Position among the bolts, End Rod Single (HRRS)

Single Rod vs. Two Rods at the End



Quantity	Fult	D@Fult	El.stiffness	Ductility	Energy dis
Specimen	[kN]	[mm]	[kN/mm]	[]	[Nm]
HRR-2	333.95	5.77	119.5	10.53	8467.43
HRRS-1	343.08	6.24	9525.15	10.1	9525.15

Rods Offset from the Central Position

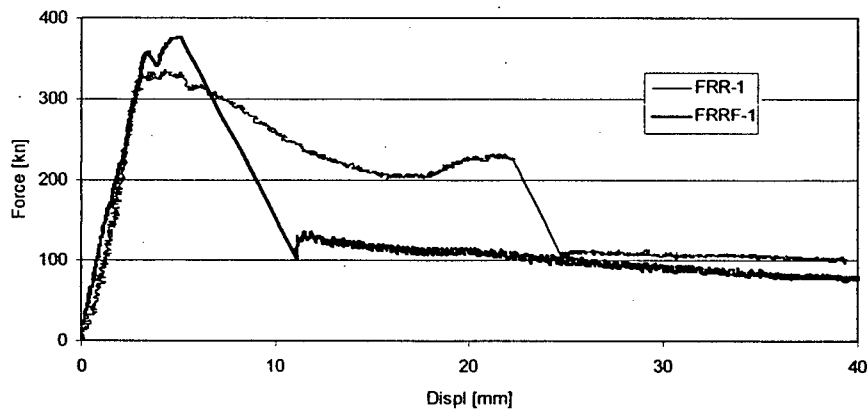


Quantity	Fult	D@Fult	El.stiffness	Ductility	Energy dis
Specimen	[kN]	[mm]	[kN/mm]	[]	[Nm]
HRR-2	333.95	5.77	119.5	10.53	8467.43
HRRSH-1	368.5	8.16	123.35	12.58	11781.4

Thread Size Comparisons

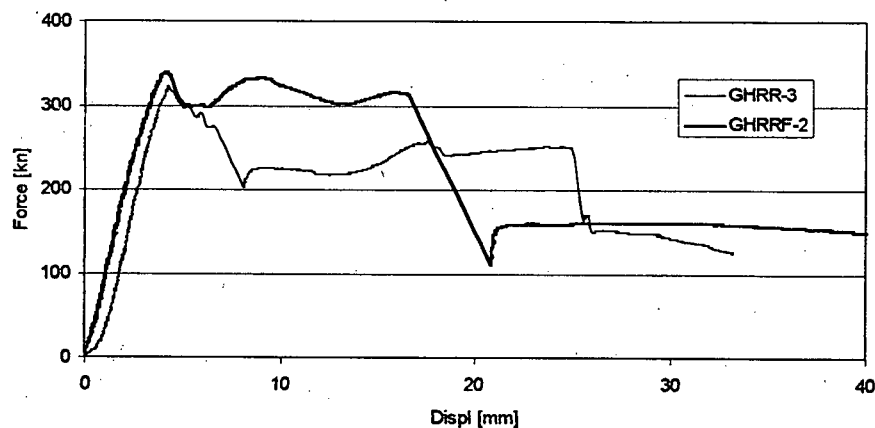
5/8" 10-Bolt Joint in PSL -Lag Screw (FRR) vs. Ready Rod (FRRF)
 1/2" 10-Bolt Joint in Glulam -Lag Screw (GHRR) vs. Ready Rod (GHRRF)

1/2" 10-Bolt PSL Connection



Quantity	Fult	D@Fult	El.stiffness	Ductility	Energy dis
Specimen	[kN]	[mm]	[kN/mm]	[]	[Nm]
FRR-1	336.22	4.31	160.57	5.28	7300.94
FRRF-1	376.97	5.12	98.5	4.23	5569.01

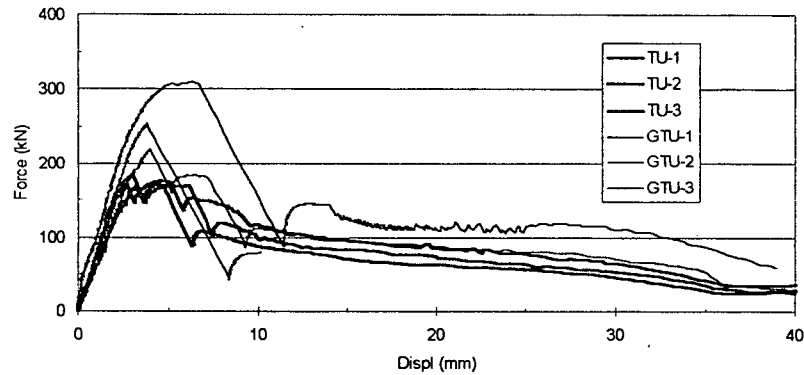
1/2" 10-Bolt Glulam Connection



Quantity	Fult	D@Fult	El.stiffness	Ductility	Energy dis
Specimen	[kN]	[mm]	[kN/mm]	[]	[Nm]
GHRR-3	322.44	4.25	108.39	2.92	7630.08
GHRRF-2	338.30	4.20	108.36	11.00	5500.00

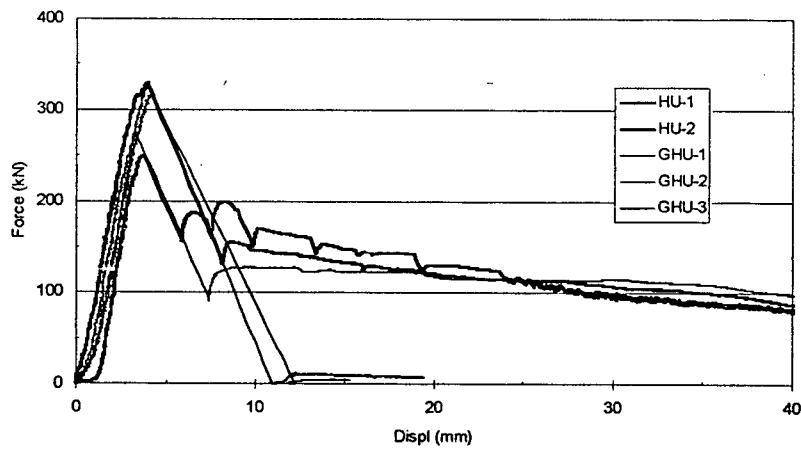
PSL (Parallam®) vs Glulam
 3/8" 10-Bolt Unreinforced Joint - TU vs GTU
 1/2" 10-Bolt Unreinforced Joint - HU vs GHU

3/8" 10-Bolt Unreinforced Connection



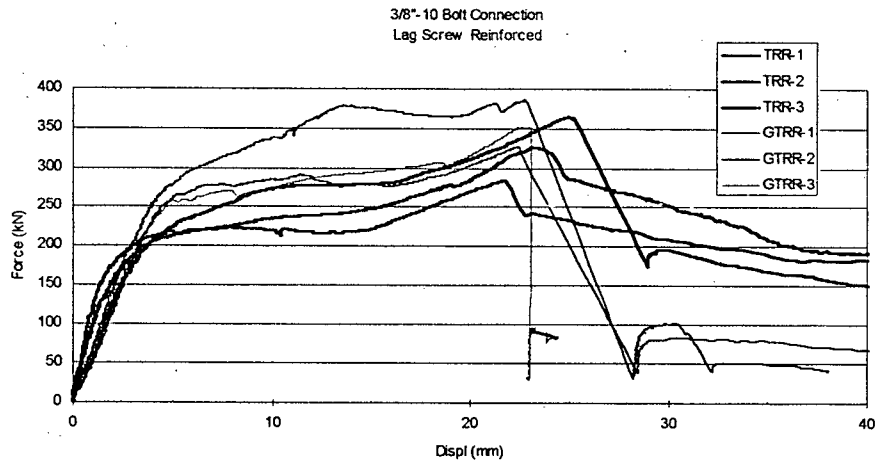
Quantity	Fult	D@Fult	El.stiffness	Ductility	Energy dis
Specimen	[kN]	[mm]	[kN/mm]	[]	[Nm]
TU-Avg	175.34	4.21	79.77	4.85	3113.22
GTU-Avg	260.80	4.67	78.53	4.13	3458.54

1/2" 10-Bolt Unreinforced Connection

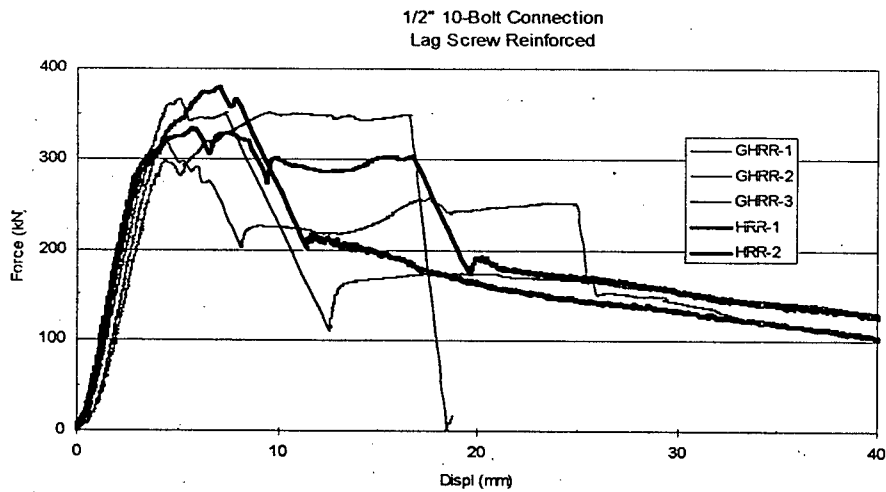


Quantity	Fult	D@Fult	El.stiffness	Ductility	Energy dis
Specimen	[kN]	[mm]	[kN/mm]	[]	[Nm]
HU-Avg	288.32	3.87	119.35	2.62	5245.95
GHU-Avg	306.57	3.80	115.03	2.34	2841.32

PSL (Parallam®) vs Glulam
 3/8" 10-Bolt Lag Screw Reinforced Joint -TRR vs GTRR
 1/2" 10-Bolt Lag Screw Reinforced Joint - HRR vs GHRR



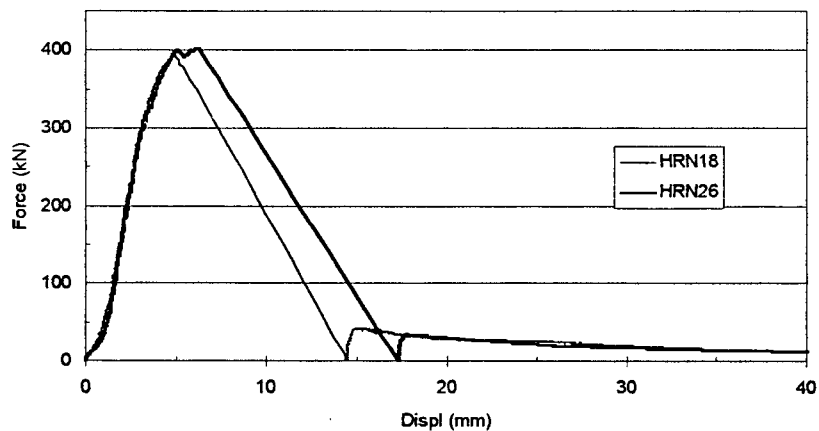
Quantity	Fult	D@Fult	El.stiffness	Ductility	Energy dis
Specimen	[kN]	[mm]	[kN/mm]	[]	[Nm]
TRR-Avg	325.26	23.37	87.35	15.18	9186.34
GTRR-Avg	354.26	22.83	74.60	8.75	7531.71



Quantity	Fult	D@Fult	El.stiffness	Ductility	Energy dis
Specimen	[kN]	[mm]	[kN/mm]	[]	[Nm]
HRR-Avg	356.98	6.44	124.93	6.22	7900.24
GHRR-Avg	346.34	6.33	100.59	4.69	6659.66

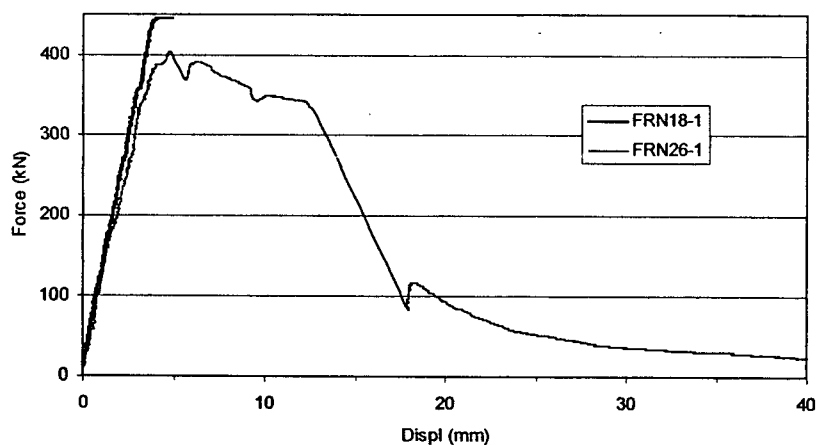
Thickness of the Nailed Plate
 $\frac{1}{2}$ ", $\frac{5}{8}$ " 10-Bolt Joint in PSL - Nailed Plate Reinforced
 Galvanized Plate Gauge 18 (1.2 mm) vs Gauge 26 (0.6mm)

1/2" 10-Bolt PSL Connection
 Nailed Plate Reinforced



Quantity	Fult	D@Fult	El.stiffness	Ductility	Energy dis
Specimen	[kN]	[mm]	[kN/mm]	[]	[Nm]
HRN18	392.80	5.00	134.92	3.02	3529.22
HRN26	398.92	6.39	131.28	3.74	4195.35

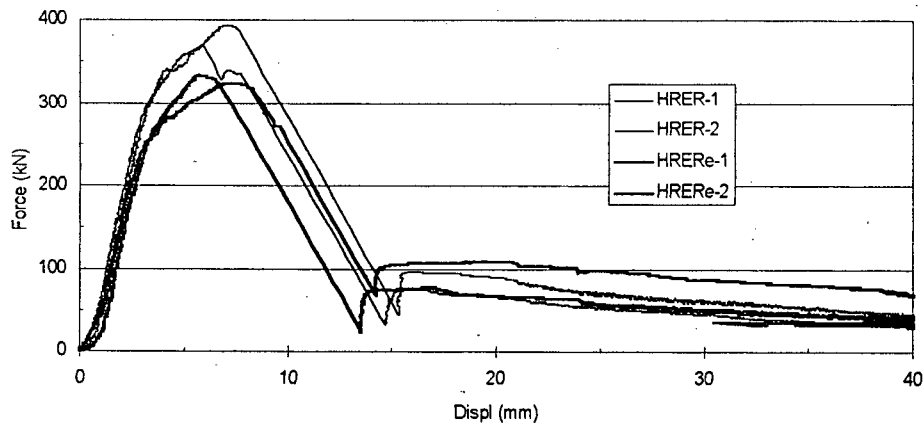
5/8" 10-Bolt PSL Connection
 Nailed plate Reinforced



Quantity	Fult	D@Fult	El.stiffness	Ductility	Energy dis
Specimen	[kN]	[mm]	[kN/mm]	[]	[Nm]
FRN18	>445	N/A	N/A	N/A	N/A
FRN26	400.22	4.875	95.07	6.77	6176.65

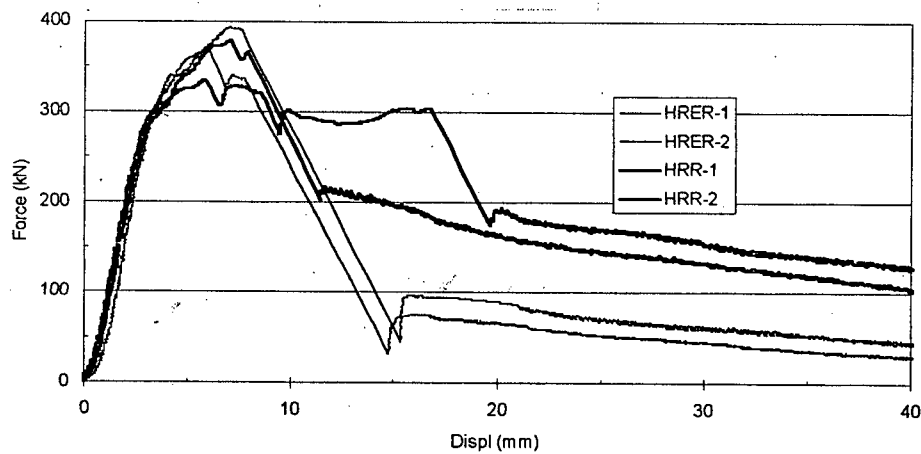
Glued-in Rod Influence
 1/2" 10-Bolt Joint in PSL – Glued-in Rods
 Glued-in Lag Screws vs Glued-in Rebars
 Lag Screws vs Glued-in Lag Screws

1/2" 10-Bolt PSL Connection
 Glued-in Lag Screws vs Glued-in Rebars Reinforced



Quantity	Fult	D@Fult	El.stiffness	Ductility	Energy dis
Specimen	[kN]	[mm]	[kN/mm]	[]	[Nm]
HRER-Avg	380.88	10.01	96.92	4.07	6372.48
HRERe-Avg	328.74	6.31	105.45	4.23	4756.98

1/2" 10-Bolt PSL Connection
 Lag Screws vs. Glued-in Lag Screws Reinforced



Quantity	Fult	D@Fult	El.stiffness	Ductility	Energy dis
Specimen	[kN]	[mm]	[kN/mm]	[]	[Nm]
HRER-Avg	380.88	10.01	96.92	4.07	6372.48
HRR-Avg	356.98	6.435	124.93	6.20	7900.24

APPENDIX III

- (a) Static Tension Tests - Numerical Data Summary
- (b) Reverse Cyclic Tests - Numerical Data Summary
- (c) Statistical Data from Single-Connector Bending Tests
- (d) Bolts Bending Deflection Values Measured after the Failure of the Connections Tested in Static Tension
- (e) Density and Moisture Content Summary

Total Test Results for 5/8" 10-Bolt Connections Tested in Static Tension

Quantity	Fult	D@Fult	80%Fult	D@80	D@50	Ductility	Avg El.Stiff	Avg En Dis
Specimen	[kN]	[mm]	[kN]	[mm]	[mm]		[kN/mm]	[Nm]
FU1	339.21	1.71	271.37	3.13	0.85	3.7	275.29	4170.78
FU2	352.36	1.92	281.89	3.33	0.98	3.4		
FU3	383.88	1.95	307.1	3.56	0.9	4		
FU4	381.39	1.8	305.11	3.39	0.95	3.6		
FU5	327.64	1.89	262.11	3.53	0.85	4.2		
FU6	388.87	1.9	311.1	3.57	1.06	3.4		
FU7	390.68	2.11	312.54	4.2	0.96	4.4		
FU8	391.81	2.39	313.45	3.96	1.08	3.7		
FU9	360.07	1.84	288.06	3.63	0.95	3.8		
FU10	409.04	1.65	327.23	3.39	0.78	4.3		
FRT1	337.4	3.6	269.92	11.34	1.31	8.7	179.15	7165.1
FRT2	361.88	2.18	289.5	3.88	1.2	3.2		
FRT3	346.69	2.37	277.35	3.7	1.32	2.8		
FRT4	325.6	3.24	260.48	5.85	1.39	4.2		
FRT5	347.82	2.38	278.25	3.84	1.25	3.1		
FRT6	447.59	3.01	358.07	4.76	1.6	3		
FRT7	Data Saturation							
FRT8	394.31	2.76	315.44	4.99	1.41	3.5	179.15	7165.1
FRT9	374.58	2.33	299.66	3.57	1.2	3		
FRT10	348.5	3.98	278.8	6.43	1.32	4.9		

Tests Conducted Earlier (B.Hockey, thesis, 1999)

Quantity Specimen	Fult [kN]	D@Fult [mm]	80%Fult [kN]	D@80 [mm]	D@50 [mm]	Ductility	Stiffness [kN/mm]	Energy [Nm]
FRTT1	374.36	3.98	299.48	5.91	1.71	3.45	101.82	2510.05
FRTT2	366.54	4.36	293.23	6.2	1.54	3.9	84.55	2472.5
FRR1	336.22	4.31	268.98	9.46	1.79	5.28	160.57	7300.94
FRR2	356.42	3.41	285.14	8.7	1.8	4.83	151.43	5887.54
FRRF1	376.97	5.12	301.58	6.76	1.6	4.23	98.5	5569.01
FRRF2	369.37	4.63	295.50	11.3	2.15	5.26	86.74	6914.85
FRRS1	418.47	5	334.78	7.89	1.84	4.29	111.5	4231.22
FRRS2	360.02	4.09	288.02	7.99	1.9	4.21	128.31	9330.75
FRE1(6bolt)	358.48	4.15	286.78	6.54	2.07	3.16	131.52	1416.03
FRE2(6bolt)	373.67	3.92	298.94	5.38	1.96	2.74	127.87	2009.8
FRNtype1	409.27	4.31	327.42	6.74	1.52	4.43	154.65	5454.49
FRNtype2	368.23	1.98	294.58	3.48	1.05	3.31	270.33	6645
FRN18	>445	N/A	N/A	N/A	N/A	N/A	N/A	N/A
FRN26	400.22	4.875	320.18	13	1.92	6.77	95.07	6176.65

Total Test Results for 1/2" 10-Bolt Connections Tested in Static Tension

Quantity Specimen	Fult [kN]	D@Fult [mm]	80%Fult [kN]	D@80 [mm]	D@50 [mm]	Ductility	Stiffness [kN/mm]	Energy [Nm]
HU1	328.08	3.96	262.46	5.33	1.74	3.06	110.36	5566
HU2	248.56	3.77	198.85	4.9	2.25	2.18	128.34	4925.9
HRT1	325.48	6.52	260.38	11.9	2.41	4.94	104.94	7863.95
HRT2	307.88	5.34	246.3	13.13	2.45	5.36	89.16	7936.32
HRTW	254.21	4.505	203.37	7.76	2.35	3.3	62.02	4930.5
HRR1	380.01	7.1	304.01	3.9	2.05	1.9	130.36	7333.04
HRR2	333.95	5.77	267.16	17.58	1.67	10.53	119.5	8467.43
HRRS1	343.08	6.24	274.46	16.87	1.67	10.1	134.5	9525.15
HRRS2	338.51	15.33	270.81	20.18	1.35	14.95	121.99	7969.92
HRRSH1	368.5	8.16	294.8	31.7	2.52	12.58	123.35	11781.4
HRRSH2	357.6	8.5	286.08	10.4	2.06	5.05	96.99	8199.41
HRN18	392.80	5.00	314.24	7.00	2.32	3.02	134.92	3529.22
HRN26	398.92	6.39	319.14	8.60	2.30	3.74	131.28	4195.35
HRER-1	393.05	14.08	314.44	18.50	4.28	4.32	58.33	8271.60
HRER-2	368.71	5.93	294.97	8.60	2.25	3.82	135.51	4473.36
HRERe-1	324.61	6.69	259.69	9.80	2.00	4.90	105.38	5443.99
HRERe-2	332.86	5.93	266.29	8.00	2.25	3.56	105.51	4069.97
GHU-1	330.04	3.98	264.03	4.40	2.31	1.90	111.59	1724.09
GHU-2	274.63	3.30	219.70	4.46	1.80	2.48	116.82	4928.11
GHU-3	315.05	4.11	252.04	5.80	2.20	2.64	116.68	1871.75
GHRR-1	350.25	9.67	280.20	17.00	2.10	8.10	95.23	5040.38
GHRR-2	366.32	5.06	293.06	8.60	2.80	3.07	98.15	7308.52
GHRR-3	322.44	4.25	257.95	7.00	2.40	2.92	108.39	7630.08
GHRRF-1	346.68	6.96	277.34	8.90	2.10	4.24	96.92	5233.51
GHRRF-2	338.30	4.20	270.64	17.60	1.60	11.00	108.36	8606.69
GHRRF-3	327.65	9.42	262.12	12.50	4.00	3.13	63.60	5500.00

Total Test Results for 3/8" 10-Bolt Connections Tested in Static Tension

Quantity Specimen	Fult [kN]	D@Fult [mm]	80%Fult [kN]	D@80 [mm]	D@50 [mm]	Ductility	Stiffness [kN/mm]	Energy [Nm]
TU-1	168.82	5.14	135.06	6.85	1.35	5.07	58.97	3070.92
TU-2	174.69	4.48	139.75	5.70	1.15	4.96	89.08	3523.98
TU-3	182.51	3.01	146.01	5.20	1.15	4.52	91.25	2744.76
TRR-1	365.02	24.97	292.02	26.60	3.20	8.31	72.37	9491.67
TRR-2	284.41	21.72	227.53	26.50	1.10	24.09	106.13	3636.06
TRR-3	326.35	23.42	261.08	28.90	2.20	13.14	83.54	9431.28
GTU-1	254.20	3.80	203.36	5.00	1.60	3.13	83.13	1243.40
GTU-2	218.80	4.00	175.04	7.15	1.70	4.21	64.40	3684.79
GTU-3	309.40	6.20	247.52	8.10	1.60	5.06	88.05	5447.43
GTRR-1	384.14	22.88	307.31	24.10	2.70	8.93	88.05	8850.07
GTRR-2	326.13	22.50	260.90	23.70	2.70	8.77	64.92	7663.35
GTRR-3	352.50	23.10	282.00	23.10	2.70	8.55	70.82	6081.70

Total Test Results for All 10-Bolt Connections - Reverse Cyclic Tests

Quantity Specimen	Fult [kN]	D@Fult [mm]	Cyc Nr.	80%Fult [kN]	D@80 [mm]	Cyc Nr.	D@50 [mm]	Ductility []	Elast.Stiff. [kN/mm]	En.Dis.* [Nm]	Step [mm]
FU1-C	290.50	2.82	23	232.40	4.20	31	1.62	2.59	171.43	398	0.40
FU2-C	244.43	2.87	21	195.54	4.12	29	1.62	2.54	138.67	288	0.40
FU3-C	282.24	3.09	23	225.79	4.60	25	1.58	2.91	160.00	762	0.40
FRR1-C	298.75	4.07	17	239.00	5.35	23	1.70	3.15	160.71	1080	0.80
FRR2-C	336.99	2.55	11	269.59	6.20	21	1.24	5.00	168.00	1375	0.80
FRR3-C	292.45	5.07	16	233.96	11.50	37	1.80	6.39	97.78	1340	0.80
FRT1-C	326.35	3.64	13	261.08	6.10	22	2.40	2.54	141.46	2546	0.80
FRT2-C	287.24	3.44	10	229.79	7.40	25	2.20	3.36	123.81	2079	0.80
FRT3-C	350.03	3.98	15	280.02	6.40	22	2.02	3.17	131.88	2737	0.80
HU1-C	298.97	4.12	7	239.18	5.40	7	1.77	3.05	108.84	2420	0.80
HU2-C	282.02	3.44	10	225.62	4.10	13	1.70	2.41	130.96	2044	0.80
HU3-C	297.67	3.70	10	238.14	5.20	10	1.70	3.06	113.32	2110	0.80
HRR1-C	295.28	7.82	28	236.22	21.28	73	2.20	9.67	118.41	1743	0.80
HRR2-C	262.25	5.50	19	209.80	18.60	67	1.98	9.39	134.28	1833	0.80
HRR3-C	290.06	7.09	25	232.05	12.20	46	2.10	5.81	130.00	1886	0.80
HRT1-C	263.99	4.71	13	211.19	6.96	22	2.24	3.10	99.22	1569	0.80
HRT2-C	290.06	4.58	13	232.05	6.50	19	1.90	3.42	89.87	2503	0.80
HRT3-C	280.72	6.09	19	224.58	10.42	34	2.90	3.59	84.85	2003	0.80
TU-C	164.04	5.12	13	131.23	7.50	19	1.38	5.43	69.26	1580	0.80
TRR-C	262.90	16.60	13	210.32	20.45	16	2.36	8.67	52.23	4784	4.00
GTRR-C	267.70	7.90	7	214.16	17.68	19	2.05	8.62	64.46	3579	2.50

*Calculated after 100 mm of Cumulative Cyclic Displacement

Bolt Grade 5 - 3/8" Diameter

Quantity	LOAD	LOAD	LOAD	LOAD	LOAD	Mean	St.Dev	COV
Displ	Bolt Nr. 1	2	3	4	5	$m = \sum(x_i)/n$	$\sum(x_i - m)^2/n$	s/m
0	0	0	0	0	0	0		
0.5	2.2	2.17	1.82	1.74	2.25	2.036		
$(x_i - m)^2$	0.026896	0.017956	0.046656	0.087616	0.045796		0.21	0.10
1	4.2	4.6	4	4	4.4	4.24		
$(x_i - m)^2$	0.0016	0.1296	0.0576	0.0576	0.0256		0.23	0.06
1.2	4.9	5.1	4.9	4.8	5	4.94		
$(x_i - m)^2$	0.0016	0.0256	0.0016	0.0196	0.0036		0.10	0.02
1.4	5.3	5.5	5.3	5.3	5.5	5.38		
$(x_i - m)^2$	0.0064	0.0144	0.0064	0.0064	0.0144		0.10	0.02
1.6	5.5	5.7	5.4	5.5	5.6	5.54		
$(x_i - m)^2$	0.0016	0.0256	0.0196	0.0016	0.0036		0.10	0.02
1.8	5.7	5.9	5.8	5.7	5.8	5.78		
$(x_i - m)^2$	0.0064	0.0144	0.0064	0.0064	0.0064		0.07	0.01
2	5.95	6.2	5.8	5.95	6.12	6.004		
$(x_i - m)^2$	0.002916	0.038416	0.041616	0.002916	0.013456		0.14	0.02
2.5	6.1	6.3	6.2	6.1	6.5	6.24		
$(x_i - m)^2$	0.0196	0.0036	0.0016	0.0196	0.0676		0.15	0.02
3	6.4	6.6	6.3	6.3	6.5	6.42		
$(x_i - m)^2$	0.0004	0.0324	0.0144	0.0144	0.0064		0.12	0.02
4	6.6	6.8	6.6	6.7	6.7	6.68		
$(x_i - m)^2$	0.0064	0.0144	0.0064	0.0004	0.0004		0.07	0.01
6	6.9	7.3	7.1	7	7.1	7.08		
$(x_i - m)^2$	0.0324	0.0484	0.0004	0.0064	0.0004		0.13	0.02
8	7.3	7.6	7.3	7.5	7.5	7.44		
$(x_i - m)^2$	0.0196	0.0256	0.0196	0.0036	0.0036		0.12	0.02
10	7.4	7.8	7.6	7.7	7.5	7.6		
$(x_i - m)^2$	0.04	0.04	0	0.01	0.01		0.14	0.02
12	7.5	8	7.9	7.7	7.8	7.78		
$(x_i - m)^2$	0.0784	0.0484	0.0144	0.0064	0.0004		0.17	0.02
14	7.7	8.1	8	7.8	7.95	7.91		
$(x_i - m)^2$	0.0441	0.0361	0.0081	0.0121	0.0016		0.14	0.02
15	7.8	8	8	7.9	7.9	7.92		
$(x_i - m)^2$	0.0144	0.0064	0.0064	0.0004	0.0004		0.07	0.01
							0.13	0.03
							Mean s	Mean COV

Lag Screw - 1/2" Diameter

Quantity	LOAD	LOAD	LOAD	LOAD	LOAD	Mean	St.Dev	COV
Displ	Bolt Nr. 1	2	3	4	5	$m = \sum(x_i)/n$	$\sum(x_i - m)^2/n$	s/m
0	0	0	0	0	0	0		
0.5	1.35	1.5	1.7	1.4	1.5	1.49		
$(x_i - m)^2$	0.0196	0.0001	0.0441	0.0081	0.0001		0.12	0.08
1	2.82	3	3.2	3.1	3.1	3.044		
$(x_i - m)^2$	0.050176	0.001936	0.024336	0.003136	0.003136		0.13	0.04
1.2	3.52	3.5	3.6	3.5	3.4	3.504		
$(x_i - m)^2$	0.000256	0.000016	0.009216	0.000016	0.010816		0.06	0.02
1.4	3.8	3.8	3.9	3.7	3.9	3.82		
$(x_i - m)^2$	0.0004	0.0004	0.0064	0.0144	0.0064		0.07	0.02
1.6	4	4.1	4.1	3.8	3.8	3.96		
$(x_i - m)^2$	0.0016	0.0196	0.0196	0.0256	0.0256		0.14	0.03
1.8	4.1	4.3	4.1	4.2	4	4.14		
$(x_i - m)^2$	0.0016	0.0256	0.0016	0.0036	0.0196		0.10	0.02
2	4.4	4.2	4.1	4.1	4.1	4.18		
$(x_i - m)^2$	0.0484	0.0004	0.0064	0.0064	0.0064		0.12	0.03
2.5	4.4	4.4	4.3	4.3	4.3	4.34		
$(x_i - m)^2$	0.0036	0.0036	0.0016	0.0016	0.0016		0.05	0.01
3	4.6	4.6	4.4	4.3	4.6	4.5		
$(x_i - m)^2$	0.01	0.01	0.01	0.04	0.01		0.13	0.03
4	4.8	4.7	4.8	4.6	4.7	4.72		
$(x_i - m)^2$	0.0064	0.0004	0.0064	0.0144	0.0004		0.07	0.02
6	4.7	5	4.8	4.7	4.7	4.78		
$(x_i - m)^2$	0.0064	0.0484	0.0004	0.0064	0.0064		0.12	0.02
8	4.9	5.1	4.9	4.8	4.8	4.9		
$(x_i - m)^2$	0	0.04	0	0.01	0.01		0.11	0.02
10	4.9	5.1	5	4.9	4.9	4.96		
$(x_i - m)^2$	0.0036	0.0196	0.0016	0.0036	0.0036		0.08	0.02
12	5.4	5.4	5.2	5.2	5.1	5.26		
$(x_i - m)^2$	0.0196	0.0196	0.0036	0.0036	0.0256		0.12	0.02
14	5.4	5.4	5.3	5.3	5.4	5.36		
$(x_i - m)^2$	0.0016	0.0016	0.0036	0.0036	0.0016		0.05	0.01
15	5.5	5.5	5.3	5.3	5.5	5.42		
$(x_i - m)^2$	0.0064	0.0064	0.0144	0.0144	0.0064		0.10	0.02
							0.10	0.03
							Mean st.dev	Mean COV

Bolt Grade 5 - 1/2" Diameter

Quantity	LOAD	LOAD	LOAD	LOAD	LOAD	Mean	St.Dev	COV
Displ	Bolt Nr. 1	2	3	4	5	$m = \sum(x_i)/n$	$s = \sqrt{\sum(x_i - m)^2/n}$	s/m
0	0	0	0	0	0	0		
0.5	5.86	5.89	5.7	4.9	5.9	5.61		
	0.0625	0.0064	0.0081	0.5041	0.0841		0.36	0.07
1	11.55	11.55	11.55	10.4	11.3	11.27		
	0.0784	0.0784	0.0784	0.7569	0.0009		0.45	0.04
1.2	12.55	12.86	12.7	12	12.7	12.562		
	0.000144	0.088804	0.019044	0.315844	0.019044		0.30	0.02
1.4	13.25	13.7	13.6	13	13.4	13.39		
	0.0196	0.0961	0.0441	0.1521	1E-04		0.25	0.02
1.6	13.6	14.1	13.9	13.4	13.8	13.76		
	0.0256	0.1156	0.0196	0.1296	0.0016		0.24	0.02
1.8	13.9	14.4	14.4	13.9	14.2	14.16		
	0.0676	0.0576	0.0576	0.0676	0.0016		0.22	0.02
2	14.4	14.9	14.6	14.5	14.5	14.58		
	0.0324	0.1024	0.0004	0.0064	0.0064		0.17	0.01
2.5	14.9	15.4	15.1	14.9	15.1	15.08		
	0.0324	0.1024	0.0004	0.0324	0.0004		0.18	0.01
3	15.4	15.9	15.6	15.4	15.5	15.56		
	0.0256	0.1156	0.0016	0.0256	0.0036		0.19	0.01
4	15.9	16.6	16.3	16.3	16.1	16.24		
	0.1156	0.1296	0.0036	0.0036	0.0196		0.23	0.01
6	17	17.6	17.2	17.3	17	17.22		
	0.0484	0.1444	0.0004	0.0064	0.0484		0.22	0.01
8	17.5	18	17.7	17.8	17.9	17.78		
	0.0784	0.0484	0.0064	0.0004	0.0144		0.17	0.01
10	18	18.7	18.6	18.5	18.5	18.46		
	0.2116	0.0576	0.0196	0.0016	0.0016		0.24	0.01
12	18.5	19.24	18.9	18.8	18.9	18.868		
	0.135424	0.138384	0.001024	0.004624	0.001024		0.24	0.01
14	19	19.9	19.3	19.2	19.3	19.34		
	0.1156	0.3136	0.0016	0.0196	0.0016		0.30	0.02
15	19.3	20.1	19.5	19.3	19.5	19.54		
	0.0576	0.3136	0.0016	0.0576	0.0016		0.29	0.02
							0.25	0.02
							Mean s	Mean COV

Bolt Grade 5 - 5/8" Diameter

Quantity	LOAD	LOAD	LOAD	LOAD	LOAD	Mean	St.Dev	COV
Displ	Bolt Nr. 1	2	3	4	5	$m = \sum(x_i)/n$	$s = \sqrt{\sum(x_i - m)^2/n}$	s/m
0	0	0	0	0	0	0		
0.5	11.5	10.2	9	12.4	11.7	10.96		
	0.2916	0.5776	3.8416	2.0736	0.5476		1.21	0.11
1	23.4	21	20.8	22.5	22.7	22.08		
	1.7424	1.1664	1.6384	0.1764	0.3844		1.01	0.05
1.2	25.6	24.3	24.2	25.1	25.4	24.92		
	0.4624	0.3844	0.5184	0.0324	0.2304		0.57	0.02
1.4	27.2	26.1	26.6	26.9	26.8	26.72		
	0.2304	0.3844	0.0144	0.0324	0.0064		0.37	0.01
1.6	28.1	27.4	27.7	28	27.9	27.82		
	0.0784	0.1764	0.0144	0.0324	0.0064		0.25	0.01
1.8	28.9	28.2	28.6	28.9	28.5	28.62		
	0.0784	0.1764	0.0004	0.0784	0.0144		0.26	0.01
2	29.6	28.8	29.2	29.5	29.2	29.26		
	0.1156	0.2116	0.0036	0.0576	0.0036		0.28	0.01
2.5	30.7	30	30.4	30.7	30.2	30.4		
	0.09	0.16	0	0.09	0.04		0.28	0.01
3	31.7	30.9	31.4	31.4	31.3	31.34		
	0.1296	0.1836	0.0036	0.0036	0.0016		0.26	0.01
4	33.2	32.4	33.2	33	32.9	32.94		
	0.0676	0.2916	0.0676	0.0036	0.0016		0.29	0.01
6	35.3	34.7	35.1	35.3	34.8	35.04		
	0.0676	0.1156	0.0036	0.0676	0.0576		0.25	0.01
8	36.5	35.6	36.4	36.7	36	36.24		
	0.0676	0.4096	0.0256	0.2116	0.0576		0.39	0.01
10	37.5	36.7	37.2	37.4	36.9	37.14		
	0.1296	0.1836	0.0036	0.0676	0.0576		0.30	0.01
12	38.5	37.8	38.4	38.3	37.9	38.18		
	0.1024	0.1444	0.0484	0.0144	0.0784		0.28	0.01
14	39.7	39.2	39.5	39.5	39.6	39.5		
	0.04	0.09	0	0	0.01		0.17	0.00
15	40	39.7	39.8	40	39.9	39.9		
	0.01	0.04	0.01	0.01	0.01		0.13	0.00
							0.39	0.02
							Mean s	Mean COV

Bending Deflection of 12.7 mm Bolts in PSL -Tension Tests [mm]

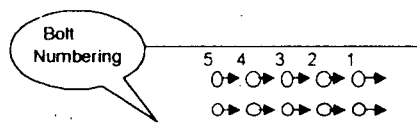
Specimen	Bolt Nr	Calc. Displ. [mm]					Displ.off Dial Gauge[1/1000"]				
		5	4	3	2	1	5	4	3	2	1
HU2	1. Row	0.3	0.1	0.1	0.3	1.4	23	10	10	25	113
	2. Row	0.2	0.1	0.1	0.2	1.2	19	10	8	15	92
HRR1	1. Row	1.8	1.1	2.3	2.8	3.5	138	90	192	242	345
	2. Row	1.4	1.1	2.4	3.1	4.4	111	86	180	224	273
HRR2	1. Row	1.9	1.4	1.3	1.3	3.2	156	90	120	110	311
	2. Row	2	1.1	1.5	1.4	3.9	150	109	105	105	250
HRRS2	1. Row	1	1.3	2.8	2.3	3.5	82	105	218	183	276
	2. Row	0.9	1.1	2.6	1.9	2.9	74	90	201	146	231
HRRSH1	1. Row	1.9	1.8	2.1	2.5	5	151	140	163	195	390
	2. Row	1.8	1.6	1.9	2.4	3.3	142	125	152	187	263
HRRSH2	1. Row	1.6	0.9	2.2	2.4	3.8	128	74	173	189	299
	2. Row	0.7	0.6	1.9	2.2	3.1	58	45	146	170	245
HRT1	1. Row	2.4	2.2	3.3	3.3	3	189	173	260	258	235
	2. Row	1.6	0.9	1.9	1.3	4.2	128	73	152	102	330
HRTW	1. Row	0.4	0.8	1.1	0.6	1.4	31	60	90	48	114
	2. Row	1	0.8	1.2	0.8	1.7	79	64	94	64	137
HRER-1	1. Row	3	2.9	3.9	4.1	3.9	234	230	310	325	305
	2. Row	1.8	2.5	3.2	3.8	4.7	141	194	253	302	372
HRER-2	1. Row	3.6	2.7	3.6	3.6	3.6	285	215	286	280	286
	2. Row	2.4	2	4	3	2.6	189	154	314	239	205
HRERe-1	1. Row	4.1	1.7	1.8	2.8	3.6	325	135	145	222	283
	2. Row	2.2	2.3	4.1	3.6	4.3	171	182	320	284	335
HRERe-2	1. Row	2.4	2.3	3	2.4	3	190	183	235	188	236
	2. Row	2.3	2.9	2.7	3.1	1.9	184	230	214	248	153
HRN26	1. Row	1.8	2.3	3.4	2.8	3.1	140	182	268	220	244
	2. Row	1.3	1.1	1.9	1.7	1.5	106	89	152	135	120
HRN18	1. Row	1.4	1.1	1.7	1	0.3	112	87	130	80	24
	2. Row	1.5	1.5	1.9	0.9	1.5	117	117	150	70	120
GHU-1	1. Row	0.6	0.5	1.7	0.8	0.9	48	42	130	60	72
	2. Row	0.3	0.7	0.9	0.7	0.2	23	58	70	55	17
GHU-2	1. Row	0.1	1.1	1.2	0.9	2.4	8	85	96	72	192
	2. Row	0.1	0	1.5	0.7	0.4	10	3	120	53	30
GHU-3	1. Row	0.5	1.2	1.7	1.1	0.2	38	92	132	90	13
	2. Row	1	1.6	2.6	1.4	1.9	80	126	205	108	149
GHRRF-1	1. Row	1.2	1.2	2.1	2.4	1.8	98	97	167	186	140
	2. Row	1.4	1.7	2.7	2.5	3.2	114	132	215	195	251
GHRRF-2	1. Row	1.2	2	2.7	2.6	3.2	91	155	211	207	250
	2. Row	1.3	2.1	3.3	3.4	4.7	105	168	256	270	369
GHRRF-3	1. Row	0.6	1.3	1.7	1.5	0.4	46	100	136	115	35
	2. Row	0.6	0.5	1.6	0.7	1.1	45	43	124	53	87
GHRR-1	1. Row	2	1.8	3.1	3	4.1	159	143	247	236	322
	2. Row	0.7	0.9	1.6	2.7	4.7	55	70	128	209	374
GHRR-2	1. Row	2.7	1.9	3	2.5	1.6	216	150	240	198	129
	2. Row	1.4	2.2	2.9	3.1	1.7	111	172	228	241	134
GHRR-3	1. Row	1.3	1.2	2.1	1.7	2.2	106	95	165	130	171
	2. Row	1.1	1	1.6	1.7	2.3	89	78	125	137	181

Bending Deflection of 15.9 mm Bolts -Tension Tests [mm]

Specimen	Bolt Nr	Calc. Displ. [mm]					Displ.off Dial Gauge[1/1000"]				
		5	4	3	2	1	5	4	3	2	1
FRRS1	1. Row	0.2	0.3	0.4	0.4	0.2	13	20	28	32	15
	2. Row	0.1	0.4	0.4	0.4	0.9	8	28	31	33	72
FRRS2	1. Row	0.1	0	0.2	0.1	0.4	10	3	16	8	32
	2. Row	0.2	0.2	0.4	0.7	1	17	15	35	55	78
FRRF1	1. Row	0.1	0.4	0.2	0.2	0.1	8	28	13	13	8
	2. Row	0.2	0.4	1	1	1	12	30	78	82	82
FRRF2	1. Row	0.2	0.3	0.2	0.5	0.3	17	25	18	43	25
	2. Row	0.3	0.3	0.7	0.7	1.7	20	26	55	55	132
FRTT1	1. Row	0.1	0.1	0.3	0.3	0.2	5	11	20	22	19
	2. Row	0.1	0.2	0.5	0.3	0.8	6	14	40	24	60
FRTT2	1. Row	0.1	0.2	0.1	0.3	0.1	5	17	10	21	8
	2. Row	0.1	0.7	0.8	0.3	1.1	10	53	64	27	86
FRN18	1. Row	0.1	0.1	0.6	0.5	0.1	4	4	47	42	8
	2. Row	0	1.6	0.3	0.6	0.4	2	123	24	44	28
FRN26	1. Row	0.2	0.1	0.2	1.5	1.2	15	5	19	115	93
	2. Row	0.2	0.7	0.5	0.4	1.3	15	57	39	35	105

Bending Deflection of 9.5 mm Bolts -Tension Tests [mm]

Specimen	Bolt Nr	Calc. Displ. [mm]					Displ.off Dial Gauge[1/1000"]				
		5	4	3	2	1	5	4	3	2	1
TU-1	1. Row	1.4	1.5	2	1.4	1.3	110	115	155	109	101
	2. Row	2.7	2.6	2.9	2.3	1.8	214	204	228	178	140
TU-2	1. Row	4.1	2.9	3.5	2.4	2.6	325	229	276	189	203
	2. Row	1.4	1.3	1.4	1.6	1.1	107	99	109	125	86
TU-3	1. Row	2	2.6	2.4	2	1.6	159	207	187	156	123
	2. Row	1.7	1.3	1.4	0.8	1.1	130	103	112	66	84
TRR-2	1. Row	8.9	9.3	10	11	11	697	731	790	850	855
	2. Row	8.7	9.5	9.8	10	11	685	750	770	812	852
TRR-1	1. Row	8.1	8.8	9.3	9.7	10	638	690	730	763	826
	2. Row	8.4	8.9	9.7	10	10	665	703	764	795	820
TRR-3	1. Row	11	11	12	12	13	833	835	910	931	1000
	2. Row	9.2	11	11	12	14	726	870	895	954	1100
GTU-1	1. Row	2.1	1.3	1.5	1.4	1	165	102	120	110	80
	2. Row	0.6	1.5	1	0.8	1.1	51	115	80	65	87
GTU-2	1. Row	1.6	1.5	1.7	1.3	1.8	123	115	136	105	142
	2. Row	3.7	2.6	3.6	3.6	2.3	295	205	286	285	180
GTU-3	1. Row	3.5	3.8	3	3	3.4	272	298	236	239	269
	2. Row	3.1	2.4	3.4	3.3	2	247	190	266	258	160
GTRR-2	1. Row	8.5	7.6	6.5	6.9	3.5	276	540	515	598	669
	2. Row	7.4	7.1	6.2	6.6	6.2	490	519	490	558	580



☐ Not in the true order

DENSITY AND MOISTURE CONTENT SUMMARY - 10 BOLT JOINTS IN GLULAM AND PSL - STATIC TENSION TESTS

Loading Test			Moisture content, density													
Test (Nr.)	Specimen (short)	Done (Date)	Measured after test				Measured after oven drying									
			Dimensions (mm)	Volume (m³)	Mass (g)	Density (kg/m³)	Dimensions (mm)	Volume (m³)	Mass (g)	Density (kg/m³)	Moist (%)	M.vol (%)				
1	HU1	6.7.99	140	90	25	0.00032	204.9	650.38	137	86	25	0.00029	189.2	642.336	8.28	1.25
2	HU2	5.7.99	140	89	25	0.00031	209.2	671.44	137	87	25	0.0003	193.1	648.007	8.32	3.62
3	HRT1	14.7.99	139	89	23	0.00028	192	674.86	136	87	23	0.00027	176.3	647.691	8.94	4.19
4	HRT2	14.7.99	139	88	29	0.00035	231.9	653.8	136	86	29	0.00034	212.6	626.769	9.09	4.31
5	HRRSH1	5.7.99	140	88	23	0.00028	179.9	634.78	138	86	23	0.00027	165.7	607.186	8.53	4.54
6	HRRSH2	6.7.99	140	90	23	0.00029	176.2	608.07	138	87	23	0.00028	162.1	586.989	8.72	3.59
7	HRR1	7.7.99	140	89	23	0.00029	186.9	652.1	138	88	24	0.00029	172.7	592.577	8.2	10
8	HRR2	6.7.99	142	90	22	0.00028	183.7	653.36	140	86	22	0.00026	170.1	642.064	8.01	1.76
9	HRRS1	6.7.99	141	87	26	0.00031	201	642.47	139	87	26	0.00031	185.9	602.844	8.11	6.57
10	HRRS2	15.7.99	140	89	27	0.00034	228.3	678.59	137	87	27	0.00032	211	658.031	8.2	3.12
11	HRTW1	16.7.99	139	87	19	0.00023	147.4	641.52	135	86	19	0.00022	134.4	609.048	9.71	5.33
12-21	FU1-10	*														
22	FRTT1	12.7.99	139	87	30	0.00036	232.9	642.02	136	85	30	0.00035	214.4	618.339	8.62	3.83
23	FRTT2	13.7.99	139	87	29	0.00035	221.9	632.85	135	86	29	0.00034	203.6	604.8	8.99	4.64
24-32	FRT1-9	*														
33	FRRS1	7.7.99	140	89	26	0.00032	211.1	651.69	138	88	27	0.00033	192.5	586.999	9.69	11
34	FRRS2	9.7.99	139	89	23	0.00028	171.4	602.29	137	86	23	0.00027	159.5	588.702	7.42	2.31
35	FRR1	13.5.99	140	88	24	0.0003	196.3	663.83	137	87	24	0.00029	178.9	625.472	9.7	6.13
36	FRR2	13.5.99	140	88	22	0.00026	179.5	677.48	136	86	22	0.00025	164.1	652.658	9.34	3.8
37	FRE1-6b	19.2.99	141	89	27	0.00034	222.7	657.33	138	87	27	0.00032	205	632.431	8.64	3.94
38	FRE2-6b	19.2.99	143	88	26	0.00032	204.7	637.88	139	86	26	0.0003	186.4	611.429	9.82	4.33
39	FRN-I	18.2.99	141	89	24	0.0003	199.6	662.8	138	86	24	0.00028	183.7	644.942	8.67	2.77
40	FRN-II	18.2.99	140	89	22	0.00027	182.1	664.42	137	86	22	0.00026	167.8	647.251	8.56	2.65
41	FRRF1	13.7.99	139	87	29	0.00035	235.6	671.78	135	86	29	0.00034	216	641.421	9.09	4.73
42	FRRF2	13.7.99	139	88	30	0.00037	217.4	592.44	136	86	30	0.00035	199.1	567.373	9.2	4.42
43	FRN18-1	22.12.99	139	87	27	0.00033	222.2	680.59	135	85	27	0.0003	201.1	661.389	10.5	2.9
44	FRN26-1	22.12.99	139	89	28	0.00035	232.2	670.35	134	86	28	0.00032	210.1	651.157	10.5	2.95
45	HRN18-1	16.12.99	140	88	32	0.00039	249.8	633.5	136	86	31	0.00036	228.8	631.15	9.14	0.37
46	HRN26-1	16.12.99	140	87	26	0.00032	192.9	609.16	137	87	25	0.0003	177	593.976	8.99	2.56
47	HRER1	16.12.99	140	88	33	0.0004	249.3	622.6	137	86	32	0.00038	228.5	606.168	9.08	2.71
48	HRER2	16.12.99	140	88	36	0.00044	284	649.28	136	85	35	0.0004	259.4	645.02	9.45	0.66
49	HRERe1	15.12.99	140	89	35	0.00044	273.3	626.71	136	85	34	0.00039	250.5	637.263	9.12	1.66
50	HRERe2	15.12.99	139	88	31	0.00037	238.8	639.95	135	86	30	0.00035	218.9	628.424	9.08	1.83
51	GHU1	16.12.99	130	87	31	0.00034	203	588.37	126	86	30	0.00033	182.1	560.078	11.5	5.05
52	GHU2	17.12.99	129	89	25	0.00028	174.2	619.12	124	87	25	0.00027	155.5	576.567	12	7.38
53	GHU3	17.12.99	129	89	34	0.00039	227.9	583.78	126	86	34	0.00036	203.6	560.735	12	4.11
54	GHRR1	22.12.99	96	89	34	0.00029	167	574.78	87	93	34	0.00028	149	541.633	12.1	6.12
55	GHRR2	20.12.99	129	89	29	0.00033	191	573.6	124	87	29	0.00031	170.4	544.635	12.1	5.32
56	GHRR3	20.12.99	85	85	33	0.00023	143.7	615.68	85	87	32	0.00024	129.3	546.484	11.1	12.7
57	GHRRF1	17.12.99	129	87	26	0.00029	181.8	622.93	125	85	25	0.00027	162.4	611.501	11.9	1.87
58	GHRRF2	17.12.99	130	89	20	0.00023	135.6	586.04	126	86	20	0.00021	121.1	573.208	12	2.24
59	GHRRF3	20.12.99	130	88	23	0.00026	148.2	575.84	126	86	22	0.00024	132.3	555.136	12	3.73
60	GTU1	10.2.00	130	88	17	0.00019	116.6	617.5	126	86	17	0.00018	103.8	580.556	12.3	6.36
61	GTU2	10.2.00	130	88	24	0.00027	167.3	622.23	126	86	24	0.00025	148.8	584.144	12.5	6.52
62	GTU3	10.2.00	130	89	27	0.0003	179.5	588.65	127	86	27	0.00029	159.9	552.459	12.2	6.55
63	GTRR1	10.2.00	130	89	25	0.00029	178.2	616.04	126	86	25	0.00027	159.3	588.151	11.8	4.74
64	GTRR2	14.2.00	128	88	28	0.00032	193.4	613.05	124	86	28	0.0003	171.1	572.922	13	7
65	GTRR3	14.2.00	130	88	30	0.00034	208.5	617.76	128	85	30	0.00032	187.9	587.696	11	5.11
66	TU1	17.2.00	139	88	30	0.00037	227.4	619.71	137	85	30	0.00035	208.7	599.612	8.96	3.35
67	TU2	17.2.00	140	89	28	0.00035	219.5	629.04	136	86	29	0.00034	201.1	592.864	9.14	6.1
68	TU3	17.2.00	140	88	25	0.00031	213.8	694.22	137	86	27	0.00031	196.3	628.781	8.91	10.4
69	TRR1	18.2.00	140	89	18	0.00022	151.7	676.34	138	87	19	0.00022	139.9	635.719	8.44	6.39
70	TRR2	18.2.00	140	89	24	0.00029	173.8	593.7	138	87	24	0.00029	161.7	561.074	7.53	5.81
71	TRR3	18.2.00	140	89	34	0.00042	267.4	640.64	138	87	34	0.0004	247.1	616.653	8.21	3.89

DENSITY AND MOISTURE CONTENT SUMMARY - 10 BOLT JOINTS IN GLULAM AND PSL - CYCLIC TESTS

Loading Test			Moisture content, density											
Test (Nr.)	Specimen (short)	Done (Date)	Measured after test						Measured after oven drying					
			Dimensions			Volume	Mass	Density	Dimensions			Volume	Mass	Density
			(mm)	(mm)	(mm)	(m ³)	(g)	(kg/m ³)	(mm)	(mm)	(mm)	(m ³)	(g)	(kg/m ³)
72	HU1-C	20.1.00	140	89	20	0.00025	166.5	667.94	135	88	20	0.00024	152	639.52
73	HU2-C	20.1.00	140	89	19	0.00024	154.9	654.30	136	88	19	0.00023	141.8	627.29
74	HU3-C	20.1.00	140	89	27	0.00034	221	656.95	137	87	27	0.00032	202.9	630.43
75	HRR1-C	20.1.00	140	89	21	0.00026	170.7	652.34	136	87	21	0.00024	156.7	645.91
76	HRR2-C	24.1.00	142	90	22	0.00027	185.7	675.77	139	88	22	0.00026	171	652.41
77	HRR3-C	24.1.00	140	89	22	0.00027	184.8	674.16	138	87	22	0.00026	170.2	646.83
78	HRT1-C	25.1.00	141	90	25	0.00032	222.5	701.34	139	88	25	0.0003	204.9	673.81
79	HRT2-C	25.1.00	139	89	25	0.0003	206	679.54	136	85	25	0.00028	186.6	658.85
80	HRT3-C	26.1.00	139	89	23	0.00028	203.6	715.42	136	86	23	0.00027	184.1	686.97
81	FU1-C	17.1.00	140	89	24	0.0003	189.8	634.53	137	87	24	0.00029	174.5	610.09
82	FU2-C	19.1.00	139	89	28	0.00035	213.1	615.23	137	87	28	0.00033	196	587.42
83	FU3-C	17.1.00	139	89	23	0.00028	184.9	664.35	136	87	23	0.00027	169.2	635.68
84	FRR1-C	19.1.00	139	89	23	0.00028	182	639.68	137	86	23	0.00027	166.6	628.27
85	FRR2-C	19.1.00	139	89	22	0.00027	165.9	623.85	135	87	21	0.00025	152.1	616.72
86	FRR3-C	19.1.00	139	89	25	0.00031	196.6	635.81	136	86	25	0.00029	179.8	627.39
87	FRT1-C	19.1.00	139	89	29	0.00036	211.8	590.23	137	87	28	0.00033	194.6	582.98
88	FRT2-C	21.1.00	139	88	23	0.00028	185.2	658.29	136	86	23	0.00027	169.2	628.83
89	FRT3-C	21.1.00	140	89	27	0.00033	229.7	695.75	136	87	27	0.00031	211.8	675.59
90	GTRR-C	14.2.00	130	89	20	0.00023	144.1	638.65	124	87	20	0.00021	128.4	610.51
91	TU-C	18.2.00	140	89	29	0.00036	244.27	676.01	137	87	30	0.00035	224.1	643.24
92	TRR-C	18.2.00	140	89	26	0.00032	186.88	576.86	137	87	27	0.00032	172.9	547.25

T	3/8" Bolt	E	Epoxy Glued	SH	Shifted Rod (away from the Bolt)
H	1/2" Bolt	F	Fine Threaded (Ready) Rod	TT	Truss Plate Transversely Rotated
F	5/8" Bolt	N	Nailed Plate	W	On-Truss Plate Welded Steel Plate
U	Unreinforced	T	Truss Plate (Gang Nail)	Re	Reinforcing Bar No.10 (11.3mm)
R	Reinforced	R	Threaded Rod	18	18 gauge (1.2 mm) galvanized steel plate
G	Glulam	S	Single Rod at the End	26	26 gauge (0.6mm) galvanized steel plate

* Tests Performed Earlier (B. Hockey, thesis, 1999)